Section I

Novel Electroactive Polymers as Environmentally Compliant Coatings for Corrosion Control

SERDP Project Number: Weapons Platforms/Systems (WP) 1148

Performing Organization: Naval Air Warfare Center Weapons Division
Polymer Science & Engineering Branch (Code 498220D)
1900 N. Knox Road (Stop 6303)
China Lake, CA 93555-6106

Lead Principal Investigator: Dr. Peter Zarras
(P) 760-939-1396
(F) 760-939-1617
E-mail: peter.zarras@navy.mil

Date: February 3, 2006

Revision Number: NA

REPORT DOCUMENTATION PAGE

Form Approved
OMB No. 0704-0188

1. REPORT DATE *(DD-MM-YYYY)*	**2. REPORT TYPE**	**3. DATES COVERED** *(From - To)*
19-06-2006	Final Technical Report	June 2000-September 2004; February 2006

4. TITLE AND SUBTITLE
Novel Electroactive Polymers as Environmentally Compliant Coatings for Corrosion Control

5a. CONTRACT NUMBER
NA

5b. GRANT NUMBER
NA

5c. PROGRAM ELEMENT NUMBER
603716D

6. AUTHOR(S)
Zarras, Peter; Mansfeld, Florian; Wynne, Kenneth, J.; Tallman, Dennis, E; Benicewicz Xu, Jun; and Kendall, Gay

5d. PROJECT NUMBER
WP 1148

5e. TASK NUMBER
NA

5f. WORK UNIT NUMBER
NA

7. PERFORMING ORGANIZATION NAME(S) AND ADDRESS(ES)
NAWCWD (Code 498220D)
1900 N. Knox Road (Stop 6303)
China Lake, CA 93555-6106

8. PERFORMING ORGANIZATION REPORT NUMBER NA

9. SPONSORING / MONITORING AGENCY NAME(S) AND ADDRESS(ES)
SERDP & ESTCP Program Office
901 North Stuart Street
Suite 303
Arlington, VA 22203

10. SPONSOR/MONITOR'S ACRONYM(S)
SERDP

11. SPONSOR/MONITOR'S REPORT NUMBER(S)

12. DISTRIBUTION / AVAILABILITY STATEMENT
unlimited

13. SUPPLEMENTARY NOTES

14. ABSTRACT The objectives of this SERDP program (WP 1148) have been completed successfully. The synthesis, scale-up and characterization of new monomers based on a bis-amino derivative of poly-*p*-phenylene vinylene (PPV) called poly(2,5-bis(N-methyl-N-hexylamino)phenylene vinylene, (BAM-PPV) and oligomers of polyaniline have been completed. These polymers have been thoroughly characterized using advanced spectroscopic and analytical methods. The details regarding the EAP synthesis has been published in the literature for duplication including potential industrial use. BAM-PPV pretreatment coating on Al 2024-T3 processed from different solvents passed 336 hours neutral salt fog exposure. This test is required for new pretreatment coatings on aluminum alloys. Additional pretreatments were also studied including trivalent chromium pretreatment (TCP). BAM-PPV coatings in several cases exceeded the 336 hour requirement. BAM-PPV has also been incorporated into full military coating systems that include non-chrome primers and topcoats. These coatings have been tested against known controls such as chromium primers and TCP pretreatment with non-chrome primer and topcoat. BAM-PPV performed as well as the TCP pretreatment with non-chrome primer and topcoat. However, in both cases, each coating did not pass the 2000 hours neutral salt fog exposure test. When BAM-PPV was used with chromium primer and topcoat, this coating system lasted over 4000 hours in a neutral salt fog chamber. Studies by ENM, SVET and XPS showed evidence that BAM-PPV provides more than simply barrier protection to corrosive environments and may passivate the metal surface.

15. SUBJECT TERMS electroactive polymers, passivation, neutral salt fog exposure

16. SECURITY CLASSIFICATION OF: U			**17. LIMITATION OF ABSTRACT**	**18. NUMBER OF PAGES**	**19a. NAME OF RESPONSIBLE PERSON**
a. REPORT	**b. ABSTRACT**	**c. THIS PAGE**			Dr. Peter Zarras
U	U	U	UU	189	**19b. TELEPHONE NUMBER** *(include area code)* 760-939-1396

Section II

Table of Contents:

Section II

Front Matter:

List of Acronyms:

aq. NaOCl	aqueous sodium hypochlorite
ATR-FTIR	Attenuated Total reflectance fourier transform infrared spectrometry
AIBN	α,α-azobis(isobutyronitrile)
BAM-PPV	poly(2,5-bis(N-methyl-N-hexylamino) phenylene vinylene
Br_2	Bromine
CARC	Chemical Agent resistant Coating
CCC	Chromate conversion coating
CV	Cyclic voltammetry
DBAR	Doppler Broadening of Annihilation Radiation
DSC	Differential Scanning Calorimetry
DHS	Dilute Harrison solution
DMF	Dimethylformamide
DIBAL-H	Diisobutylaluminum hydride solution
EAP	Electroactive polymer
EIS	Electrochemical Impedance Spectroscopy
ENM	Electrochemnical Noise Technique
EO3-PPV	Poly [2,5-bis (triethoxy-methoxy)-1,4-phenylene vinylene]
ESTCP	Environmental Security Technology Certification Program
GPC	Gel Permeation Chromatography
g	gram
HCl	hydrogen chloride
IV	Inherent viscometry
FTIR	Fourier Transform Infrared Spectrometry
kg	kilogram
LSCM	Laser Scanning Confocal Microscopy
LVDT	linear variable displacement transducer
L	Liter
$LiAlH_4$	Lithium aluminum hydride
mp	melting point
MCT	MicroCoating Technologies
mg	milligrams
$MgSO_4$	Magnesium sulfate
ml	milliliters
mmol	millimoles
MDSC	Modulated differential scanning calorimetry
NAWCAD	Naval Air Warfare Center Aircraft Division
NAWCWD	Naval Air Warfare Center Weapons Division

$NiCl_2*6H_2O$	nickel(II) chloride hexahydrate
NMR	Nuclear Magnetic Resonance Spectroscopy
ORNL	Oak Ridge National Laboratory
Pd	Palladium metal
PANI	Polyaniline
PALS	Positron Annihilation Lifetime Spectroscopy
K-*t*-OBu	Potassium-*tert*-butoxide
RPI	Rensselaer Polytechnic Institute
NaH	Sodium hydride
SEM	Scanning Electron Microscopy
SVET	Scanning Vibrating Electrode Technique
SBIR	Small Business Innovative Research Program
$SCCO_2$	Supercritical carbon dioxide
T_g	Glass transition temperature
T_c	Crystalline melting point temperature
T_d	Decomposition temperature
T_m	Melting point temperature
TGIC	Triglycidyl isocyanurate
TGA	Thermal Gravametric Analysis
THF	Tetrahydrofuran
TMA	Thermomechanical analysis
$SOCl_2$	Thionyl Chloride
TCP	Trivalent chromium pretreatment
UV-Vis	Ultraviolet-visible spectrum
UTD	University of Texas at Dallas
USC	University of Southern California
VCU	Virginia Commonwealth University
VOC	Volatile organic compounds
XPS	X-ray photoelectron scpectroscopy
WAM-PPV	water-dispersible BAM-PPV derivative

List of Tables

List of Schemes

List of Figures

Section III

Acknowledgements:

The work performed under this SERDP project (WP1148) was directed by the Naval Air Warfare Center Weapons Division (NAWCWD), China Lake, California. Dr. Peter Zarras was the project lead for coordinating activities between the various co-performers (industry, academia, government laboratories) and worked on scale-up and synthesis of EAP compounds. Ms. Nicole Anderson, Ms. Cindy Webber, Dr. David Irvin, Dr. Michael E. Wright and Dr. John Stenger-Smith worked on synthesis, scale-up and characterization of poly(2,5-bis(N-methyl-N-hexylamino)phenylene vinylene (BAM-PPV) and derivatives. Ms. Nicole Anderson and Ms. Cindy Webber were both involved in the coating of BAM-PPV films onto Al and steel alloys. Dr. Samantha Hawkins and Dr. Lawrence Baldwin characterized several BAM-PPV samples and derivatives using FTIR and NMR spectroscopy. Dr. Andrew Guenthner did extensive characterization of BAM-PPV using thermal analysis. Mr. Brett Tanner of the NAWCWD Environmental Laboratory provided their neutral salt fog chamber for extensive accelerated weathering testing of BAM-PPV coatings. Dr. Nick Prokopuk examined BAM-PPV films for pH stability and corrosion protection using electrochemical impedance measurements (EIS). In addition, Dr. Prokopuk used the XPS facilities in the Beckman Institute at the California Institute of Technology for analysis of BAM-PPV films on aluminum substrates. Drs. Craig Matzdorf and Kevin Kovaleski of NAWCAD coated several primers and topcoats onto BAM-PPV coated Al and steel alloys. MicroCoating Technologies Inc.(MCT) provided several BAM-PPV coated Al and steel coupons using their proprietary flame deposition technique for testing in neutral salt fog chamber. Dr. Gay Kendall and Mr. Mark Fleszar (US Army Research Laboratory, Benet Labs, Troy, New York) evaluated several BAM-PPV films on Al and steel coupons. They measured these BAM-PPV coupons using LSCM and coated several BAM-PPV films with CARC coatings and tested them. Dr. Ron Burr and Dr. Wade Popham of MacroSonix Inc. prepared the powder formulations using BAM-PPV. Mr. Mark S. Barilla of the NAVAIR, NADEP, Jacksonville, Florida applied this powder formulation using electrostatic-coating (e-coat).

Dr. Florian Mansfeld and Ms. Esra Kus (USC) used EIS to measure the corrosion performance of BAM-PPV powder coated samples.

Dr. Kenneth J. Wynne (VCU) performed critical studies on BAM-PPV samples for their dissolution and film forming properties in supercritical carbon dioxide ($SCCO_2$) and thermal analysis of BAM-PPV specimens.

Dr. Dennis E. Tallman and Dr. Jie He (North Dakota Sate University) used SVET and ENM spectroscopy to analyze BAM-PPV films and powder coatings in order to evaluate their corrosion protection mechanism.

Dr. Jun Xu of Oak Ridge National Laboratory examined BAM-PPV films on Al substrates using PALS and BDAR spectroscopy.

Dr. Brian C. Benicewicz and Dr. Ru Chen (RPI) worked on the synthesis, characterization and preparation of films using alternative EAP polymers based on oligomers of polyaniline.

Section IV

Executive Summary:

The aerospace industry and DoD currently enhance the corrosion resistance and paint adhesion performance of aluminum alloys with hexavalent-chromium (Cr(VI)) based pretreatments. These pretreatments are known as chromate conversion coatings (CCC) and are used to treat aluminum alloys such as 7075-T6, 7075-T3 and 2024-T3. Chromate conversion coatings are applied by either immersion, spray or wipe techniques that produce a thin coating that is inexpensive and extremely robust.

However, hexavalent chromium has been identified as a health threat, and is a known carcinogen. Due to its toxicity, it is currently highly regulated and the introduction of new, lower OSHA permissible exposure limits (PEL) will greatly reduce the levels of Cr(VI) allowed to be discharged into the industrial environment. Therefore, chromate-free coatings are needed that exhibit equal or superior corrosion protection, while reducing or eliminating volatile organic compounds (VOCs) and hazardous air pollutants (HAPs).

Electroactive polymers (EAPs) coatings have demonstrated corrosion protection even when the coating is scratched and exposed to aqueous salts and hydrochloric acid. EAP based polymer coatings are robust materials that are environmentally benign. A comprehensive study of EAP coatings, including synthesis, scale-up, benign coating formulations, testing in accelerated weathering chambers and an examination of their corrosion protective mechanisms has been carried out during this study. These novel EAPs are now potential candidates to replace CCC. In addition, these new EAP coatings have been incorporated into military coating systems using non-chrome primers and topcoats. Thus, potentially providing the DoD community a replacement for chromate containing military coating systems.

The objectives of this SERDP program (WP 1148) have been completed successfully. The synthesis, scale-up and characterization of new monomers based on a bis-amino derivative of poly-*p*-phenylene vinylene (PPV) called poly(2,5-bis(N-methyl-N-hexylamino)phenylene vinylene, (BAM-PPV) and oligomers of polyaniline have been completed. These polymers have been thoroughly characterized using advanced spectroscopic and analytical methods. The details regarding the EAP synthesis has been published in the literature for duplication including potential industrial use. BAM-PPV has been processed using a variety of conditions including both high VOC and zero VOC processing conditions. Initial studies focused on xylenes as a processing solvent with good quality films being produced. Further studies using *d*-limonene, a commercial food and cosmetic additive (environmentally friendly and zero HAP) as the processing solvent also produced high quality films. BAM-PPV pretreatment coating on Al 2024-T3 processed from both of these solvents passed 336 hours neutral salt fog exposure. This test is required for new pretreatment coatings on aluminum alloys. Additional pretreatments were also studied including trivalent chromium pretreatment (TCP). BAM-PPV coatings in several cases exceeded the 336 hour requirement. BAM-PPV has also been incorporated into full military coating systems that include non-chrome primers and topcoats. These coatings have been tested against known controls such as chromium primers and TCP pretreatment with non-chrome primer and topcoat. BAM-PPV performed as well as the TCP pretreatment with non-chrome primer and topcoat. However, in both cases, each coating did not pass the 2000 hours neutral salt fog exposure test. When BAM-PPV was used with chromium primer and topcoat, this coating system lasted over 4000 hours in a neutral salt fog chamber. Additionally, BAM-PPV has been incorporated into a zero VOC powder formulation and has matched a commercial

polyester powder resin (control) performance in neutral salt fog. Both the BAM-PPV powder coating and the control failed at 1500 hours in neutral salt fog. Oligomers of aniline have been attached to methacarylate and acrylate backbones and polymerized. The coatings based on polyaniline, however, did not pass neutral salt fog testing, failing before 336 hours.

BAM-PPV coatings were investigated in several ways to help elucidate the mechanism of corrosion protection. Studies by electrochemical noise methods (ENM,) scanning vibrating electrode technique (SVET) and X-ray photeoelectron spectroscopy (XPS) showed evidence that BAM-PPV provides more than simply barrier protection to corrosive environments. The mechanism includes barrier protection and may passivate the metal surface during exposure to corrosive environments. This evidence is demonstrated by spontaneous oxidation/doping, rendering the polymer sufficiently conductive to mediate electron transfer from the metal/polymer interface to polymer/solution interface. The corresponding electronic or electrochemical interaction between the polymer and the metal may provide evidence for the passivation of the metal.

The results to date (summarized below) demonstrate that the program has achieved the objectives of the NAWCWD team. The objectives of this program include the following;

- The new EAP polymeric materials that contain no heavy metals (Cd, Cr, Ni, Zn, Cu, etc.).
- BAM-PPV was successfully scaled up to the kilogram quantity and the synthesis was improved for potential industrial production.
- New and known EAP monomers (BAM-PPV and oligomers of aniline), polymers and co-polymers were processed to produce thin films on aluminum and steel substrates.
- Solution spraying produced uniform, non-porous, dense films that provided the minimum barrier protection for corrosive environments.
- EAPs were coated onto various substrates using benign coating processes.
- BAM-PPV powder can be coated onto aluminum and steel substrates using a variety of coatings processes. These processes included solvent based and environmentally friendly solvents. Additionally, zero VOC powder coatings incorporating BAM-PPV as the corrosion inhibitor were prepared. BAM-PPV was solvent sprayed onto aluminum alloys and non-chromium primers or chromium primers and topcoats added using standard DoD equipment currently used at NAWCAD.
- BAM-PPV has successfully passed the 336 hours neutral salt fog exposure test as a viable alternative to CCC.
- BAM-PPV has shown both barrier and may passivate the metal surface during exposure to a corrosive environment.
- BAM-PPV has been transitioned into a demonstration/validation program (Environmental Security Technology Certification Program, ESTCP).
- The program has produced 26 publications in the open literature and several patent disclosures (see Appendix B).
- This SERDP program has also supported one graduate student (FY00-04) and two post-doctoral students (FY03-04).

In conclusion, the program has resulted in the acquisition of both basic and applied knowledge regarding synthesis, scale-up, coating processing and performance of EAP polymers used in corrosive environments. The application of this knowledge is enabling the transition of the technology to fleet-wide use under the ESTCP program (FY05-08).

Section V

Objective: This SERDP project (WP1148) addressed the environmental limitations of current corrosion-protection coatings that use hexavalent chromium in the pretreatment and/or in primers. The objectives of the research were fourfold: a) to synthesize, characterize and scale-up novel electroactive polymers (EAPs); b) apply films of these EAPs onto aluminum and steel substrates via environmentally friendly applications; c) to test these coatings in accelerated weathering chambers and to measure their performance against known standards and 4) understand the mechanism by which these novel EAPs can retard or inhibit corrosion when exposed to corrosive environments.

Section VI

Background: Corrosion protection using current barrier coating systems have been found to be deficient in the areas of pitting, stress and intergranular corrosion. Pitting corrosion on Department of Defense (DoD) aircraft has been observed on aluminum skins surrounding steel fasteners, aluminum substructures bolted onto graphite epoxy substrate materials, honey comb structures consisting of aluminum-titanium alloys and aluminum facesheets bonded structures. Stress corrosion cracking on aluminum forgings and intergranular corrosion of 7075 T6 alloys (thick sections) found on the wings of DoD aircraft and lockjoints has also been observed. The aerospace and DoD currently enhance the corrosion resistance and paint adhesion performance of aluminum alloys with hexavalent-chromium (Cr(VI)) based pretreatments.[1] For years these chromate-containing coatings have been used to treat aluminum alloys such as 7075-T6, 7075-T3 and 2024-T3. Many DoD platforms such as the F-18, F-16, F-22, Joint Strike Fighter, MV-22, CV-22, H-60, C-141, C-130, C-5 and P-3 Orion aircraft use these chromium treated alloys. These pretreatment coatings are applied by immersion, spray and wipe techniques that produce a thin coating that is inexpensive and an extremely flexible process.[2]

However, hexavalent chromium has been identified as a health threat, and is a known carcinogen.[3] Due to its toxicity, is currently highly regulated.[4] Potentially new EPA regulations governing air emissions and lower OSHA permissible exposure limits (PEL) will greatly reduce the levels of Cr(VI) allowed to be discharged into the industrial environment where workers will risk exposure to this known carcinogen.[5] Therefore, chromate-free coatings are needed that also exhibit equal or superior corrosion protection. Disposal costs for hazardous waste generated from painting and depainting operations continue to soar. All three of the armed services have seen a significant increase in disposal costs associated with this waste generation. In order to meet new federal/state environmental and OSHA regulations, and to protect worker safety, alternative-coating systems that reduce or eliminate volatile organic compounds (VOCs) and hazardous air pollutants (HAPs) are urgently needed.

Additionally, current corrosion inhibitor paint chemistry for aluminum alloys relies on the extensive use of Cr(VI) such as strontium or barium chromate.[6] Strontium and/or barium chromate are incorporated into primers as highly effective corrosion inhibitor additives which provide excellent resistance even if the paint system has been subjected to mechanical damage. Several current military coating systems used on aluminum alloys for corrosion resistance containing chromates are shown in Table 1. As formulation technology has moved toward environmental compliance, current environmentally compliant coatings systems have performed less than satisfactory.

Table 1: Military Coatings Specifications
(All coatings systems listed below contain chromates)

MIL-Spec	Description
TT-2756	solvent based PUR self-priming topcoat
TT-P-2760	solvent based polyurethane flexible primer
MIL-PRF-85582, Type II, Class C2	water reducible epoxy primer strontium chromate based
MIL-PRF-23377G Type 1, Class C	solvent based epoxy primer strontium chromate based
DOD-P-15328	wash pretreatment (primer)
DOD-P-5541 MIL-C-81706	chromate conversion coating chromate conversion coating

Corrosion costs associated with corrosion prevention and/or correction of corrosion generated failures accounts for approximately 25% of the armed services annual maintenance budgets.[7] The costs associated in this 25% figure includes compliance with new environmental regulations regarding hazardous waste generation. These costs have risen dramatically over the past several years and as high as 20% in some DoD facilities. This increase accounts for a significant portion of non-compliance with new environmental regulations, systems down-time and failure of mission readiness.

Recently, new concepts based on EAP [also sometimes referred to as conductive or conjugated polymers (CP)] coatings such as polyaniline for corrosion inhibition have been proposed and tested.[8] These EAP coatings have demonstrated corrosion protection even when the coating is scratched and exposed to aqueous salts and hydrochloric acid.[9] Several researchers have demonstrated and proved with quantitative evidence that corrosion inhibition on metal alloy substrates is scientifically feasible and practical.[10-15] EAP based polymer coatings have recently shown evidence to meet the military pretreatment requirement as a viable alternative to Cr(VI) pretreatments.[16] From this solid scientific foundation our efforts have focused on using novel EAP coatings as replacements for CCCs.

Section VII

The SERDP Program (PP1148) was funded from FY00-04 and will be presented in Sections VII A-C and VIII A-C by each corresponding funding period.

SECTION VIIA-Synthesis and Characterization of EAP Materials

SERDP FY00

Materials:

Dimethyl-1,4-cyclohexanedione-2,5-dicraboxylate was obtained from ACROS Organics and used as received. Tetrahydrofuran (THF), methanol, n-hexylamine, bromine (Br_2), sodium hydride (NaH), thionyl chloride ($SOCl_2$) and diisobutylaluminum hydride solution (DIBAL-H) were purchased from Aldrich Chemical Co. and used as received.

General Analytical Methods:

^1H and ^{13}C NMR data was acquired using a Bruker 400MHz NMR spectrometer at 300K. The FTIR spectrum was collected using a Nicolet Nexus 870 FTIR spectrometer with a liquid nitrogen cooled MCT detector. The spectrum is an average of 100 scans with 4 cm^{-1} resolution. The polymer film was placed in contact with a Germanium crystal on a "Thunderdome" attenuated total reflectance (ATR) accessory. Melting points (mp) were taken with a Melt-Temp apparatus and are uncorrected.

Methods:

Synthesis Section:

The first phase of this program (FY00) was to scale-up the synthesis of poly(2,5-bis(N-methyl-N-hexylamino)phenylene vinylene (BAM-PPV). The BAM-PPV compound was prepared in milligram and gram quantities prior to the start of the SERDP WP1148 program and was tested for corrosion prevention on Al 2024-T3 alloy in simulated seawater.[17, 18]

The monomer and polymer synthesis are shown in Scheme I and is a scale-up of the original BAM-PPV synthesis. During FY00, the BAM-PPV synthesis was produced in the hundreds of gram quantities.

Scheme I: Original Synthesis of BAM-PPV

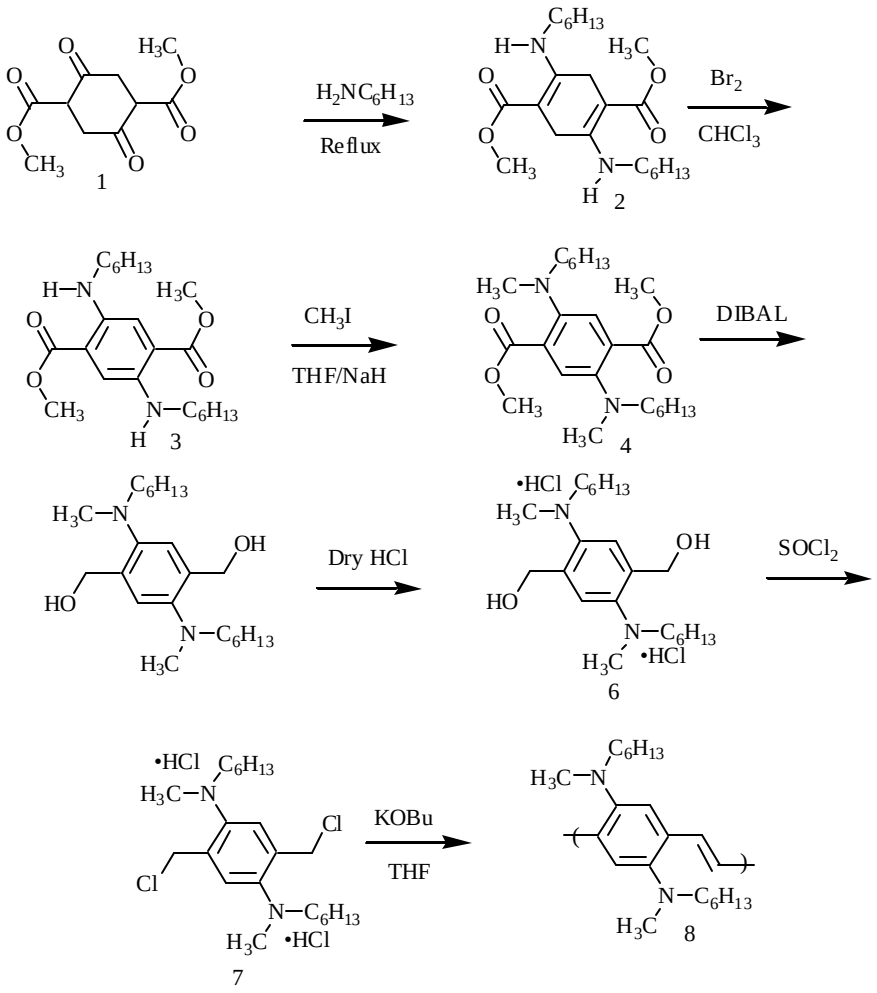

Compound 2: Methyl-2,5-Bis(hexylamino)-4-(methoxycarbonyl)cyclohexa-1,4-diene Carboxylate: Into a round bottom flask was added 1100g (4.82mol) of dimethyl-1,4-cyclohexanedione-2,5-dicarboxylate (Compound 1) and 11L methanol. To this suspension was added 1.267 L of n-hexylamine. The mixture was refluxed overnight @ 65°C. An orange-yellow precipitate was observed and the contents cooled to room temperature. The suspension filtered, and the residue washed with ether. The product was dried overnight under vacuum and the crude product was recrystallized from methanol/methylene chloride mixture (8:1). The yield was 1755g (91%) of orange crystals: mp = 120-122°C. ^{1}H NMR ($CDCL_3$): 8.8, m, 4H; 3.65, s,6H; 3.21, t, 4H; 1.5, m, 4H; 1.35,m(br), 12H, 0.9, t, 6H.

Compound 3: Methyl-2,5-Bis(hexylamino)-4-(methoxycarbonyl)benzoate: Into a round bottom flask was added 1755g (4.45 mol) of compound 2 and 10L of methylene chloride. To this solution was added 713g of bromine drop wise. The color changed from orange-red to yellow-orange. The contents were refluxed for 5 hours and cooled to room temperature. The solution was poured into 5L of an aqueous solution of sodium carbonate. A red slurry appeared and separated from the aqueous phase. The aqueous phase was extracted twice with

dichloromethane. The combined organic phases were filtered and the filtrate was rotovapped and dried overnight under vacuum. The crude product was recrystallized from a mixture of methanol/methylene chloride (2:1). The yield was 1200g (69%): mp = 104-105°C. ^{1}H NMR (CD_2Cl_2): 7.28, s, 2H; 3.86, s, 6H; 3.14, t, 4H; 1.62, m, 4H; 1.36 m(br), 12H; 0.91, t, 6H.

Compound 4: Methyl-2,5-Bis(hexylmethylamino)-4-(methoxycarbonyl)benzoate: Into a round bottom flask was added 1200g (3.06 mol) of compound 3. Approximately 694g (17.3 mol) of sodium hydride and 6L of dry THF was then added to the round bottom flask. The mixture was stirred for 2 hours and 695 mL (11.2 mol) of methyl iodide was added to the suspension. After all the methyl iodide was added, the red mixture was heated to 58°C overnight. The mixture turned from red to yellow overnight and was cooled to room temperature. NMR verified the completion of the reaction. The mixture was filtered; the residue rinsed with dry THF and the filtrate rotovapped to dryness. The semisolid was redissolved in 4L of hexane, the solution stirred overnight after which 500g silica gel was added. The mixture was stirred overnight and filtered, the residue was rinsed with hexanes and the combined filtrates rotovapped and dried overnight under vacuum. The yield was 931g (72%) of a yellow-orange oil. ^{1}HNMR (CD_2Cl_2): 7.18, s, 2H; 3.58, s, 6H; 2.92, t, 4H; 2.70, s, 6H; 1.49, m, 4H; 1.26, m, 12H; 0.87, t, 6H.

Compound 5: 2,5-Bis(hexylmethylamino)-4-(hydroxymethyl)phenylmethan-1-ol: Into a round bottom flask was added 931 g (2.21 mol) of compound 4 and 1.5L dry THF. 177g lithium aluminum hydride was suspended in THF and compound 4 solution was added slowly to the suspension. After complete of compound 4 solution, the contents were stirred at ambient temperature for 2 days. The reaction was then quenched with 500 mL 4N sodium hydroxide solution. The mixture was filtered, the residue washed with methanol and the filtrate rotovapped and dried for one week. A solid residue was obtained with a yield of 610 g (76%). The product was used immediately for the next step.

Compound 6: 2,5-Bis (hexylmethylamino)-4-(hydroxymethyl)phenyl)methan-1-ol Dihydrichloride: Into a round bottom flask was added 610g (1.67 mol) dissolved in 3L methanol. 150 g dry HCl was bubbled through the solution for 2.5 hours. The solution was stirred while warming to room temperature. The methanol was removed using the rotary evaporator, leaving a semi-solid residue. The residue was dissolved in methanol, then precipitated into 1L of acetone and stirred overnight. The suspension was filtered; the residue washed three times with cold acetone and the residue dried overnight under vacuum. The product was obtained as a white solid in 465g (64%) yield, mp = 146°C (dec). ^{1}H NMR (CD_3OD): 7.98, s, 2H; 5.07, s, 4H; 3.66, t, 4H; 3.34, s, 6H, 1.55 m(br), 4H; 1.30, m(br), 12H; 0.88, t, 6H. ^{13}C NMR (CD_3OD): 145.0, 139.7, 126.8, 66.3, 64.1, 49.7, 35.1, 29.8, 29.2, 26.3, 17.1.

Compound 7: 2,5-Bis(chloromethyl)-4-(hexylmethylamino)-phenyl)hexylmethylamine Dihydrohloride: Into a round bottom flask cooled in an ice-bath was added 465g (1.06 mol) suspended in 3L of methylene chloride . 200 mL Thionyl chloride was added drop wise after 1 hour of reaction time a white precipitate had formed. The white precipitate was filtered and the residue rinsed with dry acetone. The residue was dried overnight under vacuum. The product was obtained as an off-white solid with a yield of 386g (80%). ^{1}H NMR (CD_3OD): 8.13, s, 2H; 5.07, s, 4H; 3.68, t, 4H; 3.33, s, 6H; 1.29, m(br), 12H; 0.87, t, 6H. ^{13}C NMR (CD_3OD): 144.7,

138.3, 128.5, 75.0, 64.7, 51.5, 35.1, 29.7, 29.2, 26.3, 17.1; mp = 156-161^{o}C (dec). Mass spectrometry m/z(HCl comes off under probe conditions):400, 365, 329, 315, 295, 279, 259, 245, 209, 201, 187, 173, 159, 145, 130, 117, 103, 77. Infrared(cm^{-1}): 512, 522, 625, 678, 732, 832, 898, 930, 978, 1103, 1126, 1140, 1200, 1220, 1258, 1274, 1295, 1393, 1408, 1439, 1452, 1468, 1483, 1529, 2433, 1531, 2618, 2854, 2869, 2924, 2946, 2996, 3015, 3168.

Compound 8: Polymer(BAMPPV) : Into a round bottom flask was added 550 g potassium tert-butoxide and 3.5L THF. To this solution was added 386 g (0.8 mol) of compound 7. The suspension was stirred overnight at room temperature. The solution was then quenched with methanol and the suspension filtered. The polymer was dried under vacuum for one day. The crude polymer was purified by extraction with hot methanol and dried to constant weight. Approximately 200grams of polymer was obtained by the above procedure and the ^{1}H (Figure 1) and ^{13}C NMR (Figure 2) of the product are shown below.

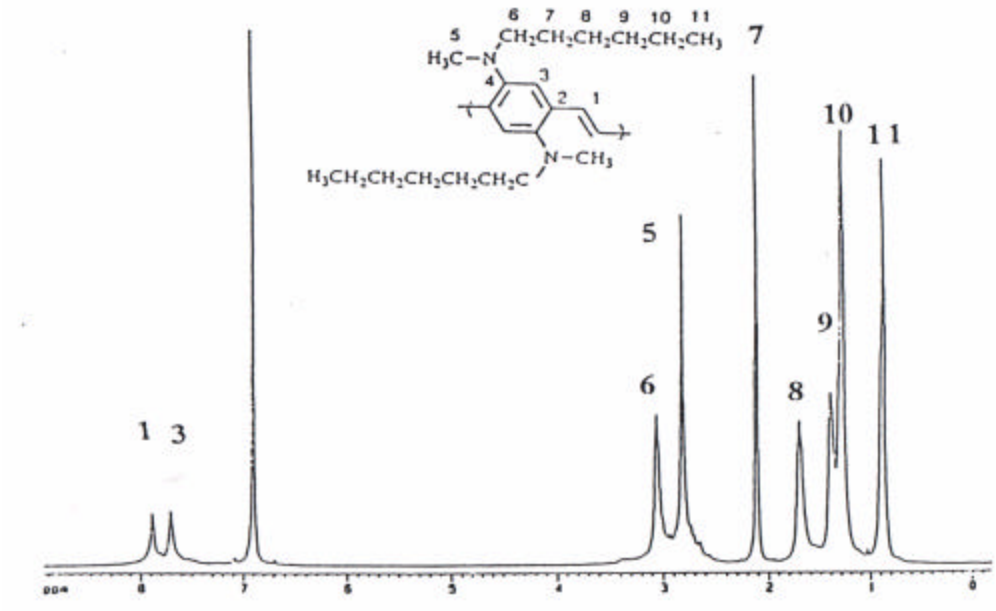

Figure 1: ^{1}H NMR of BAMPPV

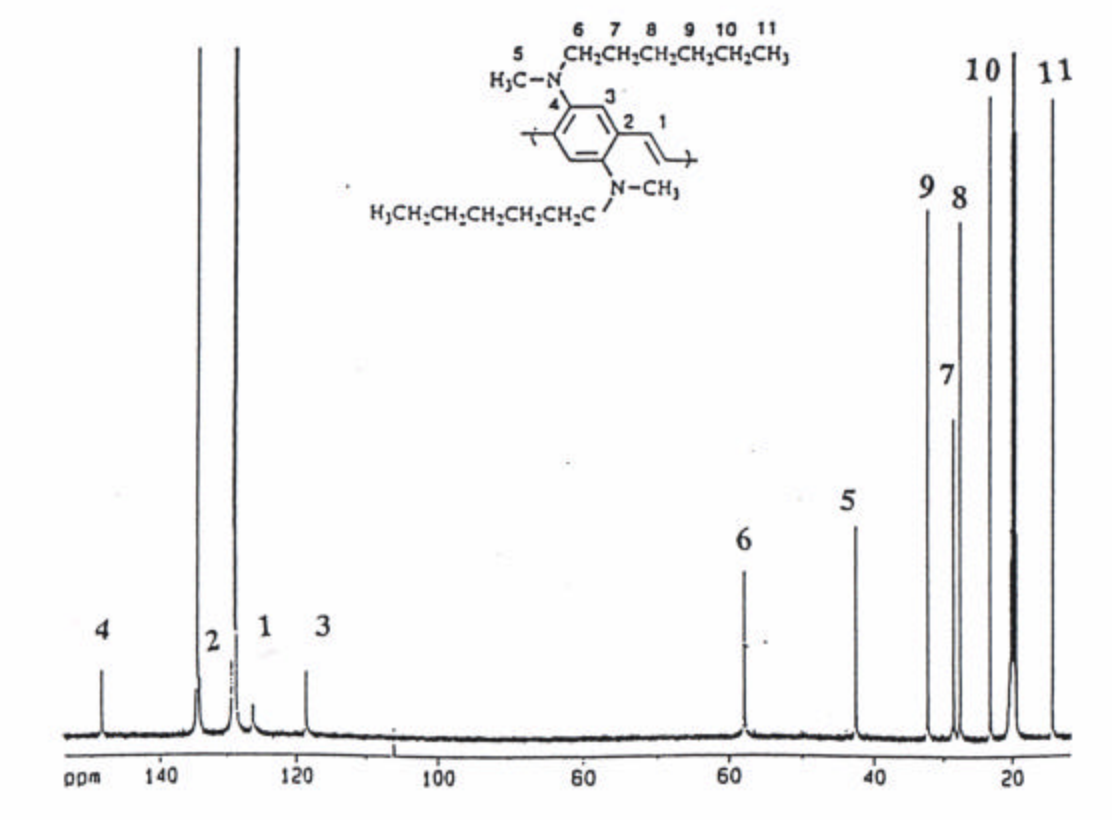

Figure 2: ^{13}C NMR of BAMPPV

SERDP FY01

Materials:

Dimethyl-1,4-cyclohexanedione-2,5-dicraboxylate was obtained from ACROS Organics and used as received. Tetrahydrofuran (THF), methanol, n-hexylamine, household bleach (10 % aqueous sodium hypochlorite (NaOCl)) obtained from K Mart, NaH, $SOCl_2$ and lithium aluminum hydride ($LiAlH_4$) were purchased from Aldrich Chemical Co. and used as received.

General Analytical Methods

^1H and ^{13}C NMR data was acquired using a Bruker 400MHz NMR spectrometer at 300K. The FTIR spectrum was collected using a Nicolet Nexus 870 FTIR spectrometer with a liquid nitrogen cooled MCT detector. The spectrum is an average of 100 scans with 4 cm^{-1} resolution. The polymer film was placed in contact with a Germanium crystal on a "Thunderdome" attenuated total reflectance (ATR) accessory. MP's were taken with a Melt-Temp apparatus and are uncorrected.

Methods:

Synthesis Section:

The second phase of this program during FY01 was to continue the scale-up of BAM-PPV to the kilogram quantity. The monomer and polymer new synthesis is shown in Scheme 2 and represented a dramatic scale-up in quantities produced from FY00.

Scheme 2: Scale Up of BAM-PPV (New Synthesis Route)

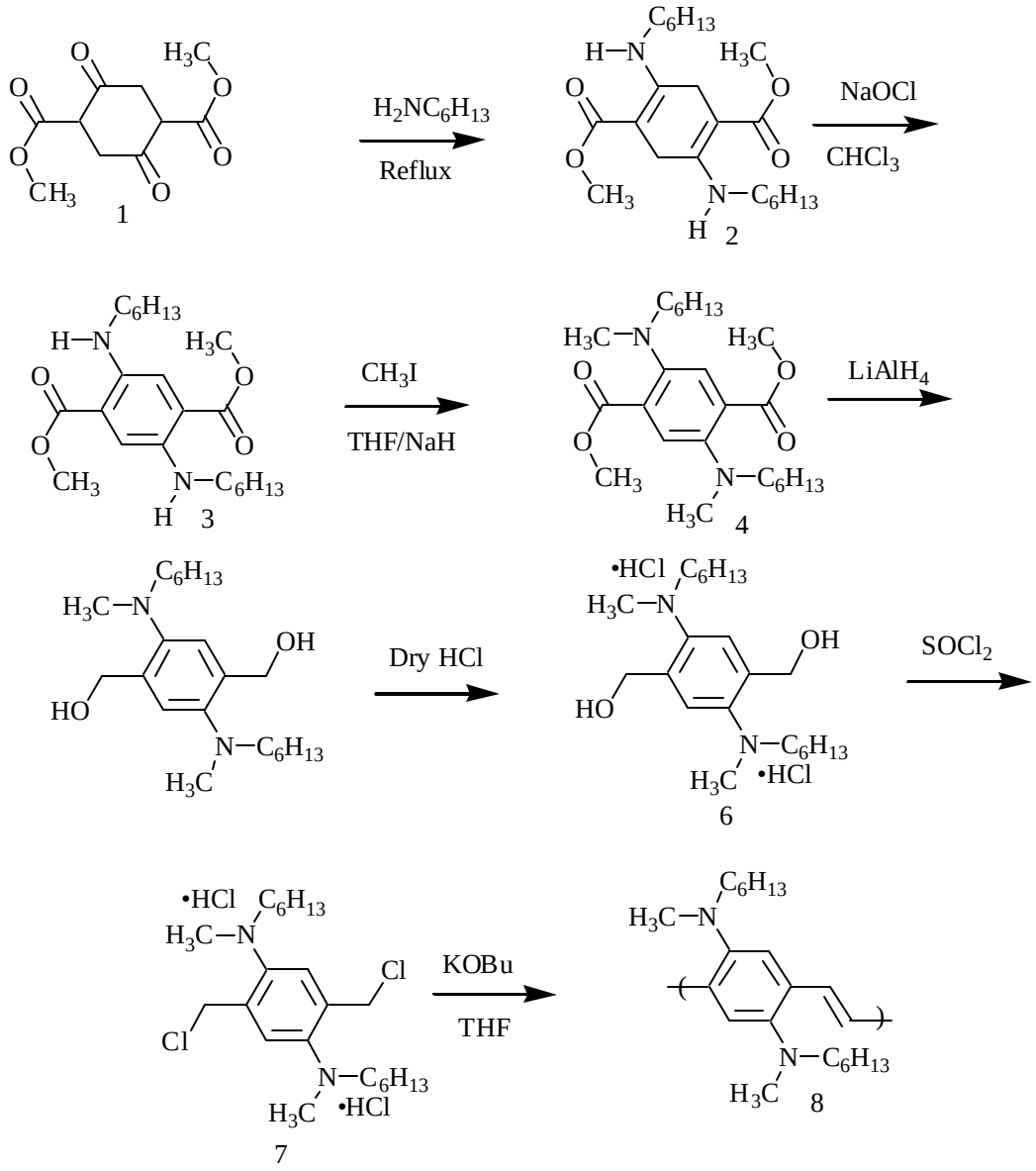

Compound 2: Synthesis of 2,5-bis(N-hexylamino)-cyclohexa-1,4-diene carboxylic acid methyl ester

Dimethyl-1,4-cyclohexanedione-2,5-dicarboxylate (compound 1, 2499g, 11mol) was added to 12L methanol in a 20L reaction vessel. *n*-Hexylamine (2.6L) was added drop wise. The mixture was heated at reflux overnight. The product, a pink-orange solid, was collected by vacuum filtration and rinsed with methanol. The product, 2,5-bis(N-hexylamino)-cyclohexa-1,4-diene carboxylic acid methyl ester (compound 2), was dried under vacuum over night. The product was verified by ^{1}H NMR (Figure 3). Average yield: 74%.

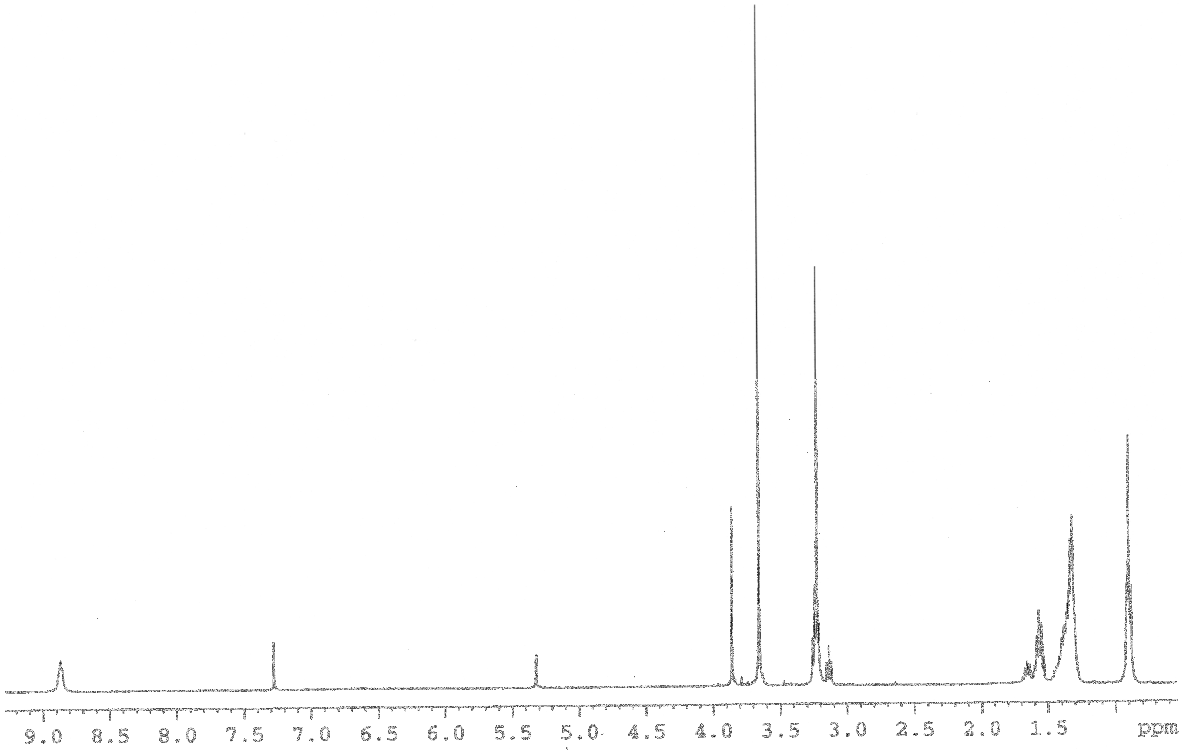

Figure 3: ^{1}H NMR of Compound 2

Compound 3: Synthesis of 2,5-bis(N-hexylamino)terephthalic acid dimethyl ester

The aromatization step in the scale-up synthesis was done using a synthesis route developed by The Spectra Group, Inc. under a Small Business Innovative Research (SBIR) Program. The SBIR resulted in the replacement of bromine with sodium hypochlorite (household bleach), a safer reactant. A typical batch involved the addition of 1053g of compound 2 to 4L methylene chloride in an open 5 gallon reactor. After the mixture was cooled to 0°C, one gallon of 10% sodium hypochlorite solution was added drop wise. The reaction mixture was allowed to warm to ambient temperature while stirring overnight. After several hours of stirring in the open reactor, the majority of the methylene chloride was evaporated. The

resulting viscous red mixture was then rinsed with hexanes to obtain 1493g of a red crystalline product, 2,5-bis(N-hexylamino)terephthalic acid dimethyl ester (compound 3). The product was verified by ^{1}H NMR (Figure 4). Subsequent batches were produced in the same way with the exception of using methanol to precipitate and rinse the product. Average yield: 74%.

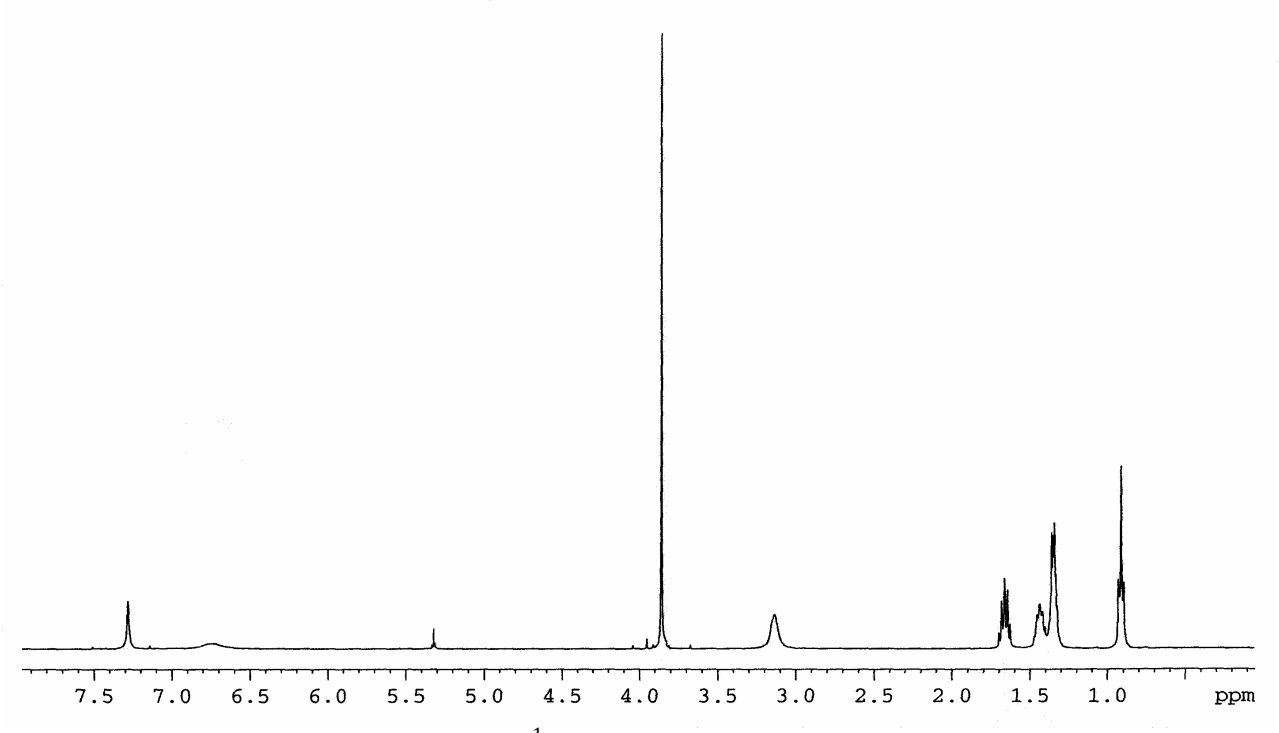

Figure 4: ^{1}H NMR of compound 3

Compound 4: Synthesis of 2,5-bis(N-hexyl-N-methylamino)terephthalic acid dimethyl ester

The methylation step was also performed in multiple batches. Compound 3 (1544g, 3.9mol) was added to a 22L reaction vessel containing 8L tetrahydrofuran. Sodium hydride (758g, 19mol) in oil was rinsed with hexanes and added to the reaction vessel and allowed to stir for 1h. Iodomethane (500mL) was added to reactor drop wise, while the reaction was kept under a nitrogen purge. The reactor temperature was then set to 60°C for 16h. Hexanes (4L) were added to the reactor and stirred overnight. The reaction mixture was then filtered through Celite, and solvent was removed under reduced pressure, yielding the dark brown oil 2,5-bis(N-hexyl-N-methylamino)-terephthalic acid dimethyl ester (compound 4). Completion of the reaction was verified by ^{1}H NMR (Figure 5) and GC-MS. Average yield: 68%.

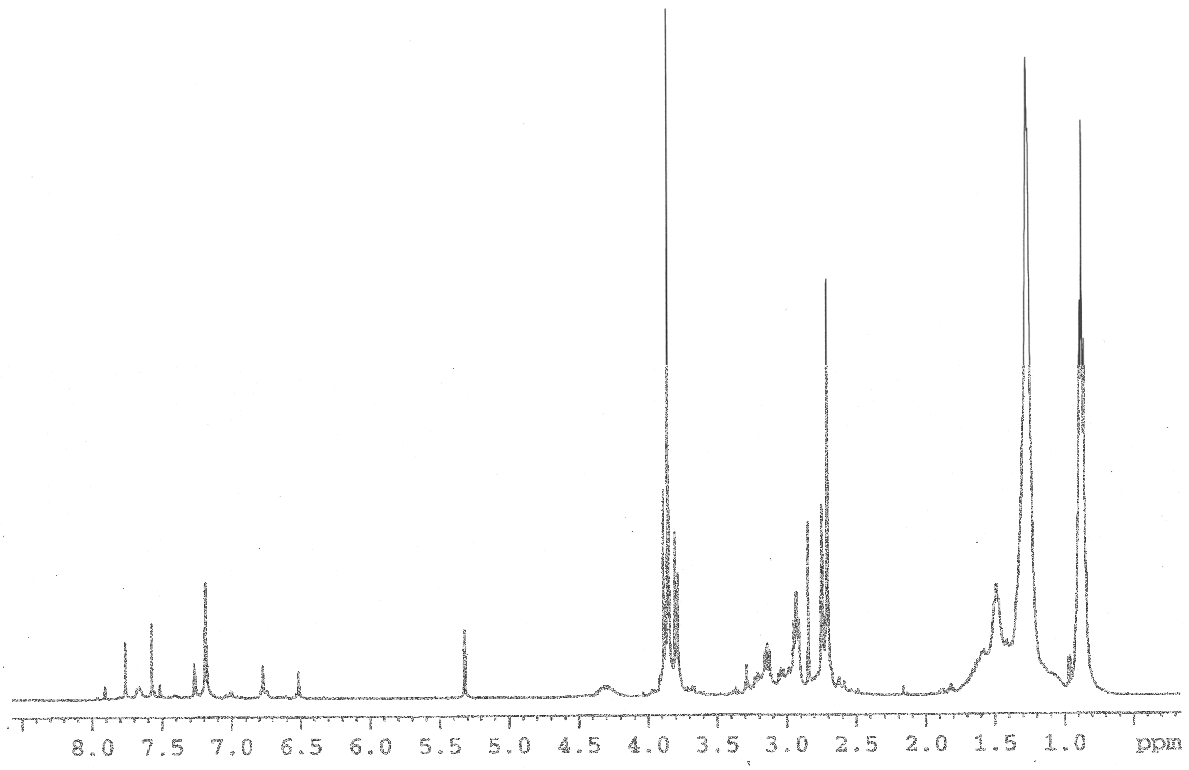

Figure 5: ^{1}H NMR of compound 4

Compound 5: Synthesis of

2,5-bis(N-hexyl-N-methylamino)-1,4-bis(hydroxymethyl)benzene

The reduction step was done in multiple batches using a 22L reaction vessel. $LiAlH_4$, (110g) was added to 9L tetrahydrofuran that had been cooled to 7°C (under nitrogen). Compound 4 (1054g) was added drop wise. The reaction mixture was heated at 40°C for 16h with stirring under nitrogen. The reaction was then quenched with 4M NaOH (300mL) and filtered through Celite. The organic layer was isolated, and solvent was removed under reduced pressure to yield a viscous brown oil, 2,5-bis(N-hexyl-N-methylamino)-1,4-bis(hydroxymethyl)benzene (compound 5). Completion of the reaction was verified by ^{1}H NMR (Figure 6). Average yield: 90%

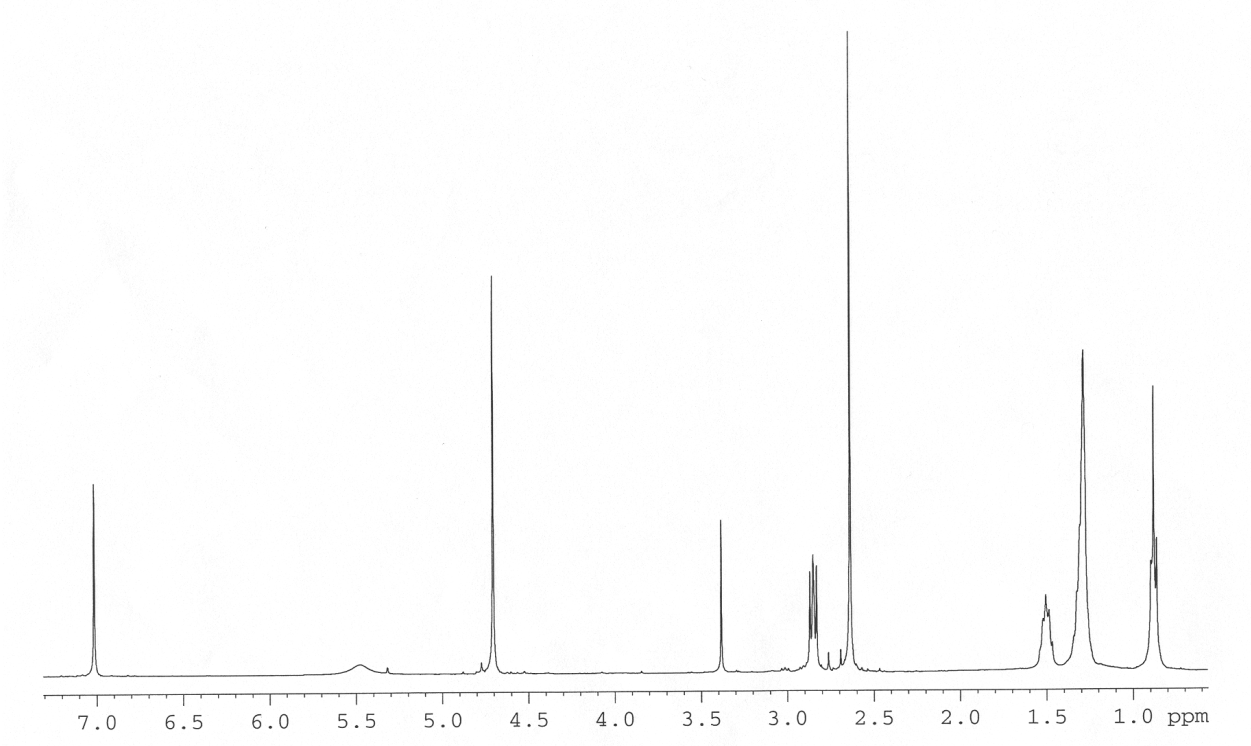

Figure 6: ^{1}H NMR of compound 5

Compound 6: Synthesis of
2,5-bis(N-hexyl-N-methylamino)-1,4-bis(hydroxymethyl)benzene dihydrochloride

The formation of the HCl salt was accomplished in multiple batches using a 4L reaction vessel. Compound 5 (1021g, 2.3mol) was added to 3L methanol. While stirring and under nitrogen, 247g (6.9mol) HCl was bubbled into the solution. The reaction was complete after 2h. The product, an off-white solid, was precipitated and rinsed with cold acetone, the dried overnight under vacuum to yield 2,5-bis(N-hexyl-N-methylamino)-1,4-bis(hydroxymethyl)benzene dihydrochloride (compound 6). Completion of the reaction was verified by ^{1}H NMR (Figure 7). Average yield: 35%.

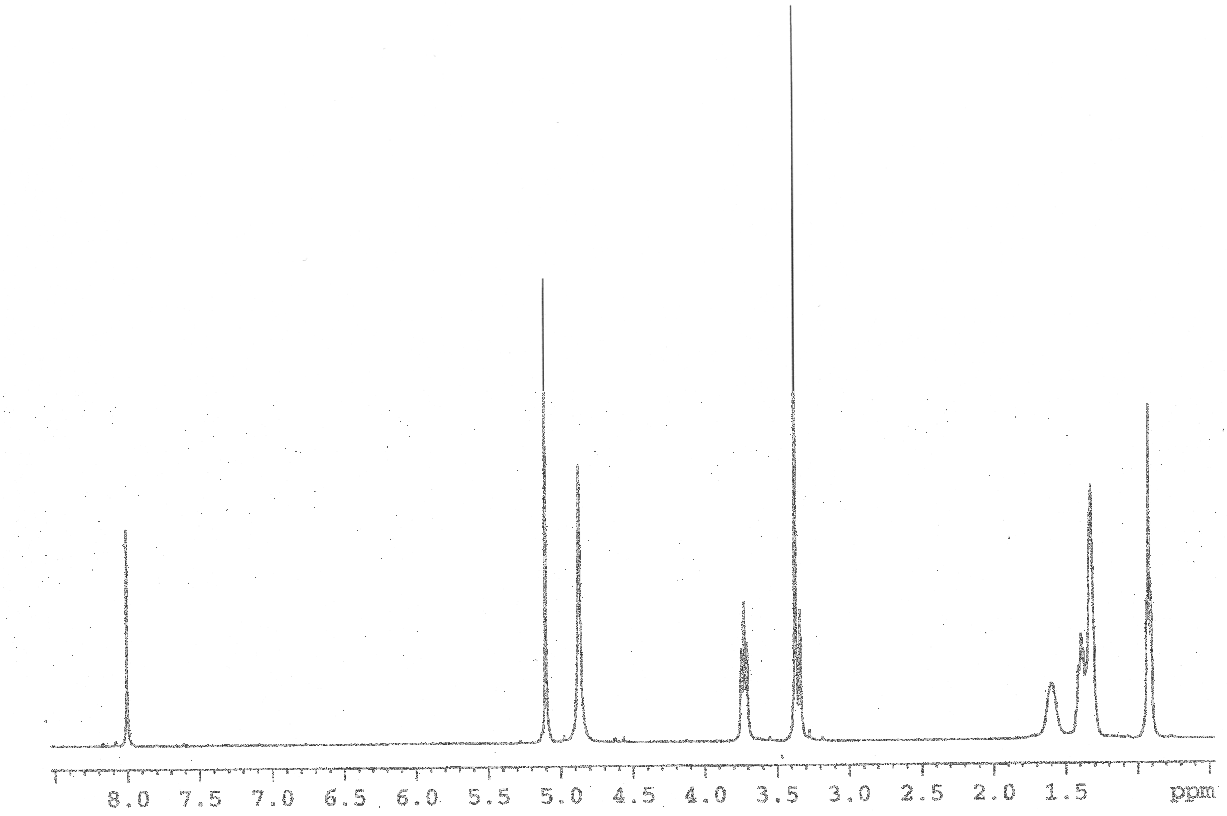

Figure 7: ^{1}H NMR of compound 6

Compound 7: Synthesis of
2,5-bis(N-hexyl-N-methylamino)-1,4-bis(chloromethyl)benzene dihydrochloride

The chloromethylation step was performed in multiple batches using 1- and 2L reactors. A typical 1L reaction consisted of the addition of 197g (0.45mol) of compound 6 to 700mL thionyl chloride at 0°C. The thionyl chloride was removed under vacuum. The resulting solid had a slight purple tint. The solid was dissolved in methanol and precipitated from acetone. A white solid, 2,5-bis(N-hexyl-N-methylamino)-1,4-bis(chloromethyl)benzene dihydrochloride (compound 7) was obtained. Completion of the reaction was verified by ^{1}H NMR (Figure 9). Yield: 75%.

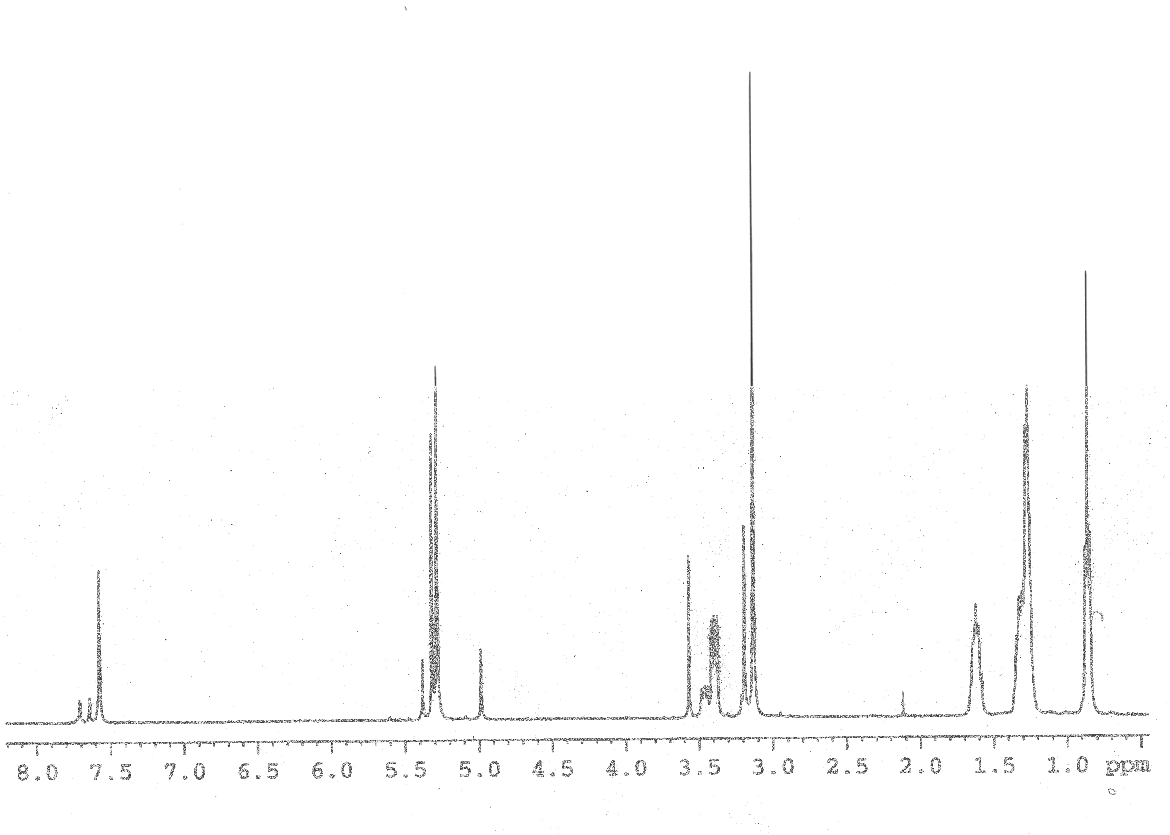

Figure 8: ^{1}H NMR of compound 7

Compound 8: Synthesis of BAM-PPV

The polymerization was performed at –45°C in a solvent mixture of 50% toluene and 50% THF by volume. Into a total of 3L of cooled solvent, 50g (0.11mol) of monomer (compound 7) was added and dissolved. Potassium *t*-butoxide (105g, 0.94mol) was then added incrementally. The reaction was kept between –50°C and –40°C for 2h. The reaction was allowed to warm to room temperature overnight while stirring under nitrogen. The orange polymer, now a gelatinous mass, was collected and precipitated into room temperature methanol. To purify the product, the polymer was dissolved into xylenes and reprecipitated into methanol, repeatedly. The polymer, BAM-PPV (compound 8), was verified by ^{1}H and ^{13}C NMR (Figure 9). Yield: 84%.

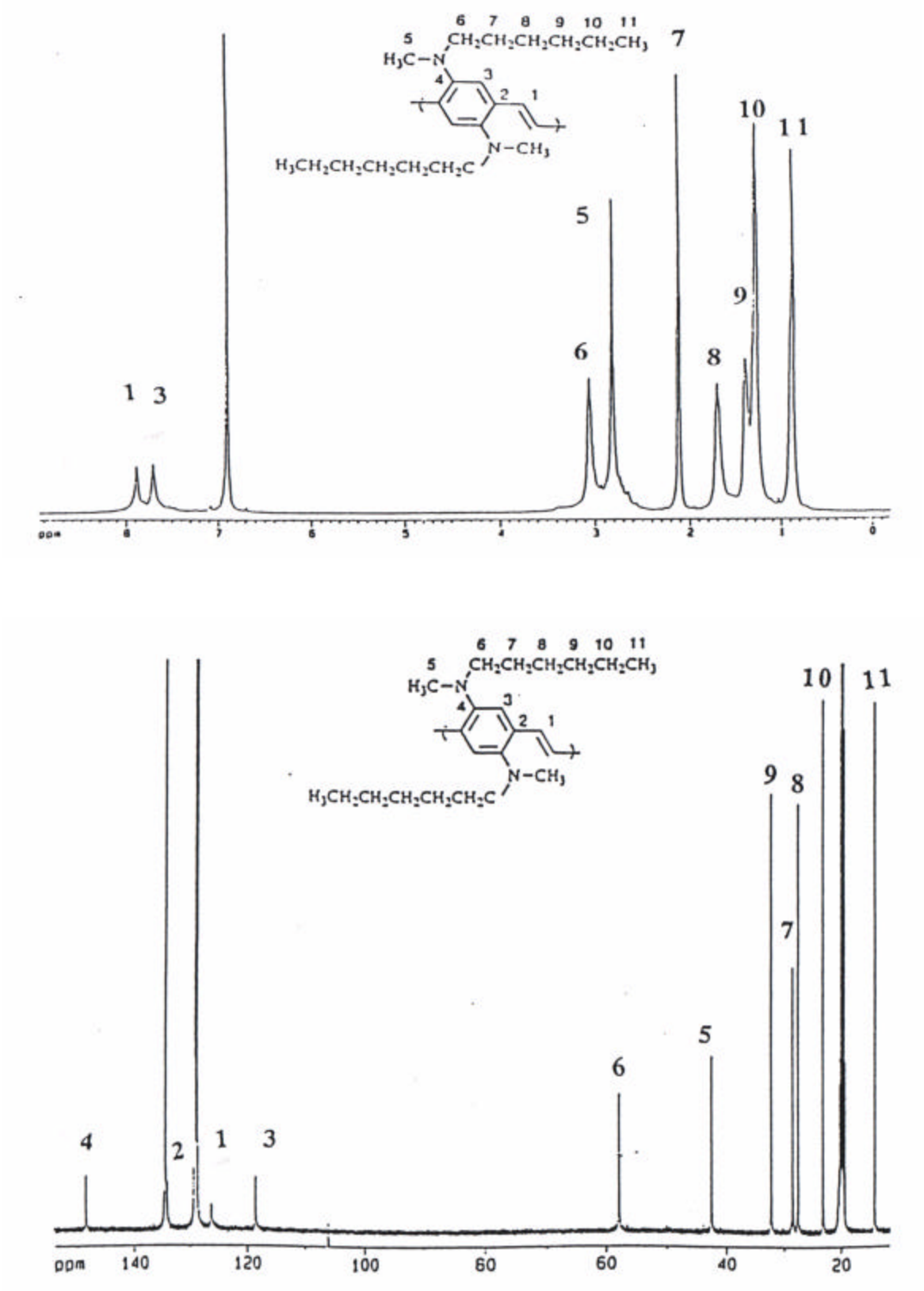

Figure 9: ^{1}H NMR (top) and ^{13}C NMR (bottom) of BAM-PPV, compound 8

Alternate 3-Step Synthesis Route to produce BAM-PPV:

In order to reduce the number of steps (and cost) of BAM-PPV, we tried to devise a three-step synthesis (Scheme 3). The first step relies on new catalyst technology enabling an aryl halide to be coupled to an alkyl amine. The catalyst and required ligand are now commercially available and the starting aryl halide is inexpensive. We have been able to synthesize this material in a 77% yield with only trace quantities of the mono-substituted compound. Both ^{13}C and ^{1}H NMR are in agreement with the desired structure. The second step involves the selective chlorination at the two benzylic sites. This process failed to yield the desired results and alternative methods were tried but unsuccessfully.

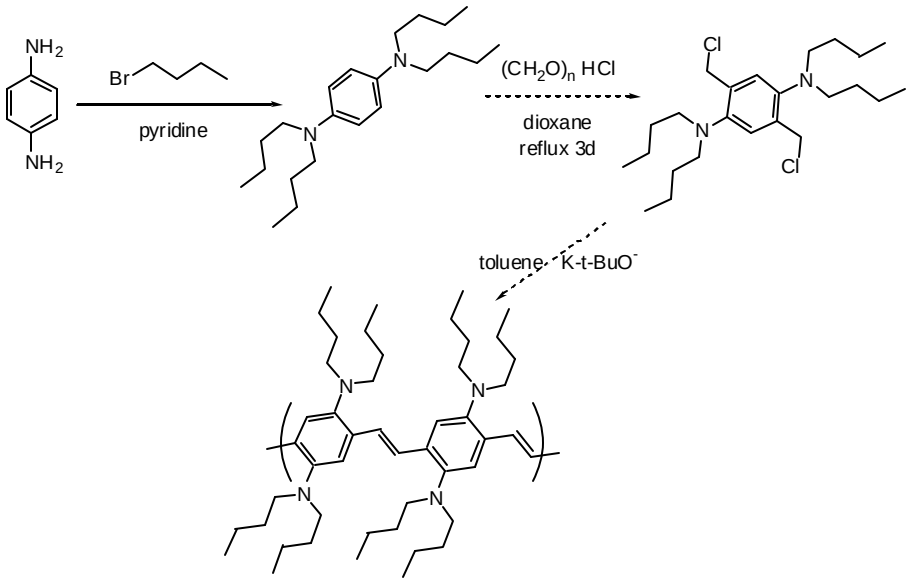

Scheme 3: Proposed three-step route to BAM-PPV

Alternate 4-Step Synthesis Route to produce BAM-PPV:

Another synthesis effort is also underway to produce BAM-PPV. The following 4-step synthesis (Scheme 4) was investigated on a 25 gram scale. To date, the first step of the reaction has been completed; and the product was purified. Further attempts to produce the final desired product were also unsuccessful.

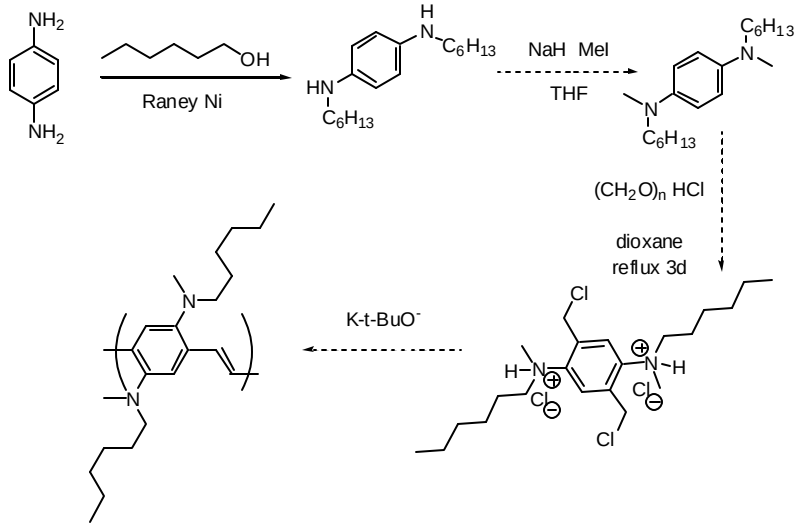

Scheme 4: Proposed four-step route to BAM-PPV

WAM-PPV Synthesis

A number of attempts were made to synthesize water-borne BAM-PPV polymers based on the nickel-catalyzed amination (Buckwald chemistry) as in the three-step synthesis method (Scheme 5). None of the routes shown below were able to produce significant quantities of the desired products. An example of this type of reaction follows: A 50mL Schlenk tube was dried for 2h in an oven at 120°C. The dried Schlenk tube was cooled to ambient temperature, and the tube was charged with 0.50g (3.4mmol) dichlorobenzene, 2.41g (4.08mmol) bis-2-[2-(2-methoxyethyoxy)-ethoxy]ethylamine, 0.031g $Pd_2(dba)_3$, 0.020g ligand (2-dicyclohexylphosphine-2'-[N,N-dimethylamino]-biphenyl), 0.46g NaO-*t*-butoxide and 5.0mL dry toluene. The contents were stirred at ambient temperature for 3h under positive nitrogen flow. The reaction flask was heated at 80°C for 48h, then the solution was allowed to cool to ambient temperature, and 30mL dry ether was added. The suspension was filtered through Celite, and the filtrate was concentrated under vacuum to yield an oil. ^{1}H NMR showed only starting material; none of the desired product was detected.

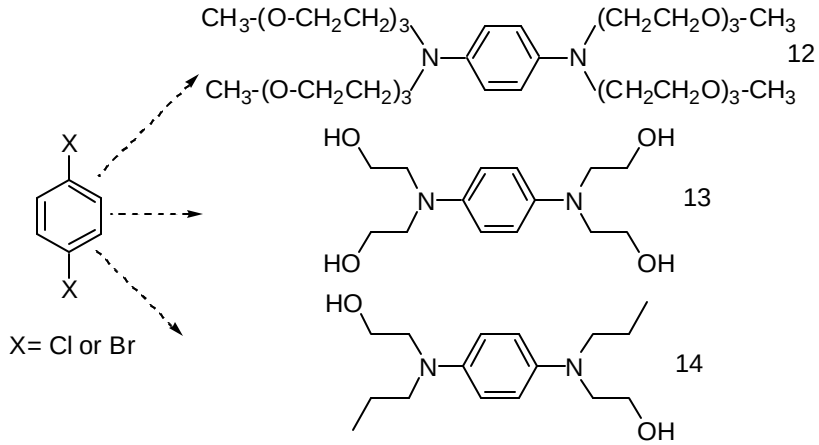

Scheme 5: Attempted syntheses of water-borne BAM-PPV monomers based on Buckwald chemistry

EAPs based on Oligomers of Polyaniline:

Rensselaer Polytechnic Institute (RPI), Troy, New York began the synthesis of a series of vinyl monomers with oligoaniline side chain functionality during FY00/01. Homopolymers and copolymers with widely used co-monomers in latex paint formulations are prepared by free radical polymerization. The combination of a flexible backbone with the aniline side chain allows easy control of polymer electroactivity and overall properties, such as glass transition temperature, adhesion to metal surfaces, and film forming ability. Following the synthesis and screening of several classes of related monomers and polymers, several candidates were selected for scale-up and corrosion testing. Initial work on this project is focused on the synthesis and characterization of monomers and testing their ability to polymerize by conventional radical polymerization methods. Figure 10 show the complete list of monomers prepared during FY01. The complete details of their synthesis are given below in the monomer synthesis section.

Materials:

α, α –Azobis(isobutyronitrile) (AIBN), N-phenyl-*p*-phenyldiamine, acetic anhydride, dimethylformamide (DMF), nickel (II) chloride hexahydrate ($NiCl_2*6H_2O$) potassium hydroxide, zinc chloride, THF, di-*tert*-butyldicarbonate, (4-dimethylamino)pyridine, sodium-*tert*-butoxide, palladium(II) acetate, and ammonium formate were obtained from Aldrich Chemical Co. and used without further purification.

General Analytical Methods:

^{1}H NMR data were obtained on a 500MHz NMR spectrometer. Gel permeation chromatography and thermal analysis were performed of polymer samples. Molecular weights of the polymers were measured by Gel Permeation Chromatography (GPC) in THF relative to polystyrene standards. The inherent viscosity (IV) was obtained in DMF with an Ubbelohde viscometer at 5mg/mL and 30°C. Temperature of 5% weight loss and T_g were measured by Thermal Gravametric Analysis (TGA) and Differential Scanning Calorimetry (DSC), respectively. In this work the polymers were characterized by cyclic voltametry (CV) using a three-electrode electrochemical cell.

Monomer Synthesis:

Compound 25: 4-(4'-aminophenylamino)diphenylamine: The synthesis is shown in Scheme 6. Acetic anhydride (40.0mL, 0.426mol) was added slowly into N-phenyl-*p*-phenylenediamine (compound 22, 20.00g, 0.109mol) in acetic acid (100mL). The reaction mixture was heated to 70°C for 2h. The solvent was removed by rotary evaporation, and the residue was recrystallized from ethyl acetate/hexanes, which afforded a white crystalline solid (21.90g, 75.2%): mp 132 – 134°C. ^{1}H NMR (500MHz, $CDCl_3$) δ 7.99 (s, 1H), 7.20 – 7.53 (m, 9H), 2.10 (s, 3H), 2.06 (s, 3H). MS (EI) m/z 268 (M^+). Anal. Calcd for $C_{16}H_{16}N_2O_2$: C, 71.62; H, 6.01; N, 10.44. Found: C, 71.58; H, 6.07; N, 10.34.

The amide product (5.00g, 18.7mmol) was dissolved in DMF (50mL). 4-Iodonitrobenzene (13.00g, 52.4mmol) and copper (4.90g, 76.6mmol) were added to the solution. The reaction mixture was heated to 130°C for 24 h. The hot mixture was filtered to remove copper powder. After removal of solvent, the residue was recrystallized from toluene, providing compound 23 as a pale yellow solid (5.36g, 73.9%): mp 162 – 163°C. ^{1}H NMR (500MHz, $CDCl_3$) δ 8.17 (d,2H), 7.20 – 7.46 (m, 11H), 2.08 (s, 3H), 2.07 (s, 3H). MS (EI) m/z 389 (M^+). Anal. Calcd for $C_{22}H_{19}N_3O_4$: C, 67.79; H, 4.92; N, 10.79. Found: C, 67.85; H, 4.88; N, 10.42.

The next step in the synthesis required taking compound 23 (2.00g, 5.14mmol) and nickel chloride hexahydrate (2.58g, 10.8mmol) and dissolving them in methanol (50mL). Sodium borohydride (1.04g, 27.4mmol) was added in portions with stirring under cooling with an ice bath. The reaction was continued for 2h at room temperature. The solvent was removed by rotary evaporation. The residue was dissolved in aqueous hydrochloride (30mL, 1.0M), and then alkalinized with ammonium hydroxide (35mL, 1.0M). After filtration, the solid was extracted with chloroform. Solvent was removed by rotary evaporation, providing compound 24 as a white solid (1.67g, 90.5%): mp 243 – 244°C. ^{1}H NMR (500MHz, $CDCl_3$) δ 7.20 – 7.35 (m,9H), 7.00 (d, 2H), 6.65 (d, 2H), 3.83 (s, 2H), 2.04 (s, 3H), 2.02 (s, 3H). MS (EI) m/z 359 (M^+). Anal. Calcd. for $C_{22}H_{21}N_3O_2$: C, 73.52; H, 5.89; N, 11.69. Found: C, 73.23; H, 5.87; N, 11.62.

The final step of the synthesis taking compound 24 (3.50g, 9.75mmol) was refluxed for 24h in potassium hydroxide ethanol solution (100mL, 1.5M). The reaction mixture was cooled to room temperature and filtered. The solid was recrystallized from methanol, providing a slightly purple solid 25 (2.33g, 86.9%): mp 156 – 158 °C. ^{1}H NMR (500MHz, DMSO-d_6) δ 7.61 (m, 1H), 7.23 (m, 1H), 7.11 (m, 2H), 6.90-6.93 (m, 2H), 6.85 (m, 2H), 6.79(m, 4H), 6.64 (m, 1H), 6.51-6.53 (m, 2H), 4.65 (s, 2H). ^{13}C NMR (125MHz, DMSO-d_6) δ 145.98, 142.97, 141.03, 133.43, 133.04, 129.00, 121.41, 121.03, 117.48, 115.49, 114.85, 114.16. MS (EI) m/z 275 (M^+).

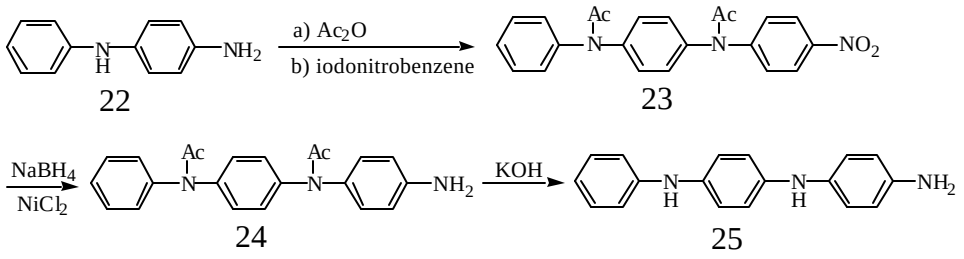

Scheme 6: Synthesis of 4-(4'-aminophenylamino)diphenylamine

Compound 26: 4-{[4-(phenylamino)phenyl]amino}phenol: This compound, 26, was prepared according to Scheme 7. N-Phenyl-*p*-phenylenediamine (5.00g, 27.2mmol), hydroquinone (5.68g, 51.6mmol) and zinc chloride (0.72g, 5.3mmol) were combined in a three-necked flask. The mixture was heated at 180°C with stirring in nitrogen atmosphere for 4h. The reaction mixture was cooled to room temperature, and 0.1M HCl (aq.) solution (50mL) was added. The mixture was heated at 100°C with stirring for 1h and filtered. The product was recrystallized from toluene in the presence of small amount of phenylhydrazine to yield slightly pink crystals, 3.92g, 52% yield: mp = 140-141°C. ^{1}H NMR (500MHz, DMSO-d_6) δ 8.87 (s, 1H), 7.70 (s, 1H), 7.44 (s, 1H), 7.13 (t, J= 7.3 Hz, 2H), 6.98-6.93 (m, 2H), 6.90-6.82 (m, 6H), 6.69-6.62 (m, 3H). MS (EI) m/z 276 (M^+). Anal. Calcd. for $C_{18}H_{16}N_2O$: C, 78.24; H, 5.84; N, 10.14. Found: C, 78.10; H, 5.89; N, 9.90.

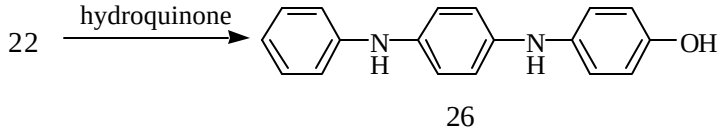

Scheme 7: Synthesis of 4-{[4-(phenylamino)phenyl]amino}phenol

Compound 32*:* (The overall synthesis can be found in Scheme 8) N-Phenyl-*p*-phenylenediamine (22.32g, 121.3mmol) and benzophenone (20.00g, 109.9mmol) were added to toluene (125mL). 5Å molecular sieves (30.0g) were added to the solution under a nitrogen atmosphere. The mixture was refluxed for 48h. The solution was decanted, and the molecular sieves were washed with ethyl ether until the filtrate was colorless. The organic solutions were combined and solvent was removed. The solid residue was taken up in ethyl acetate and washed with NaOH solution and brine. The organic solution was dried with anhydrous sodium sulfate and concentrated. The yellow solid was dried in vacuo at 50°C for 24h to yield compound 27: 37.80g. Compound 27 (25.00g, 71.84mmol) was dissolved in THF (180mL). Di-*tert*-butyl dicarbonate (18.79g, 86.19mmol) and 4-(dimethylamino)pyridine (1.31g, 10.74mmol) were added. The solution was refluxed for 6h, after which the solvent was removed by rotary evaporation. The solid was recrystallized from ethyl acetate/hexane and dried in vacuo at 50°C for 24h to yield compound 28 as pale yellow needles, 25.73g, 80% yield: mp = 154-155°C. ^{1}H NMR (500MHz, $CDCl_3$) δ 7.74 (d, J=8.3Hz, 2H), 7.49-7.44 (m, 1H), 7.43-7.33 (m, 2H), 7.32-7.20 (m,5H), 7.18-7.06 (m, 5H), 6.97 (d, J=8.5Hz, 2H), 6.67 (d, J=8.3Hz, 2H), 1.40 (s, 9H). Anal. Calcd. for $C_{30}H_{28}N_2O_2$: C, 80.33; H, 6.29; N, 6.25. Found: C, 79.78; H, 6.31; N, 6.32.

Compound 27 (8.53g, 24.5mmol) was dissolved in dichloromethane (50mL), and tetra-n-butylammonium tribromide (13.03g, 27.03mmol) was added in one portion. The solution was stirred at room temperature for 1h, then saturated sodium sulfite solution (50mL) was added with stirring for 30min followed by sodium hydroxide solution (2.0M, 25mL). The layers were separated, and the organic phase was washed with distilled water, dried over anhydrous sodium sulfate, and concentrated. The residue was dissolved in THF (60mL), then di-*tert*-butyl bicarbonate (6.41g, 29.40mmol) and 4-(dimethylamino)pyridine (0.45g, 3.7mmol) were added. The solution was refluxed for 6h and concentrated. The residue was recrystallized in methanol and dried in vacuo at 50 °C for 24h to yield slightly pink crystals 29, 8.86g, 69% yield: mp = 163-165°C. ^{1}H NMR (500MHz, $CDCl_3$) δ 7.74 (d,J=7.3Hz, 2H), 7.50-7.33 (m, 5H), 7.31-7.20 (m, 3H), 7.11 (dd, J= 7.9, 1.3Hz, 2H), 7.02 (d, J=8.8Hz, 2H), 6.94 (d, J=8.5Hz, 2H), 6.68 (d, J= 8.5Hz, 2H), 1.39 (s, 9H). Anal. Calcd. for $C_{30}H_{27}BrN_2O_2$: C, 68.31; H, 5.16; N, 5.31. Found: C, 68.27; H, 5.20; N, 5.30.

Compound 28 (24.00g, 53.57mmol), ammonium formate (40.61g, 644.6mmol) and palladium on carbon (5%, 2.83g, 1.33mmol Pd) were charged into a round-bottom flask and purged with argon. THF (100mL) and methanol (250mL) were added. The reaction mixture was heated at 55°C for 12h. The solution was concentrated and taken up with dichloromethane, filtered through Celite and concentrated. The solid was triturated with hexanes and filtered. The white powder was dried in vacuo at 50 °C for 24hto yield product 30 (14.92g). Compound 30 (0.50g, 1.76mol), palladium acetate (6.6mg, 2.9×10^{-2}mmol) and DPEphos (21.0mg, 3.9×10^{-2}mmol) were charged into a flask and purged with argon. Compound 29 (0.77g, 1.46mmol) was added, followed by toluene (6mL). The solution was warmed to 50°C to help the dissolution. Sodium *tert*-butoxide (0.21g, 2.19mmol) was added in one portion. Additional toluene (4mL) was added to wash the flask wall. The reaction mixture was heated at 100°C with stirring for 24h. The solvent was removed by rotary evaporation. The residue was dissolved in dichloromethane, washed with distilled water, dried over anhydrous sodium sulfate, and concentrated. The residue was dissolved in THF (10mL) and di-*tert*-butyl bicarbonate (0.47g, 2.2mmol) and 4-(dimethylamino)pyridine (43.3mg, 0.355mmol) were added. The reaction mixture was heated at 60°C for 12h. The solvent was removed, and the solid was recrystallized

from methanol to yield pink powder 31, 0.59g, 49% yield: mp = 184-185°C. ^{1}H NMR (500MHz, $CDCl_3$) δ 7.74 (d, J= 8.3Hz, 2H), 7.50-7.44 (m, 1H), 7.43-7.38 (m, 2H), 7.33-7.22 (m, 5H), 7.21-7.06 (m, 13H), 6.95 (d, J=8.5Hz, 2H), 6.67 (d, J= 8.4Hz, 2H), 1.44 (s, 9H); 1.43 (s, 9H); 1.39 (s, 9H). Anal. Calcd. for $C_{52}H_{54}N_4O_6$: C, 75.16; H, 6.55; N, 6.74. Found: C, 74.94; H, 6.63; N, 6.75.

Compound 32 was prepared using a procedure similar to that used to prepare compound 30, yielding a white powder in 96% yield. ^{1}H NMR (500MHz, $CDCl_3$) δ 7.34-7.25 (m, 2H); 7.22-7.07 (m, 11H); 6.96 (dd, J= 8.5, 1.2Hz, 2H); 6.61 (dd, J= 8.7, 1.3Hz, 2H); 3.65 (broad, 2H), 1.46-1.42 (m, 27H).

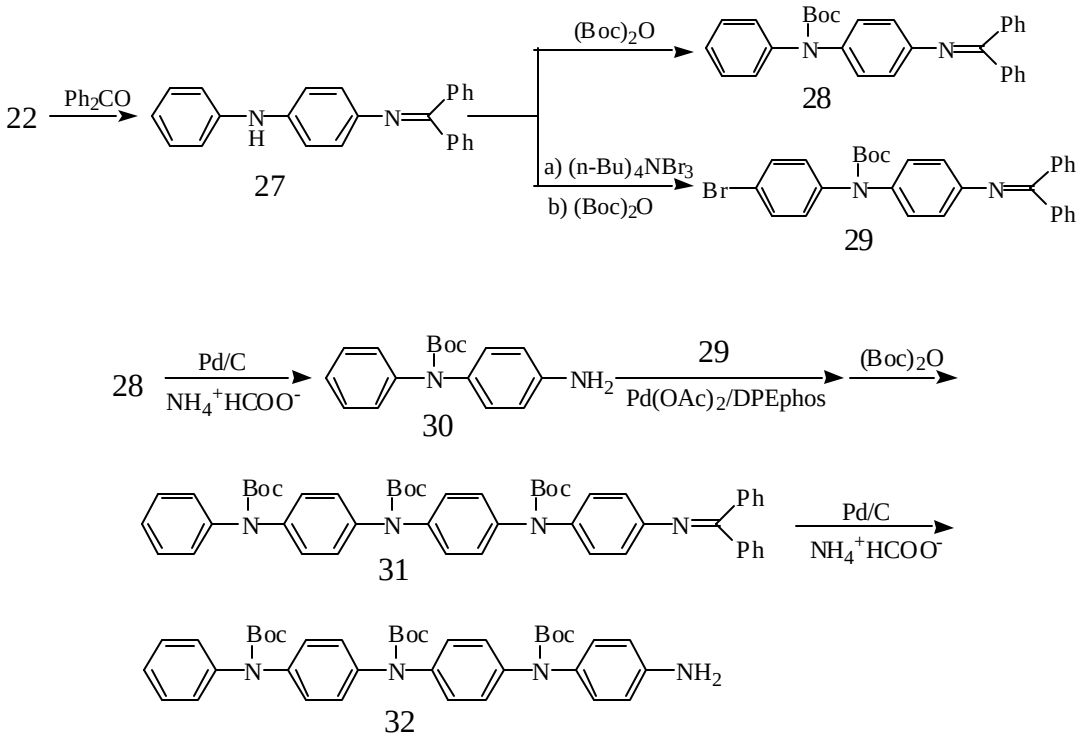

Scheme 8: Synthesis of Compound 32

Compound 35*:* The synthesis of compound 33 is similar to that of compound 27 (see Scheme 9). Product: slightly yellow crystals, 87% yield, mp = 82-83 °C; MS EI m/z 335 (M^+).

The synthesis of compound 34 is similar to that of compound 31. Product: slightly red crystals, 73% yield, mp=149-151 °C. ^{1}H NMR (500MHz, $CDCl_3$) δ 7.74 (d, 2H), 7.47 (t, 1H), 7.40 (t, 2H), 7.33-7.22 (m, 5H), 7.21-7.06 (m, 9H), 6.96 (d, 2H), 6.67 (d, 2H), 1.44 (s, 9H); 1.38 (s, 9H). Anal. Calcd. for $C_{41}H_{41}N_3O_4$: C, 76.97; H, 6.46; N, 6.57. Found: C, 76.70; H, 6.65; N, 6.54.

The synthesis of compound 35 is similar to that of compound 32 (see Scheme 9). Product: white powder, 94% yield; ^{1}H NMR (500MHz, DMSO-d_6) δ 7.37-7.31 (m, 2H); 7.24-7.16 (m, 3H); 7.16 –7.08 (m, 4H), 6.84 (d, 2H); 6.50 (d, 2H); 5.12 (s, 2H), 1.36 (d, 18H).

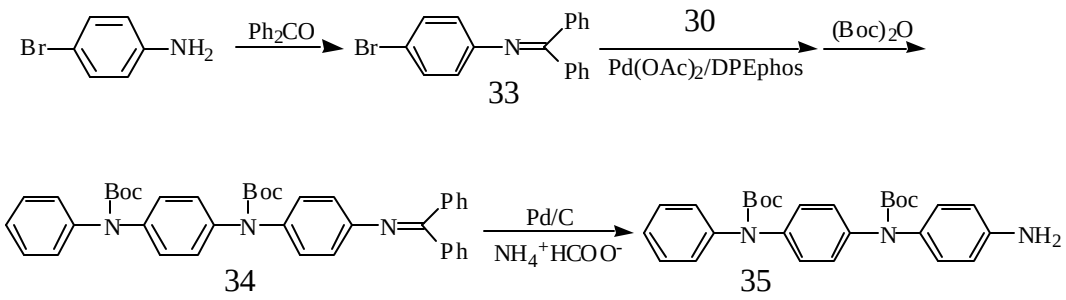

Scheme 9: Synthesis of Compound 35

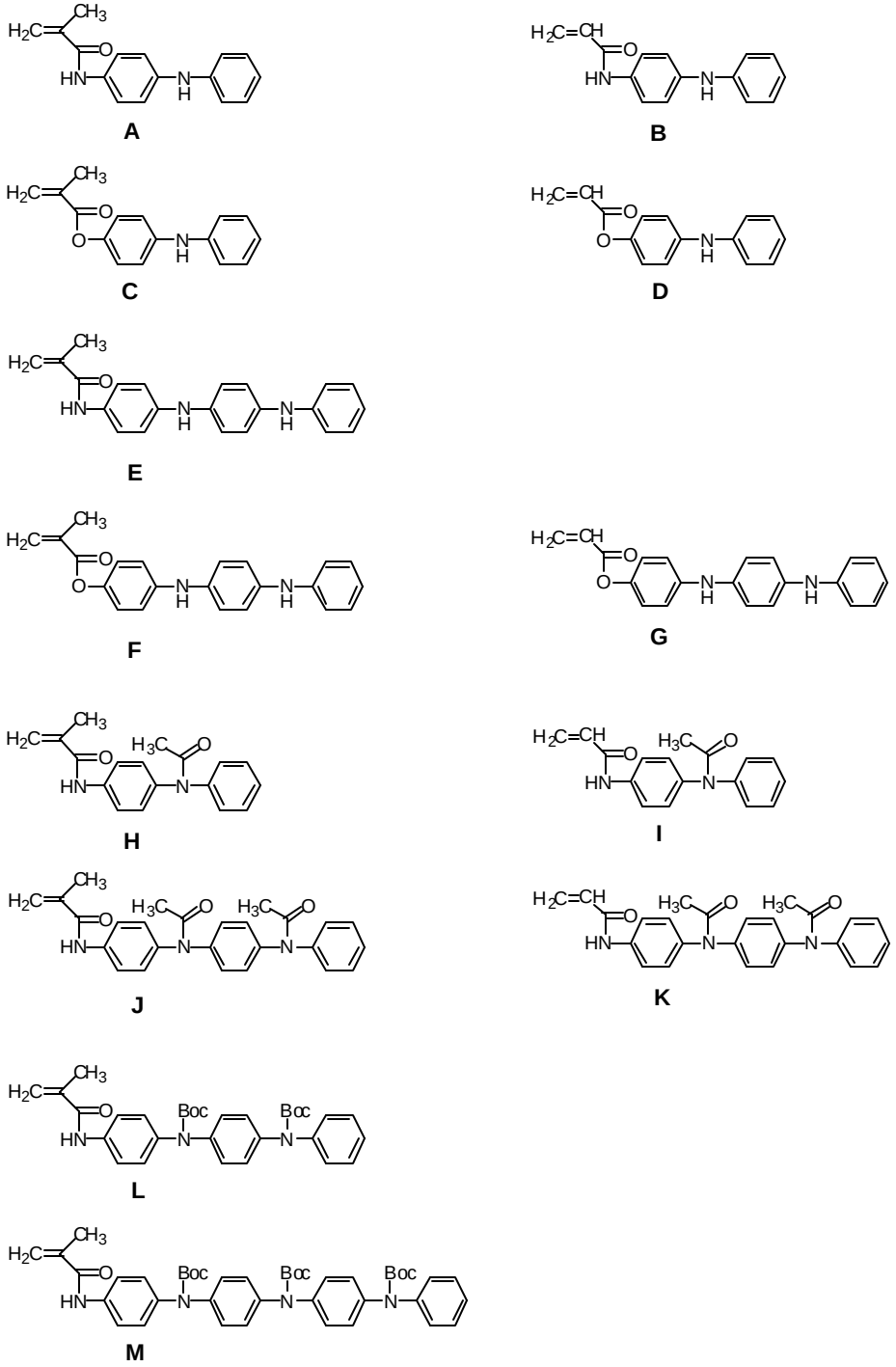

Figure 10: Monomer Structures A-M

Monomer A: (N-[4-Anilinophenyl]-methacrylamide: N-phenyl-p-phenylenediamine (11.52g, 62.61mmol), methyl methacrylate (25.96g, 259.6mmol), dibutyltin oxide (0.92g, 3.7mmol), and phenothiazine (0.06g, 0.3mmol) were combined in a three-necked flask. The mixture was heated at reflux for 15h, and the methanol/methyl methacrylate co-distillation product was removed continuously. The MMA was removed on a rotary evaporator. The residue was recrystallized from toluene. The product was dried to give light blue crystals (12.61g, 80%): mp 109 - 110°C.

^{1}H NMR (500 MHz, $CDCl_3$) δ 7.49 (s, 1H), 7.47–7.38 (dt, 2H), 7.28-7.20 (m, 2), 7.09-6.96 (m, 4H), 6.93-6.84 (tt, 1H), 5.80-5.76 (m, 1H), 5.70 (s, 1H), 5.46-5.40 (m, 1H), 2.07-2.04 (m, 3H). GC/MS (EI) m/z 252(M^+). Anal. Calcd for $C_{16}H_{16}N_2O$: C, 76.16; H, 6.39; N, 11.10. Found: C, 76.11; H, 6.44; N, 11.04.

Monomer B: (N-[4-Anilinophenyl]-acrylamide): N-phenyl-p-phenylenediamine 5.00g, 27.1mmol), triethylamine (5.40g, 53.5mmol) and THF (20mL) were charged into a round-bottomed flask. The solution was stirred and cooled in an ice bath. Acryloyl chloride (2.95g, 32.6mmol) in THF (40mL) was added slowly into the solution. Stirring was continued at room temperature for 12h. The precipitate was removed by filtration. The filtrate was concentrated and recrystallized from toluene and dried in vacuo for 24h to give a pale yellow solid (3.25g, 50%): mp 150-152°C. ^{1}H NMR (500MHz, DMSO-d_6) δ 7.54 (s, 1H), 7.50-7.38 (d, 2H), 7.32-7.12 (t, 2H), 7.10-6.94 (m, 4H), 6.94-6.75 (t, 1H), 6.45-6.33 (d, 1H), 6.32-6.16 (q, 1H), 5.80-5.60 (m, 2H). GC/MS (EI) m/z 238 (M^+). Anal. Calcd for $C_{15}H_{14}N_2O$: C, 75.61; H, 5.92; N, 11.76. Found: C, 75.11; H, 5.97; N, 11.20.

Monomer C: (4-Anilinophenyl methacrylate): The synthesis of monomer C is similar to that of monomer B, yielding white crystals from heptane in 60% yield: mp 72-73°C. ^{1}H NMR (500MHz, DMSO-d_6) δ 8.19 (s, 1H), 7.26-7.20 (m, 2H), 7.14-6.96 (m, 6H), 6.87 – 6.79 (tt, 1H), 6.25 (m, 1H), 5.86 (m, 1H), 2.06-1.94 (m, 3H). GC/MS (EI) m/z 253 (M^+). Anal. Calcd for $C_{16}H_{15}NO_2$: C, 75.87; H, 5.97; N, 5.53. Found: C, 76.65; H, 6.00; N, 5.55.

Monomer D: (4-Anilinophenylacrylate): The synthesis of monomer D is similar to that of monomer B, yielding pale yellow crystals from heptane in 40% yield: mp 47-49 °C. ^{1}H NMR (500MHz, DMSO-d_6) δ 8.20 (s, 1H), 7.28-7.19 (m, 2H), 7.14-6.96 (m, 6H), 6.86-6.78 (t, 1H), 6.56-6.46 (dd, 1H), 6.44-6.33 (q, 1H), 6.17-6.06 (dd, 1H). GC/MS (EI) m/z 239(M^+). Anal. Calcd for $C_{15}H_{13}NO_2$: C, 75.30; H, 5.48; N, 5.85. Found: C, 74.91; H, 5.49; N, 5.82.

Monomer E: The synthesis of monomer **E** is similar to that of monomer **B**, yielding pink powder from ethanol, 80% yield: mp 163-164°C. ^{1}H NMR (500MHz, $CDCl_3$) δ 7.39-7.30 (m, 3H), 7.20-7.13 (m, 2H), 7.01-6.86 (m, 8H), 6.78 (t, J=7.3Hz, 1H), 5.70 (s, 1H), 5.49 (s, 2H), 5.36 (s, 1H), 1.99 (s, 3H). GC/MS (EI) m/z 343(M^+). Anal. Calcd for $C_{22}H_{21}N_3O$: C, 76.94; H, 6.16; N, 12.24. Found: C, 74.38; H, 6.30; N, 11.58.

Monomer F: The synthesis of monomer **F** is similar to that of monomer **B**, yielding blue solid, 82% yield: mp 99-100°C. ^{1}H NMR (500MHz, DMSO-d_6) δ 7.93 (s, 1H), 7.89 (s, 1H), 7.20-7.15 (m, 2H), 7.06-6.88 (m, 10H), 6.72 (t, J= 7.3Hz, 1H), 6.24 (s,1H), 5.85 (s, 1H), 1.99 (s,3H). GC/MS (EI) m/z 344(M^+). Anal. Calcd for $C_{22}H_{20}N_2O_2$: C, 76.70; H, 5.85; N, 8.13. Found: C, 76.19; H, 5.70; N, 8.03.

Monomer G: The synthesis of monomer **G** is similar to that of monomer **B**, yielding pale blue solid by liquid chromatography, 26% yield: mp 107-110°C. ^{1}H NMR (500MHz, DMSO-d_6) δ 7.94 (s, 1H), 7.89 (s, 1H), 7.20-7.15 (m, 2H), 7.07-6.90 (m, 10H), 6.72 (t, J= 7.3Hz, 1H), 6.50 (dd, J=17.3Hz, 1.5Hz, 1H), 6.38 (dd, J= 10.4, 1.5Hz, 1H), 6.10 (dd, J=10.3Hz, 1.5Hz, 1H).

GC/MS (EI) m/z 330 (M^+); Anal. Calcd for $C_{21}H_{18}N_2O_2$: C, 76.34; H, 5.49; N, 8.48. Found: C 76.13; H, 5.61; N, 8.36.

Monomer H: Monomer **A** (5.19g, 20.6mmol) was dissolved in acetic acid (50mL). Acetic anhydride (10mL, 106.5mmol) was slowly added to the solution. The mixture was heated at 70°C for 8h. The solvent was removed by rotary evaporation at reduced pressure. The residue was recrystallized from ethyl acetate/hexanes, providing a white crystalline solid (4.93g, 81.4%): mp 136-137 °C. ^{1}H NMR (500MHz, $CDCl_3$) δ 7.80 (s, 1H), 7.20-7.52 (m,9H), 5.77 (s, 1H), 5.45 (s, 1H), 2.04 (s, 3H), 2.02 (s, 3H). MS (EI) m/z 294 (M^+).

Monomer I: The synthesis of monomer **I** is similar to that of monomer **H**, yielding pale yellow solid, 63% yield. ^{1}H NMR (500MHz, $CDCl_3$) δ 8.30 (s, 1H), 7.70-6.90 (m, 9H), 6.39 (d, 1H), 6.25 (dd, 1H), 5.69 (d, 1H), 2.07 (s, 3H). Anal. Calcd for $C_{17}H_{16}N_2O_2$: C, 72.84; H, 5.75; N, 9.99. Found: C 72.68; H, 5.83; N, 10.18.

Monomer J: The synthesis of monomer **J** is similar to that of monomer **B**, yielding white powder from acetone, 51% yield: mp 194-195°C. ^{1}H NMR (500MHz, $CDCl_3$) δ 7.88 (s, 1H), 7.70-6.92 (m, 13H), 5.78 (s, 1H), 5.46 (s, 1H), 2.04 (s, 9H). GC/MS (EI) m/z 427 (M^+). Anal. Calcd for $C_{26}H_{25}N_3O_3$: C, 73.05; H, 5.89, N, 9.83. Found: C, 72.64; H, 5.97; N, 9.38.

Monomer K: The synthesis of monomer **K** is similar to that of monomer **B**, yielding pale yellow powder from ethyl acetate, 72% yield: mp 203-204°C. ^{1}H NMR (500MHz, $CDCl_3$) δ 8.30 (s, 1H), 7.75-6.90 (m, 13H), 6.40 (d, J=16.8Hz, 1H), 6.23 (dd, J=16.8Hz, 10.3Hz, 1H), 5.69 (d, J=10.3Hz, 1H), 2.06 (d, 6H); Anal. Calcd for $C_{25}H_{23}N_3O_3$: C, 72.62; H, 5.61; N, 10.16. Found: C, 71.24; H, 5.60; N, 9.64.

Monomer L: Compound 35 (3.00g, 6.31mmol) was dissolved in THF (25mL) and cooled in an ice bath. Methacryloyl chloride (0.79g, 7.6mmol) in THF (25mL) was added drop wise. The reaction was continued at room temperature for 24h. The reaction mixture was filtered, and the solvent was removed from the filtrate. The solid residue was dissolved in dichloromethane and washed with water. The product was purified by liquid chromatography (silica gel, ethyl acetate/ hexanes 1:1). Product: white crystals, 2.34g, 68% yield. ^{1}H NMR (500 MHz, DMSO-d_6) δ 9.84 (s, 1H), 7.66 (d, 2H), 7.34 (t, 2H), 7.25 – 7.10 (m, 9H), 5.79 (s, 1H), 5.51 (s, 1H), 1.94 (s, 3H), 1.37 (s, 18H). Anal. Calcd for $C_{32}H_{37}N_3O_5$: C, 70.70; H, 6.86; N, 7.73. Found: C, 69.11; H, 6.80; N, 7.29.

Monomer M: The synthesis is similar to that of **L**. Product: white crystals, 93% yield. ^{1}H NMR (500 MHz, DMSO-d_6) δ 9.84 (s, 1H), 7.68 (d, 2H), 7.34 (t, 2H), 7.25 – 7.10 (m, 13H), 5.81 (s, 1H), 5.51 (s, 1H), 1.95 (s, 3H), 1.37 (s, 27H). Anal. Calcd for $C_{43}H_{50}N_4O_7$: C, 70.28; H, 6.86; N, 7.62. Found: C, 69.58; H, 6.83; N, 7.38.

General Polymerization Procedure

Monomer (0.50g), AIBN (5.0mg) and DMF (5mL) were combined in a Schlenk tube. The solution was degassed by three freeze-pump-thaw cycles. The tube was heated at 70°C with stirring for 24h. The polymer was precipitated from methanol, filtered and dried in vacuo oven at 60°C for 24h.

Polymer Characterization: All polymers were prepared from their corresponding monomer (e.g. monomer A = polymer A); please see Table 2 for polymer properties (A-M) and a representative TGA is shown in Figure 11.

Table 2: Physical Properties of Polymers A-M

Polymer	**Yield (%)**	**M_n**	**M_w**	**IV (dL/g)**	**Td (^{o}C) (5wt% loss)**	**Tg (^{o}C)**
Polymer A Poly[N-(4-Anilinophenyl)-methacrylamide)	81	$58.4x10^3$	$134.9x10^3$	0.27	263	184
Polymer B Poly[N-(4-Anilinophenyl)-acrylamide]	72	$28.4x10^3$	X*	0.25	280	155
Polymer C Poly(4-Anilinophenyl methacrylate)	88	$30.1x10^3$	$80.3x10^3$	0.26	250	116
Polymer D Poly(4-Anilinophenyl acrylate)	42	$13.3x10^3$	$24.4x10^3$	0.12	269	73
Polymer E	DNP#	X	X	X	X	X
Polymer F	60	$27x10^3$	$57x10^3$	0.26	X	X
Polymer G	10	$11x10^3$	$16x10^3$	X	X	X
Polymer H	99	X	X	0.48	X	X
Polymer I	80	X	X	0.1	X	X
Polymer J	80	X	X	0.28	X	X
Polymer K	58	X	X	0.1	X	X
Polymer L	X	$34x10^3$	$56x10^3$	X	X	X
Polymer M	X	$8.5x10^3$	$24x10^3$	X	X	X

*Not determined
Did not polymerize

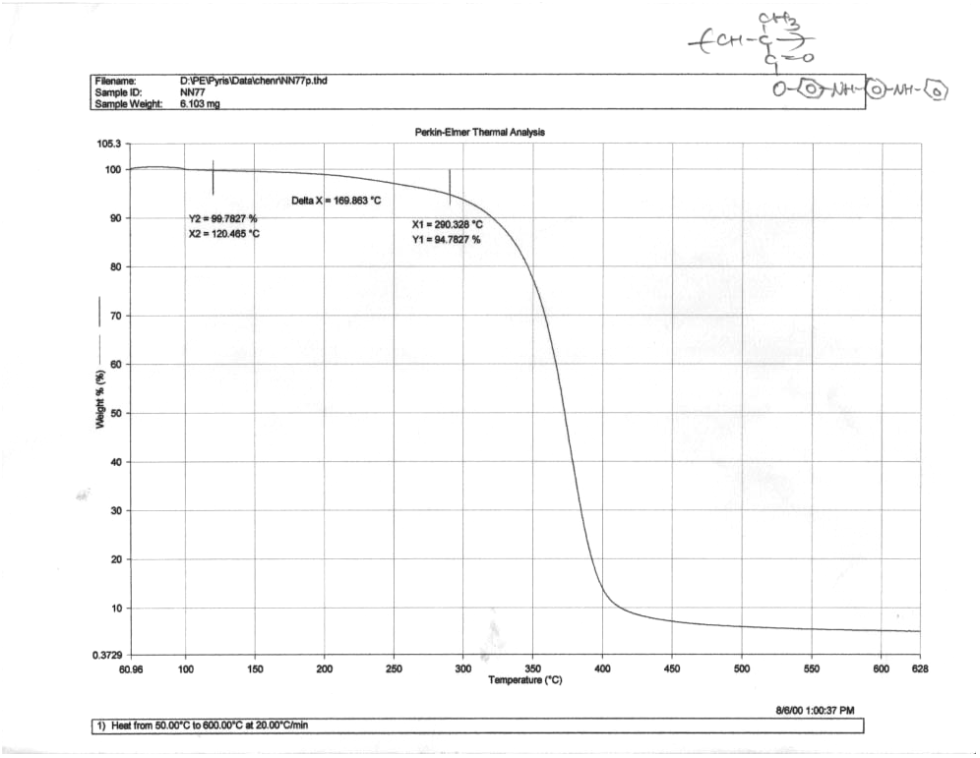

Figure 11: TGA of polymer D

UV-Vis spectroscopy *of* polymer F in DMF. The reduced colorless polymer exhibited a single strong absorption at 311nm (2.3×10^4). After oxidation in the air, the blue polymer solution showed a sharp peak at 300nm (2.2×10^4) and a broad band at 578nm (6.3×10^3). The higher energy band is believed due to the $\pi \rightarrow \pi^*$ transition of the benzenoid ring, while the lower energy is due to the charge transfer from benzenoid ring to quinoid ring. The solution turned green when doped with sulfuric acid, and the UV-Vis spectrum changed to reveal three peaks: 292nm, 396nm and 830nm. The new absorption appearing at 396nm is attributed to the polaron transition. The characteristic absorption of polymer **F** is similar to that of polyaniline.

Conductivity: Polymer F powder was doped with iodine for a week and pressed into pellet. The conductivity was measured using the four-point probe method. The conductivity was low, 6×10^{-7} S/cm.

SERDP FY02

Materials:

Dimethyl-1,4-cyclohexanedione-2,5-dicraboxylate was obtained from ACROS Organics and used as received. THF, methanol, n-hexylamine, household bleach (10 % aqueous NaOCl)) obtained from K Mart, NaH, $SOCl_2$ and $LiAlH_4$ were purchased from Aldrich Chemical Co. and used as received.

General Analytical Methods

^1H and ^{13}C NMR data was acquired using a Bruker 400MHz NMR spectrometer at 300K. The FTIR spectrum was collected using a Nicolet Nexus 870 FTIR spectrometer with a liquid nitrogen cooled MCT detector. The spectrum is an average of 100 scans with 4 cm^{-1} resolution.

The polymer film was placed in contact with a Germanium crystal on a "Thunderdome" attenuated total reflectance (ATR) accessory. Melting points (mp) were taken with a Melt-Temp apparatus and are uncorrected.

Methods:

Synthesis Section:

The second phase of this program during FY02 was continuation of the BAM-PPV scale-up. The scale up procedure used in FY01 was previously described. While this procedure was successful, environmental and financial concerns warranted investigation of alternative synthetic approaches. Efforts at NAWCWD to synthesize BAM-PPV in three to four steps from starting material were promising; however, the scale-up process had to begin before the synthetic details could be finalized, so the original seven-step synthesis was used with modifications. Spectra Group Limited, Inc. was chartered under an SBIR to investigate alternative synthetic methods. In FY02, Spectra Group provided some very important environmentally beneficial changes to the synthesis scheme (Scheme 10). One such change was doing step 1 and 2 in the same 'pot' without isolating step 1 product. This was accomplished by replacing the methanol of step 1 and the methylene chloride of step 2 with toluene for both step one and two. To reduce costs, the THF in step 4 was changed to toluene, with only a small amount of THF added for solubility. Another change was made in step 5; dry HCl gas was replaced with aqueous HCl, which was much easier to work with. In an additional timesaving change made at NAWCWD, the first four steps of the FY02 scale up were performed in a 50-gallon Pfaudler reactor, allowing for up to 10 kg of starting material at a time demonstrating that this process can be scaled-up to multi-kilogram quantity batches.

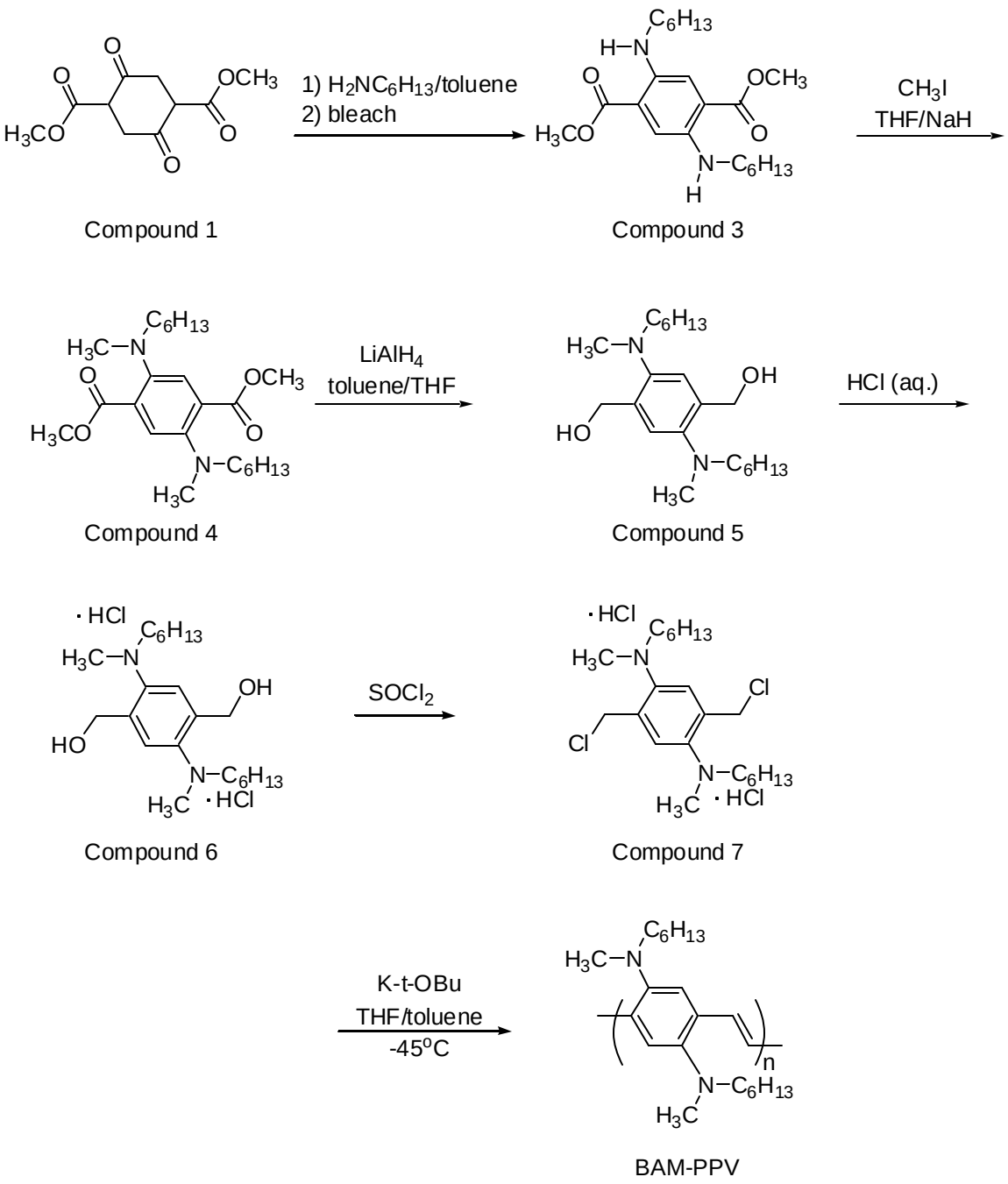

Scheme 10: Reduction in Synthesis Steps of BAM-PPV

Intermediate product for Compound 3: Synthesis of 2,5-bis(N-hexylamino)-cyclohexa-1,4-diene carboxylic acid methyl ester: Dimethyl-1,4-cyclohexanedione-2,5-dicarboxylate (compound 1, 10kg, 43.9 mol) was added to 30L toluene in a 50-gallon reactor. N-Hexylamine (12.2L) was pumped in slowly. The mixture was heated at 70°C overnight. After 24 hours the reaction was determined to be complete by ^{1}H NMR. The product was not isolated. The mixture

remained in the reactor, and step 2 was performed immediately. ^{1}H NMR ($CDCl_3$): 8.8, m, 4H; 3.65, s, 6H; 3.21, t, 4H; 1.5, m, 4H; 1.35, m (br) 12H; 0.9 t, 6H.

Compound 3: Synthesis of 2,5-bis(N-hexylamino)terephthalic acid dimethyl ester: The temperature in the 50-gallon Pfaudler was lowered to 55°C, and 64L of 10% sodium hypochlorite was pumped in at a rate of 1.4L/hour. When all the bleach was added, the temperature was raised to 70°C for 4 days. Completion of the reaction was determined by ^{1}H NMR. Upon completion the temperature was lowered to 55°C and stirring halted to allow separation of the layers. The water layer was removed and discarded. The toluene layer was removed from the reactor, and the toluene was removed from the mixture by rotary evaporation, leaving red crystals of 2,5-bis(N-hexylamino)terephthalic acid dimethyl ester (compound 3). The crystals were filtered on a glass frit, rinsed with methanol, and dried in a vacuum oven overnight. Steps 1 and 2 were completed in three batches. mp: 104-105°C. ^{1}H NMR (CD_2Cl_2): 7.28, s, 2H; 3.86, s, 6H; 3.14, t, 4H; 1.62, m, 4H; 1.36, m (br) 12H; 0.91 t, 6H. Average yield over 2 steps: 72%.

Compound 4: Synthesis of 2,5-bis(N-hexyl-N-methylamino)terephthalic acid dimethyl ester:
The methylation step was also performed in three batches. Compound 3 (7kg, 17.9mol) was added to the 50-gallon reactor containing 48L tetrahydrofuran. Sodium hydride (1786g, 44.6mol) in oil was rinsed with hexanes and added to cooled THF. The THF/NaH slurry was then added to the reaction vessel and allowed to stir for 1h. Iodomethane (7623g) was pumped through Viton® tubing into the reactor using a peristaltic pump while the reaction was kept under an argon purge. The reactor temperature was then set at 60°C for 1-3 days. Completion of the reaction was determined by ^{1}H NMR. Upon completion the reaction mixture was allowed to cool to room temperature and was pumped out of the reactor. The THF was removed with a rotary evaporator; the hexanes were added and stirred. The mixture was then filtered through Celite, and hexanes were removed under reduced pressure, yielding the dark brown oil 2,5-bis(N-hexyl-N-methylamino)-terephthalic acid dimethyl ester (compound 4). ^{1}H NMR (CD_2Cl_2): 7.18, s, 2H; 3.58, s, 6H; 2.92, t, 4H; 2.70, s, 6H, 1.49, m, 4H; 1.26, m, 12H; 0.87, t, 6H. Average yield: 92.5%.

Compound 5: Synthesis of 2,5-bis(N-hexyl-N-methylamino)-1,4-bis(hydroxymethyl)-benzene: The reduction step was done in multiple batches using a 50-gallon reactor. $LiAlH_4$ (843g) was added to 32L toluene that had been cooled to 0°C (under argon). THF (3.5L) was added to the mixture and allowed to stir for 1 hour. Compound 4 (7.1kg) mixed with 16L toluene was slowly pumped into the reactor. The reaction mixture was allowed to reach room temperature and stir overnight. The reaction was then quenched with 4M NaOH (3.5L). Completion of the reaction was verified by ^{1}H NMR. The product mixture was used as-is in step 5 without further isolation of the product. ^{1}H NMR (CD_2Cl_2): 6.99, s, 2H; 4.69, s, 4H; 3.41, d, 2H, 2.84, t, 4H; 2.63, s, 6H; 1.53, m (b), 4 H, 1.27, s (br); 12H, 0.97, m (br), 6H.

Compound 6: Synthesis of 2,5-bis(N-hexyl-N-methylamino)-1,4-bis(hydroxymethyl)-benzene dihydrochloride: The formation of the HCl salt was accomplished in multiple batches using 4L, 5L, 12L, and 22L reaction vessels. Typical procedure in the 22L reactor is as follows: 20L of compound 5 mixed with toluene, THF and water from previous step (approximately 1184g of actual starting material) was added to the reactor. This mixture was chilled to 10°C. While stirring under nitrogen, 675mL of 36% HCl was added drop wise to the solution. The reaction

was allowed to stir for ca. 4 hours. The solvent was removed using a rotary evaporator and the product, an off-white solid, was precipitated and rinsed with acetone followed by vacuum drying to yield 2,5-bis(N-hexyl-N-methylamino)-1,4-bis(hydroxymethyl)benzene dihydrochloride (compound 6). Completion of the reaction was verified by ^{1}H NMR. mp: 146°C (dec). ^{1}H NMR (CD_3OD): 7.98, s, 2H; 5.07, s, 4H; 3.66, t, 4H; 3.34, s, 6H; 1.55, m, 4H; 1.30, m, 12H; 0.88, t, 6H. Average yield over steps 4 and 5: 58%.

Compound 7: Synthesis of 2,5-bis(N-hexyl-N-methylamino)-1,4-bis(chloromethyl)benzene dihydrochloride: The chloromethylation step was performed in multiple batches using 1 and 22L reactors. A typical 22L reaction consisted of the addition of 1794g (4.1mol) of compound 6 to 8L thionyl chloride at 10°C. The reaction was allowed to stir overnight. The thionyl chloride was removed under vacuum. The resulting solid had a slight purple tint. The solid was precipitated from ethyl acetate, filtered and rinsed with acetone to yield an off white/tan solid, 2,5-bis(N-hexyl-N-methylamino)-1,4-bis(chloromethyl)benzene dihydrochloride (compound 7), which was dried under vacuum. Completion of the reaction was verified by ^{1}H NMR. mp: 156-161°C (dec). ^{1}H NMR (CD_3OD): 8.13, s, 2H; 5.07, s, 4H; 3.68, t, 4H; 3.33, s, 6H; 1.54, m(br), 4H; 1.29, m(br), 12H; 0.87, t, 6H. Average yield: 67%.

Compound 8: Synthesis of BAM-PPV: 152g (0.32mol) of monomer (compound 7) was dissolved in 4L of solvent (2L toluene, 2L THF) at –45°C. Potassium t-butoxide (289g, 2.6mol) was then added incrementally. The reaction was kept between –50°C and –40°C for 2h. The reaction was allowed to warm to room temperature overnight while stirring under nitrogen. The orange polymer, now a gelatinous mass, was collected and precipitated into room temperature methanol and then dried under vacuum. Purification of the polymer will not occur in FY02. ^{1}H NMR (CD_2Cl_2): 7.48, s, 2H; 7.40, s, 2H; 2.96, m, 4H; 2.78, s, 6H; 1.63, m (br),4H; 1.53, s (br), 4H; 1.30,m, 8H; 0.85 s (br), 6H. Average yield for unpurified polymer: 200% (this is consistent with incorporation of solvent and salt.). The scale-up synthesis of BAM-PPV proceeded as planned. We prepared at this milestone (FY02) 3.2kg of crude polymer. In addition 2-3kg of compound 5 product was prepared for further scale-up in FY03.

EAPs based on Oligomers of Polyaniline:

Electroactive Polymethacrylamides: Poly(methacrylamide)s containing trimeric and tetrameric anilines were synthesized and characterized (Scheme 11) at RPI. Methacrylamides containing the protected oligoaniline were polymerized by free radical polymerization in DMF using AIBN as initiator. These polymers show good solubility in common organic solvents, such as toluene, THF, DMSO and DMF. The number average molecular weight of protected polymers 15 and 16 were 2.8×10^4 and 5.8×10^3, respectively. The molecular structures of the polymers were confirmed by proton NMR and FTIR. To obtain electroactive polymers the protective groups need to be removed after the polymerization. Thermolysis of protected oligoaniline in an inert atmosphere results in a quantitative removal of the t-Boc group affording oligoaniline in its reduced state. In the TGA study in nitrogen, protected polymers 15 and 16 started to lose weight at about 140 °C (Figure 12). The total weight loss in the first step of decomposition for polymers 15 and 16 were 36% (theoretical loss 37%, calculated from molecular weight of repeating unit) and 39% (theoretical loss 41%), respectively. This showed that the removal of the t-Boc group was quantitative. The thermograms also indicated that the resulting polymers 15 and 16 were

stable up to about 250 °C. Polymers 15 and 16 were prepared by heating precursors in Schlenk tubes under argon at 180 °C for 10h.

The resulting polymers, **15** and **16**, were soluble in THF, DMSO and DMF. GPC analysis showed that the molecular weights were slightly lower than those of the precursors, 2.0×10^4 and 3.4×10^3 respectively. This may be attributed to the loss of the bulky t-Boc groups, causing a decrease in the hydrodynamic volume of the macromolecules in solution. Proton NMR in DMSO-d_6 showed that the proton resonance of the tert-butyl group (1.31ppm) disappeared completely. New resonances due to amine groups appeared after thermolysis (7.72, 7.28 ppm for polymer **15**, 7.72, 7.60, and 7.30 ppm for polymer **16**). The FTIR spectrum was obtained by casting a film on a KBr pellet (Figure 13). The protected polymers exhibit peaks at 1712 and 1161 cm^{-1}, which can be assigned to the stretching vibration of carbonyl and the stretching of O-$C(CH_3)_3$ from the tert-butyl carbamate protective groups. After the thermolysis these peaks disappeared. A new peak appeared at 3385 cm^{-1}, which can be attributed to the N-H stretching of the diphenylamine moiety. The spectra of polymer **15** and the precursor were similar to that of polymer **16**.

Polymers **15** and **16** in the reduced state were dissolved in DMF and then oxidized by bubbling oxygen into the solution. The reduced polymer **15** exhibited a single strong absorption at 317 nm. Oxidation of the colorless solution resulted in an intense blue-purple solution, with a sharp peak at 308nm and a broad peak at 481nm. The first peak was ascribed to the π - π^* transition in the benzenoid ring. The second one was associated with a benzenoid to quinoid excitonic transition. The oxidized polymer was doped with sulfuric acid and the solution turned green. Three peaks were displayed in the UV-Vis spectrum at 270, 391 and 752nm (Figure 14). The protonation of the oxidized polymer caused the low wavelength absorption to split. The high wavelength absorption red-shifted and extended toward near-IR with an increase in intensity. The spectrum of polymer **16** was similar to that of polymer **15**, except that the absorption peaks shifted slightly to longer wavelengths. It is easy to understand that the chromophore (conjugated oligoaniline) in polymer **16** is one unit longer than that in polymer **15**. The absorption shifts to longer wavelength with the increase in conjugation length, which has been observed in many series of conjugated oligomers. The reduced state of polymer **16** exhibited a single strong absorption at 320nm, while the oxidized state showed a sharp peak at 311nm and a broad peak at 565nm. The acidified solution displayed three peaks at 302, 420 and 789nm.

Cyclic voltammetry (CV) has been widely used to characterize the electrochemical properties of conducting polymers. The polymer was first dissolved in tetrahydrofuran and added to the surface of the Pt working electrode. After the solvent evaporation a layer of thin film was formed. The experiment was carried out in 1.0 M sulfuric acid aqueous solution with a scan rate at 100mV/s. Two reversible oxidation peaks (0.385V and 0.597V) were observed in the cyclic voltammogram of polymer **15**. It has been shown in the literature that the phenyl-end aniline dimer displays two reversible oxidation peaks that correspond to two one-electron transfer processes (Scheme 12). The first oxidation involves the transfer of a single electron, giving rise to a radical cation. The second one results in the transfer of another electron followed by the loss of two protons leaving the uncharged imine form. As the length of conjugation increases, for example in phenyl-end capped aniline tetramer, the electron-transfer tends to occur in pairs and two two-electron transfer processes are observed. The leucoemeraldine structure was converted first into emeraldine, and then into pernigraniline. This is the case in the experiment for polyaniline. In the repeat unit of polymer **15**, trimer aniline was attached to the backbone through an amide group whose oxidation was not observed in the potential range of the

experiment. In the polymer structure the redox properties of this oligoaniline unit should resemble that of the phenyl-end dimer. The same is true for polymer **16**. The oligomer unit behaved like substituted phenyl-end trimer aniline and displayed a similar CV response. Only one peak was observed at 0.561V (Figure 15), which may correspond to one two-electron transfer process (Scheme 13). It has been shown in the literature that oxidation of oligoaniline occurs through an even-electron transition when possible and the odd-numbered oligomers generate radical cations only transiently and at high potential. Unfortunately, to the best our knowledge there is no previous report on the electrochemistry of phenyl-end trimer aniline.

For comparison, poly(N-(4-anilinophenyl)-methacrylamide), a polymer similar to polymer **15** and **16** except that the side chain is dimeric rather than trimeric and tetrameric aniline, was synthesized and characterized. The electrochemical properties of the polymer have not been reported before. Our work showed that this polymer was not oxidized by bubbling oxygen; there was no change in UV-Vis absorption occurred upon oxygen exposure. Cyclic voltammetry showed that the polymer could not be oxidized under the same experimental conditions as those for polymer **15** and **16**.

Copolymers with n-Butyl Acrylate: In order to improve film-forming properties, a series of copolymers (including polymers 17 and 18 in Scheme 11) were synthesized by free radical polymerization. The characteristics of these polymers are given in Tables 3 and 4, respectively. The properties include number average molecular weight, polydispersity index, and composition (mol% oligoaniline monomer).

Table 3: Characterization of copolymer 17

	M_n	PDI	Feed (%)	NMR (%)	Elemental (%)
1	42k	2.5	10	17	13
2	86k	2.6	30	36	37
3	179k	1.9	50	49	52
4	23k	8.2	70	70	89
5	30k	2.7	100	-	-

Table 4: Characterization of copolymer 18

	M_n	PDI	Feed (%)	NMR (%)	Elemental (%)
1	43k	1.9	10	15	12
2	59k	2.6	30	31	30
3	98k	2.5	46	49	50
4	60k	2.9	70	70	59
5	58k	2.3	100	-	-

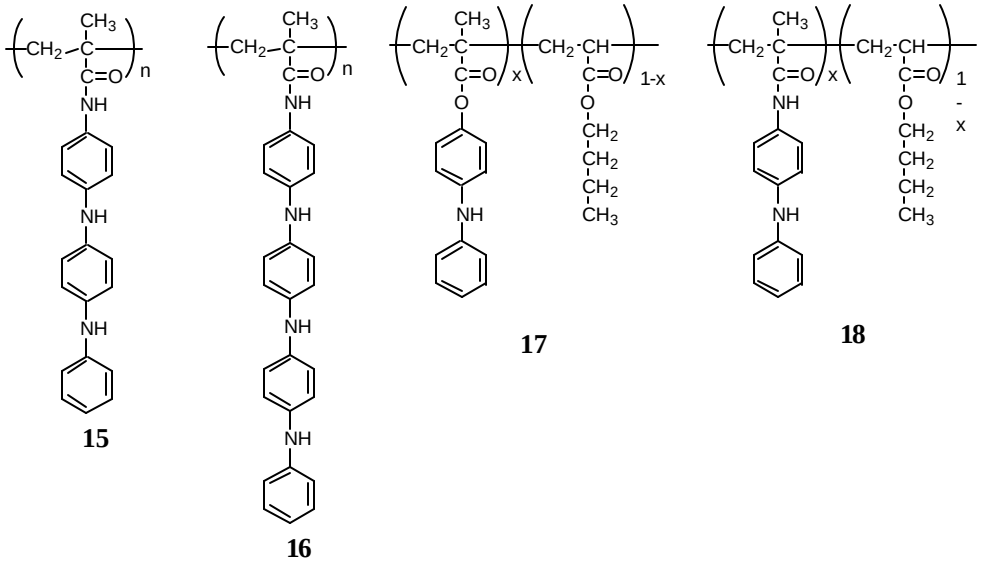

Scheme 11: Chemical structures of polymethacrylamides and copolymers

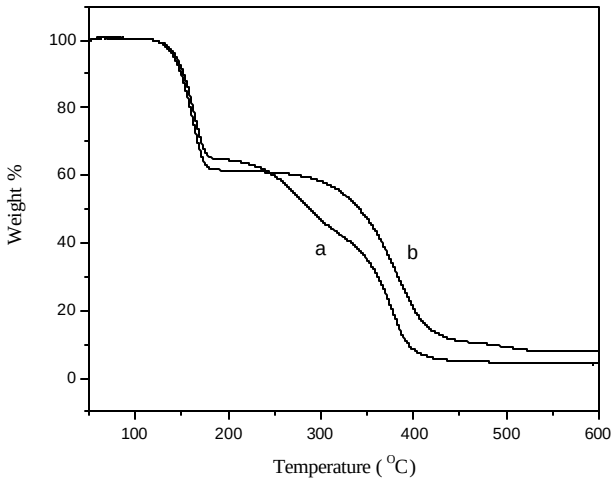

Figure 12: TGA thermograms of protected a) polymer 15;
b) polymer 16.

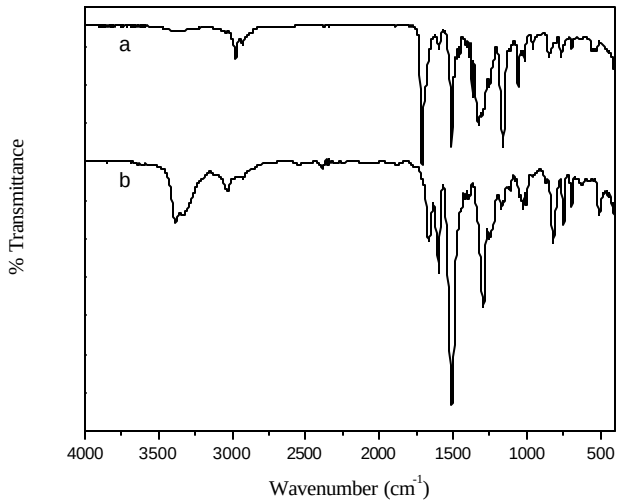

Figure 13: FTIR spectra of polymer 16: a) precursor; b) polymer 16.

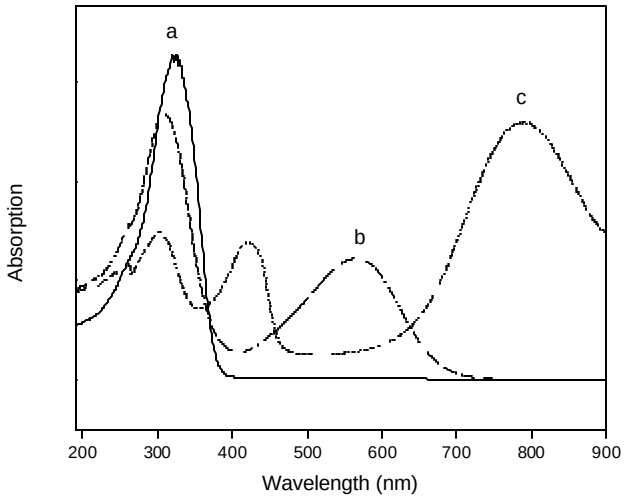

Figure 14: UV-Vis spectra of polymer 16: a) reduced, b) oxidized and c) doped with sulfuric acid

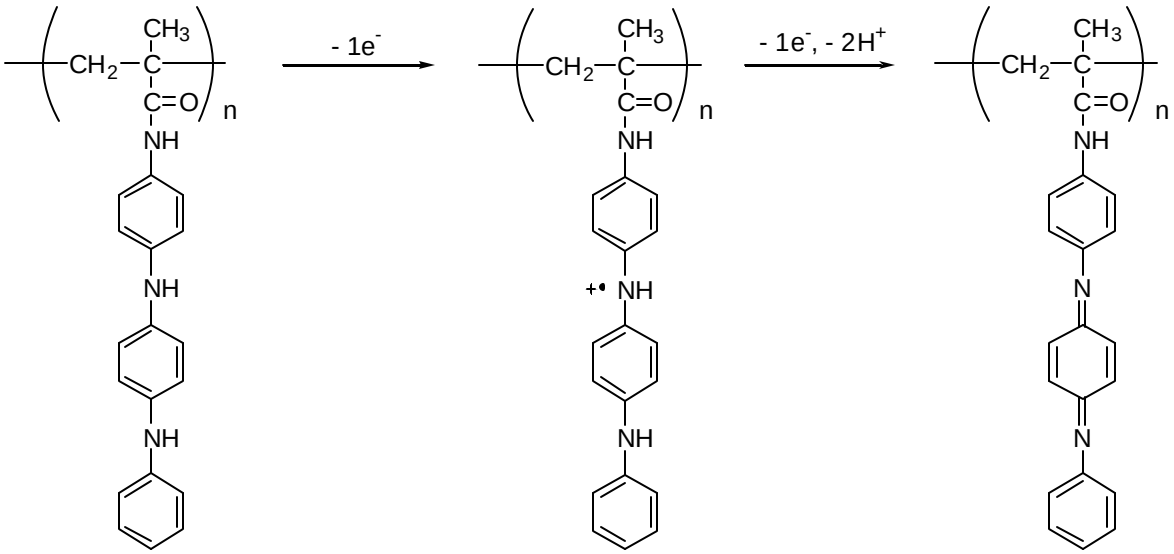

Scheme 12: Proposed oxidation mechanism of polymer 15 in aqueous H_2SO_4 (0.1M).

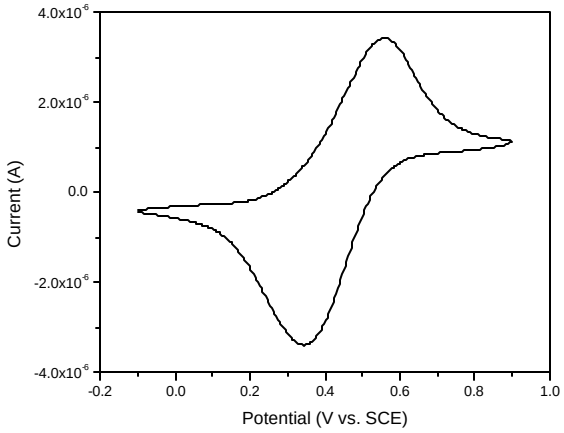

Figure 15: Cyclic voltammogram of polymer 16 in aqueous H_2SO_4 (0.1M).

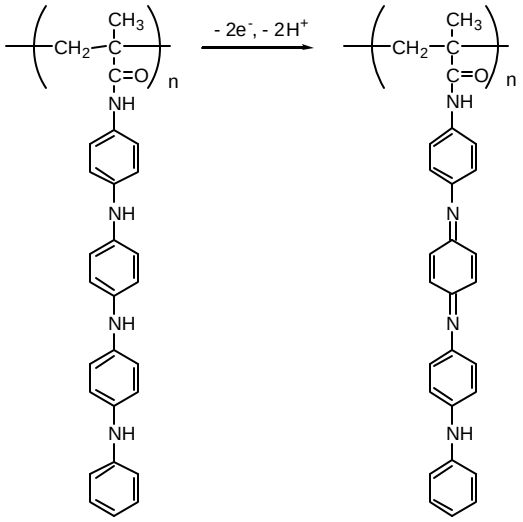

Scheme 13: Proposed oxidation mechanism of polymer 16 in aqueous sulfuric acid (0.1 M)

SERDP FY03

Purification of BAM-PPV:

The scale-up task for FY02 was to produce over 1kg of polymer. 3kg of crude polymer was produced during this period. With the final purification efforts in FY03 more than 2kg of purified polymer was obtained. Soxhlet extraction was used to remove residual potassium chloride produced during the polymerization process. The extraction solvent was a mixture of methanol and water. Samples were taken from each batch and sent to independent laboratories for elemental analysis, which verified that the potassium chloride levels in the polymer had been reduced from approximately 50% by weight to <0.40 % by weight. There are sufficient quantities of monomer precursor (compound 6) and monomer (compound 7) available to produce several additional kg of polymer if necessary (see Scheme 10). Purified polymer yield after Soxhlet extraction (liquid-liquid) was >70%, giving an overall synthesis yield of >30%. Quality assurance was determined by elemental analysis of BAM-PPV polymer for total chloride content. Elemental analysis of BAM-PPV samples which showed an overall chloride content <0.45 % would not result in corrosion failure during neutral salt fog testing. Additional methods of purification of BAM-PPV included mechanical stirring of BAM-PPV in an excess volume of de-ionized water for several days under nitrogen. This process resulted in pure product after drying to constant weight in a vacuum chamber. The chloride content was checked via elemental analysis and the purification procedure could be scaled up for potential industrial use.

EAPs based on Oligomers of Polyaniline:

At RPI in FY03, efforts continued to develop an adherent coating with a high content of aniline oligomer. A series of copolymers containing trimeric methacrylate and n-butyl acrylate was synthesized. The chemical structures of all oligoanilines are shown in Figure 16, and the properties are listed in Table 5.

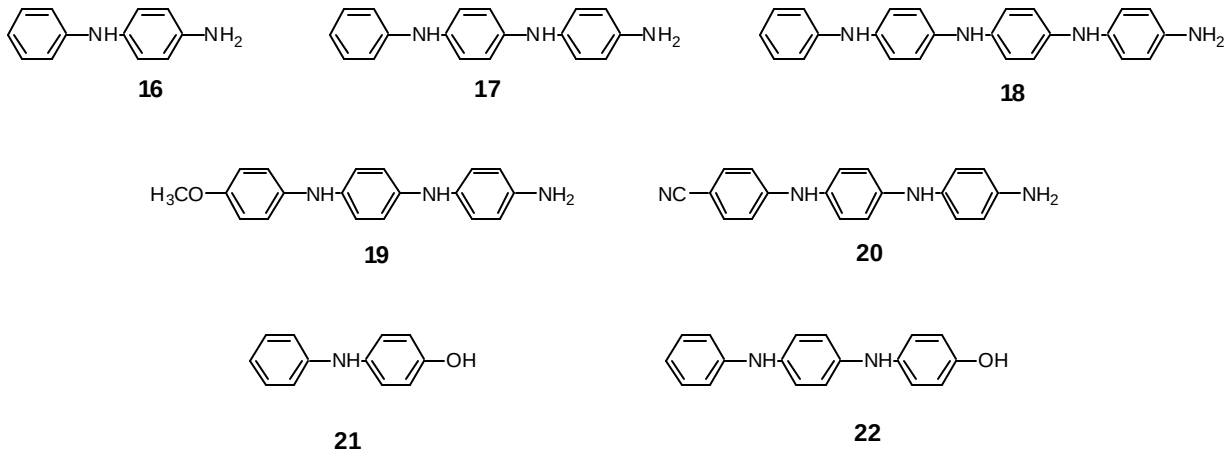

Figure 16: Chemical structures of oligoanilines

Table 5: Optical and Electrochemical Properties of Oligoanilines

	UV-vis (reduced, nm)	*UV-vis (oxidized, nm)*	*Oxidation Potential (V)*	*Conductivity (S/cm)*
16	291	290, 427	0.45, 0.94	3×10^{-6}
17	311	304, 555	0.33, 0.67, 1.40	6×10^{-3}
18	323	303, 577	0.27, 0.54, 0.90, 1.08	4×10^{-2}
19	311	304, 554	0.29, 0.62, 1.25	2×10^{-3}
20	332	329, 565	0.40, 0.76, 1.46	9×10^{-5}
21	285	285, 456	0.75, 1.88	1×10^{-6}
22	309	303, 583	0.44, 0.83, 1.69	9×10^{-5}

A series of oligoanilines were synthesized using palladium-catalyzed aromatic amination reactions (Figure 17), which proved to be an effective reaction for the synthesis of aniline oligomers with controlled length and structure. These oligomers were investigated by NMR (Figure 18), UV-Vis spectroscopy, cyclic voltammetry (Figure 19) and electrical conductivity measurements. The results showed that the electronic absorption, oxidation potential and conductivity were dependent on the length and substitution of the oligoaniline unit. For all oligoanilines, the number of oxidation peaks was equal to the number of repeat phenyl rings in the oligomers, indicating that every unit in the oligomers could be oxidized. The first oxidation potential depended on the chain length of the oligomers. The potentials decreased from 0.45 V (dimer 16) to 0.33 V (trimer 17) and 0.27 V (tetramer 18). The trend of the ease of oxidation indicated that the stability of cation radicals generated in the oxidation increased with the chain length because of longer delocalization range. Electron-donating groups decreased the oxidation potential and had no effect the UV-vis absorption, while electron-withdrawing groups increased the oxidation potential and the UV-vis absorption wavelength. Electrical conductivity was in the range from 10^{-5}-10^{-3} S/cm when the oligoanilines were doped with iodine.

N-(4-aminophenyl)-N'-phenyl-1,4-benzenediamine (17): off – white granules; mp: 148-150 °C. ^{1}H NMR (500 MHz, DMSO-d_6): d 7.64 (s, 1H), 7.26 (s, 1H), 7.12 (t, 2H), 6.92 (d, 2H), 6.85 (d, 2H), 6.81-6.78 (m, 4H), 6.64 (t, 1H), 6.52 (d, 2H), 4.67 (s, 2H). MALDI – TOF MS (MW 275.4). IR (KBr, cm^{-1}): 3381, 3024, 1597, 1514, 1302. Anal. Cacld. For $C_{18}H_{17}N_3$: C, 78.52; H, 6.22; N, 15.26. Found: C, 78.14; H, 6.22; N, 14.96.

N-(4-aminophenyl)-N'-(4-methoxyphenyl)-1,4-benzenediamine (19): off – white granules; mp: 150 – 152 °C. ^{1}H NMR (500 MHz, DMSO-d_6): d 7.34 (s, 1H), 7.14 (s, 1H), 6.86-6.82 (m, 4H), 6.78-6.74 (m, 6H), 6.50 (d, 2H), 4.63 (s, 2H), 3.67 (s, 3H). MALDI – TOF MS (MW 305.4). IR (KBr, cm^{-1}): 3389, 3028, 2931, 1613, 1513, 1238. Anal. Cald. for $C_{19}H_{19}N_3O$: C, 74.73; H, 6.27; N, 13.76. Found: C, 74.46; H, 5.84; N, 12.29.

N-(4-aminophenyl)-N'-(4-cyanophenyl)-1,4-benzenediamine (20): off – white clump; mp: 79 – 181 °C. ^{1}H NMR (500 MHz, DMSO-d_6): d 8.50 (s, 1H), 7.49 (s, 2H), 7.47 (s, 1H), 6.96 (d, 2H), 6.84-6.80 (m, 6H), 6.54 (d, 2H), 4.76 (s, 2H). MALDI – TOF MS (MW 300.4). IR (KBr, cm^{-1}): 3352, 3030, 2207, 1602, 1513, 1307. Anal. Calcd. for $C_{19}H_{16}N_4$: C, 75.98; H, 5.37; N, 18.65. Found: C, 76.65; H, 5.38; N, 18.40.

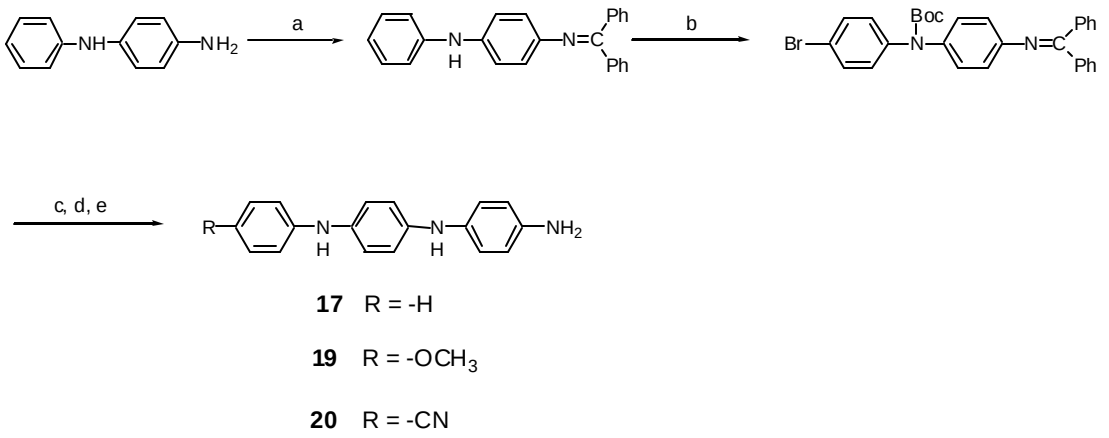

Figure 17: Synthetic procedure to prepare substituted anilines. Key: a) Ph_2O, toluene, reflux, 48h; b) n-Bu_4NBr_3, CH_2Cl_2, RT, 1h; c) aniline or aniline derivatives (4-methoxyaniline or 4-cyanoaniline), $Pd(OAc)_2$, DPEPhos, NaOt-Bu, toluene, 110 °C, 24h; d) compound 17, 19: NH_4HCO_2, Pd/C, THF/MeOH, reflux, 24h; compound 20: $HONH_2$, pyridine, CH_3Cl/THF/EtOH, RT, 15h; e) 180 °C, 10h.

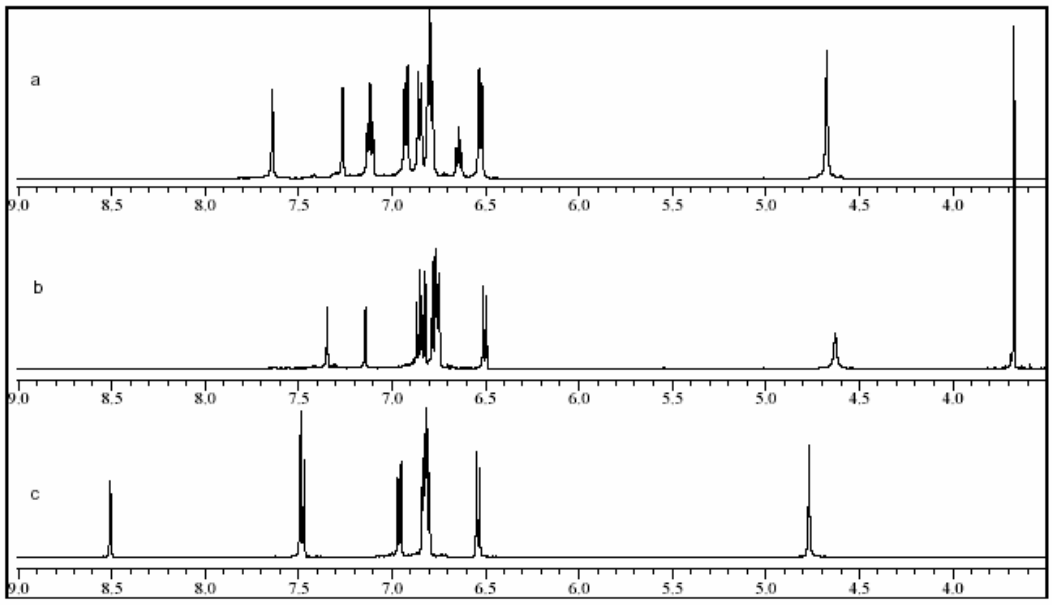

Figure 18: ^{1}H NMR in DMSO-d_6 of a) compound 17;
b) compound 19; and c) compound 20

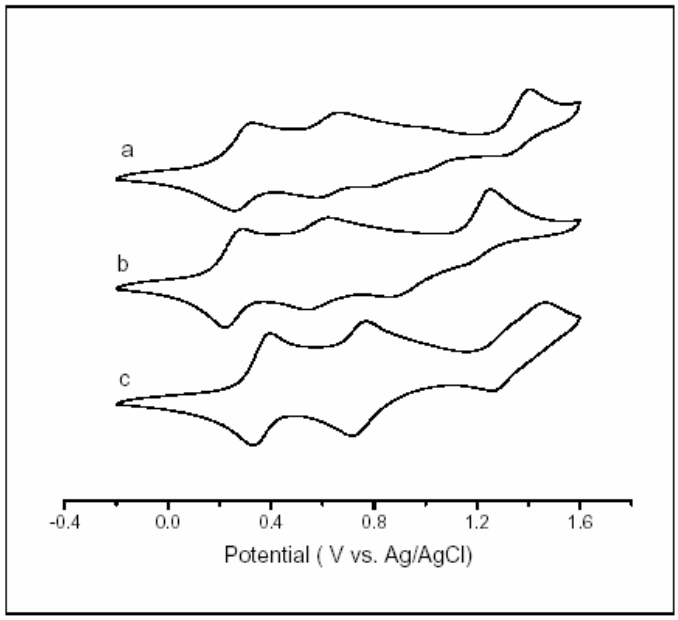

Figure 19: Cyclic voltammograms of a) compound 17; b) compound 19 and c) compound 20 measured in tetrabutylammonium perchlorate (0.1M) at 100mV/s

Once the oligomers were prepared, monomers containing short oligoaniline side chains were directly polymerized by free radical polymerization through careful selection of initiators.

For the monomers containing long oligoaniline side chains, protection of the secondary amine with *tert*-butoxycarbonyl group was crucial for their successful polymerization. The *tert*-butoxycarbonyl groups improved the solubility of the resulting polymers in common organic solvents and were readily removed by thermolysis in an inert atmosphere (Figure 20). The properties of these polymers were summarized in Table 6. Electronic absorption and electrochemical properties of polymers containing oligoaniline side chains were investigated. These properties were dependent on the nature of the oligoaniline side chains and not affected by the polymer backbones. The UV-vis spectra of the polymers in the reduced, oxidized and doped states were similar to that of oligoanilines or polyaniline (Table 7). The wavelength of the absorption maximums changed with oligomer chain length. Both one-electron and two-electron transfer processes were observed during the electrochemical oxidation, and were also dependent on the oligomer chain length.

Monomer 23b: white solid; mp: 178-179 °C. ^{1}H NMR (500 MHz, DMSO-d6): d 10.20 (s, 1H), 7.64(d, 2H), 7.36 (t, 2H), 7.25–7.10 (m, 9H), 6.42 (dd, 1H), 6.25 (d, 1H), 5.75 (d, 1H), 1.37 (s, 18H). IR (KBr, cm^{-1}): 3315, 3043, 2978, 2930, 1711, 1511, 1325, 1161, 1058. Anal. Calcd. for $C_{31}H_{35}N_3O_5$: C, 70.30; H, 6.66; N, 7.93. Found: C, 70.26; H, 6.70; N, 7.92.

Monomer 24b: white solid; mp: 120-121 °C. ^{1}H NMR (500 MHz, DMSO-d_6): d 10.20 (s, 1H), 7.64 (d, 2H), 7.34 (t, 2H), 7.25–7.10 (m, 13H), 6.42 (dd, 1H), 6.25 (d, 1H), 5.75 (d, 1H), 1.36 (s, 27H). IR (KBr, cm^{-1}): 3321, 3044, 2977, 2932, 1711, 1510, 1327, 1161, 1058.Anal. Calcd. for $C_{42}H_{48}N_4O_7$: C, 69.98; H, 6.71; N, 7.77. Found: C, 69.96; H, 6.75; N, 7.75.

Polymer 25b: ^{1}H NMR (500 MHz, DMSO-d_6): d 9.52 (s, 1H, -C(O)NH-), 7.67 (s, 1H, -NH-), 7.29 (s, 1H, -NH-), 7.20-6.50 (m, 13H, Ar), 2.80-2.10 (m, 1H, -CH-), 2.10-0.80 (m, 2H, -CH_2-). IR (KBr, cm^{-1}): 3385, 3035, 2932, 1664, 1601, 1513, 1303, 1024.

Polymer 26b: ^{1}H NMR (500 MHz, DMSO-d_6): d 9.52 (s, 1H, -C(O)NH-), 7.67 (s, 1H, -NH-), 7.59 (s, 1H, -NH-), 7.29 (s, 1H, -NH-), 7.20-6.50 (m, 17H, Ar), 2.80-2.10 (m, 1H, -CH-), 2.10-0.80 (m, 2H, -CH^2-). IR (KBr, cm^{-1}): 3384, 3039, 2930, 1663, 1600, 1511, 1298, 1024.

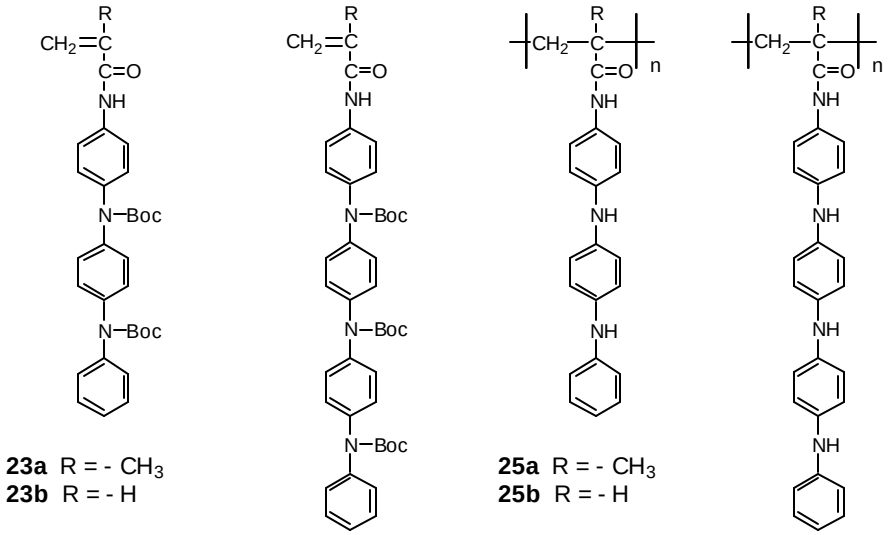

Figure 20: Chemical structures of poly(acrylamide)s

Table 6: Properties of Deprotected Polymers

	M_n (10^3)	M_w (10^3)	*PDI*	$T_{5\%}$ (ºC)	T_g (ºC)
25a	20	33	1.6	261	162
25b	14	25	1.8	298	142
26a	3.4	4.6	1.4	317	120
26b	13	25	1.9	316	112

Table 7: Peaks From UV-vis Spectra of Oligoaniline Side Chain Polymers

	Reduced (nm)	*Oxidized (nm)*	*Doped (nm)*
25a, 25b	317	308, 481	270, 391, 752
26a, 26b	320	311, 565	302, 420, 789

Additional work for FY03 focused on preparing monomers containing oligoaniline side chains that were incorporated into copolymers by free radical polymerization. Copolymerization was carried out in DMF at 70 ºC with AIBN as an initiator. The composition of the copolymers was calculated from the integration ratio of the proton resonance at 4.0 ppm (-OCH_2-) and approximately 8 ppm (Ar-NH-Ar) in proton NMR spectra (Figure 21). The composition was also obtained from the nitrogen content in the copolymers from elemental analysis. The molecular weights of copolymers 27 were in the range from 2.3×10^4 to 5.1×10^4. These polymers were stable up to 300 ºC. The glass transition temperature T_g increased from –2 ºC to 96 ºC when the fraction

of oligoaniline methacrylate increased from 10% to 70% (Table 8). This demonstrated that the monomers with oligoaniline side chains were able to polymerize with butyl acrylate. Polymer properties such as glass transition temperature were adjusted through copolymer composition. The cyclic voltammetry of copolymers 27 was carried out in H_2SO_4 (1.0 M) solution. The voltammograms have similar features as that of oligoaniline methacrylate homopolymer. The electroactivity of the side chains was observed through the entire copolymer composition range. The oxidation peaks were observed and the oxidation potentials did not change with the composition, indicating that the butyl acrylate repeat units did not alter the fundamental electrochemistry of the oligoaniline side chains.

Sixteen samples were prepared for corrosion testing at NAWCWD. These samples consisted of standard polyaniline made at RPI and spray-coated onto test panels. These samples were sent to China Lake for neutral salt-fog testing (see Section VII B).

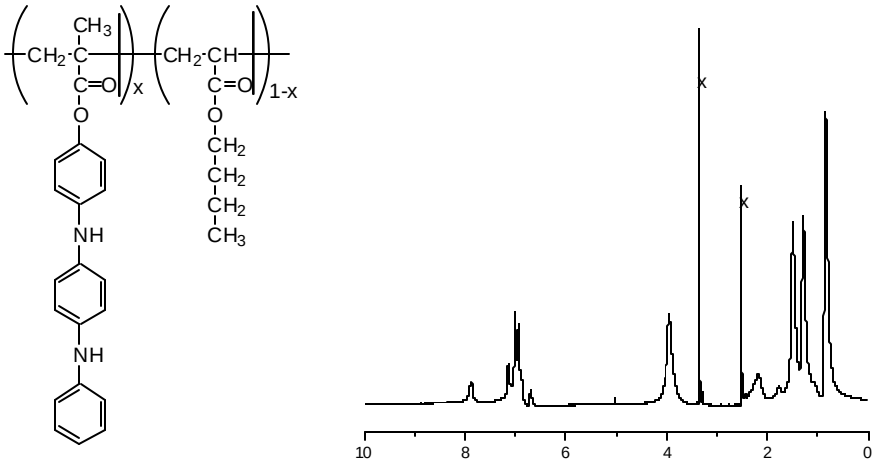

27

Figure 21: ^{1}H NMR of copolymer 27 in DMSO-d_6

Table 8: Properties of Copolymers 27

	Feed Oligoaniline Methacrylate (mol%)	*NMR (mol%)*	***Elemental*** *(mol%)*	M_n (10^3)	M_w (10^3)	*PDI*	$T_{5\%}$ (°C)	T_g (°C)
a	10	12.5	13.6	51	120	2.3	302	-2
b	27	40.6	43.7	23	43	1.9	304	65
c	50	61.1	67.3	50	120	2.3	304	94
d	59	71.5	78.9	32	63	2.0	299	96

Initial Studies Assessing the Interactions of BAM-PPV with Supercritical carbon dioxide ($SCCO_2$):

The objective of this work, performed at Virginia Commonwealth University (VCU), was to measure the degree of interaction of BAM-PPV with $SCCO_2$. These interactions became the

foundation of a database that guided the choice of polymer compositions that can be applied as coatings from this environmentally benign solvent. Few polymers are completely soluble in $SCCO_2$. Amorphous polymers including poly(dimethylsiloxane)s and fluoropolymers are often miscible. While most polymers are immiscible in $SCCO_2$, $SCCO_2$ shows surprising solubility in the polymer solid state. That is, most polymers investigated thus far are *swollen* by $SCCO_2$. The degree of swelling (interaction) depends on functional groups present, crystallinity, temperature, and pressure. The interaction of polymers with $SCCO_2$ is highly variable. The degree of swelling depends on crystallinity, polymer microstructure (nature of the repeat), functionalization, pressure, and temperature.

The apparatus for measuring swelling behavior (Figure 22) employs a linear variable displacement transducer (LVDT) that is commonly used in quality control measurements. This is coupled with a pressure / temperature capability. In our high-pressure system, we measure the linear dimensional change of a solid polymer in contact with $SCCO_2$ with an accuracy of 1%. Our current system measures the linear dimensional change over the temperature range from 25 – 300 °C and at pressures up to 680 bar (10kpsi).

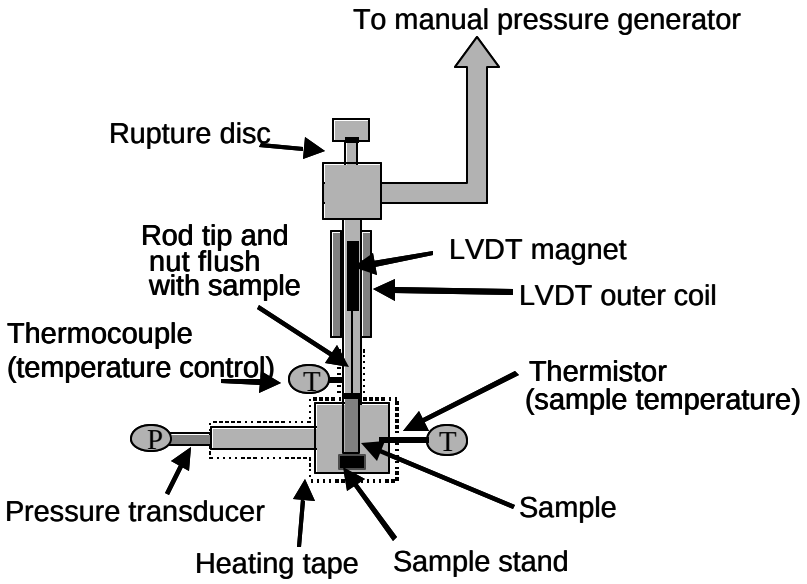

Figure 22: LVDT apparatus for measuring swelling of BAM-PPV.

Materials:

Liquid CO_2 (bone dry, 99.8%) was obtained from Roberts Gas Company. Two groups of samples of BAM-PPV were obtained "BAM-PPV-1" and BAM-PPV-2. All BAM-PPV samples were supplied by China Lake and were from the same polymerization batch; thus, molecular weights and other characteristics of the various samples used by VCU are identical—only processing methods change. BAM-PPV-1 was received in February 02 while BAM-PPV-2 was received in May 02. BAM-PPV-1 samples had two processing histories. BAM-PPV-1CL were compression pressed at China Lake. The samples were easily fractured back into flakes. Other samples were melt pressed at VCU (BAM-PPV-1VCU) in a cylindrical shape (4 mm in diameter

and 10 mm in length). BAM-PPV-2 samples were melt pressed and cut at China Lake; bars were 2 mm x 3 mm and 7 mm "high").

General Analytical Procedure:

Differential scanning calorimetry (DSC) measurements were carried out using a Perkin Elmer DSC Pyris-1. *LVDT System:* All pipes and fittings were stainless steel (316SS) parts (pressure rating 1360 bar) from High Pressure Company (HiP), Erie, PA. A Loctite Silver Grade Anti-Size joint lubricant obtained from McMaster-Carr was applied to chamber fittings to extend coupling life. Polymer swelling measurements in $SCCO_2$ were carried out in an apparatus consisting of two sections, a pressure generating section and a sample chamber (Figure 23). The pressure generating section (not shown) is similar to that employed previously for measuring polymer phase behavior in supercritical fluids.[19]

A standard LF9 T-fitting was employed as the sample chamber. A pressure transducer (Omega PX-602) rated at ±0.4% full scale (±3 bar) and resistive temperature device (RTD) were attached to the arms of the T. The vertical T-opening was attached to a nonmagnetic steel pressure pipe that was surrounded by the LVDT outer coil. The entire assembly was connected to the pressure generating section through LF6 T-fitting.

Polymer swelling was measured with a linear variable differential transformer (LVDT) coil (Schaevitz Sensors, Hampton, VA). The coil surrounded a section of the nonmagnetic steel pressure pipe described above. A thin (1.8mm) nonmagnetic threaded follower rod (Schaevitz catalog # 05282945-006) was fitted with a cylindrical magnet (2.8mm OD) and placed inside the steel pressure pipe.

Safety features: A rupture disk (» 850 bar) was connected to the top of the T-fitting as shown in Figure 22. In addition to pressure measurement near the sample on the $SCCO_2$ side, a gauge was used to measure pressure on the water side (Standard Gauge 6PG20, HiP). The lowest pressure rated component in the system was rated to at least 1020 bar giving a substantial safety margin. A well secured ¼ inch thick polycarbonate shield was placed between personnel and the high-pressure system. The pressure, temperature, and displacement meters were placed on the personnel side of the system.

Linear Swelling: The sample bar was placed in the chamber on an insulated stage consisting of a thin graphite rod wrapped in aluminum foil. A small nut was fitted on the follower rod to distribute the mass of the magnet and follower rod (3 g) over the sample. The follower rod was then placed on the sample. Applying appropriate torque to the fitting connecting the sample chamber to the steel pressure pipe/LVDT assembly sealed the system. The sample chamber was purged with CO_2 and pressurized.

The sample size (≈ 0.07cc, 0.14g) resulted in a convenient rate of dilation for manual data collection. Typically, total time for data acquisition after a change in P or T was 2 hrs. The swelling results are reported as % fractional change in the sample length $(\Delta L/L_o)\%$, where $\Delta L = L_t - L_o$, L_t is the length of the sample at time t, and L_o is the initial sample length. Data was not curve-fit; curves in figures are guides for the eye.

For constant temperature experiments, the sample was first heated to the desired temperature. Then, CO_2 was slowly introduced into the chamber, and the pressure was increased to the first pressure stage, 138 bar. LVDT readings were noted at regular intervals. When the sample had attained its maximum swelling, LVDT readings remained constant for 20-30 minutes. The pressure was then increased slowly to the next stage (276 bar) with the help of the manual pressure generator and the LVDT readings noted again. LVDT data was obtained for

pressures from 138 bar to 690 bar. The same methodology was followed as the pressure was decreased from 690 bar to 138 bar. This allowed measurement and evaluation of hysteresis.

For constant pressure experiments, $SCCO_2$ pressure was increased to the desired value at a temperature below T_m. LVDT readings were noted at regular intervals. When the sample attained maximum swelling, the LVDT readings remained constant for 20-30 minutes. The temperature was then increased by 2-3°C incrementally, while employing the manual pressure generator to maintain constant $SCCO_2$ pressure. At T_m, $\Delta L/L$ decreased markedly due to sample softening / melting. The experiment was terminated a few degrees above T_m.

VCU began their experiments with BAM-PPV powder (BAM-PPV-1) provided by NAWCWD. From this material VCU melt pressed several pellets, designated BAM-PPV-1VCU. Further experiments were then conducted on samples BAM-PPV that were melt pressed at NAWCWD, designated BAM-PPV-2. The data for BAM-PPV-1 samples are discussed first followed by those BAM-PPV-2 samples.

As received BAM-PPV-1 samples "flaked", that is these samples had a laminated appearance and fractured along the lamination interfaces. A few BAM-PPV-1 samples were manually melt pressed at VCU and are designated BAM-PPV-1VCU (vs. as received samples from China Lake, BAM-PPV-1CL). Figure 23 shows swelling as a function of pressure at 110°C for BAM-PPV-1VCU. At relatively low pressure, 138 bar (2000 psi), the sample swells 2%, a modest amount at best. By increasing the pressure to 276 bar (400 psi) resulted in a 3% swelling, while at higher pressures yielded only a maximum swelling of about 4%.

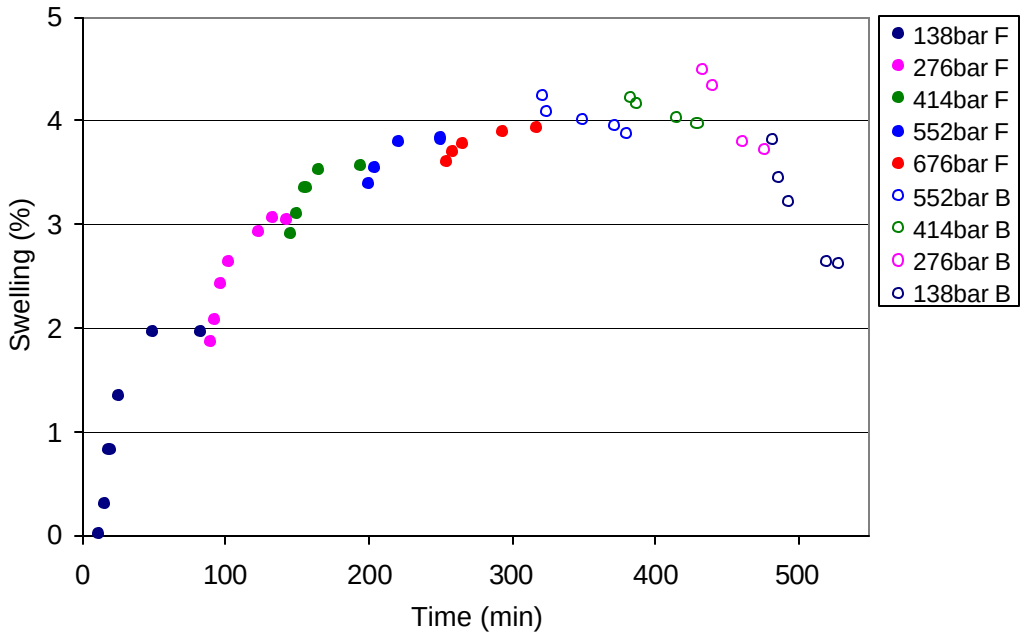

Figure 23: BAM-PPV swelling ($\Delta L/L_o$) result for LVDT constant temperature experiment at 110 °C (P = 138-676 bar).

Lowering the pressure after reaching 680 bar (10 kpsi) resulted in some hysteresis characteristic of sample distortion (Figure 24). This means that at the higher pressures we are close to T_m of BAM-PPV-1VCU. Indeed, inspection of the data at 130°C shows an irreversible loss in linear dimension characteristic of reaching T_m. An important conclusion is that the T_m of BAM-PPV-1VCU is very sensitive to CO_2 pressure. That is, less than 280 bar (4000 psi) $SCCO_2$ lowers the melting point of BAM-PPV-1VCU by about 40°C.

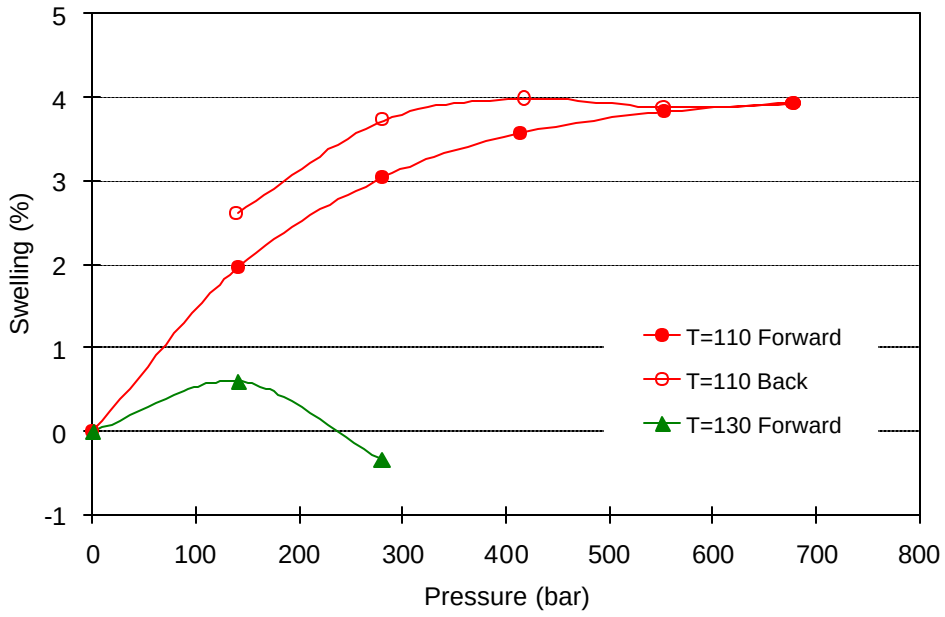

Figure 24: BAM-PPV swelling ($\Delta L/L_o$) results for LVDT constant temperature experiments at 110, 130 °C.

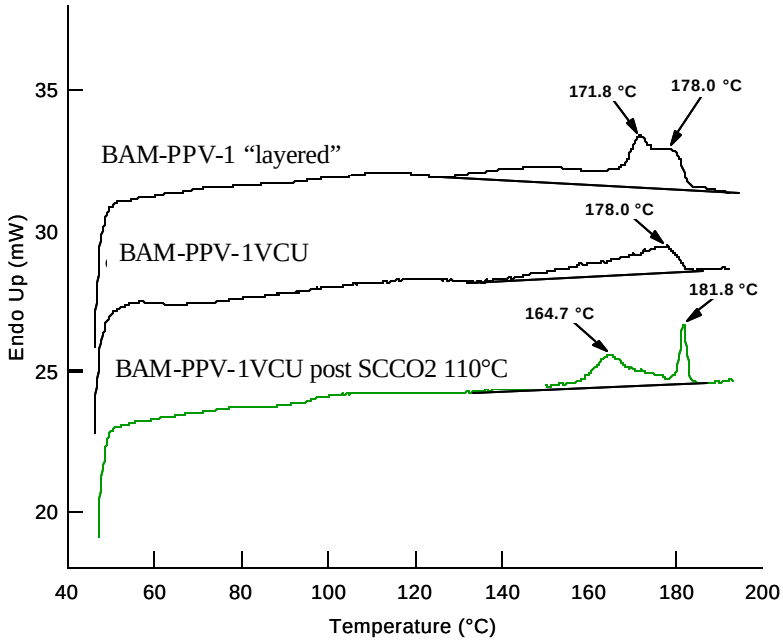

Figure 25: DSC data for BAM-PPV-1

The DSC data for BAM-PPV-1VCU before and after $SCCO_2$ processing are shown in Figure 25. The topmost curves are for the as-received sample. The middle curves are for VCU-melt pressed material and the lowest curve is the post-110°C $SCCO_2$ processed material. The VCU melt pressed sample (middle curve) was cooled quickly in air from 200°C. The DSC is

rather broad in the melting range of 175°C. After treatment with $SCCO_2$ in the course of swelling experiments (140 – 680 bar, then 680 bar – 140 bar or 2-10 kpsi, then 10 – 2 kpsi) the DSC shows markedly improved crystallinity characterized by sharp melting peaks at 164.7°C and 181.8°C. Note that the lower melting broad endotherm at 150°C is absent; this is another sign of increased order in the $SCCO_2$ treated samples.

BAM-PPV-2 samples were melt-pressed at China Lake. Various sized blocks were received and swelling measurements were made directly on these materials. Figure 26 shows typical constant temperature (90°C) LVDT data for BAM-PPV-2. While the overall trend is the same (as for BAM-PPV-1VCU), the quantitative result is quite different. The maximum linear expansion is barely greater than 2%.

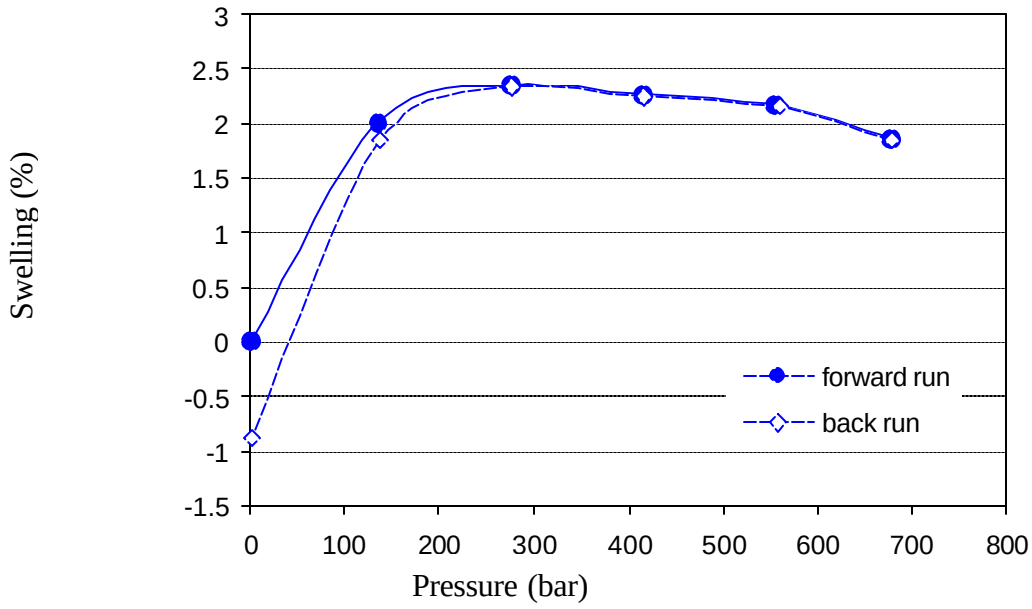

Figure 26: BAM-PPV-2 swelling (?L/L_o) results for LVDT constant temperature (90°C) experiments.

Figure 27 summarizes swelling data at constant pressure for BAM-PPV-2. It is best to consider the data in nitrogen first. The LVDT data show that the sample in nitrogen never shows signs of swelling. This is in keeping with the fact that nitrogen is a "noninteracting" gas.[20] BAM-PPV-2 starts to lose its dimensional integrity even at 120°C. This is a very slow process as each data point represents attainment of equilibrium over the course of an hour. BAM-PPV-2 continues to shrink a small amount with increasing temperature until melting is observed at about 160°C.

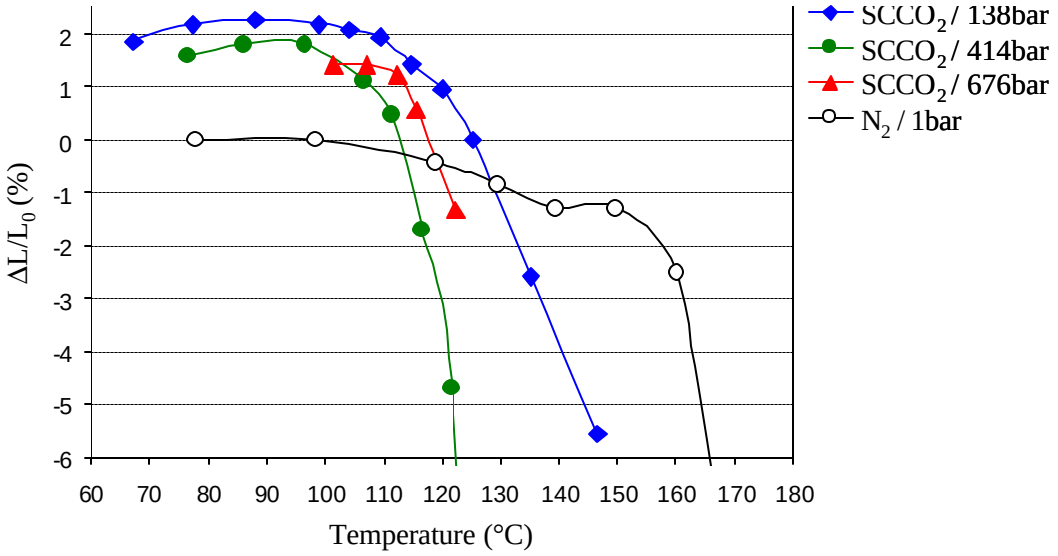

Figure 27: LVDT swelling data for BAM-PPV-2.

The results for $SCCO_2$ depression of T_m at constant pressure are shown in Figure 28 and summarized in Table 9. It is seen that the T_m of BAM-PPV-2 is depressed around 50°C. This is quite remarkable considering the low solubility evidenced by the low swelling. Even at 140 bar (2 kpsi), T_m is depressed by 40°C. An important point is that the maximum depression in T_m occurs at 414 bar (6 kpsi). At 680 bar (10 kpsi) T_m increases due to hydrostatic pressure effects. A puzzling feature of all the DSC's is a more-or-less prominent low temperature endotherm in the vicinity of 120°C, which is strikingly ***absent*** in the DSC of the "nitrogen" sample.

Table 9: Summary of melting point depression and maximum swelling of BAM-PPV-2 samples.

	Pressure (bar)	Melting T (°C)	max. $\Delta L/L_o$ (%)
$SCCO_2$	138	117	2.3
$SCCO_2$	414	105	1.9
$SCCO_2$	676	112	1.4
N_2	1	158	-

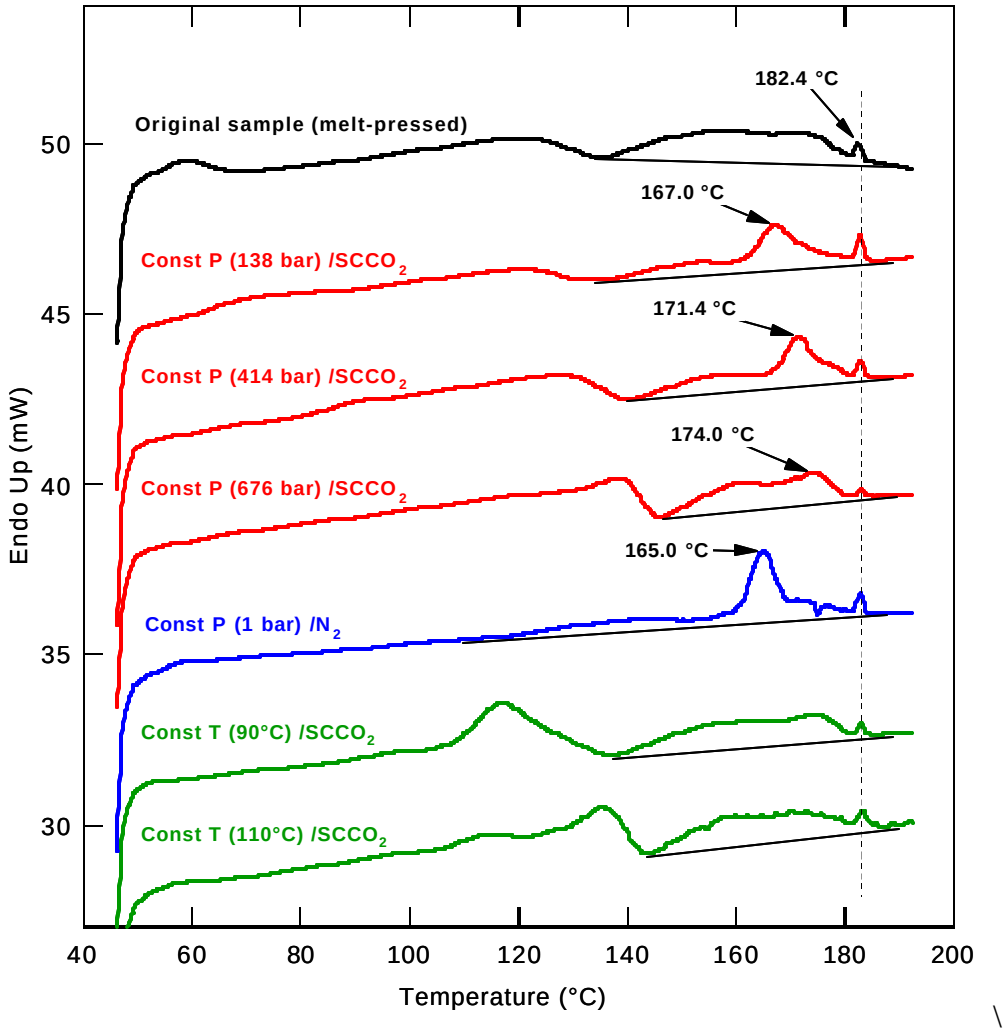

Figure 28: DSC data for BAM-PPV-2. Top curve is as-received.

The DSC of the latter was run after the LVDT experiment shown in Figure 28. That is, the sample was heated in nitrogen to about 10°C above (170°C) the LVDT determined T_m (160°C) and cooled to ambient temperature. The resultant DSC is labeled "constant P, N_2 1bar. The DSC is striking in showing a minimal low temperature endotherm and well-resolved melting peaks at 165 and 182°C. It is emphasized that "second scans" of all samples after finishing each first run at 190°C were identical with the topmost "as received" BAM-PPV-2 sample. That is to say, the "170°C" nitrogen DSC first scan reverts to the topmost DSC scan, which is indistinguishable from any of the "190°C" second scans. It is noted that the cooling rates in the LVDT experiment are much slower than in the DSC experiment.

A consistent feature is the increased temperature of the melting endotherms in the $SCCO_2$ processed samples. This is easily understood as crystallization is more facile in the plasticized material and crystalline phases have higher order leading to higher T_m's. BAM-PPV is poorly crystalline with very low heats of melting (8-16 J/g). The thermal transitions of BAM-PPV are highly processing dependent. The T_m of BAM-PPV can be lowered by 40-50 °C under moderate $SCCO_2$ pressures. After $SCCO_2$ processing, samples have higher order as reflected in higher

temperature DSC melting endotherms. Despite similar processing histories, BAM-PPV-1VCU has different swelling behavior and different DSC characteristics than BAM-PPV-2.

Several approaches were undertaken to improve the processability of BAM-PPV in $SCCO_2$ during FY04. A co-solvent was investigated that could also be used with $SCCO_2$ to improve processability.

FY04 RESULTS

Synthesis of Water-Dispersible BAM-PPV Derivatives

A modified synthetic route was developed for EO3-PPV (Poly [2,5-bis (triethoxy-methoxy)-1,4-phenylene vinylene], also called ' BTEM-PPV'), and a further modified Gilch polymerization process (simultaneous addition of base and monomer at a controlled rate) was developed for the preparation of its random copolymers with BAM-PPV (poly [2,5-bis (N-methyl-N-hexylamino)-1,4-phenylene vinylene]) at various monomer ratios. One of the BAM/EO3-PPV random polymer with composition BAM: EO3 ≈ 1:1.8 showed no less than 20 wt% water-dispersibility. The BAM-PPV derivatives were prepared by Dr. John Ferrais at the University of Texas, Dallas (UTD). Although there's a reported synthetic route to prepare the bis-chloromethyl monomer of EO3-PPV, a new synthetic route for the bromomethyl derivative was developed to achieve a better yield and more facile purification (Scheme 14).[21] An overall yield of 34% for the EO3-PPV monomer was achieved in this synthetic route, which was a significant improvement from the <10% yield reported for the chloromethyl derivative, due in part to the facile purification procedure (purification of 1 was achieved through simple filtration through alumina; 2 could be used as isolated; and 3 was purified by recrystallization of the crude product from ether. The resulting product was copolymerized with the monomer, 2,5-bis-(chloromethyl)-4-hexamethylamino)phenyl)hexamethylamine dihydrochloride, for BAM-PPV polymer. The BAM/EO3 random copolymers with different composition ratios (BAM:EO3 = 4:1; 1:1; 1.8) were successfully prepared and fully characterized. Scheme 15 outlines the preparation of random copolymers at different monomer ratios.

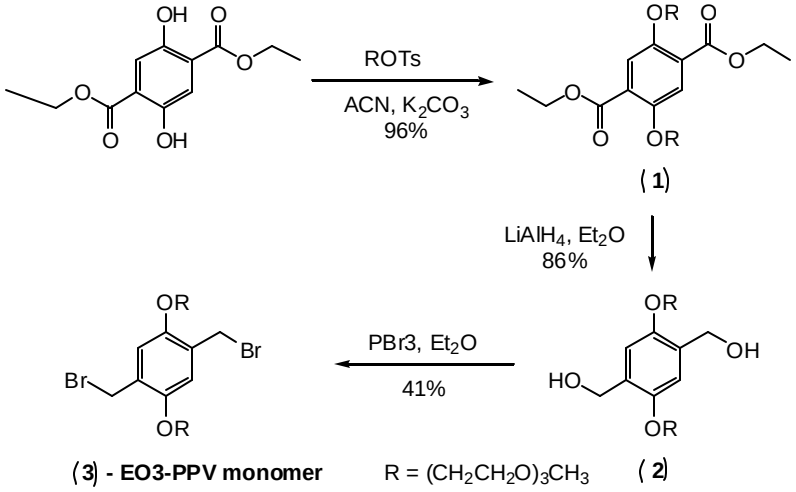

Scheme 14: BTEM-PPV Improved Synthetic Route

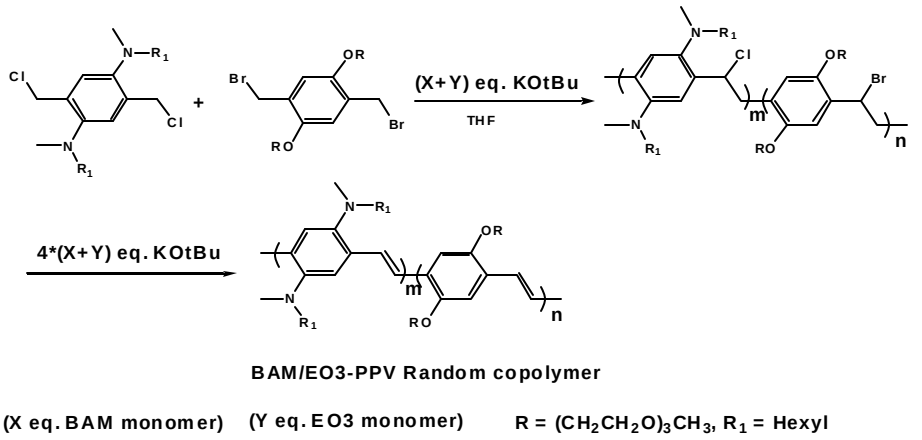

Scheme 15: Preparation of Random Copolymers of BAM/EO3-PPV

A representative procedure for preparing these copolymers is presented below. A three-neck round bottom flask is equipped with N_2 inlet and charged with 100ml dry THF. N_2 is bubbled into THF for 1hr, and the temperature is lowered to 0 °C using an ice-water bath. BAM monomer free-base (freed from the HCl salt by dissolution in water, neutralization by cold aqueous NaOH, extraction with ether and dried over magnesium sulfate ($MgSO_4$)) (0.60 g, 1.5 mmol) and EO3 monomer (2.65 g, 3.0 mmol) in 20 ml dry THF in one syringe and KOtBu (0.708 g, 6 mmol) in 20 ml dry THF in another syringe are simultaneously injected into the reaction at a rate of 20 ml / hr via a syringe pump. Upon completion, KOtBu (2.832 g, 24 mmol)/50 ml dry THF is injected at the rate of 17 ml/hr. Then the ice-water bath is removed and reaction is heated to reflux for 3hr. The reaction is then cooled to room temperature, and the polymer is precipitated by adding 800 ml MeOH. The suspension was filtered through a 0.45µ filter paper, and the solids washed with MeOH and H_2O until pH was neutral. The resulting red brown polymer was dried in a vacuum oven (50 °C for 4hr) to obtain 1.6g (70 %, actual composition ratio was BAM: EO3 ≈ 1:1.8 as estimated by ^1H NMR spectrum). The polymer was tested for its water dispersiblity and results are described as follows: 10 mg of each BAM/EO3 copolymer samples with different composition ratios were placed into separate vials containing 20ml distilled water and a small magnetic stirrer, and the samples were stirred at room temperature continuously for 1-2 weeks. Only BAM/EO3 copolymer sample (B:E ≈ 1:1.8) gave a visually homogeneous red solution/suspension. Filtration of this sample through a 0.45 micron membrane filter gave a colorless liquid filtrate with all solids retained on the filter membrane. This indicates that the sample was a suspension, and not a true solution. This copolymer composition could be dispersed in water at concentrations up to 20wt% (0.20g of polymer in 1ml distilled water; stirring for 1week) to afford a visually homogeneous red solution from which a visually homogenous film on a glass substrate could be cast. These solutions were spray coated from a water-THF based system onto Al 2024-T3 substrates and dried. The resulting films were

tested in a neutral salt fog spray chamber as a pretreatment coating and all coatings failed at 24 hours.

BAM-PPV Physical Properties and $SCCO_2$ Studies

General Analytical Results:

DSC was performed using a TA Instruments 2910 Differential Scanning Calorimeter at a heating rate of 10°C/min under nitrogen. TGA was performed using a TA Instruments 2950 TGA scanning at 5°C/min (under nitrogen and air). ^{1}H and ^{13}C NMR data was acquired using a Bruker 400MHz NMR spectrometer at 300K.

Single beam FTIR spectra were acquired from the polished and freshly cleaned aluminum plates using a FT-85 Fixed 85° Grazing Angle spectral reflectance accessory with a constant *p*-polarized light component. A Nicolet 870 FTIR spectrometer was used. Spectral resolution was 8 cm^{-1} and 10,000 scans were acquired. The single beam of a clean Al plate was used for all subsequent spectra as a reference background.

Additional BAM-PPV samples were sent to Virginia Commonwealth University (VCU). These samples were 2x3x7-mm rectangular bars that had been compression molded at 150°C and 10,000 psi and are designated BAM-PPV-2, consistent with the labeling in our earlier report. The second samples were 2x4x10-mm bars that also had been compression molded at 150°C and 10,000 psi. The processing of these materials at China Lake involved additional steps and the use of methylene chloride solvent. These second samples are designated BAM-PPV-3. The third sample was a 1 g portion of polymer flake and is designated BAM-PPV-F-1.

Carbon dioxide, Ingredient Grade with a specified purity of at least 99.9%, was purchased from Roberts Oxygen Company, Inc. It was pumped directly as a liquid from a cylinder fitted with a siphon tube. Films of BAM-PPV were compression molded from BAM-PPV-F-1 polymer flake with a Model 2702 Carver Laboratory Press. The unit was equipped with 9x9" electrically heated platens that could be cooled with chilled water. Chromalox Model Number 3910-51104 controllers maintained the molding temperature within a range of about ±5°C. A 0.2-mm thick window frame was fashioned from layers of aluminum foil in which a 15x30-mm opening had been cut. To prepare a sample for molding, a piece of 24-mil 304 stainless steel sheet was the first layer, covered next with a 5-mil thick PTFE film and then the window frame. About 140 mg of the BAM-PPV flake was evenly spread in the opening of the frame, and the sandwich was completed next with the PTFE film and finally the stainless steel sheet. Two 8x8x3/8" aluminum plates were placed between the platens, and the press was closed and heated to 205-215°C. A small hole had been drilled from edge to center in each of the aluminum plates so the temperature could be monitored with a calibrated thermocouple. When the press was at temperature, it was opened briefly, and the sandwich described above was placed between the aluminum plates. The press was closed and about 5,000 lb of force was applied for approximately a minute. Then the full force of 25,000 lb was applied, and after about 10 min total time in the press, the sample was cooled by applying chilled water to the plates. The 25,000 lb force was maintained as the unit cooled to ambient temperature in about 10 min.

Thermal analysis was performed on these samples using standard and modulated DSC (MDSC) measurements were made with a TA Instruments Q1000 DSC. MDSC was the more effective technique and ultimately allowed interpretation of the polymer thermal behavior. Accurately weighed samples of 5-10 mg were sealed in tared, standard aluminum pans. Three

complementary methods were employed. Generally the calorimetry was performed in nitrogen while heating from –85 to 230°C or while cooling from 200 to –85°C. The ramp rate was always 3.0°C/min and the modulation cycle was ±1.0°C/60 sec. To assure accuracy of the sample results, the instrument calibration was checked frequently by performing standard DSC measurements on indium reference materials. The thermal stability of BAM-PPV samples was estimated with a TA Instruments Q500 TGA. Samples weighing 5-10 mg were placed directly on tared platinum pans and heated in nitrogen or air from ambient temperature to about 800°C. Measurements were conducted employing the default conditions of the High-Resolution Dynamic procedure. The heating rate was variable – as high as 50°C/min when no weight loss was occurring and very much slower when the sample was undergoing decomposition. The mechanical properties of BAM-PPV compression molded films were measured as a function of temperature with a TA Instruments Q800 DMA. The rectangular samples were about 0.24-mm thick and ranged in width from 7.6-9.0 mm. They were mounted in a Tension: Film type clamp with gauge lengths that ranged from 13.7-17.8 mm and preloaded with a force of 0.1 N. An oscillation amplitude of 10.0 µm was specified, so the maximum strain was +0.07% or less. The Temperature Step / Frequency Sweep method was employed where data were collected from –40 to 100°C and 0.1-100 Hz at a resolution of two points per decade.

Polymer linear expansion was measured with a LVDT equipment as previously described in section FY03. Unless otherwise noted, the reactor hardware was purchased from High Pressure Equipment Company (HiP) and the sensors from Omega Engineering. The body of the cell was a female to female coupling (20-21LF6LF9-SP1) connected at the top to the gas manifold by a 10x3/8" nipple (20-LM6-10) and sealed at the bottom by a thermocouple assembly through a female to male adapter (15-21AF2LM9-T). The Type-K calibrated thermocouple with a 1/8" stainless steel sheath (KQSS- 18U-07-CL5) was capped with a piece of graphite rod center-drilled to fit loosely over the sheath. The graphite rod extended about 10 mm into the cell and formed the stage on which samples stood. The LVDT coil assembly (LD200-7.5 with LVDT signal conditioner LDX-3A) fit snugly around the 10x3/8" nipple. The LVDT core that was supplied by Omega Engineering was replaced by a 0.108x2.00" core and Type 303 stainless steel threaded connecting rod from Schaevitz Sensors, Division of Measurement Specialties, Inc. (catalog number 05561639-000 and 05282976-012 respectively). The core and rod assembly was small enough to fit inside the 3/8" nipple, and when finished with a M2 hex nut as a foot to increase the area that contacted the sample, the entire unit weighed 4.59 g. The reactor was heated by a 120-watt, 9" long cylindrical BriskHeat mantle that was custom fabricated by BH Thermal Corporation (model VCU271001). The LVDT was calibrated by noting the voltage output as the connecting rod was moved up and down around the zero position with a 40-turn/in micrometer. The linear portion of the distance versus voltage curve greatly exceeded the displacement ever observed for any polymer sample. During an experiment, a rectangular polymer bar was positioned on its end on the graphite stage. The LVDT connecting rod was placed on the top end of the sample, and changes in position were noted as the temperature and CO_2 pressure were changed. Before or after the expansion of a polymer sample was measured, the dimensional changes of the empty cell were also determined in an identical sequence of temperature and pressure changes. These cell corrections were appropriately combined with the observed experimental results. In the cell correction setup, more of the LVDT connecting rod was in the heated part of the equipment than during the actual experiment with a polymer sample. The thermal expansion [17.2 µm/m-°C for 303 stainless steel] of this extra length, which is exactly equal to the sample size, was accounted for and added as a correction.

Methods :

Thermal analysis of BAM-PPV has been carried out to determine the glass transition temperature, thermal decomposition temperature and stability of the polymer. The results have shown BAM-PPV to be thermally stable and can undergo normal processing conditions without degradation.

A differential scanning calorimetry (DSC) plot of BAM-PPV powder was run. Figure 29 shows a low temperature plot (2^{nd} heating) and is measured in nitrogen atmosphere. The DSC scan shows that the glass transition temperature (Tg) of BAM-PPV is 9^{o}C. A small endotherm at this temperature indicates that the transition has some melting. This may be due to the short side chains becoming liquid-like. A high temperature DSC plot of BAM-PPV (Figure 30) reveals that the BAM-PPV contains crystal regions melting near 175^{o}C.

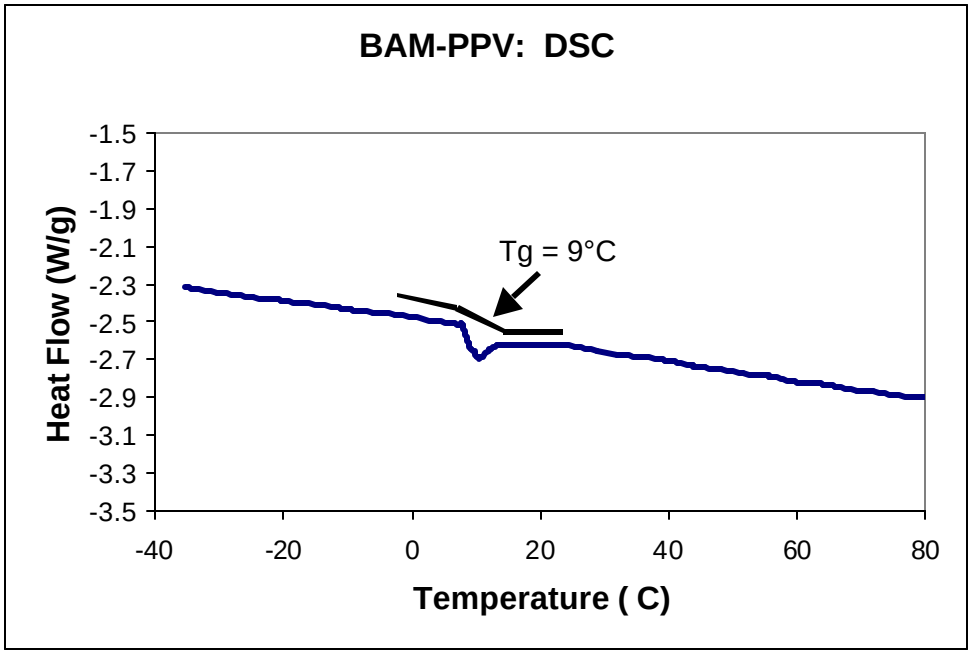

Figure 29: Low-temperature DSC plot of BAM-PPV

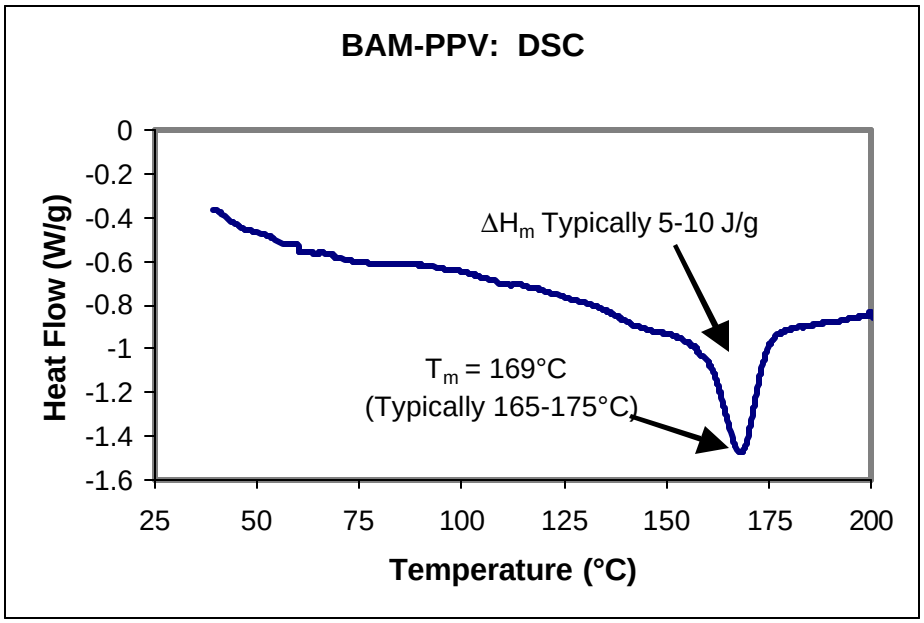

Figure 30: High-temperature DSC Plot of BAM-PPV

Thermogravimetric analysis (TGA) (Figure 31) shows the weight loss of BAM-PPV produced via Scheme 10 as a function of temperature. The 5% weight loss temperature is about 282°C in nitrogen. This weight loss is associated with a strong endotherm in the DSC plots (Figures 29 and 30), which begins at 200-250°C. Thus, the thermal analysis of BAM-PPV is confined to temperatures of 225°C or less in order to ensure the stability of the samples. Almost all processing conditions for paint formulations operate well below this temperature. The TGA plot of BAM-PPV is heated to 120°C for 2 hours and then cooled to ambient temperature. The sample is re-heated to 500°C at 10°C/minute and the plot shows complete stability of BAM-PPV at 120°C under nitrogen atmosphere (Figure 32). The polymer is shown to be thermally stable up to 225°C without degradation in a nitrogen atmosphere, when exposed to air BAM-PPV will start to degrade about 180°C (Figure 33).

The thermomechanical analysis (TMA) of BAM-PPV using a 0.02 N holding force at temperatures above 10°C, were taken at a heating rate of 10°C/minute (Figure 34). This measurement was to examine the dimensional changes of BAM-PPV. The BAM-PPV material begins to deform due to softening, lowering the net expansion rate and introducing error into the signal. Above 50°C, the material is soft enough that compression by the probe exceeds thermal expansion. The TMA of BAM-PPV was repeated using a lower holding force. Although deformation of the sample is reduced, it still takes place. When this is combed with the low holding force, only intermittent contact with the sample takes place above Tg, preventing direct measurement of expansion (Figure 35).

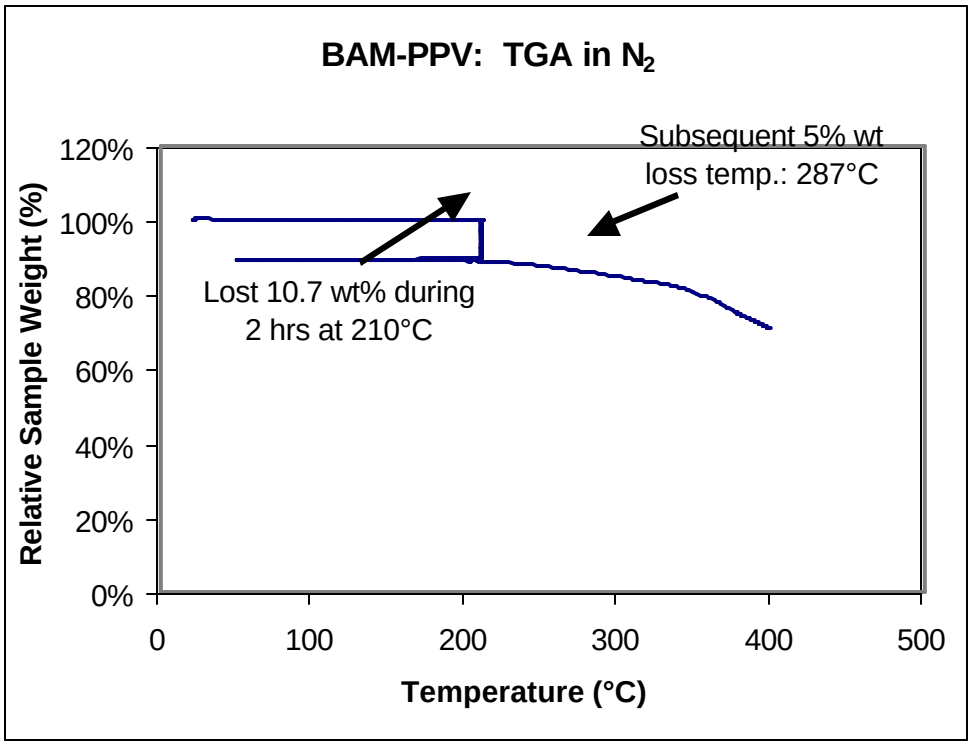

Figure 31: TGA Plot of BAM-PPV

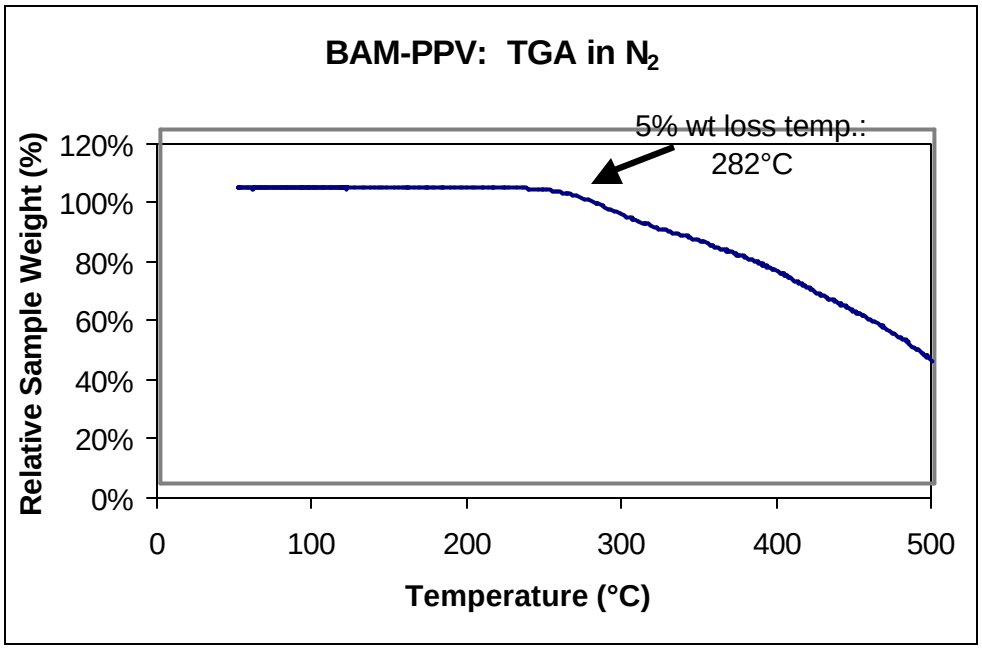

Figure 32: TGA Plot of BAM-PPV heated and re-heated to 500°C

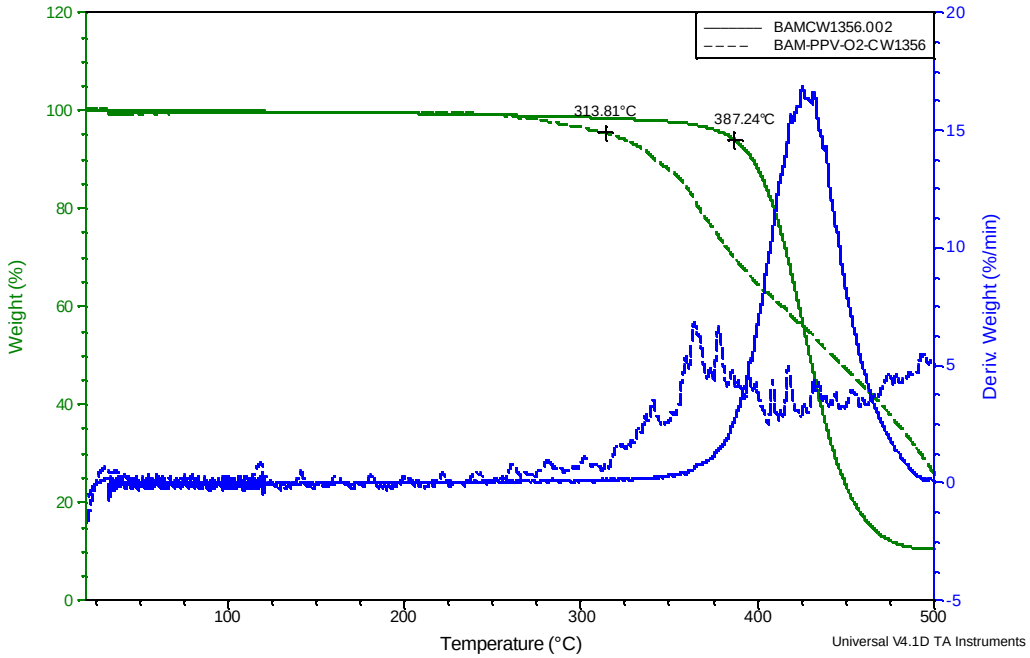

Figure 33: TGA of BAM-PPV in air and N_2

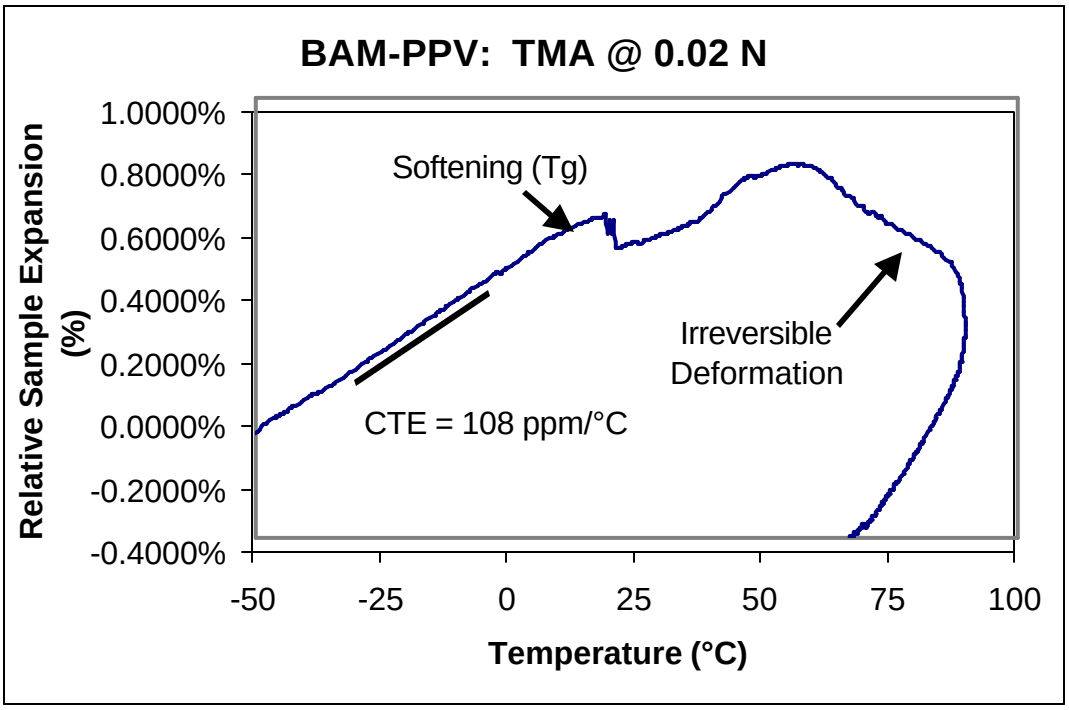

Figure 34: TMA of BAM-PPV

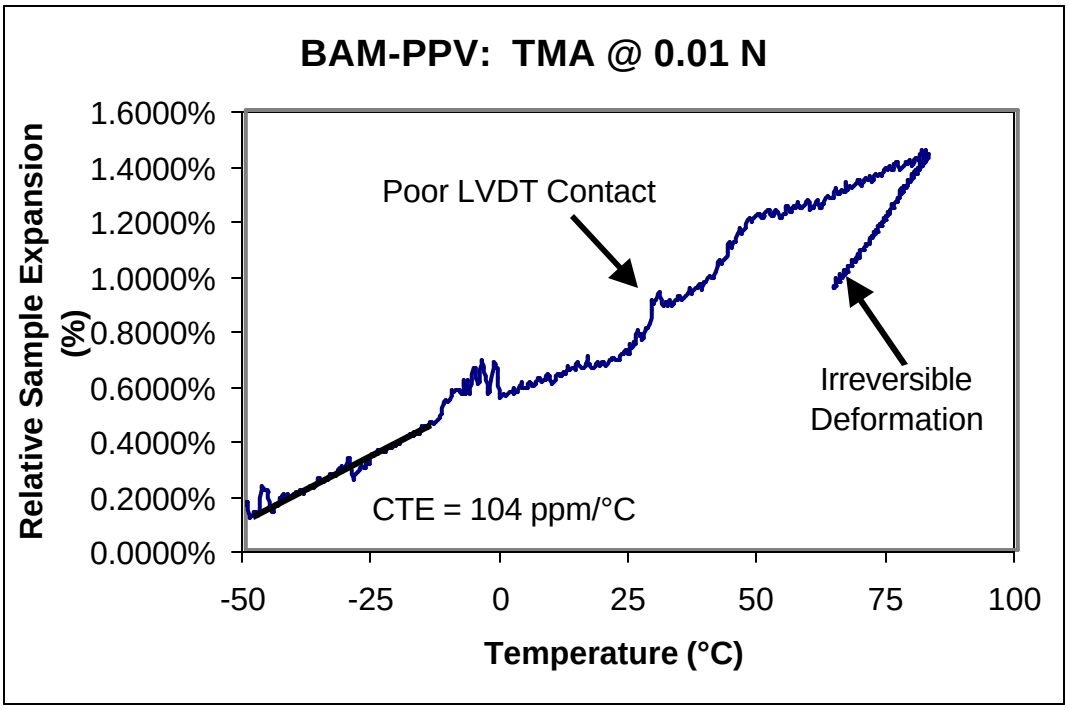

Figure 35: TMA of BAM-PPV using lower holding force

Unless noted otherwise, the following properties (Table 10) are theoretical predictions based on connectivity index methods outlined in Prediction of Polymer Properties, by J. Bicerano.[22]

Table 10: Physical Property Summary of BAM-PPV

Volumetric Properties

Molecular Weight	328.5 g/mol
Molar Volume (Bicerano 3.12)	334 cc/mol
Molar Volume (Bicerano 3.13)	343 cc/mol
Van der Waals Volume (Bicerano 3.9)	204 cc/mol
Van der Waals Volume (Bicerano 3.10)	219 cc/mol
Molar Volume (Bicerano 3.9 w/ Tg)	302 cc/mol
Molar Volume (Bicerano 3.10 w/ Tg)	345 cc/mol
Amorphous Density	0.95 – 1.09 g/cc
Crystalline Density	1.09 – 1.25 g/cc
Density (compression molded sample)	1.1 g / cc (exp)

Thermal Properties

Molar Heat Capacity (Cp) below Tg	469 J / molºK
Heat Capacity (Cp)	1.42 J / gºK
Molar Heat Capacity (Cp) above Tg	547 J / molºK
Heat Capacity (Cp)	1.66 J / gºK
Glass Transition Temperature Tg (DSC)	9ºC (exp)
Melting Temperature Tm (typical) (DSC)	170ºC (exp)

5% wt Loss Temperature (N2, TGA)	387ºC (exp)
5% wt Loss Temperature (Air, TGA)	320ºC (exp)

Solubility Properties

Fedors Cohesive Energy Density	113000 J/mol
Van Krevelen Cohesive Energy Density	110000 J/mol
Fedors Total Solubility Parameter	18.2 $(J/cc)^{1/2}$
Van Krevelen Total Solubility Parameter	17.8 $(J/cc)^{1/2}$
Dispersive Component	16.6 $(J/cc)^{1/2}$
Solubility Parameter of d-limonene	17.4 $(J/cc)^{1/2}$ (exp)
Solubility Parameter of xylenes	18.0 $(J/cc)^{1/2}$ (exp)

Surface Properties

Molar Parachor	793 (cc/mol) $(dyn/cm)^{1/4}$
Surface Tension at 25 C	47 dyn/cm

Electro-Optical Properties

Refractive Index (1300 nm, prism coupling)	1.6 (exp)
Bulk resistivity (measured film, undoped)	10^{11} ohm cm (exp, in vacuum)
Dielectric constant (as perfect insulator)	2.6
Dielectric constant (based on resistivity)	5.5

exp = experimentally determined

The results either experimentally or theoretically calculated represent a comprehensive properties summary for BAM-PPV. Since BAM-PPV is only slightly crystalline, the simpler correlations, do the best job at predicting the actual density of the polymer.[23] However, this correlation requires knowledge of the van der Waals volume and the experimental glass transition temperature. The solubility parameters appear to be validated by experiments, since both *d*-limonene and xylenes are among the best known solvents for BAM-PPV. The electro-optical properties, however, are more difficult to predict. The refractive index at 1300 nm, for instance, is predicted to be only about 1.5, whereas experiments show it to be about 0.1 higher. The anomalously high index is accompanied by a conductivity that is six orders of magnitude higher than predictions based on simple structural correlations. Both results are not unexpected since the correlations do not take into account the electroactive nature of BAM-PPV.

The BAM-PPV powder has been characterized using FTIR and the results are shown in Figure 36 and Table 11, respectively.

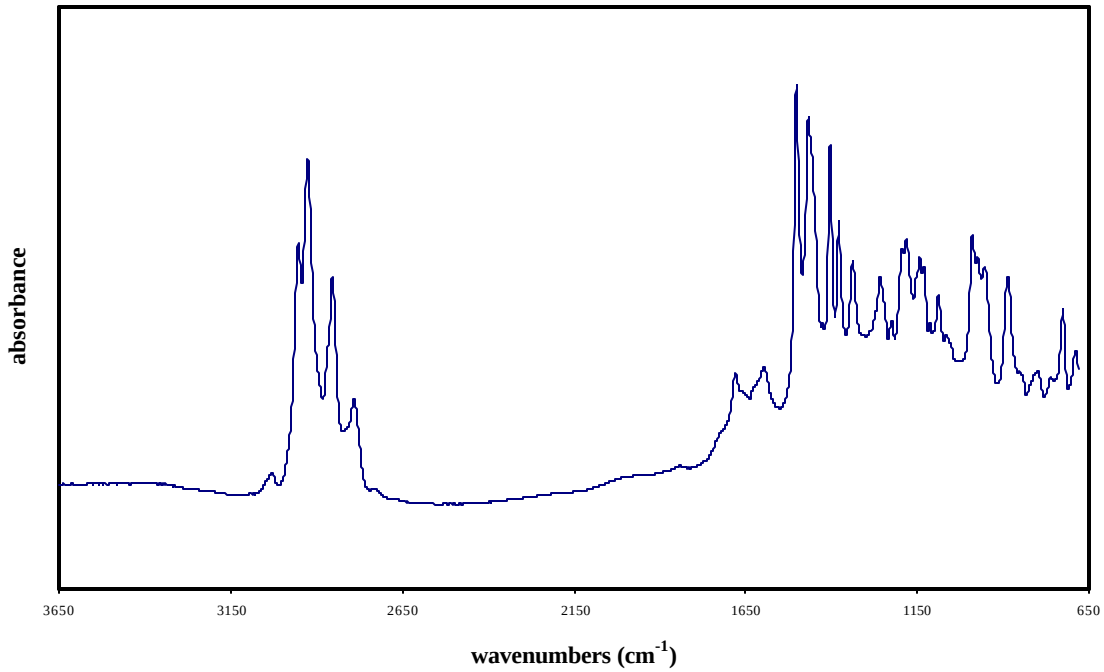

Figure 36: FTIR of BAM-PPV powder

Table 11: FTIR Peaks and Assignments for BAM-PPV Polymer

Vibrational peaks and proposed peak assignments of BAM-PPV polymer film			
peak position (cm^{-1})	assignment	peak position (cm^{-1})	assignment
3032 w	aromatic C-H stretch	1257 m	aromatic C-N stretch
2954 s	asym. methyl C-H stretch	1224 w	
2927 vs	asym. Methylene C-H stretch	1192/1179 doublet	C-N aliphatic stretch
2869 sh	sym. methyl C-H stretch	1141 m	
2855 s	sym. methylene C-H stretch	1127 m	
2792 m	C-H stretch (C bonded to N)	1111 w	
1678 w	vinyl C=C stretch	1087 m	
1593 w,b	aromatic C=C stretch	989 s	C-H out of plane on vinyl group
1500 vs	aromatic skeletal vib.	973 sh	
1465 s	asym. methyl def.	953 sh,s	
1455 sh	CH2 scissor	886 s	C-H out of plane on 1,2,4,5 sub. Phenyl
1424 w	N-CH3 sym. methyl bend	797 w	
1403 s		725 m,s	CH2 rock
1377 s	sym. CH3 bend	687 m	
1337 m			

w=weak, m=medium, s=sharp, vs=very sharp, sh=shoulder, b=broad

FTIR and UV-Visible Studies of BAM-PPV Films on Al 2024-T3

Analytical Method

FTIR analysis was performed on very thin films of BAMPPV to determine the interaction of the BAMPPV molecule on the surface of the aluminum (Al 2024-T3). Results indicate that a small amount of the BAMPPV is significantly attached, either chemisorbed or physically adsorbed, to the surface of the aluminum. Data indicates that the phenyl ring is lying flat on the surface of the aluminum, and the alkane chain interacts with the surface of the aluminum over time.

The experimental procedure for measuring the FTIR on Al 2024-T3 plates is described. Aluminum (2024-T3) plates were polished first with 600-grit silicon-carbide sandpaper and then with diamond polishing compound (6 and 1 micron, sequentially). Final polishing was done by hand using a 0.05 micron colloidal silica suspension and a Buehler microcloth polishing cloth. The sides and back of the aluminum plates were cleaned with acetone and a cotton swab to reduce the risk of contamination by residual polishing compound. The polished aluminum plates were then cleaned with several solvents (acetone, methylene chloride, methanol, and THF) sequentially in an ultrasonic cleaner for 15 minutes each. The plates were then soaked in spectral grade THF for several days. The aluminum plates were then soaked in very dilute solutions of BAMPPV (<0.002%) dissolved in THF for several days. The samples were "drip-dried" and spectra were acquired. The samples were allowed to age, face down in air, and spectra were acquired every one to four days.

Method:

To determine the interaction of BAMPPV with the surface of the surface of the aluminum plate, some of the samples were briefly rinsed with THF. The THF was allowed to evaporate and spectra were acquired. A reference "bulk" spectrum was acquired for comparison by placing a drop of the concentrated BAM-PPV in THF solution on a polished aluminum plate. The THF was allowed to evaporate and a spectrum was acquired using the same technique as the other samples. The FTIR results have shown the following: there were several differences among the bulk spectra and the very thin film spectra were observed (Figure 37). Of special interest was aromatic CH stretch peak observed in the bulk sample at about 3031 cm^{-1} (Figure 38). In the thin film spectra this peak was greatly diminished. This is likely due to the aromatic ring laying flat on the surface of the aluminum. In addition, there were significant differences noted between the spectra of "fresh" BAMPPV thin-film samples, and spectra obtained after the samples had been sitting in air for several days. Most notable was the change in the ratio of the R-CH_3 stretch (~2960 cm^{-1}) to the -CH_2- stretch (~2930 cm^{-1}) (Figure 39). The decrease over time of the CH_2 peak height relative to the CH_3 peak may indicate a change in interaction of the alkane chain on the surface of the aluminum over time, thus making the CH_2's less visible to infrared spectroscopy. It appears also that the CH_2 peak height may have broadened, which could indicate a higher degree of intermolecular interaction (such as van der Waals forces). Additionally, the disappearance of the peak at 2791 cm^{-1} (Figure 39) is observed. This peak is in the region of the CH stretching mode for an -NCH_3 group, this again is likely due to a change in the interactions of the BAM-PPV molecule with each other or with the surface of the aluminum. After rinsing a 3-day-aged BAM-PPV sample with THF, there still appeared to be some BAM-PPV on the surface of the aluminum. Figure 32 shows a "same-scale" comparison of the CH stretch region of a thin layer BAMPPV sample, the same sample aged 3-days, and the same sample briefly rinsed with THF. Even after rinsing, a significant amount of BAMPPV remains.

While not conclusive, these results indicate that there is some sort of interaction is occurring between the BAMPPV and the aluminum surface.

While the analysis described above in detail does show that after the initial deposition, no distinction may be made between a very thin layer, on the order of a few monolayers thick, and a thicker coating of the polymer on the surface. As stated above, there were changes after aging the coated samples for several days. The changes with the thin films were reproducible and did not occur with thicker deposited films, which indicates that a polymer-surface interaction may be occurring. The reason for the changes in the aged spectra has not yet been conclusively determined.

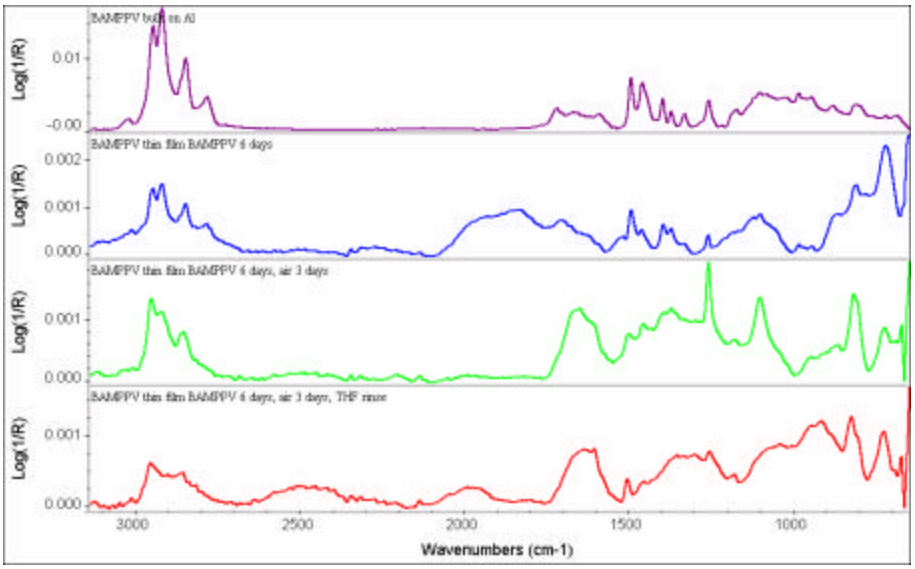

Figure 37: Comparison of "bulk" BAMPPV, thin layer BAMPPV, thin layer BAMPPV aged 3-days, and thin layer BAMPPV aged 3-days and rinsed with THF sample spectra. The spectra are all normalized to the tallest peak.

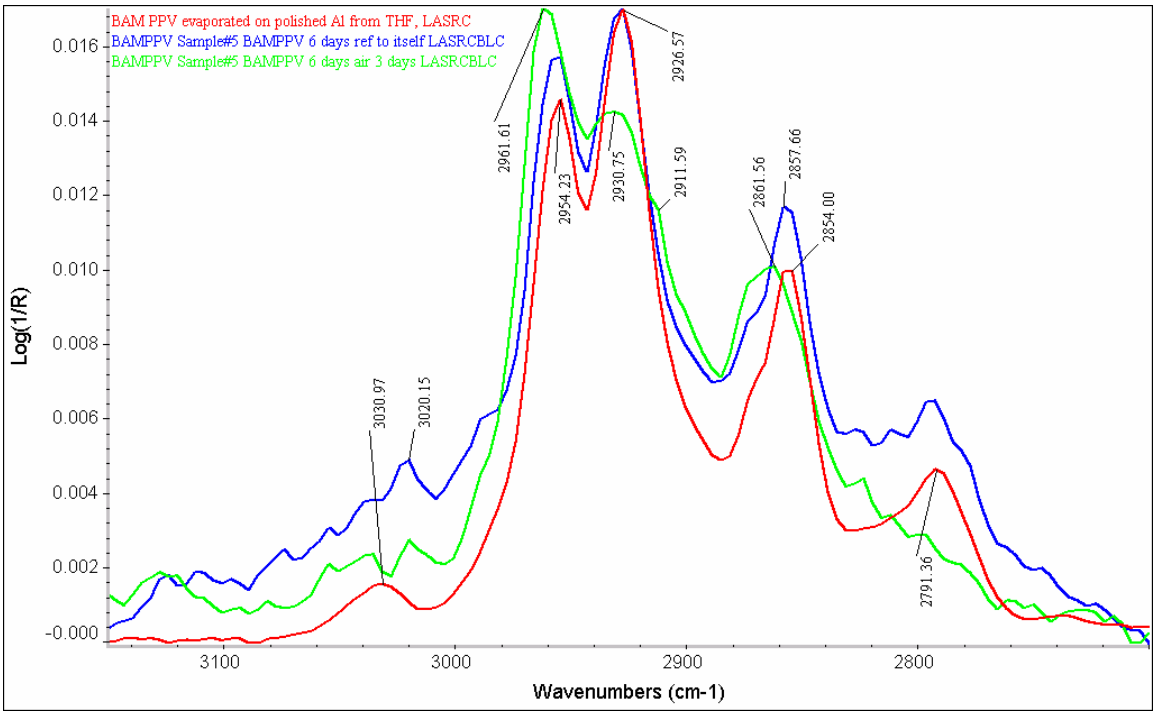

Figure 38: Comparison of CH stretch region of "bulk" BAMPPV, thin layer BAMPPV, and thin layer BAMPPV aged 3-days. The spectra are all normalized to the tallest peak.

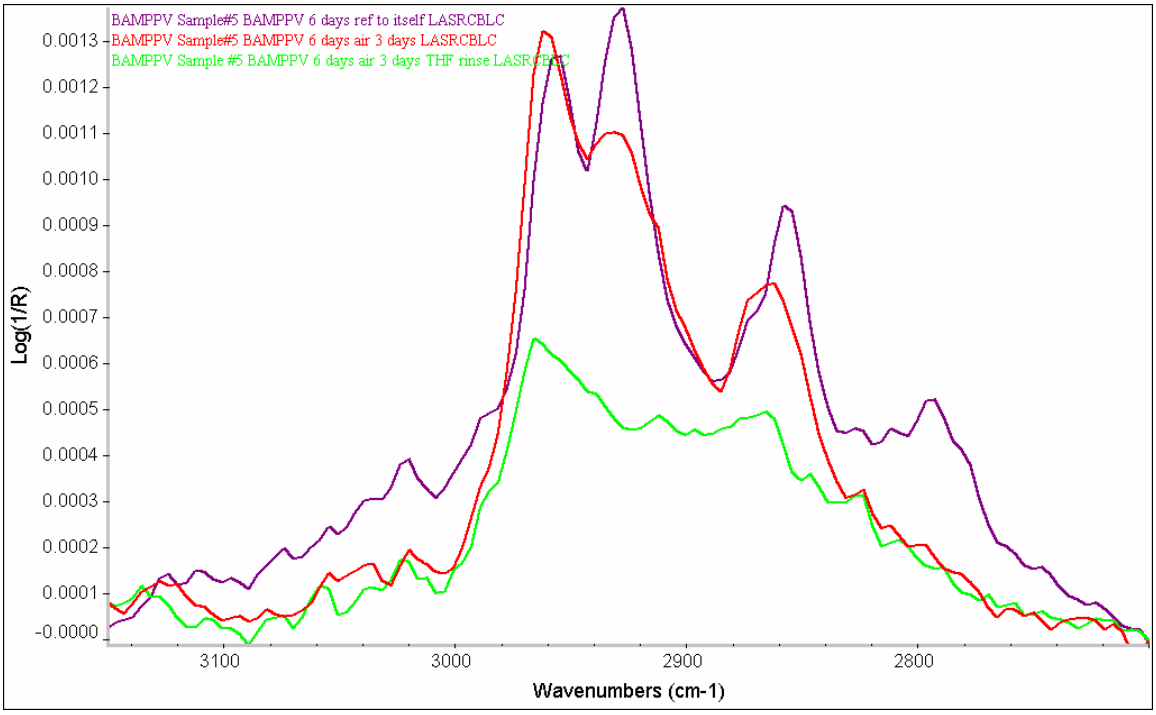

Figure 39: stretch region comparison of thin layer BAMPPV, thin layer BAMPPV aged 3-days, and sample rinsed with THF to remove easily washed away BAMPPV. The spectra are all displayed to the same scale.

UV-Visible (UV-Vis) spectroscopy was performed on BAM-PPV films coated onto Al 2024-T3 substrates to further investigate the interaction of BAM-PPV with aluminum alloys. The samples of BAM-PPV coated onto Al 2024-T3 substrates were aged for several days. The thin film absorbance maximum was observed at 431 nm and the thick film absorbance maximum was observed at 398 nm (Figure 40). For BAM-PPV a significant shift in the absorbance maximum (λ max), 33 nm shift is observed in the spectra for the thin (0.1 micron) and thick films (0.5-0.75 microns). This shift can be explained via differences in the electronic state from thin to thick films respectively.

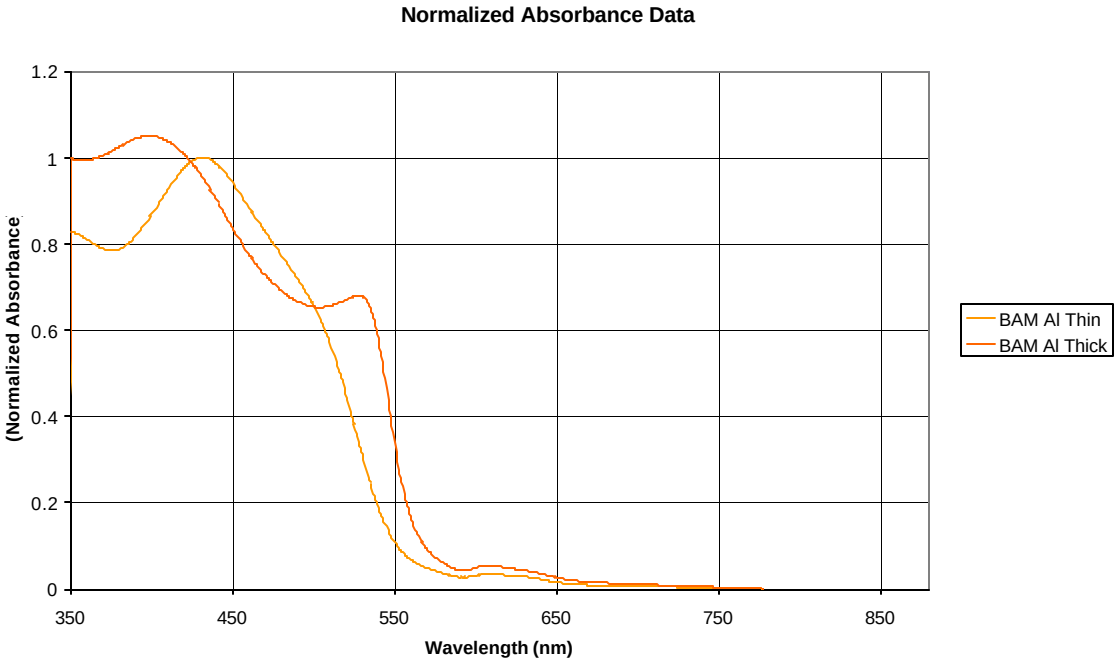

Figure 40: UV-Vis spectra of BAM-PPV
Thin films are 0.1 microns and thick films are 0.5-0.75 microns, respectively

Assessing the Interactions of BAM-PPV with Supercritical carbon dioxide ($SCCO_2$):

The work presented in this section was under the direction of Dr. Kenneth Wynne from VCU. The work focuses on the continuing effort of coating BAM-PPV onto steel and/or aluminum substrates using $SCCO_2$. The previous work showed poor processability of BAM-PPV in $SCCO_2$. This final study focused on improving the processability of BAM-PPV using $SCCO_2$ and co-solvents.

Experimental Section:

Note: barg is the symbol for “bar, gauge”, a common unit of pressure in engineering. The term "gauge" means that the pressure has been read from a gauge that actually measures the difference between the pressure of the fluid or gas and the pressure of the atmosphere.

Materials:

Several samples of BAM-PPV described in this report were received directly from Drs. Peter Zarras and Andrew Guenthner from the NAWCWD, China Lake, CA.

General Method:

The MDSC data are shown in Figure 41 for a sample of BAM-PPV flake heated from –85°C to 230°C at 3°C/min with a modulation of ±1.0°C/60 sec. The reversing heat flow curve exhibits a weak inflection at 3°C that is tentatively assigned as the glass transition temperature, T_g. The non-reversing heat flow curve shows an exothermic peak at 142.4°C that is due to recrystallization upon heating, T_{ch}. If a BAM-PPV-F-1 sample is first heated to 200°C for 5 min and then cooled at 3°C/min with a modulation of ±1.0°C/60 sec, the total heat flow curve exhibits an exothermic peak, T_{cc}, centered at 130.8°C with an onset at 137.3°C. The enthalpy of fusion, ΔH_f = 11.2 J/g, for crystallization on cooling is determined by integration with a linear baseline extended from 100-150°C. The total heat flow curve in Figure 41 shows two endothermic peaks centered at 129.3 and 162.4°C that could be designated T_m1 and T_m2. The total integrated area with a linear baseline extended from 70-180°C is 11.3 J/g.
The amorphous phase of BAM-PPV samples is in a rubbery state above about 3°C. These semicrystalline materials undergo a melt-recrystallize-remelt process beginning at about 70°C and concluding by about 180°C. In the total heat flow curve for various other BAM-PPV samples there is sometimes observed a weak inflection near 50°C. This feature does not persist if the samples are first heated to 200°C and then cooled to –85°C.

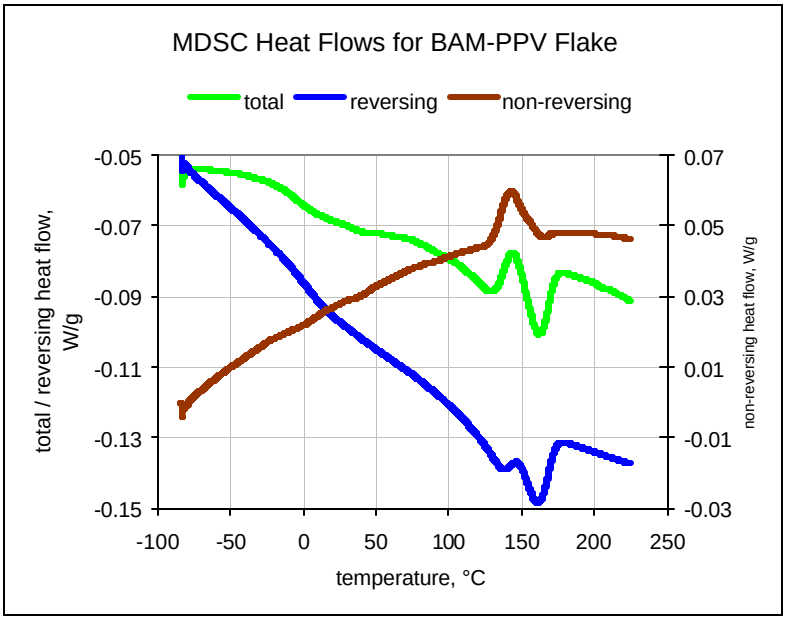

Figure 41: Modulated DSC Data for BAM-PPV Polymer Flake

The calorimetry described above was performed so that observations made when samples were heated in the LVDT experiments could be understood. It was of some concern that the BAM-PPV-2 and –3 bars had been pressed at temperatures below T_m2. The TGA measurements described below were performed to determine if BAM-PPV was thermally stable enough so that compression molding at higher temperatures was feasible.

The TGA data for BAM-PPV-F-1 is shown in Figure 42, heated from ambient temperature to about 800°C in either nitrogen or air. In nitrogen, the onset of weight loss occurs

at 402°C, and about 10% residue remains at the final temperature. In air, decomposition is observed starting at about 305°C, and the entire sample burns away by about 600°C. BAM-PPV-2 and -3 samples exhibit similar behavior in nitrogen. In air, their decomposition is slightly delayed, presumably because the surface area of the samples is reduced.

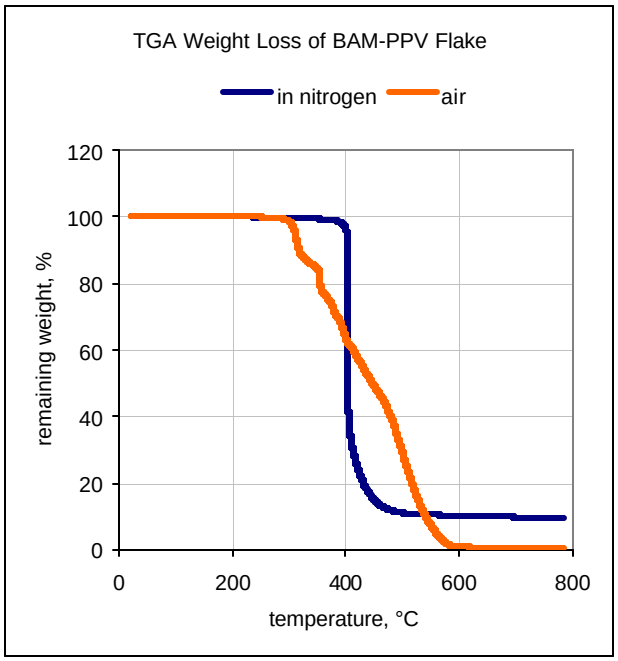

Figure 42: Stability of BAM-PPV Polymer Flake Heated in Nitrogen and Air

Even when the weight loss axis was greatly expanded, the results of the TGA experiments suggested that compression molding of BAM-PPV flake was feasible at temperatures up to about 225°C. For BAM-PPV-F-1 measured in air, only 0.14% weight loss occurred in the 100-225°C range. After some preliminary trials, four films were molded by pressing at 205-215°C for about 10 min. Figure 43 shows the remaining film left in the window frame after a center section has been cut out for DMA measurement. To give a sense of magnification, the actual width of the aluminum foil window was 15.8 mm. The films are brick red-orange and brighter than the BAM-PPV-2 and –3 bars that are reddish-brown. The VCU compression-molded films do show blotchy or mottled darker areas that suggest the polymer may be inhomogeneous or contain minor amounts of impurities.

Figure 43: Compression Molded BAM-PPV Film

Three DMA experiments were performed, each with a different BAM-PPV film. In the first and second, the temperature ranges were –40-100°C and –30-90°C respectively, both with steps of 20°C. The third experiment was measured with 10°C steps over a –35-95°C range. In all the experiments, the frequency varied from 0.1-100 Hz with a resolution of two measurements per decade. Figure 44 shows only the 10 Hz data from the three experiments. The storage and loss moduli are plotted on a logarithmic scale versus temperature. The storage modulus decreases from about 3290 MPa at –35°C to 110 MPa at 95°C, consistent with a glassy to rubbery transition.

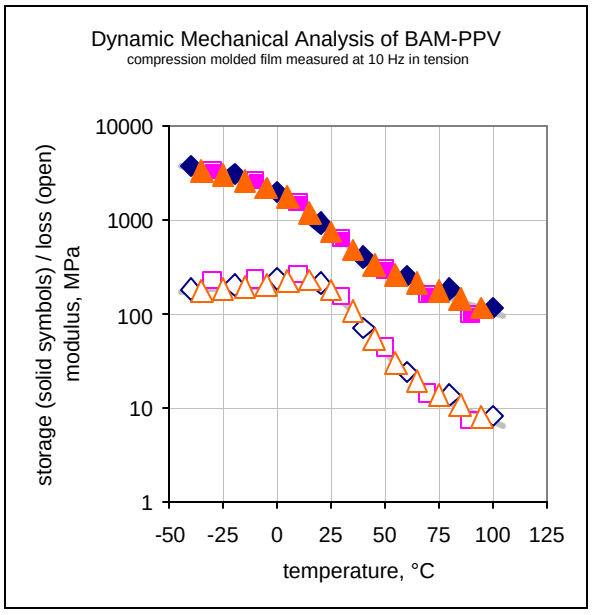

Figure 44: Storage and Loss Modulus of BAM-PPV versus Temperature

Figure 45 shows the same 10 Hz data plotted as tan δ versus temperature. This curve can be fitted to a Gaussian distribution allowing for slight linear change of baseline. As the frequency of measurement increases from 0.1-100 Hz, the center of the tan δ peak shifts to higher temperature, the width of the peak increases and the peak height does also. Figure 46 shows an Arrhenius plot of natural log frequency versus reciprocal absolute temperature. The apparent activation energy is E_a = 193. kJ/mol (46.3 kcal/mol), a value that is unremarkable for a glass transition centered at this temperature. It is amusing to note that the Arrhenius relationship predicts that the tan δ peak will shift to 4°C at 0.0167 Hz, the modulation frequency of the MDSC experiment where a weak inflection at 3°C was tentatively assigned as the T_g.

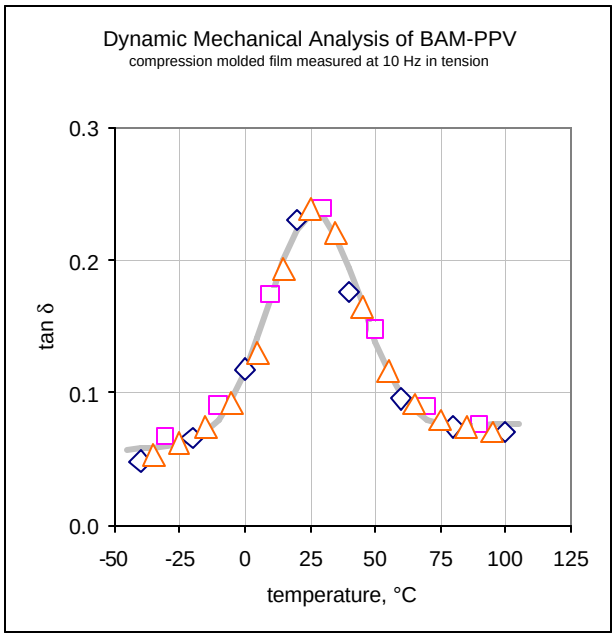

Figure 45: Tan δ Representation of Modulus of BAM-PPV versus Temperature

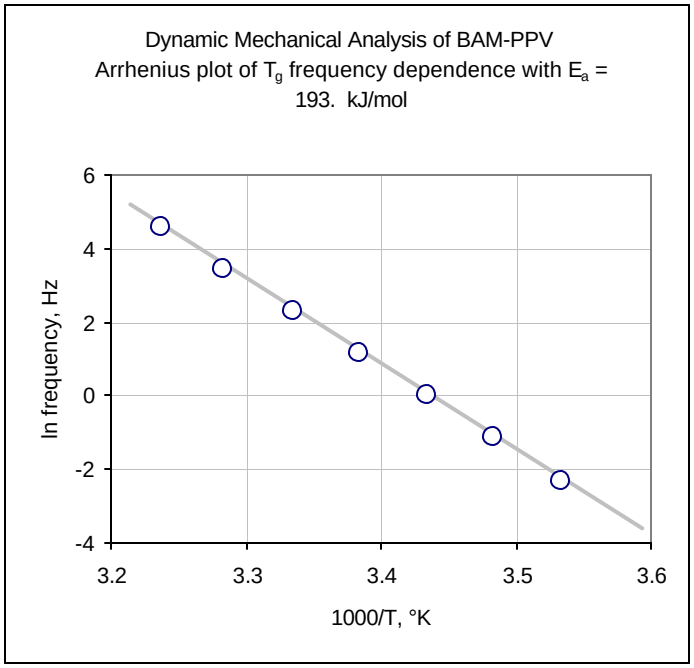

Figure 46: Arrhenius Plot of BAM-PPV Tg versus Frequency Data

The first experiment performed in the LVDT apparatus was intended to measure the coefficient of thermal expansion (CTE) of BAM-PPV in the absence of CO_2. An as received bar of BAM-PPV-2 was placed in the apparatus and heated in steps to 120°C. Instead of increasing in length, the sample size decreased, reaching a near-steady length at each new temperature. The equipment was cooled to ambient temperature overnight. It was found, based on the change in LVDT reading, that the sample length had decreased by 2.7%. The experiment was restarted without disassembling the equipment. This time, stepwise heating to 120°C produced the expected, regular increase in sample length. These data are plotted as open circles in Figure 47, accounting for the reduction in the ambient temperature sample length. As the heating was continued in steps from 120-155°C, the sample length again decreased. The equipment was cooled to ambient temperature overnight. It was found, based on the change in LVDT reading, that the sample length had decreased by a total of 6.7% compared to its length when first placed in the apparatus. The experiment was restarted without disassembling the equipment. This time, stepwise heating to 145°C produced the expected, regular increase in sample length. These data are plotted as open squares in Figure 47, accounting for the further reduction in the ambient temperature sample length. The calculation of the slope at 25°C of the fitted line provides a CTE = 196. µm/m-°C. This value is quite high but not unreasonable for a somewhat crystalline polymer above its glass transition temperature. The second experiment performed in the LVDT apparatus was intended to measure the linear expansion of BAM-PPV as a function of CO_2 pressure. A bar of BAM-PPV-2 was placed in the LVDT apparatus as before, except that the core and connecting rod were removed. The sample was heated to 155°C in steps over about 6 hr and maintained at this final temperature for about 35 min before cooling to ambient. The equipment was disassembled, the sample bar was measured, and the equipment was reassembled including the LVDT core and connecting rod. The annealed BAM-PPV-2 was heated to 110°C, and the pressure of CO_2 was increased in steps. At 60 then 138 barg, the sample length increased in the regular, expected fashion. When the pressure was increased to 345 barg, the sample slumped. That is, the length decreased steadily because the sample could no longer support the weight of the LVDT core and connecting rod. These results are plotted in Figure 48. Although

the experiments measuring thermal expansion and expansion in CO_2 are both quite self-consistent, the linear expansion measured at 0 barg in the second experiment is substantially less than that predicted from the first, thermal expansion experiment. It is possible that this discrepancy results from a difference between how the sample bar annealing was done in the two trials. In the thermal expansion measurements, the sample was annealed under the compressive force of the LVDT core and connecting rod, and there was no such load in the preparation for the second measurements.

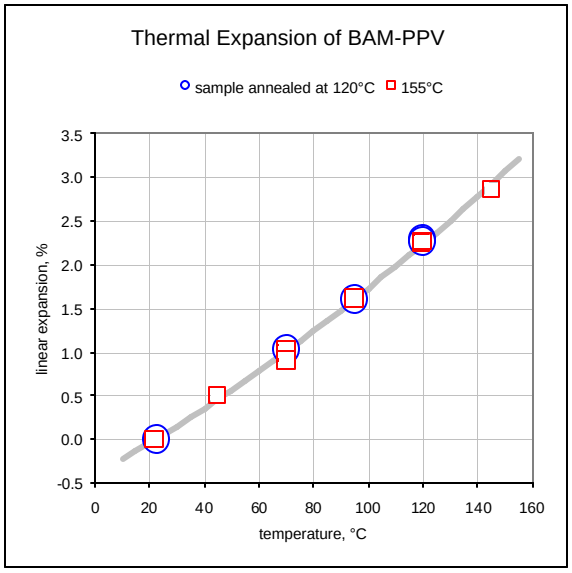

Figure 47: Thermal Linear Expansion of BAM-PPV

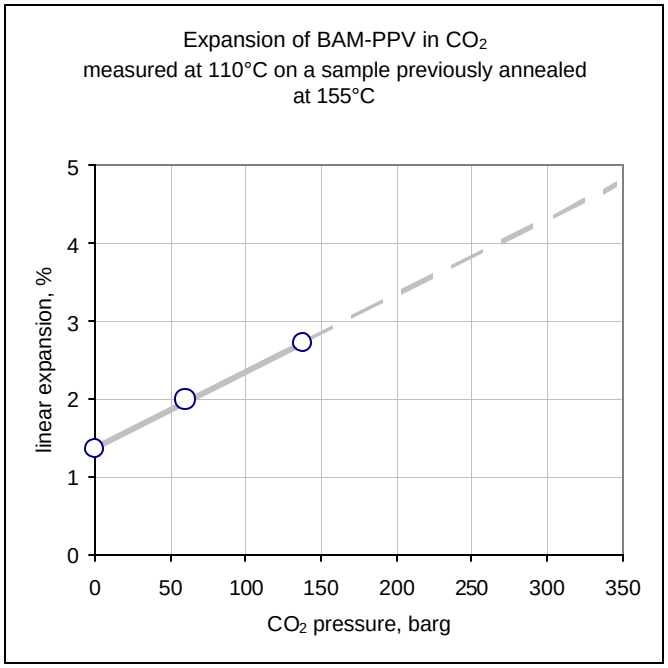

Figure 48: Linear Expansion of BAM-PPV in CO_2

The results show that BAM-PPV has a glass transition temperature at about T_g = 3°C and apparently two crystalline phases. Melting of the first at Tm1 = 129.3°C is followed by recrystallization at 142.4°C and then re-melting at 162.4°C. In nitrogen, BAM-PPV is stable to about 402°C and leaves about 10% residue at 800°C. In air, the polymer is stable to about 305°C and burns completely by 600°C. BAM-PPV films can be compression molded at 205-215°C. The DMA measurements on these films, at -40-100°C and 0.1-100 Hz confirms the observed glass transition temperature. At 10 Hz, the storage modulus decreases from about 3290 MPa at –35°C to about 110 MPa at 95°C. From an Arrhenius plot, the activation energy associated with the T_g is found to be E_a = 193. kJ/mol. The linear thermal expansion of annealed BAM-PPV was measured at 20-145°C. At 25°C the coefficient of thermal expansion was CTE = 196. µm/m-°C. At 110°C and CO_2 pressures up to 138 barg, considerable additional linear expansion is observed. At this temperature, when the pressure is increased to 345 barg, the BAM-PPV sample is unable to support the LVDT connecting rod and it slumps.

Experiments were performed on the polymer to test the solubility of BAM-PPV with several co-solvents. The polymer, BAM-PPV is swollen by supercritical CO_2 and the melting point is lowered at relatively low CO_2 pressure by about 40°C. However, BAM-PPV is not soluble in supercritical CO_2 so toluene was employed as co-solvent with supercritical CO_2. Toluene is reported to form completely miscible solutions with supercritical CO_2 over a wide range of pressure and temperatures, for example 38.1 ^oC, 74.2 atm. In our experiment, we used 41 ^oC and 2000 psi (136 atm) to ensure the complete cosolvent miscibility. About 3 ml BAM-PPV/toluene solution (approximate 0.5 % (w/v) concentration) was put into a small container, which was then placed into a cylindrical high-pressure vessel. The glass slides were also put in vessel without contacting the toluene solution. The vessel was purged with nitrogen twice and then pressurized with CO_2 at tank pressure (840 psi). The temperature was increased to 41 ^oC and then pressure was increased to 2000 psi. After 6 hours, the vessel was cooled down to room temperature and the CO_2 was slowly depressurized. The slides were taken out of the vessel to see if they were coated with BAM-PPV at this condition. Two experimental runs were done. The first experiment consisted of having the cylindrical pressure vessel horizontally arranged and the

toluene solution and glass slides were loaded into the pressure vessel bore and were separated by a few inches. After loading the CO_2 as described above and depressurization a yellow coating on glass was clearly observed, though the coating was not uniform. The second experiment consisted of having the cylindrical pressure vessel vertically arranged. The toluene solution was loaded into the pressure vessel bore first followed by the glass slides. After loading the CO_2 was described as above and depressurization. The coated slides from experiment run 1: wherein the toluene feed solution and slides were loaded into the pressure vessel in the horizonal position were examined with UV/Vis spectrometer with uncoated slides as reference. The UV/Vis spectrum (Figure 49) shows two peaks centered around 461 and 355 nm wavelengths, which are a characteristic aromatic absorbance. This result provides evidence that BAM-PPV was coated on the glass slide.

The CO_2/toluene/BAM-PPV is a ternary system and it the solubility of BAM-PPV is strongly dependent on the CO_2/toluene ratio. BAM-PPV is substantially swollen and plasticized in dense CO_2. At 110°c and 345 barg, the compliance is so greatly increased that samples will not support a load of 10 pa, that is the sample substantially melts. Therefore, BAM-PPV has limited application for processing in $SSCO_2$ even with co-solvents.

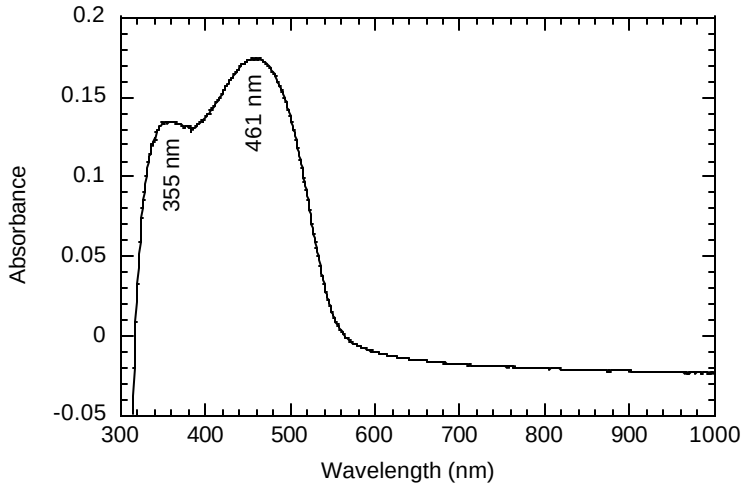

Figure 49: UV/Vis spectra of BAM-PPV coated glass slide.
(uncoated slide reference)

EAPs Based on Oligomers of Polyaniline

At RPI during FY04, a series of copolymers containing trimeric methacrylate and n-butyl acrylate were synthesized. Several test panels were prepared and sent to NAWCWD to establish a baseline for the standard polyaniline primer as a corrosion resistant coating. The chemical structures of all oligoanilines are shown in Figure 50, and the properties are listed in Table 12.

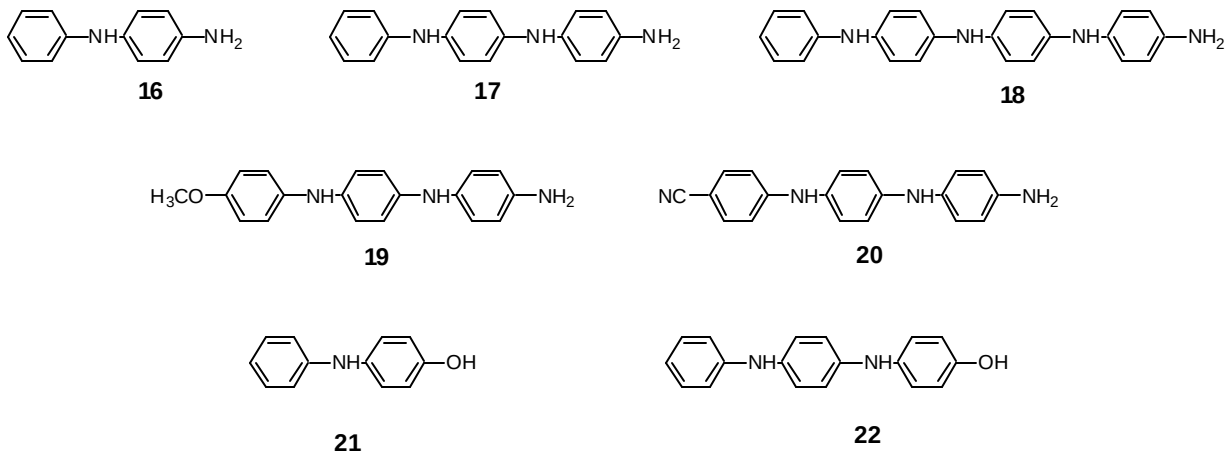

Figure 50: Chemical structures of oligoanilines

Table 12: Optical and Electrochemical Properties of Oligoanilines

	UV-vis (reduced, nm)	*UV-vis (oxidized, nm)*	*Oxidation Potential (V)*	*Conductivity (S/cm)*
16	291	290, 427	0.45, 0.94	3×10^{-6}
17	311	304, 555	0.33, 0.67, 1.40	6×10^{-3}
18	323	303, 577	0.27, 0.54, 0.90, 1.08	4×10^{-2}
19	311	304, 554	0.29, 0.62, 1.25	2×10^{-3}
20	332	329, 565	0.40, 0.76, 1.46	9×10^{-5}
21	285	285, 456	0.75, 1.88	1×10^{-6}
22	309	303, 583	0.44, 0.83, 1.69	9×10^{-5}

SECTION VIIB- Coating Methods and Accelerated Weathering Testing of EAPs Films

Flame Deposition-FY01-02 RESULTS

A coating technique using a novel flame spray deposition process developed by MicroCoating Technologies, Inc. (MCT), (Chamblee, GA) was investigated during FY00-02. A solution of BAM-PPV polymer in toluene is atomized and deposited via flame spray. The flame spray deposition coating offers a zero-VOC process due to the combustion of the solvent.

A total of 50 panels have been coated by MCT for testing. The application results in a smooth, even coating of polymer on steel and aluminum substrates. Initial test results indicate good adhesion to the substrate. In pull tests performed by MCT up to 1000psi, all of the coatings remained bonded to the substrates. Figures 51 and 52 are of the coated steel and aluminum panels, respectively.

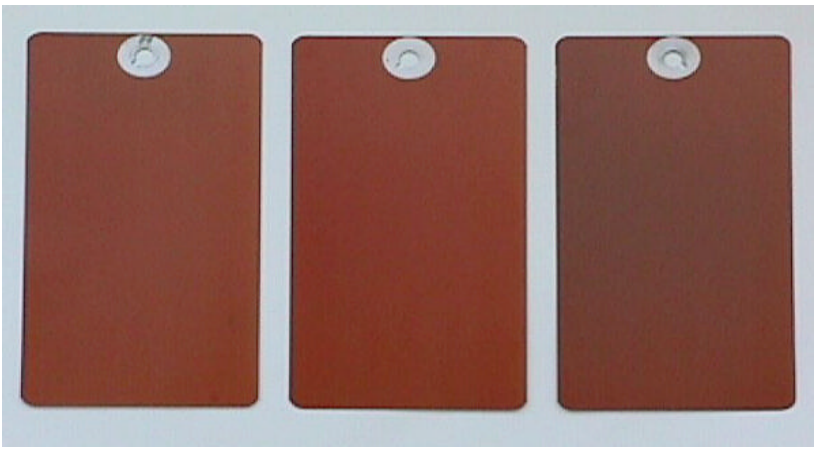

Figure 51: Steel panels (3'x 6') coated with BAM-PPV using the flame deposition process

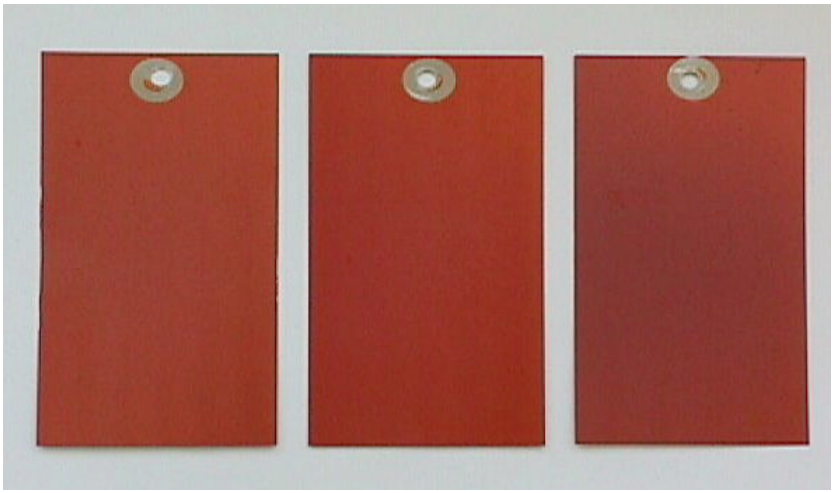

Figure 52: Aluminum panels (3'x 6', Al 2024-T3) coated with BAM-PPV using the flame deposition process

Evaluation of BAM-PPV Coated Metal Coupons

To determine the effects on the polymer surface and the substrate surfaces due to ultraviolet (UV) exposure and salt spray exposure, panels were sent to Benet Laboratories for initial evaluation using Laser Scanning Confocal Microscopy (LSCM).

Methods:

Figure 53 shows an extended-depth-of-field optical image of the surface of a standard 1008/1010 steel panel intended for use in the studies. This image was taken at a randomly selected location but is representative of the entire surface of this panel. As seen in Figure 53, the surface of the steel substrates consists of smooth, undulating features, presumably generated during the manufacturing process.

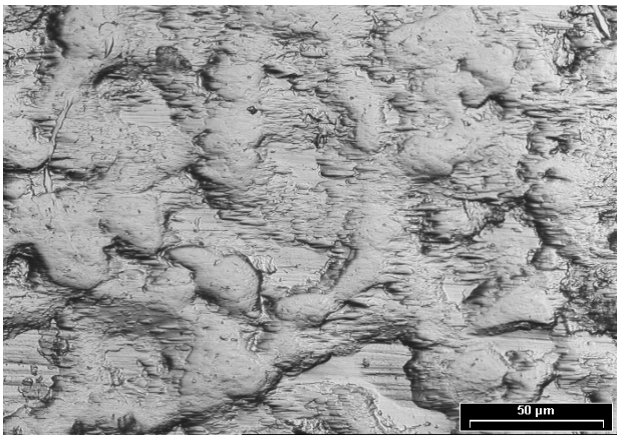

Figure 53: LSCM optical image of 1008/1010 steel surface @ 1000x

Figure 54 shows the simultaneously obtained "height-mapping" of this surface. This image consists of 640 x 480 pixels, each of which is represented as any one of 256 possible gray levels. These gray levels correspond to the height deviations along the surface, where the brightest pixel (white) indicates the highest point(s) of the surface, and darkest pixel (black) indicates the lowest point(s) of the surface. Here the minimum-maximum height deviation was measured to be approximately 6µm.

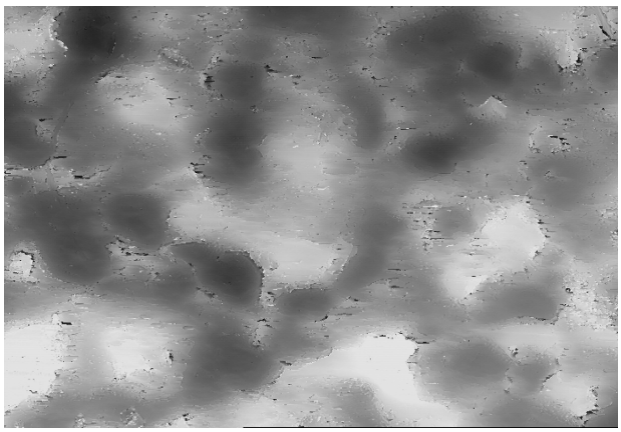

Figure 54: LSCM height-mapping of 1008/1010 steel surface @ 1000x

Either rows or columns of this 640 x 480 matrix of height information can then be plotted to extract high resolution profiles of the surface, as shown in Figure 55.

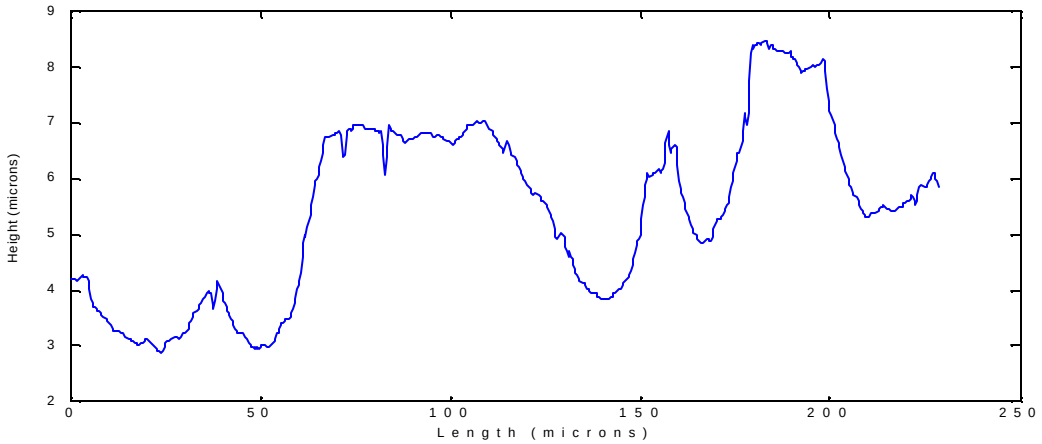

Figure 55: Surface profile generated from height information shown in Figure 51 for 1008/1010 steel panel surface @ 1000x

The surface profiles obtained from height mappings were characterized using a standard approach for obtaining roughness measurements. In these studies, the average roughness, R_a, is defined as the arithmetic average of the absolute values of the height deviations as measured from a graphical centerline that is determined from a least-squares fit to the profile. The RMS roughness, R_q, is the square root of the sum of the squared height deviations as measured from the same graphical centerline. Roughness values obtained for the 1008/1010 steel were R_a=1.16µm and R_q=1.29µm.

Figure 56 shows an extended-depth-of-field optical image of the surface of a 2024 Al 2024-T3 panel, which is intended for use in the studies. As in Figure 53, this panel was imaged at a randomly selected location, but results are representative of the entire surface.

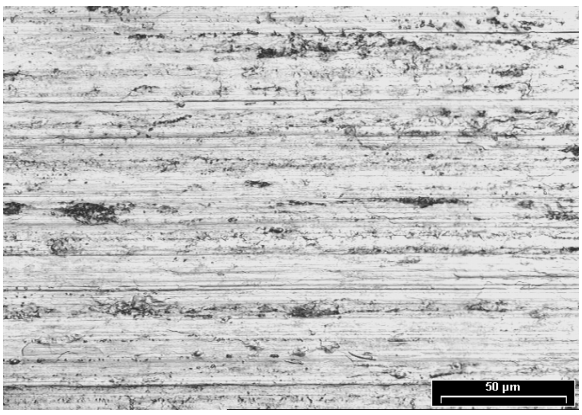

Figure 56: LSCM optical image of Al 2024 T3 panel surface @ 1000x

As seen in Figure 56, the surface of the Al 2024-T3 substrate consists of fine linear features, presumably generated during the manufacturing process. Figure 57 shows the simultaneously obtained "height-mapping" of this surface. Minimum-maximum height deviations along the surface were measured to be approximately 0.5 microns.

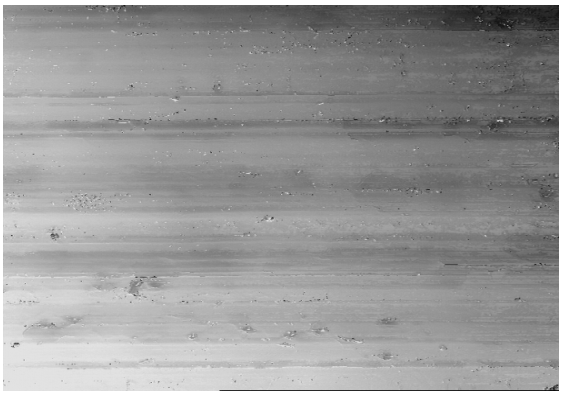

Figure 57: LSCM height-mapping of Al 2024 T3 panel surface @ 1000x

One row of data from the 640 x 480 matrix of height data shown in Figure 57 was then plotted to obtain a high resolution profile of the surface, as shown in Figure 58.

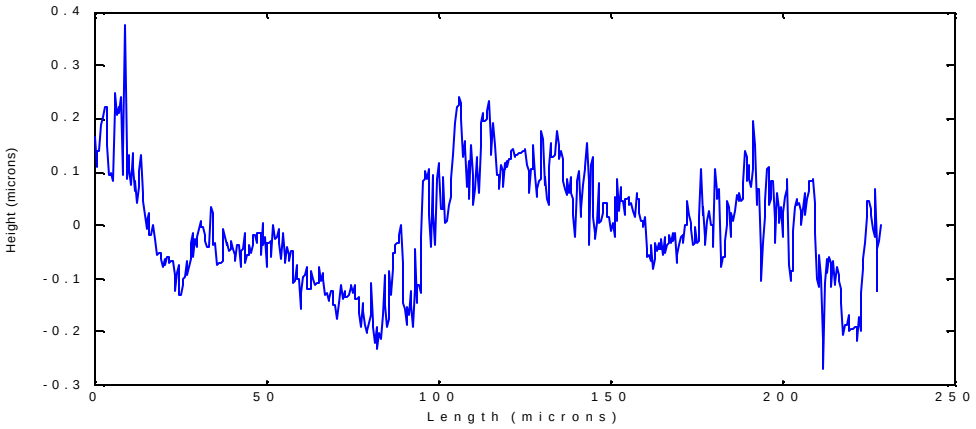

Figure 58: Surface profile generated from height information shown in Figure 47 for Al 2024 T3 panel surface @ 1000x

It is noted that a small number of "spike" features can be seen in the surface profile shown in Figure 58. These "spikes" are artifacts of the line-of-sight LSCM imaging process. Selective filtering can be used to remove these artifacts. The profile is shown here in the unaltered (unfiltered) state. Surface profiles obtained from LSCM imaging of the Al 2024 T3 panel analyzed using the same standard approach for determining roughness as was applied to the steel panels, yielding R_a=0.08µm and R_q=0.10µm.

Polymer Coatings

As illustrated in Figure 51, in the as-received state each coupon appeared to have a thin and uniform copper-colored coating on one surface. Those coatings that were applied to the

2024 T3Al substrates appeared to have inferior adhesion relative to the 1008/1010 steel substrates.

The BAM-PPV was applied by cool combustion spray, which may have given rise to the variations in gloss across the coupon surfaces, as shown in the black and white photograph of Figure 59. This change in reflectivity appears to be in the form of uniform stripes, evidently due to a raster-like application process. These stripes are not seen on the original substrate, and are attributed to small variations in coating surface roughness.

Figure 59: BAM-PPV Coated Al Panel

Figures 60 and 61 were acquired using standard optical microscopy. Figure 60 shows the BAM-PPV coating at approximately 100x magnification. Figure 61 shows the respective steel substrate underneath the BAM-PPV coating. A comparison of these two images indicates that the BAM-PPV coating appears to be closely following the inherent surface structure of the steel substrate.

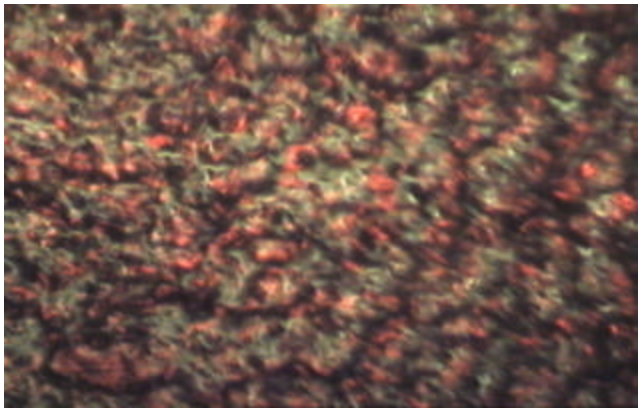

Figure 60: Optical micrograph of BAM-PPV coating of 1008/1010 steel substrate @ approx.100x

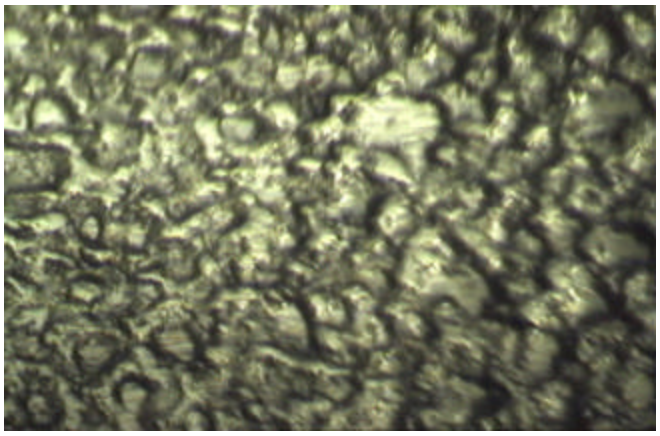

Figure 61: Optical micrograph of underlying 1008/1010 steel substrate @ approx. 100x

High resolution profilometry using LSCM at a magnification of 2000x confirms this mirroring of the substrate and EAP surface structure, as seen in Figure 62. This plot of surface profiles was generated by images taken at randomly selected locations from both the coated and uncoated regions of the panel. In good agreement with the steel surface, the roughness values obtained for the BAM-PPV surface were R_a=1.22µm and R_q=1.34µm.

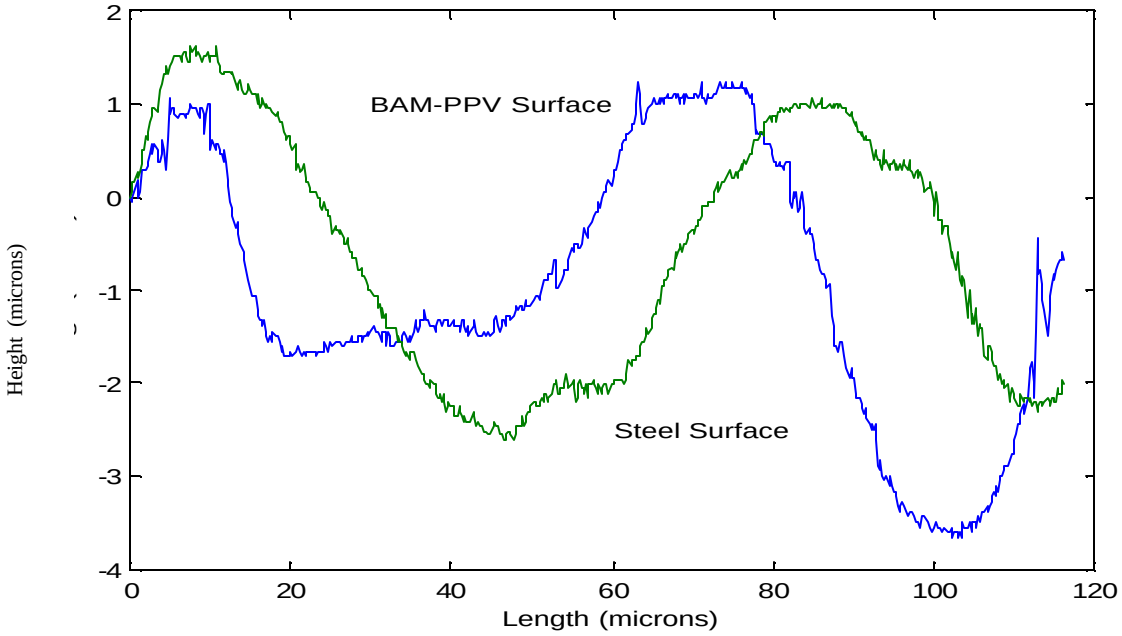

Figure 62: LSCM profilometry of EAP and steel substrate surfaces @ 2000x

LSCM profilometry was then applied to the BAM-PPV/Al 2024-T3 system to investigate the effects of substrate structure for this EAP/Al system. Results are shown in Figure 63. For this system the EAP coating does exhibit a larger min-max height deviation that that of the underlying Al surface. Because of the much smoother surface of the Al substrate, the inherent

height variations of the BAM-PPV coating can be more clearly observed. This contrasts with the BAM-PPV/steel system, where the substrate has much larger deviations. It is noted that the EAP surface profile shows several noise "spikes". This is due to the semi-transparent nature of the BAM-PPV coating, which allows some light to penetrate through to the highly reflective Al substrate below, resulting in noise spikes in the height image. As indicated previously, selective filtering can be used to remove these artifacts. The profile is shown here in the unaltered (unfiltered) state.

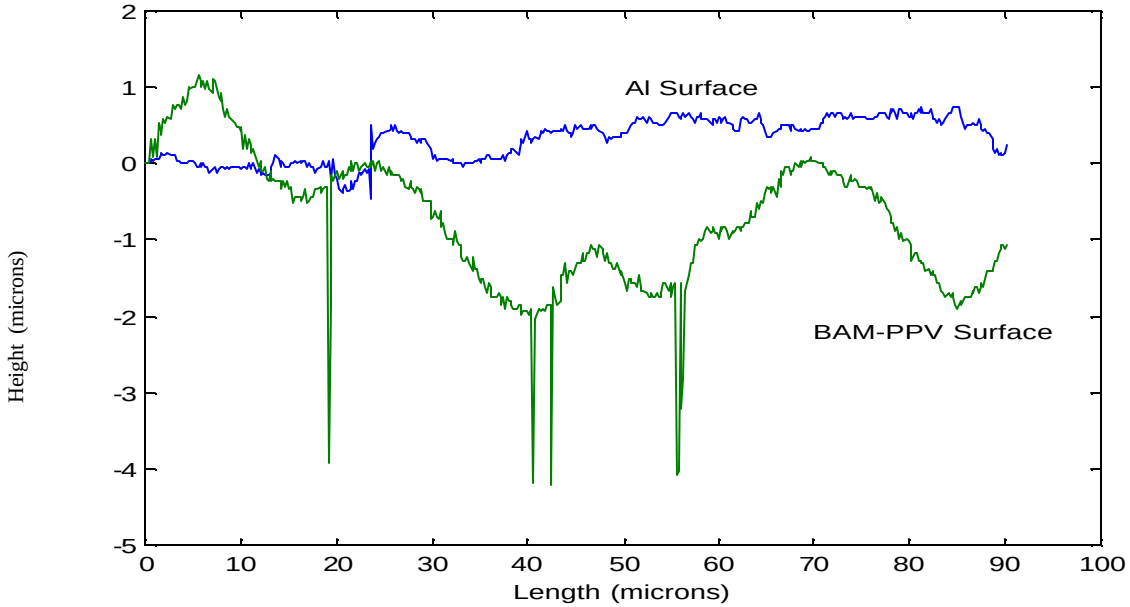

Figure 63: LSCM profilometry of EAP and aluminum substrate surfaces @ 2000x

Coatings appear to be uniformly and homogeneously applied to both steel and Al substrate surfaces. No major defects (e.g. pin holes) were observed. Surface roughness variations give rise to variations in gloss, resulting in observable stripes across the coupon surfaces. Coatings appear to follow substrate topography.

BAM-PPV Coated Films Analysis via Attenuated Total Reflectance Fourier Transform Infrared Spectroscopy (ATR-FTIR)

To investigate the flame spray application by MCT and any possible effects on the BAM-PPV, the coatings were analyzed using ATR-FTIR. BAM-PPV (15g) was sent to MCT with aluminum and steel substrates to obtain ten panels for initial testing. Spectra were taken of a pure polymer film made by evaporation at room temperature. Spectra were then taken of films that had been applied to substrates using the flame deposition process (Figures 64 and 65). In Figure 64 the absorbance peaks of the original film and the films deposited on aluminum and steel substrates indicate the same functional groups throughout all of the samples (see original BAM-PPV powder-FTIR sample, Figure 36). When the spectra are graphed simultaneously, as in Figure 65, the spectra overlap, indicating that there is no distinguishable difference between the films.

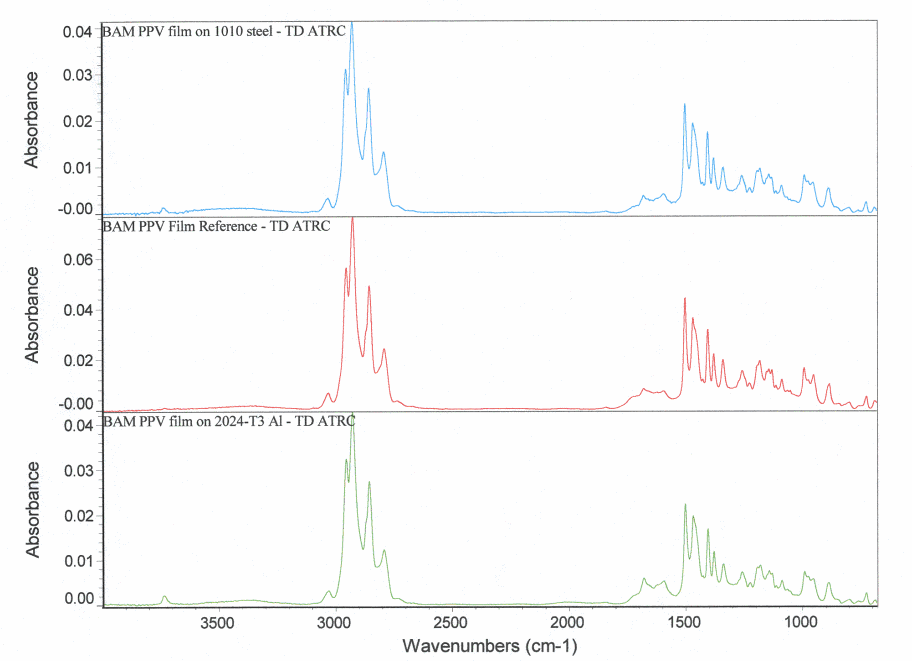

Figure 64: Absorbance spectra of BAM-PPV films using ATR-FTIR. Top: coating on steel panel, center: reference film, bottom: coating on Al 2024-T3

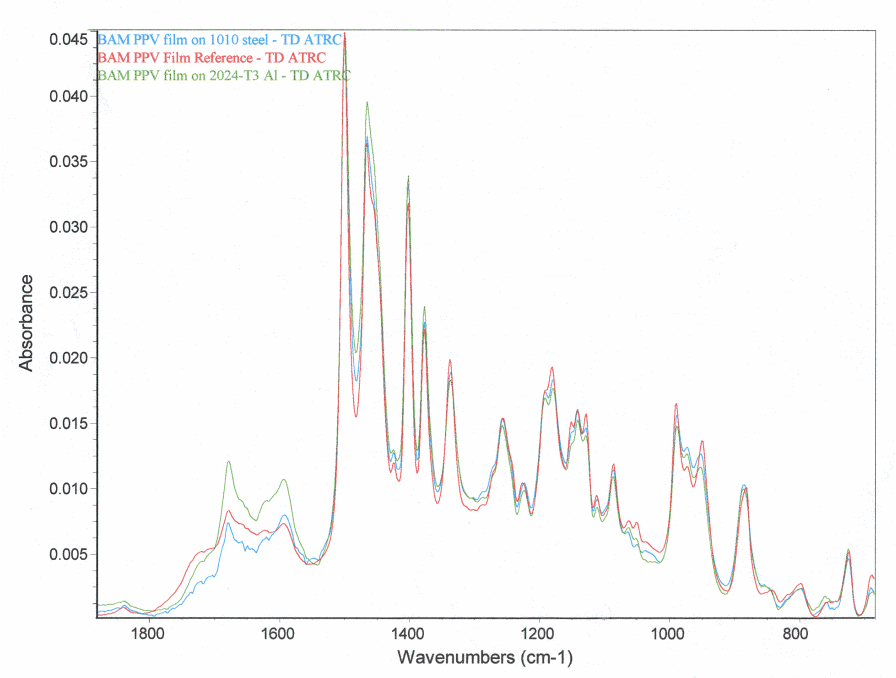

Figure 65: Overlapping spectra of the pure reference film and films applied on Al and steel substrates

The MCT flame deposition process did not alter the polymer, so fifty test panels were coated by MCT (25 Al 2024-T3 and 25 steel) for salt fog tests. The neutral salt fog testing of the

MCT Coated aluminum and steel panels began in FY01 on 16 panels according to ASTM B-117.[24] The initial tests are being done at neutral pH. The substrates coated with BAM-PPV using the flame deposition process include 2024-T3 aluminum (3 scribed and 3 unscribed) and 1008/1010 steel (3 scribed and 3 unscribed); these are being compared to control substrates, which are 2024-T3 aluminum (2 scribed and 2 unscribed) coated with a chromate conversion coating. This controlled salt spray test consisted of six aluminum 2024-T3 panels coated with BAM-PPV (3 scribed and 3 unscribed), six 1008/1010 steel panels (3 scribed and 3 unscribed), and six aluminum panels coated with a chromate conversion coating (3 scribed and 3 unscribed). Figures 66 and 67 are representative photos of scribed aluminum test panels before exposure in the salt spray chamber. These BAM-PPV coated panels for the neutral salt-fog salt spray tests were prepared by MicroCoating Technologies, Inc. (MCT, Chamblee, GA). BAM-PPV application was accomplished using a proprietary atomization and flame deposition process. The polymer films were analyzed using IR spectroscopy and compared to original BAM-PPV films that had not been exposed to flame or high temperatures. The composition of the films is not affected by MCT's atomization and flame deposition process.

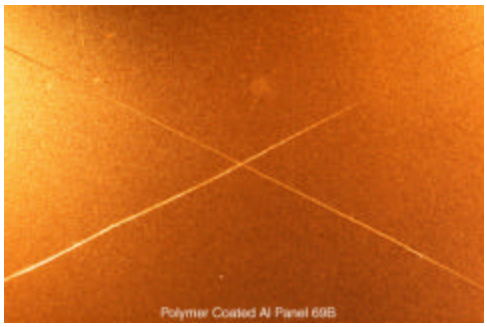

Figure 66: Polymer coated Al panel 69B before salt spray exposure.

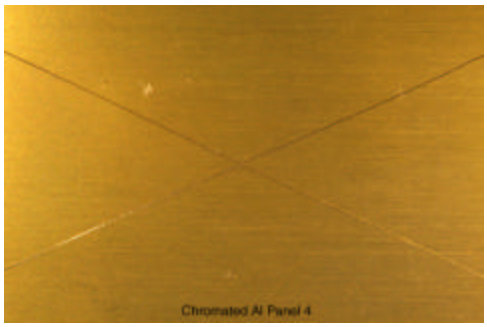

Figure 67: Chromate conversion coated Al panel before salt spray exposure.

After an exposure time of 41 hours in a salt spray chamber, it was apparent (Figure 68) that BAM-PPV did not adhere well to the untreated steel panels using the flame deposition application.

Figure 68: Steel panels after 41 hours of salt spray exposure.

After the initial 41 hours, all of the steel panels were removed from the salt spray test with the exception of one. The remaining steel panel was removed from the test after 616 hours due to failure. BAM-PPV has shown poor adhesion onto 1008/1010 steel panels when applied only as a pretreatment. Figures 69 and 70 shows the overall appearance of the scribed polymer and scribed conversion coated panels. After 616 hours of salt spray exposure, the aluminum

panels coated with BAM-PPV performed similarly to the chromated panels In Figures 71 and 72, corrosion products can be seen within the scribe lines of both the chromate conversion coated panels and the polymer coated panels; unscribed panels are shown in Figures 73 and 74. Under high magnification (60x) there are slightly more corrosion products visible within the scribes of the polymer coated panels than in the conversion-coated panels. However, the unbreached portion of the polymer coating is largely unaffected by the exposure to salt spray. Overall, the performance of the polymer coatings was similar to the performance of the conversion coatings after 616 hours of exposure in neutral salt fog.

Figure 69: Scribed polymer-coated Al panel after 616 hours of exposure.

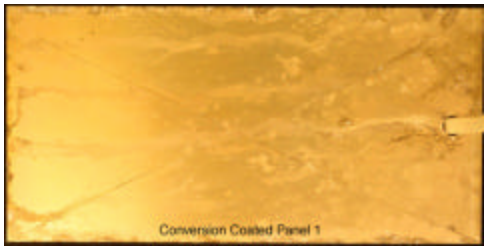

Figure 70: Scribed conversion-coated Al panel after 616 hours of exposure.

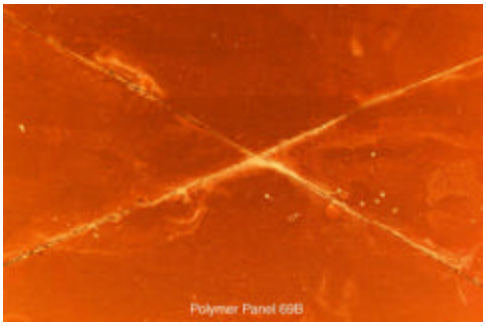

Figure 71: Scribed polymer-coated Al panel after 616 hours of exposure.

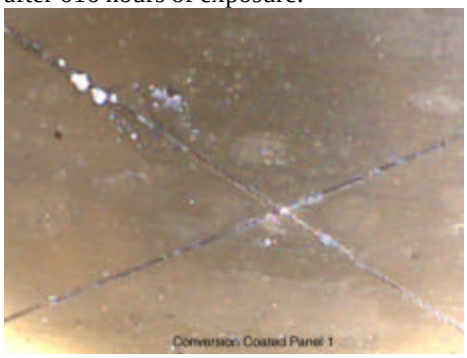

Figure 72: Scribed conversion-coated Al panel after 616 hours of exposure.

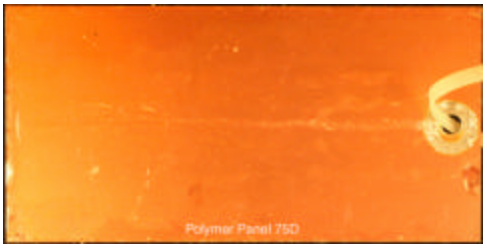

Figure 73: Unscribed polymer-coated Al panel after 616 hours of exposure.

Figure 74: Unscribed conversion-coated Al after 616 hours of exposure.

The panels were later removed from the salt fog chamber for evaluation after an exposure time of 1146 hours. It can be seen in Figures 75 and 76 that the polymer coated and chromated panels still had a similar appearance overall. Both panels had corrosion products within the scribed areas, but the overall coating was largely unaffected. Both panels also exhibited more corrosion along the edges than through the bulk of the coatings.

Figure 75: Scribed polymer coated Al panel (1146 hours of exposure).

Figure 76: Scribed conversion coated Al panel (1146 hours of exposure).

Unscribed polymer and chromated panels are compared in Figure 77 after an exposure time of 1146 hours. Just as with the scribed panels, the appearance of the two coatings is very similar.

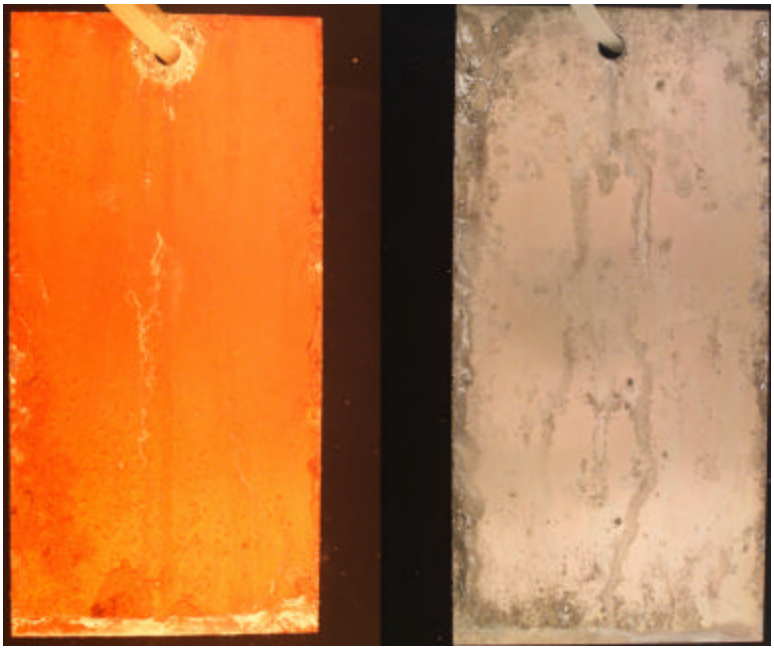

Figure 77: Comparison of polymer coated Al panel (left) to chromated Al panel (right) after 1146 hours of exposure.

The panels were returned to the salt fog chamber and removed again after an exposure time of 3000 hours. Figure 78 is the BAM-PPV polymer-coated panel, and Figure 79 is the chromated panel.

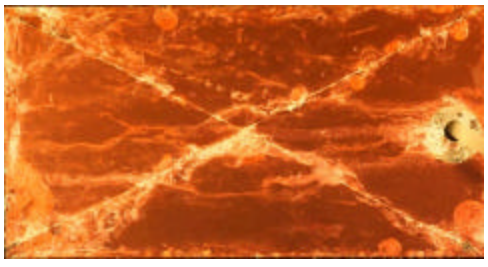

Figure 78: Scribed polymer coated Al panel (3000 hours of exposure).

Figure 79: Scribed conversion coated Al Panel (3000 hours of exposure).

A comparison of the unscribed BAMPPV coated panel and the conversion-coated panel after an exposure time of 3000 hours indicates that the polymer coating performs similarly to the hexavalent chrome conversion coating.

Neutral Salt Spray Tests of BAM-PPV-Based Coating Systems

A second set of salt spray tests (ASTM B117) began in FY02 to evaluate the BAM-PPV coatings on aluminum (Al 2024-T3) in place of a CCC with a standard military system consisting of the chromated epoxy primer Mil-P-23377 and the urethane topcoat Mil-P-85285. Multiple variables are being examined in this test matrix. One variable is the comparison of the BAM-PPV coating by MCT (flame spray) and a simple solution spray technique (air brush) using a gas carrier (nitrogen). Coating failure and inconsistencies could be seen (Figure 80) with the MCT coated panels within 19 hours. No further testing was done with BAM-PPV and primer/topcoat using the MCT method.

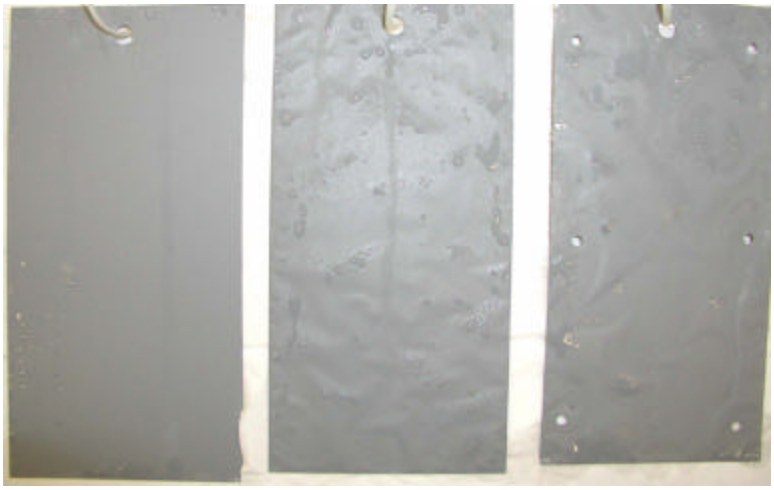

Figure 80: Failure of Al panels coated with flame deposition process after an exposure time of 19 hours.

Another variable within the test matrix was the inclusion and exclusion of the chromated epoxy primer. This was done to determine if the BAM-PPV could function as a primer and corrosion inhibitor and eliminate the need for the conversion coat and primer. Coating failures began to appear around the edges of panels that did not contain the primer within 240 hours. Panels that contained the BAM-PPV coating followed by primer and topcoat have not failed after 500+ hours of exposure (Figure 81).

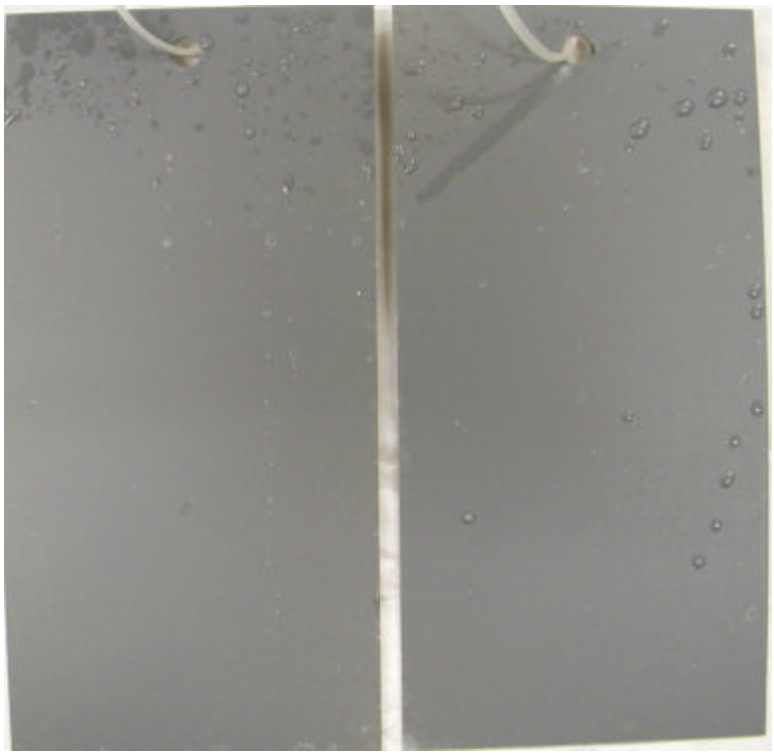

Figure 81: Al panels coated with airbrushed BAMPPV followed by primer and topcoat after 748 hours of exposure.

The neutral salt fog test results during FY02 show (Figures 82 and 83) that after 1000 hours the performance of BAM-PPV sprayed onto bare aluminum followed by the standard primer and topcoat performs as well as the control, which contains a chromate conversion coating beneath the primer. Other coatings systems that included the flame deposited polymer coatings failed before 1000 hours.

Figure 82: Panel coated with BAM-PPV/primer/topcoat. Visible spots are water droplets on the surface.

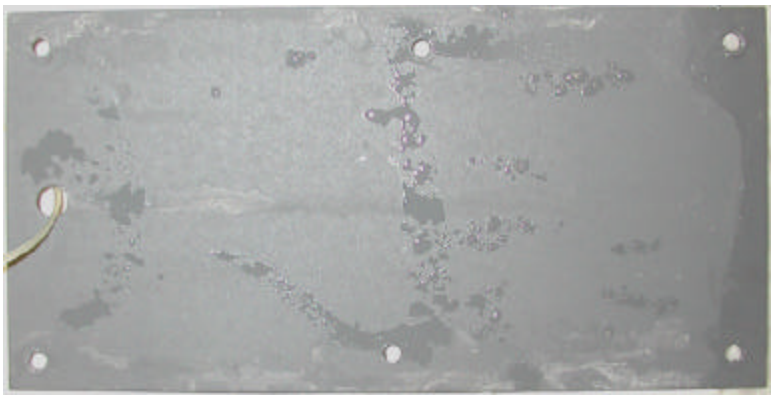

Figure 83: Panel with chromated conversion coat/primer/topcoat. Visible dark sections are water on the panel surface.

SERDP FY03/04

BAM-PPV Coating Surface Morphology:

Scanning Electron Microscopy (SEM) was used to obtain high magnification images of the surface of BAM-PPV coatings. Samples were applied to aluminum test panels with no surface treatment as well as onto mirror finish aluminum substrates. A thickness of approximately 0.2µm was examined as well as a thinner coating whose exact thickness could not be measured (due to the small sample size) but is believed to be less than 0.1µm. Figure 84 is a 50x magnification of the thin coating (<0.1µm). The notable features are the striations from the metal surface and the overall uniform appearance of the coating. Figure 85 is a 50x magnification of the 2µm thick coating also on the untreated metal surface.

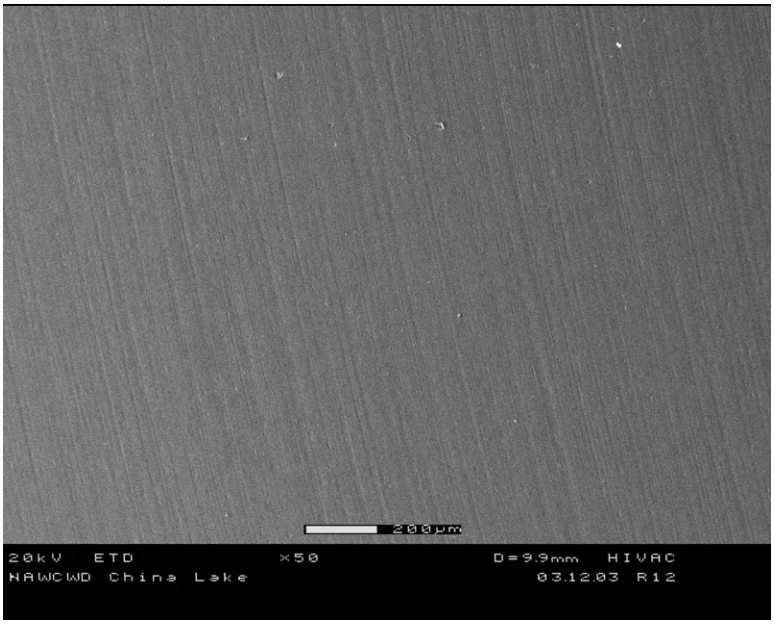

Figure 84: 50x magnification of thin coating (<0.1µm) on untreated surface.

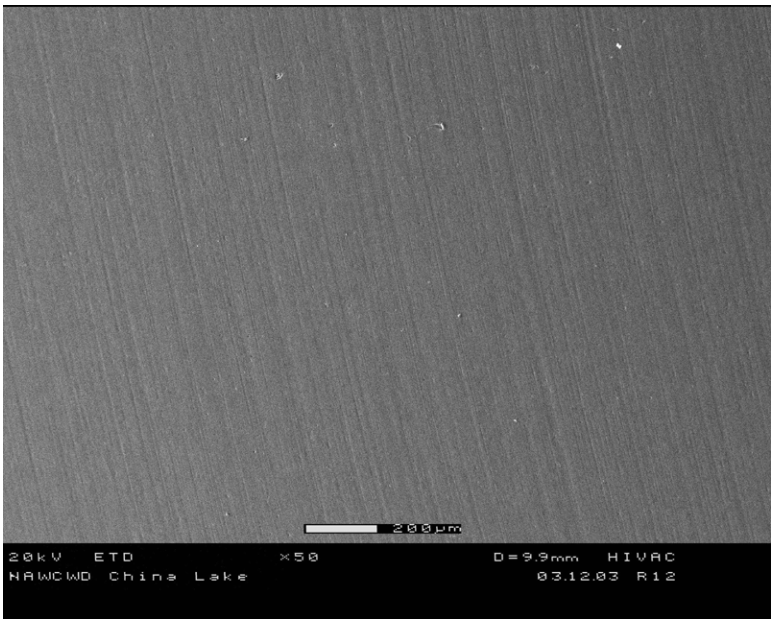

Figure 85: 50x magnification of the 2µm thick coating on untreated surface.

Figure 86 and Figure 87 show the bare polished surface and the coating on the polished surface, respectively. The surfaces were polished in order to view the features of the polymer surface more clearly and to reduce the appearance of the features of the substrate such as the striations seen in Figures 84 and 85 above. Debris and initial corrosion sites on the metal surfaces can be seen in both photos. The filament-like features are the corrosion sites that resulted from the polishing process and are not features of the polymer film. There are no visual defects in the coatings at 1000x magnification (Figures 86 and 87).

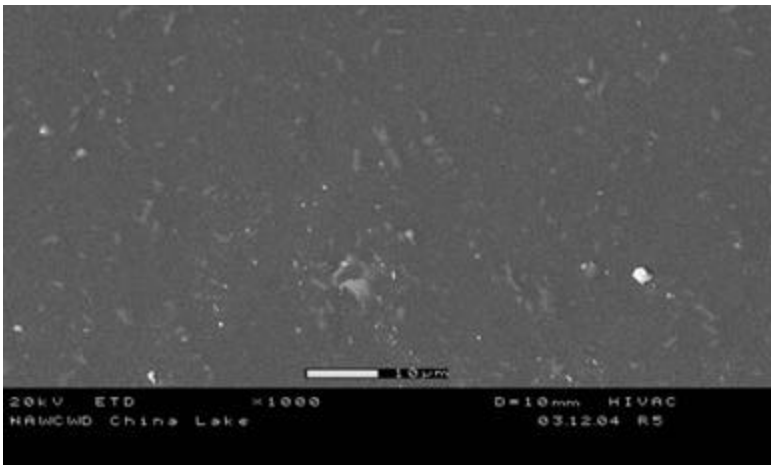

Figure 86: 1000x magnification of polished surface without coating.

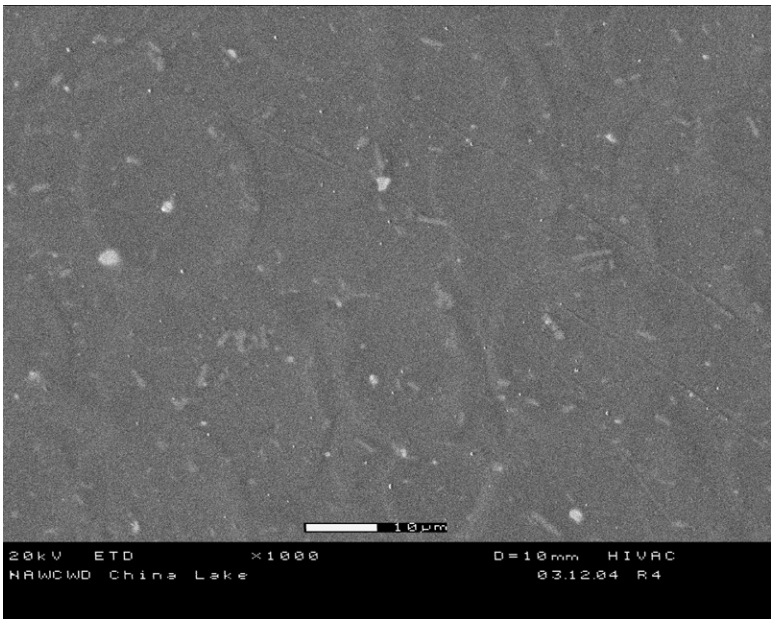

Figure 87: 1000x magnification of the thin coating on polished surface.

Figure 88 shows a 50x magnification of the interface of the coating and bare aluminum. The top portion of the image (darker) is the coated portion and the lower (lighter) portion of the image is the uncoated portion of the polished surface. Figure 89 shows a 500x magnification of the coated portion. The spray pattern and the overlap of the polymer as it impacted the surface are visible at 500x magnification. A 500x photo of the uncoated polished surface can be seen in Figure 90.

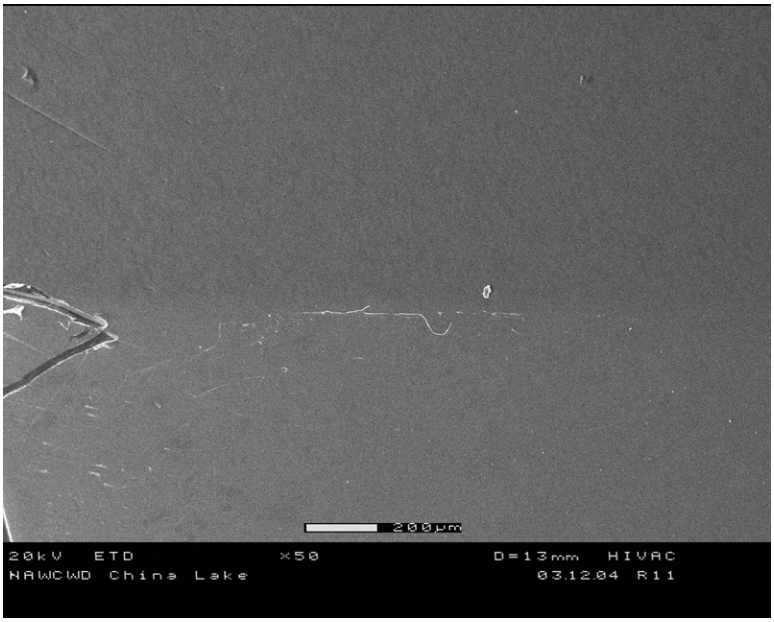

Figure 88: 50x magnification of the interface of the polymer coating with the bare aluminum polished surface.

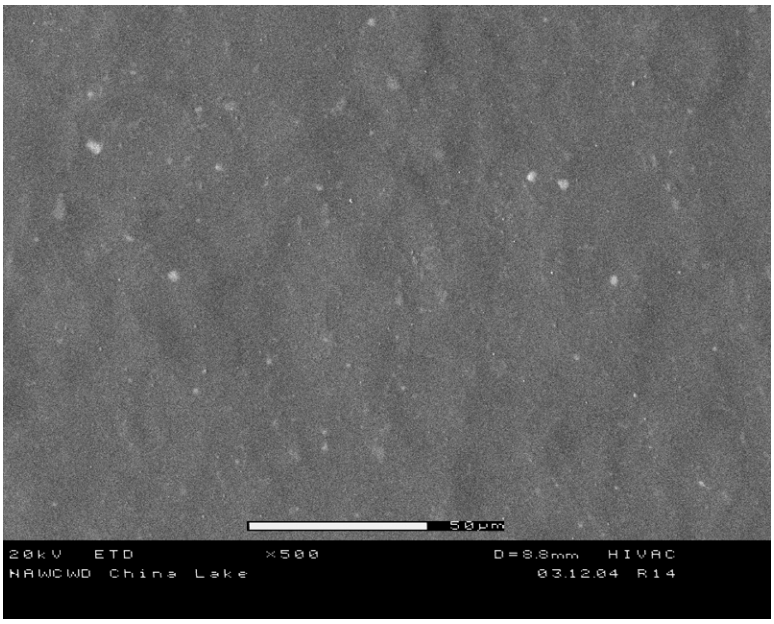

Figure 89: 500x magnification of the 0.2µm thick coating on the polished surface.

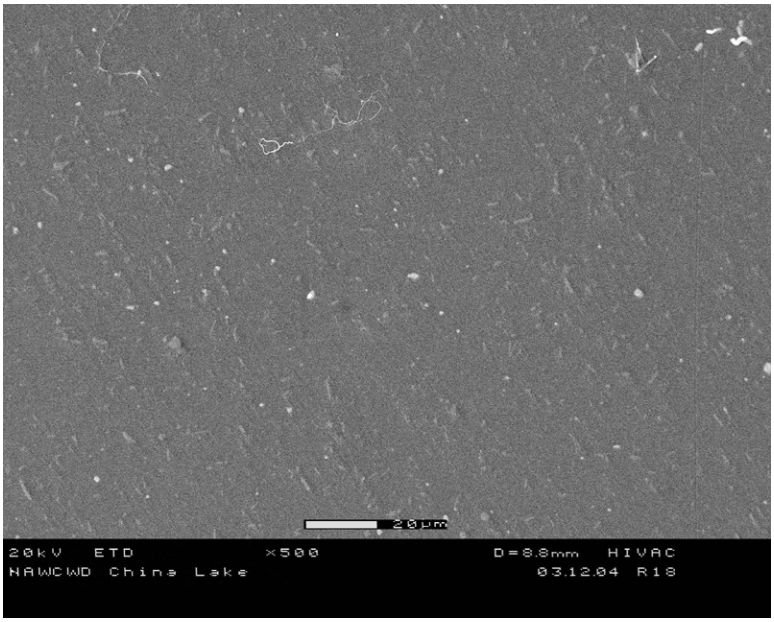

Figure 90: 500x magnification of the uncoated polished surface.

The SEM images indicate that at 0.2µm thick, the BAM-PPV coating is uniform overall and nonporous. At higher magnification (20,000x) defects can be found within the coating with diameters of 0.5 to 2µm. These defects were found very rarely within the 0.2µm coating and are expected to be rare in a standard coating of 0.5µm. The minimum coating thickness used for corrosion testing that has shown corrosion resistance to 4000 hours in the salt spray tests is approximately twice as thick at 0.4 to 0.5µm.

Neutral Salt Fog Testing of BAM-PPV vs. Alternative Pretreatment Coatings

Methods:

During FY03/04 with adequate quantities of pure BAM-PPV (>2.5 kg) on hand the polymer was used to coat various substrates for testing in neutral salt fog chamber as an alternative pretreatment to CCC. The polymer, BAM-PPV was dissolved in xylenes and *d*-limonene (Dipentene) solutions, the latter is an non-toxic solvent, EPA food additive.[25] Limonene is an non-ozone depleting chemical, and is not considered an air toxic or hazardous air pollutant (HAP) and is not regulated under the Clean Air Act or SARA Title III.

The BAM-PPV solutions were air-brushed onto Al 2024-T3 substrates and dried for 2 hours at 60°C under house vacuum for the BAM-PPV xylenes coated panels. The *d*-limonene coated panels required longer drying times between 12-16 hours at 100°C under vacuum. The panels were placed in a neutral salt fog chamber and monitored over selected time intervals for their performance. The thin films of BAM-PPV (<1.0 microns) did not pass neutral salt fog exposure (Figures 91 and 92). Corrosion was evident in these films. The thicker films (>1.0 microns) did pass neutral salt fog exposure without evidence of discoloration, corrosion, blistering or delamination of the films (Figures 93 and 94). All tests were run against the chromate conversion coating (CCC) as controls.

Figure 91: BAM-PPV Coated Al 2024-T3
Coating Thickness <1.0 micron
Time = 0 hours

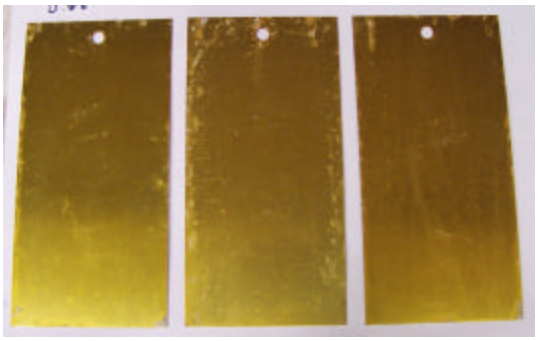

Figure 92: BAM-PPV Coated Al 2024-T3
Coating Thickness < 1.0 micron
Time = 168 hours

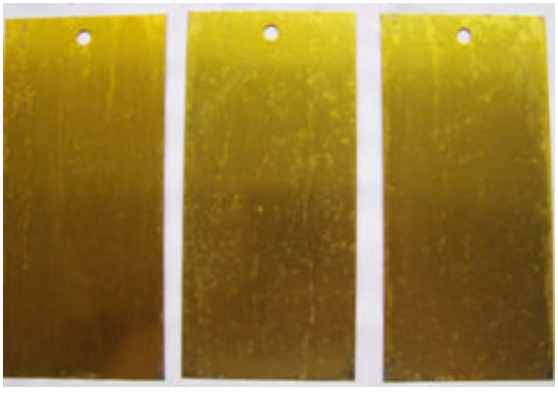

Figure 93: BAM-PPV Coated Al 2024-T3
Thickness > 1.0 micron
Time = 336 hours

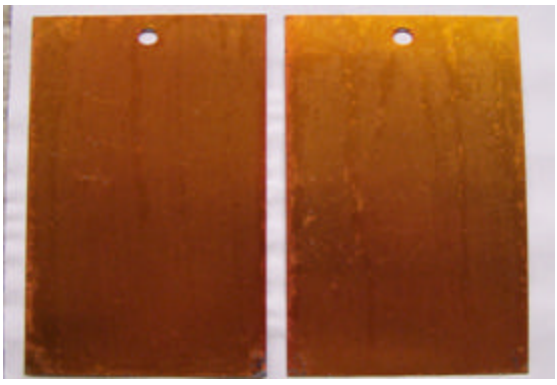

Figure 94: BAM-PPV Coated Al 2024-T3
Thickness > 1.0 micron
Time = 336 hours

Additional pretreatments were tested against BAM-PPV. Two pretreatments AC 131 (formally Bogel, a sol-gel pretreatment formulation) and Alodine 5700 (Henkel Inc, inorganic pretreatment system) were obtained via a commercial vendor and supplied to the NAWCWD. The two pretreatments were placed in neutral salt fog chamber and monitored over selected time intervals for their performance. In both cases these pretreatments did not last to the required 336 hours neutral salt fog. In fact, they failed at 24 hours, extensive corrosion damage was evident (Figure 95-99). Tri-valent chromium pretreatment (TCP) coupons were supplied by the NAWC-AD and coated onto Al 2024-T3. The TCP pretreatment samples lasted well over 1000 hours (Figures 100-103).

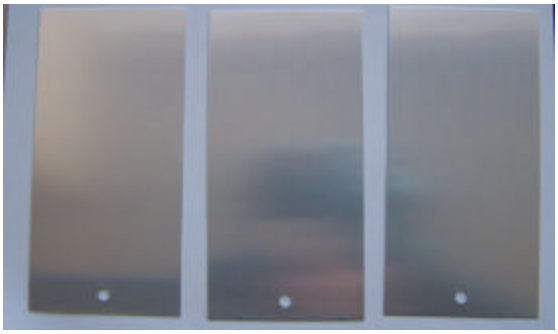

Figure 95 : AC131 Pretreatment on Al 2024-T3 Time = 0 hours

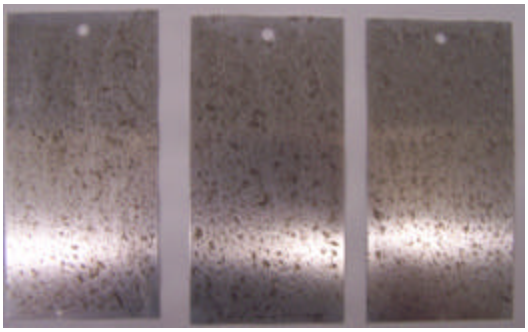

Figure 96: AC131 Pretreatment on Al 2024-T3 Time = 24 hours

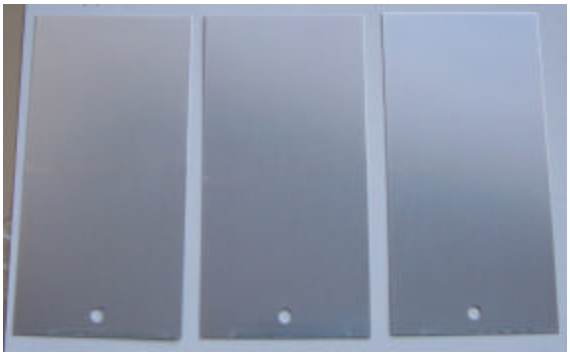

Figure 97: Alodine 5700 Pretreatment on Al 2024-T3, Time = 0 hours

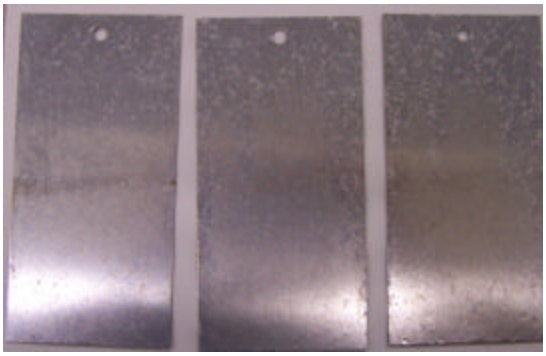

Figure 98: Alodine 5700 Pretreatment on Al 2024-T3, Time = 24 hours

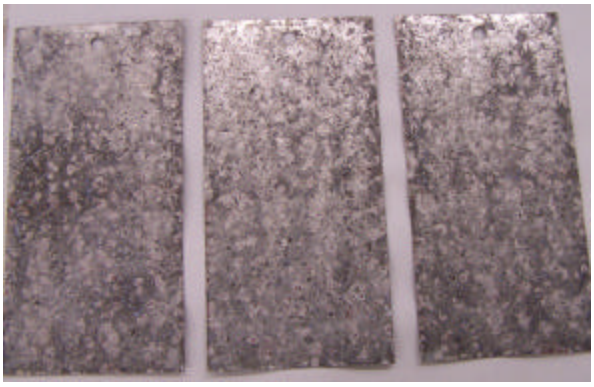

Figure 99: Alodine 5700 Pretreatment on Al 2024-T3 Time = 168 hours

Figure 100: TCP on Al 2024-T3
Time = 0 hours

Figure 101: TCP on Al 2024-T3
Time = 336 hours

Figure 102: TCP on Al 2024-T3
Time = 1000 hours

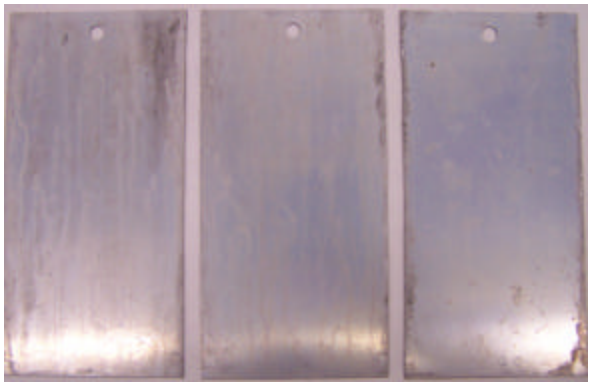

Figure 103: TCP on Al 2024-T3
Time = 1500 hours

Polyaniline and EAPs based on oligomers of aniline was also examined as an alternative coatings to CCC. Aniline (37.4g, 0.40 mol) was added to an aqueous HCl solution (2.0 M, 400 mL) and cooled to 0 ºC with ice bath. An ammonium persulfate solution (1.5 M, 400 mL) was added dropwise. The temperature of the reaction mixture was always kept below 20 ºC during the addition. After complete addition, the polymerization temperature was kept near 0 ºC, and the polymerization time was about 5 hours. The polyaniline (PANI)was washed with water, methanol and diethylether and allowed to air dry overnight. The resulting solid was crushed in a mortar and pestle and stirred in 3% ammonium hydroxide solution for two hours, and then washed with water, methanol and diethylether. The polyaniline was air dried for several hours and dried in vacuum oven overnight. The yield was 85% and the inherent viscosity was 0.7 dL/g (0.1% in conc. sulfuric acid at 30.0 ºC). Solutions of PANI were prepared as follows: Tinuvin 770 (100mg) was dissolved in 100 mL1-methyl-2-pyrrolidinone (NMP). PANI (5g) was added gradually into the solution with stirring until fully dissolved. The surface of the metal substrates was prepared by sand blasting to remove surface oxidation and increase the roughness. PANI was spray coated on the metal substrates and dried in an oven at 80 ºC for 15 min, and coated with the second layer and dried at 80 ºC for three hours. The substrates were immersed in 0.1 M

p-toluenesulfonic acid/tetrahydrofuran (THF) for 24 hours, and washed with THF and air dried overnight. The samples were aluminum coupons (Al 6061-T6) and steel coupons (1008). The neutral salt fog exposure of both aluminum and steel samples showed that PANI used as pretreatment coatings does not meet the minimum requirement for a new military coating. Discoloration was observed prior to 336 hours in neutral salt fog (Figures 104-110).

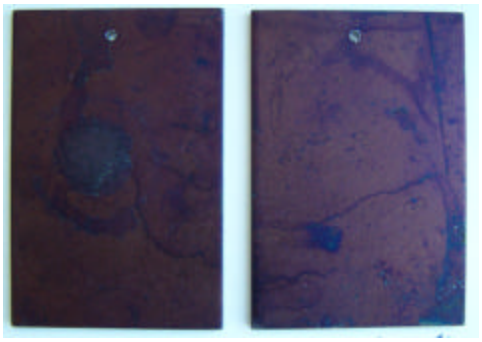

Figure 104: PANI Coated steel
Time = 0 hours

Figure 105: PANI Coated steel
Time = 168 hours

Figure 106: PANI Coated steel
Time = 336 hours

Figure 107: PANI Coated Al 6061-T6
Time = 0 hours

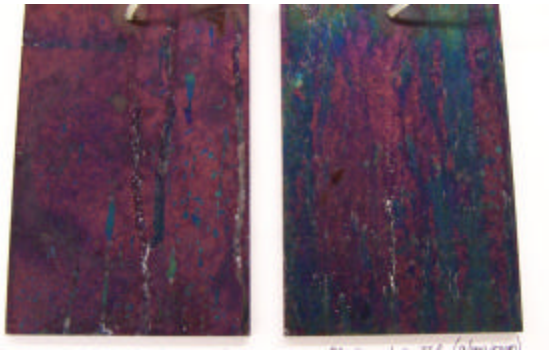

Figure 108: PANI Coated Al 6061-T6
Time = 168 hours

Figure 109: PANI Coated Al 6061-T6
Time = 336 hours

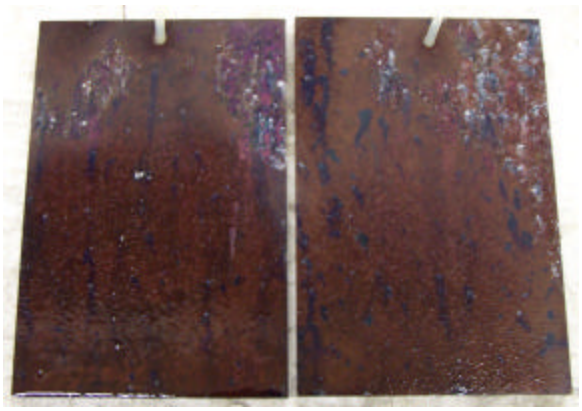

Figure 110: PANI Coated Al 6061-T6
Time = 500 hours

Neutral Salt Fog Testing of BAM-PPV and other Pretreatments with Non-Chrome Primers

The pretreatment results above have shown that BAM-PPV can provide corrosion protection in neutral salt fog exposure tests and can pass the minimum requirement for CCC pretreatment replacement. In addition, BAM-PPV can be incorporated into military coating systems using current spray technology onto Al 2024-T3 specimens. Full military coatings were prepared using BAM-PPV as the pretreatment coating (> 1.0 micron thickness), with a non-chromated primer (MIL-P-53030, epoxy, water reducible, lead and chromate free), or MIL-P-53022 (epoxy primer, corrosion inhibiting, chromate and lead free) or MIL-PRF- 85582 (epoxy, water-bourne primer, non-chromated, Class N) with a topcoat (MIL-PRF-85285, aliphatic urethane, solvent based, two component). The BAM-PPV was applied via spray technology in-house at NAWCWD and the epoxy primer and topcoat were coated onto the BAM-PPV pretreatment at the NAWCAD. The full military coatings were measured against a full chromated military coating system (MIL-DTL-81706, CCC), chromated primer (MIL-PRF-23377, epoxy polyamide) and non-chromated topcoat (MIL-PRF-85285, aliphatic urethane solvent based, two component). Additional coating comprised the TCP pretreatment with non-chromated primer (MIL-PRF-53030) and topcoat (MIL-PRF-85285). The full military coating systems were scribed and placed in neutral salt fog chamber and monitored at selected intervals for corrosion along the scribed area (Figures 111-124). The results show that the BAM-PPV military coating performed as well as the TCP military coating system. A minimum passing criteria for the non-chrome coating systems was to provide corrosion protection of scribed substrates for no less than 2000 hours. Slight corrosion in the scribe is acceptable but blistering, undercutting of the coating, or excessive corrosion constitute failing performance. None of the non-chrome primer systems passed 2000 hours of salt fog except for the controls containing hexavalent chrome pretreatment and primer. It is clear from the salt fog results that current non-chrome primers are inadequate even over a CCC. The three coating systems that prevented corrosion up to 2000 hours (utilizing a chromated primer) include hexavalent chrome, trivalent chrome and BAM-PPV pretreatments.

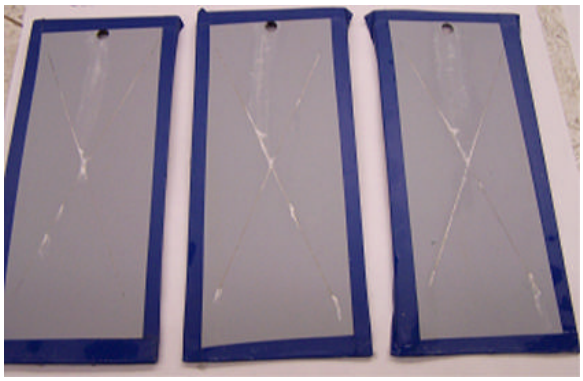

Figure 111: BAM-PPV + Mil-P-53022 + + Mil-PRF-85285 on Al 2024-T3 2000 hours of exposure

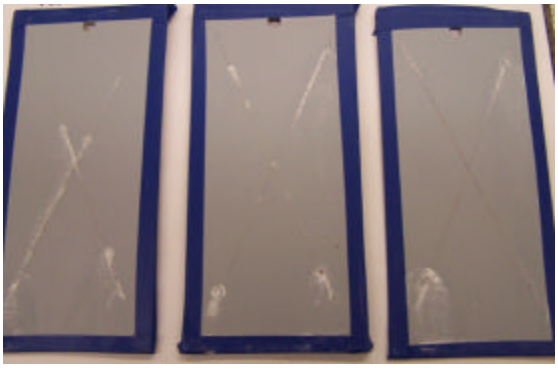

Figure 112: TCP + Mil-P-53022 + Mil-PRF -85285 on Al 2024-T3 2000 hours of exposure

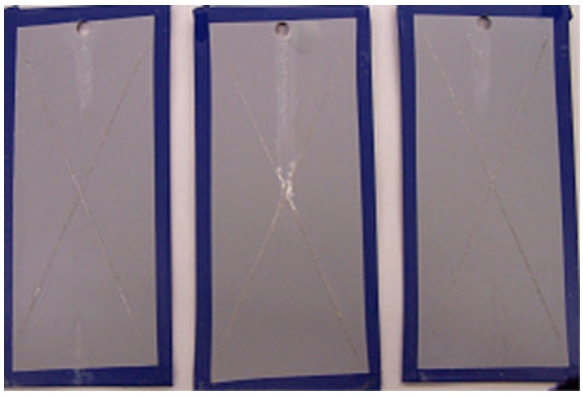

Figure 113: Alodine 5700 + Mil-P-53022 + Mil-PRF-85285 on Al 2024-T3 2000 hours of exposure

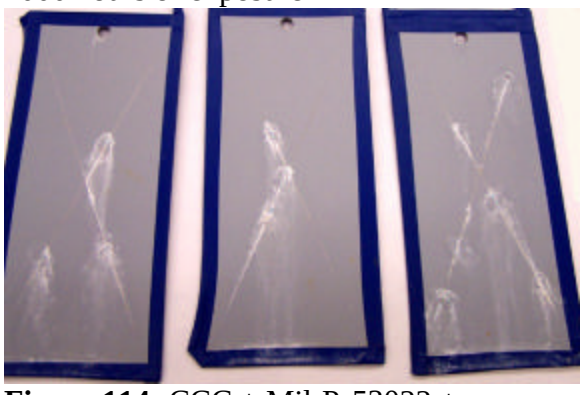

Figure 114: CCC + Mil-P-53022 + Mil-PRF-85285 on Al 2024-T3 2000 hours exposure

Figure 115: BAM+PPV + Mil-P-53030 + Mil-PRF-85285 on Al 2024-T3
2000 hours of exposure

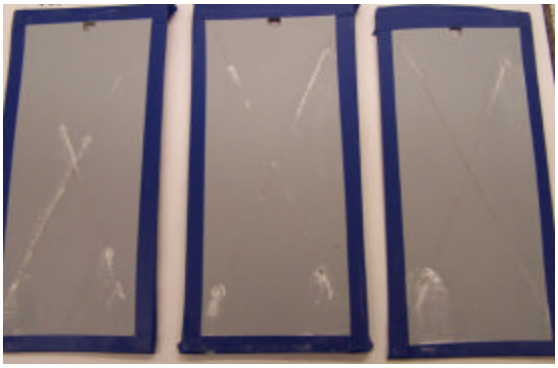

Figure 116: TCP + Mil-P-53030 + Mil-PRF -85285 on Al 2024-T3
2000 hours of exposure

Figure 117: Alodine 5700 + Mil-P-53030 + Mil-PRF-85285 on Al 2024-T3
2000 hours of exposure

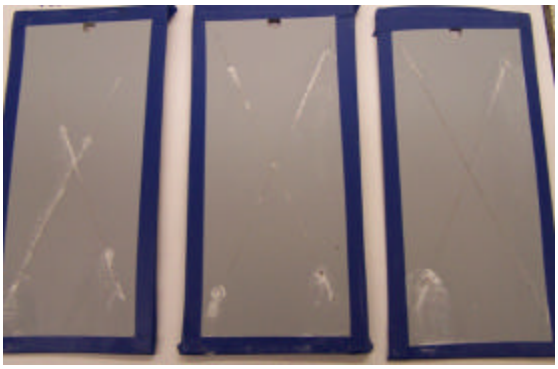

Figure 118: CCC + Mil-P-53030 + Mil-PRF -85285 on Al 2024-T3
2000 hours of exposure

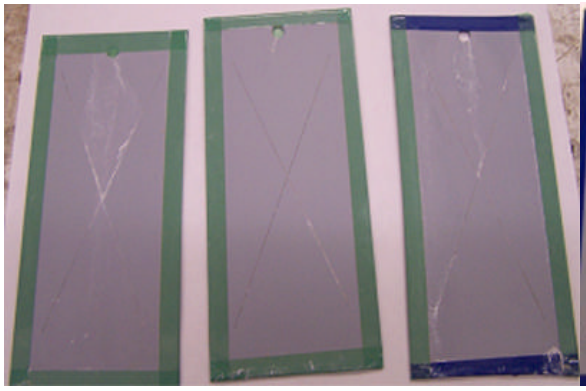

Figure 119: Alodine 5700 + Mil-PRF-85582 (N) + Mil PRF-85285 on Al 2024-T3 2000 hours of exposure

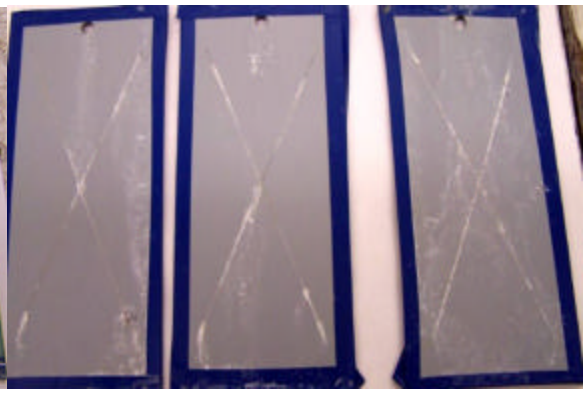

Figure 120: AC-131 + Mil-PRF+85582 (N) + Mil-PRF-85285 on Al 2024-T3 2000 hours of exposure

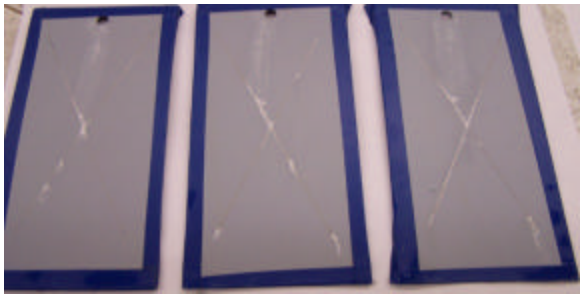

Figure 121: CCC + Mil-PRF-85582 (N) + Mil-PRF-85285 on Al 2024-T3 2000 hours of exposure

Figure 122: BAM-PPV + Mil-PRF-23377 + Mil-PRF-85285 on Al 2024-T3 2000 hours of exposure

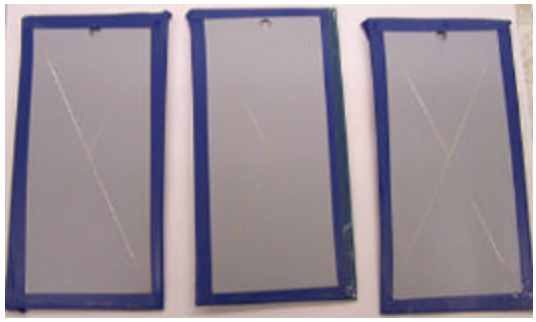

Figure 123: CCC + Mil-PRF-23377 + Mil-PRF-85285 on Al 2024-T3 2000 hours of exposure

The salt fog tests continued to 4000 hours. After 4000 hours of exposure, the only coating systems that still had a passing performance were the BAM-PPV, TCP, and

hexavalent chrome pretreatments used in conjunction with the chromated primer (Figure 124).

Figure 124: BAM-PPV + Mil-PRF-23377 + Mil-PRF-85285 on Al 2024-T3
4000 hours of exposure

Testing on Aluminum Alloy 2219-T87

BAM-PPV was applied to Al 2219-T87 panels for testing with the non-chrome primers (Figures 125-128). The only coating system that passed the required time of 2000 hours was the system that contained the chromated primer Mil-PRF-23377. BAM-PPV was the only pretreatment tested (Figure 128).

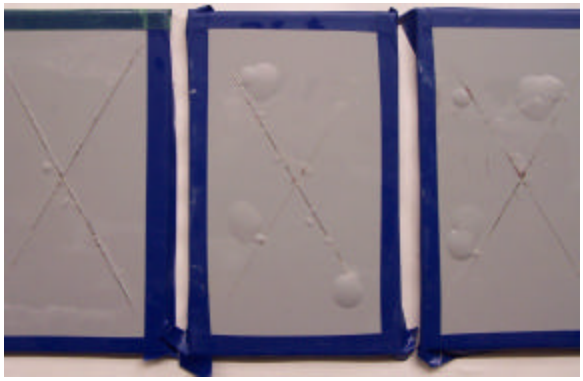

Figure 125: Al 2219-T87 with BAM-PPV + Mil-P-53030 + Mil-PRF-85285
840 hours of exposure

Figure 126: Al 2219-T87 with BAM-PPV +Mil- P-53022 + Mil-PRF-85285
500 hours of exposure

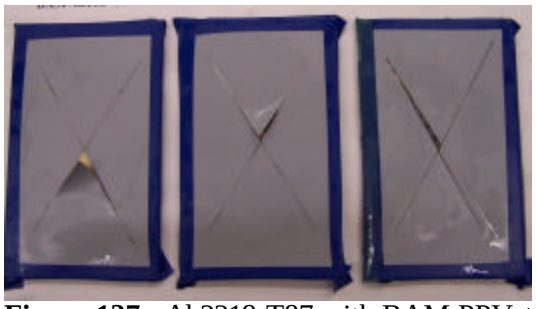

Figure 127: Al 2219-T87 with BAM-PPV + Mil-PRF-85582 + Mil-PRF-85285
500 hours of exposure

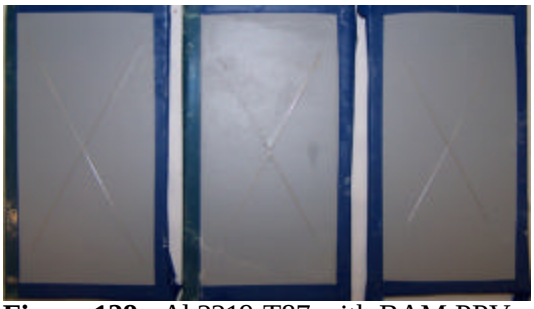

Figure 128: Al 2219-T87 with BAM-PPV Mil-PRF-23377 + Mil-PRF-85285
2560 hours of exposure

Evaluation of BAM-PPV as a Chemical Agent Resistant Coating (CARC)

BAM-PPV solutions were applied to Al 2024-T3 and 1008 steel substrates. Both solvent-borne CARC (MIL-C-46168) polyurethane and waterborne CARC polyurethane (MIL-DTL-64159) topcoats were applied by Benet Laboratories. The panels were placed in a neutral salt fog chamber and monitored over time along with CARC control panels. In all cases, there was delamination of the coating at the pretreatment/surface interface. It is likely that during the paint application, there was a solvent interaction with the BAM-PPV causing it to soften, leading to delamination. Panels that contained the solvent-borne primer had better performance than those containing the waterborne primer. Figures 129-132 are of Al 2024-T3 coated substrates.

Figure 129: Al 2024-T3 with BAM-PPV + + Mil-P-53030 + Mil-C-46168
before exposure

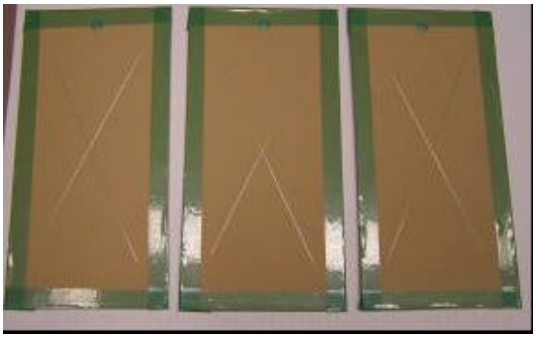

Figure 130: Al 2024-T3 with BAM-PPV Mil-P-503030 + Mil-C-46168
1250 hours of exposure

Figure 131: Al 2024-T3 with BAM-PPV + Mil-P-53030 + Mil-C-53039
before exposure

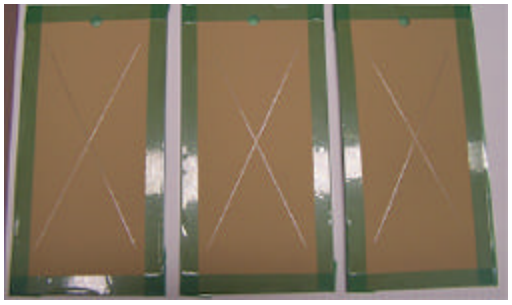

Figure 132: Al 2024-T3 with BAM-PPV + Mil-P-53030 + Mil-C-53039
718 hours of exposure

Note that in Figure132, delamination is beginning to occur at the center of the scribed portion of the paint. In all cases of CARC coatings on steel, corrosion and delamination are evident (Figures 134 and 136). The waterborne CARC coatings showed catastrophic failure after 48 hours (Figure 136), while the solvent borne coatings failed after 230 hours of exposure (Figure 134).

Figure 133: 1008 Steel with BAM-PPV + Mil-P-53030 + Mil-C-46168
before exposure

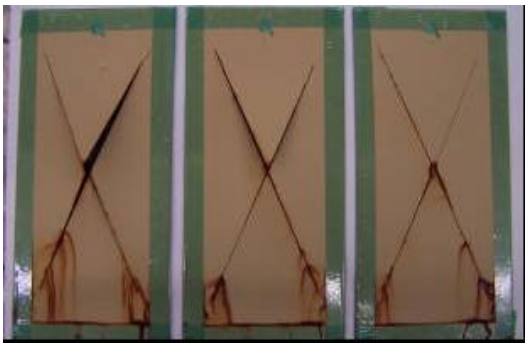

Figure 134: 1008 Steel with BAM-PPV + Mil-P -53030 + Mil-C-46168
230 hours of exposure

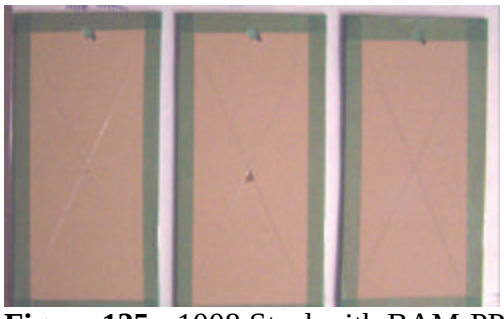

Figure 135: 1008 Steel with BAM-PPV + + Mil-P-53030 + Mil-C-53039
before exposure

Figure 136: 1008 Steel with BAM-PPV Mil- P-53030 + Mil-C-53039
48 hours of exposure

BAM-PPV Powder Coating Samples-Neutral Salt Fog Exposure Test Methods:

Several powder coating samples containing 1 wt% BAM-PPV dispersed in a commercial polyester resin were prepared by MacroSonix Inc. The commercial resin consisted of triglycidyl isocyanurate (TGIC) polyester resin with BAM-PPV average particle size range of 45-57 microns. An acoustic blending technique was used to incorporate the BAM-PPV into the resin. The BAM-PPV powder was applied via e-coat onto Al 2024-T3 substrates at the NADEP, Jacksonville, Florida. The two primary goals of this test were to (1) determine if BAM-PPV could be successfully incorporated into a powder coating and (2) determine if there was a distinguishable difference in corrosion protection by adding 1% BAM-PPV as a corrosion inhibitor. Neutral salt fog experiments for 1500 hours of exposure time showed no significant difference between BAM-PPV powder coating samples and the controls. Both steel and aluminum alloy coupons were tested. Figures 137-140 show neutral salt fog results for Al 2024-T3 coupons at various time intervals. At 1500 hours both the control and BAM-PPV coated powder panels show blisters along the scribed regions. Both of these panels failed to meet the minimum 2000 hours military salt fog exposure requirement. Figures 141-142 show neutral salt fog results for steel coupons after 336 hours of exposure and both coupons fail with extensive corrosion damage along the scribed area.

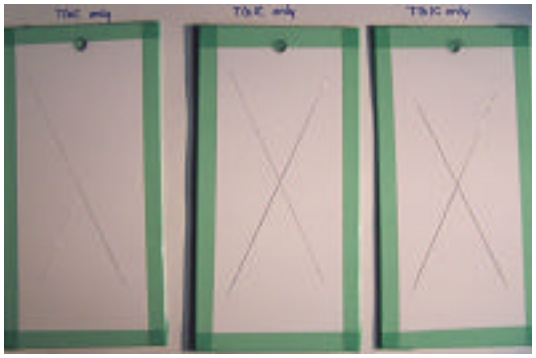

Figure 137: Powder coat control (no BAM-PPV) on Al 2024-T3 before exposure

Figure 138: Powder coat with BAM-PPV on Al 2024-T3 before exposure

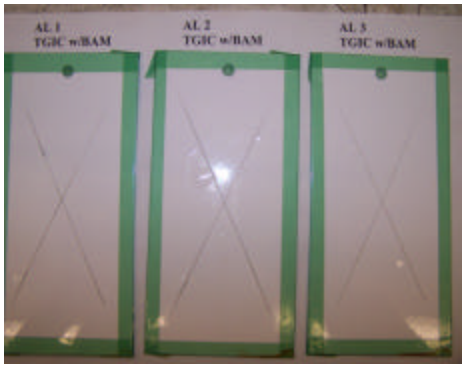

Figure 139: Powder coat control on Al 2024-T3; 1500 hours of exposure

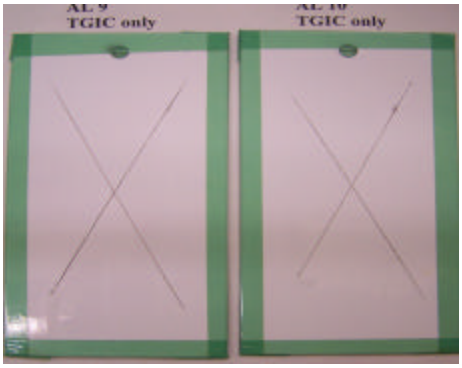

Figure 140: Powder coat w/BAM-PPV on Al 2024-T3; 1500 hours of exposure

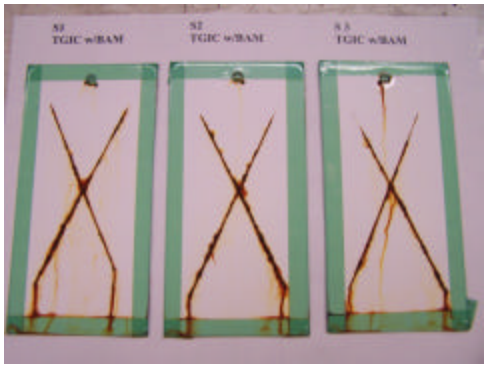

Figure 141: Powder coat control (no BAM-PPV) on 1008 steel; 336 hours of exposure

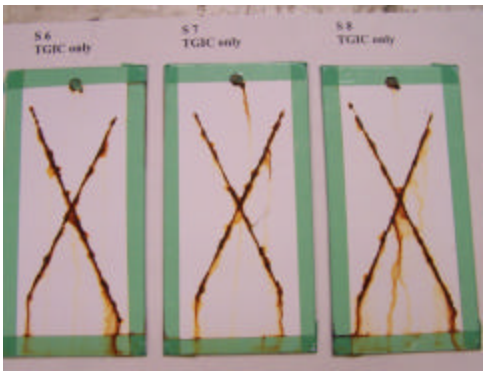

Figure 142: Powder coat w/BAM-PPV on 1008 steel; 336 hours of exposure

SERDP FY03/04
SECTION VIIC- Evaluation of Corrosion Preventive Mechanisms of EAPs

PH Dependency Study of BAM-PPV coated onto Al 2024-T3:

General Analytical Methods:

BAM-PPV solutions were prepared from a xylene solution and thin films of BAM-PPV were coated onto aluminum substrates (Al 2024-T3) using an airbrush technique (film thickness ~1.5 µm). BAM-PPV coupons were tested using electrochemical impedance spectroscopy (EIS). Bare Al 2024-T3 and BAM-PPV coated Al 2024-T3 substrates were immersed in Tris (pH 8.1) and acetate (pH 4.5) buffer solutions at room temperature. Impedance spectra were acquired with a Princeton Applied Research Model 273a potentiostat/galvanostat equipped with an EG&G Princeton Applied Research 5210 lock-in amplifier. Measurements were made over at least ten days at the open circuit potential. The frequency range extended from 120 kHz to 0.005 Hz with an amplitude of 20 mV rms. Three electrode cells were employed with a platinum counter electrode and a silver wire reference electrode. Data were fit using EQUIVCRT software.

Methods:

In order to access the stability of BAM-PPV coated Al 2024-T3 substrates; a pH dependence study of BAM-PPV coupons was investigated. These tests were performed to determine if the BAM-PPV coated onto Al 2024-T3 substrates would show any significant failure when exposed to various pH solutions. Several previous impedance studies have investigated aluminum alloys in contact with both acidic and basic solutions. The initial pH stability studies were conducted in acidic media. The Bode plots for bare Al 2024-T3 substrates exposed to acetate buffer solutions (pH 4.5) were acquired over 13 days and are presented in Figure 143.

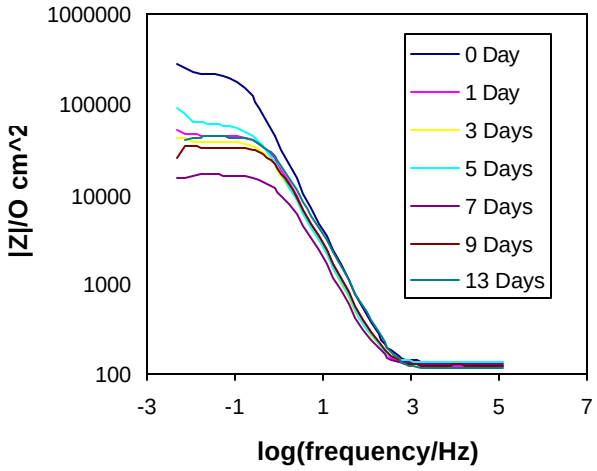

Figure 143: Bode plot of bare Al 2024-T3 substrate exposed to acetate buffer solution (pH = 4.5) over 13 days

The mostly capacitive nature of the Figure 144 data indicates that the surface does not undergo appreciable corrosion over the time scale of the experiment. Similar results are obtained for BAM-PPV coated aluminum panels as shown in Figure 145.

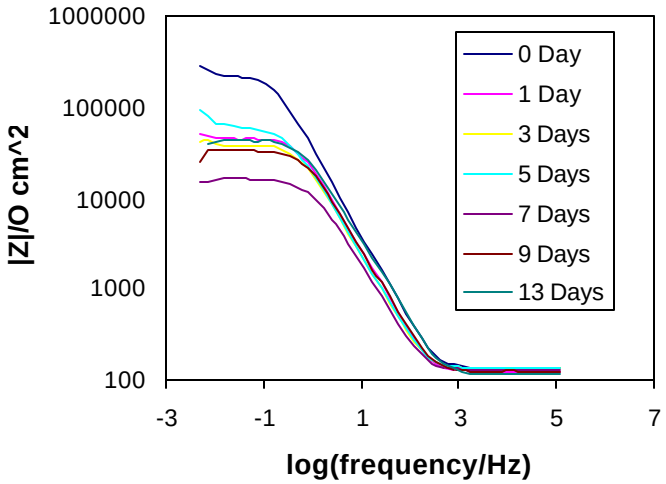

Figure 144: Bode plot of BAM-PPV coated Al 2024-T3 substrate exposed to acetate buffer sol (pH = 4.5) over 12 days

The pore resistance of the bare aluminum fluctuates slightly with an initial decrease followed by a more stable but higher resistance being attained as shown in Figure 145.

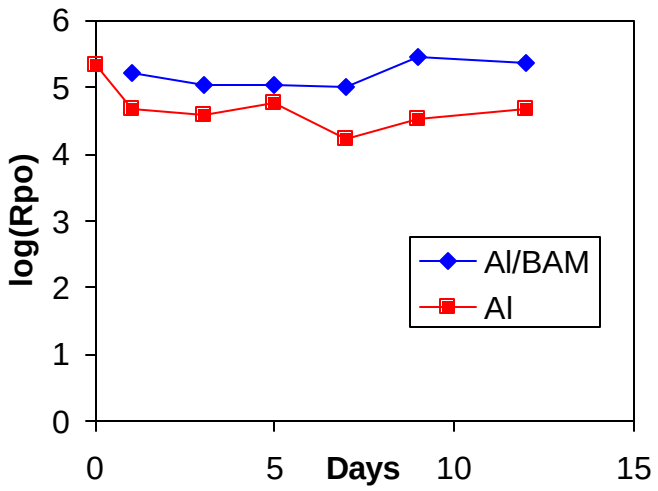

Figure 145: Plot of pore resistance (R_{po}) for bare Al 2024-T3 (red squares) and BAM-PPV coated Al 2024-T3 (blue diamonds) exposed to acetate buffer sol (ph = 4.5)

The BAM-PPV coated films also exhibit purely capacitative behavior with a slightly higher pore resistance than that observed for the bare Al 2024-T3 substrate as shown in Figure 145. In the case of the bare Al 2024-T3 substrate, a thin oxide layer is present that strongly adheres to the metal surface. The early decrease in pore resistance indicates that some loose or reactive oxide may be removed initially from the surface by the acidic conditions. However, aluminum oxide is generally insoluble at a pH of 4.5, and the plateau at the higher resistance suggests the eventual formation of a uniform and protective oxide layer. The higher pore resistances measured for the BAM-PPV coated Al 2024-T3 substrate suggest that the polymer layer also contributes to the electrical properties at the aluminum/liquid junction. In effect the polymer coating appears to function as a resistor in series with the oxide layer on the aluminum. The stability of this additional layer is indicated by the persistently higher R_{po} values obtained with the BAM-PPV coated panels versus the bare aluminum. This evidence suggests that the electronic properties of the BAM-PPV layer are not significantly altered by the buffer solution over the course of the experiments.

The addition of the BAM-PPV coating on the aluminum does alter the inductive properties of the interface. However, since the associated physical process is not well defined, a conclusive statement regarding this inductive behavior cannot be made. For example, the BAM-PPV may reduce one inductive process but stimulate another. Bode plots for the surfaces in contact with pH 8.1 buffer solutions are provided in Figures 146 and 147. The low frequency regions are dominated by the inductive loop. Pore resistances for the surfaces do not significantly change after ten days of solution exposure (Figure 148). A slight increase in R_{po} for the bare aluminum is observed. The unprotected surface likely forms a more complete and more uniform oxide layer compared to the BAM-PPV coated surface. Similar R_{po} values are obtained for the polymer-protected surfaces. Unlike the impedance data for the acidic conditions, the

BAM-PPV films do not significantly alter the resistance of the junction in basic media. One explanation for this observation is that the organic compounds in the Tris buffer can permeate the organic film, blending in with the solution resistance and not contributing to the pore resistance. Consequently, the stability of the BAM-PPV films under basic conditions cannot be conclusively determined by the impedance measurements.

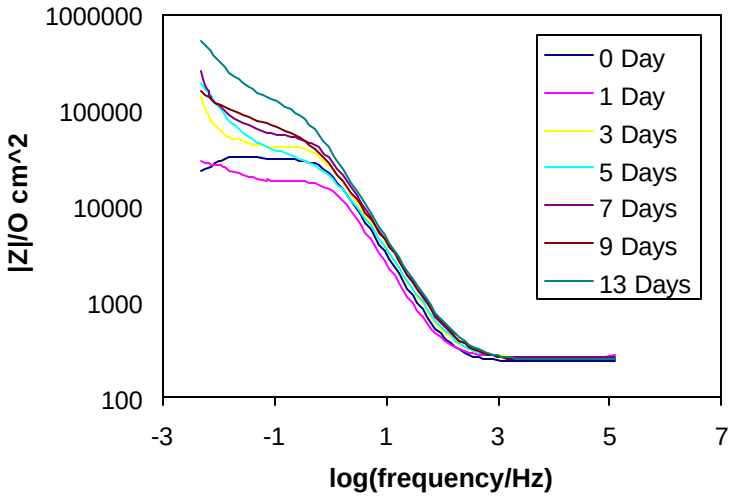

Figure 146: Bode plot of bare Al 2024-T3 substrate exposed to Tris buffer sol (pH = 8.1) over 13 days

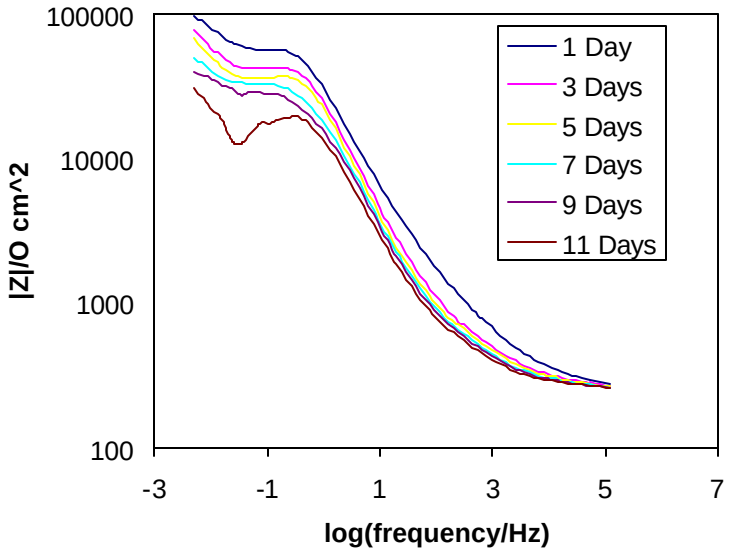

Figure 147: Bode plot of BAM-PPV coated Al 2024-T3 substrate exposed to Tris buffer sol (pH = 8.1) over 11 days

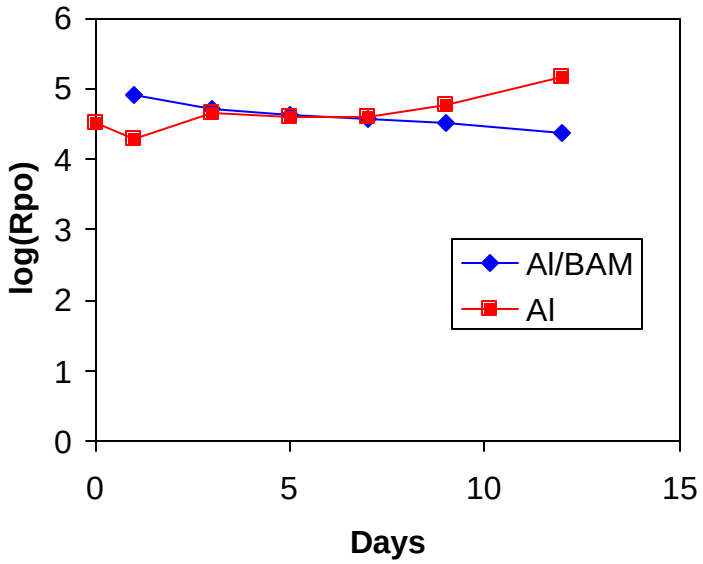

Figure 148: Plot of pore resistance (Rpo) for bare Al 2024-T3 substrate (red squares) and BAM-PPV coated Al 2024-T3 substrate (blue diamond) exposed to Tris buffer sol (pH = 8.1)

While no visible changes in the BAM-PPV coatings were apparent with either pH 4.5 or 8.1 buffered solutions, the impedance data reveals electrochemical differences that vary with pH. In general the BAM-PPV coated surfaces proved more resistive than the bare aluminum panels. However, impedance data for panels immersed in basic solutions could only be fit with model circuits that included an additional inductive element. This added complexity likely results from chemical processes between the aluminum or alumina and the contact solution rather than any specific BAM-PPV-solution interaction

Electrochemical Impedance Studies (EIS) of BAM-PPV coatings:

General Analytical Methods:

A total of six coating on aluminum panels (Al 2024-T3) were investigates: BAM-PPV, CCC, BAM-PPV/Cr-primer, CCC/Cr-primer, BAM-PPV/non-Cr-primer, and CCC/non-Cr-primer. Each surface (12.56 cm^2) was exposed to 0.5 M NaCl (aq) solutions and impedance spectra were acquired over six months. Aluminum/liquid contacts were kept at room temperature and solutions were exposed to the ambient environment and nominal light. Impedance spectra were acquired with a Princeton Applied Research Model 2273 potentiostat/galvanostat. Measurements were made over at least ten days at the open circuit potential. The frequency range extended from 2 MHz to 0.005 Hz with a rms amplitude of 20 mV. Two-electrode cells were employed with a platinum counter electrode. Data were fit using EQUIVCRT software. However, the data could not be fit to conventional equivalent circuits commonly used to describe corrosion processes at a metal/liquid interface.[27] As the impedance spectra changed with time, new elements had to be added or removed from the equivalent circuits. This complication prevents a quantitative comparison of the various corrosion mechanisms between different coatings and over time. Nevertheless, the total impedance of the cell, as measured at the lowest frequencies, provides a quantitative measure of the total cell resistance provided that the phase angles at these frequencies approach zero. With this analysis the total impedance reflects the sum of all the resistances in the cell. Since the solvent resistance remains constant over the course of the experiment, the change in impedance can be attributed to the coated aluminum/liquid interface.

Methods:

EIS provides quantitative information on the electrical properties at metal/liquid or metal/coating/liquid junctions and can be used to elucidate the mechanisms of various corrosion processes and lead to understanding on how barrier layers inhibit corrosion.[28] During the SERDP coatings program, impedance spectroscopy has been used to compare the performance of various chromate conversion treated (CCC) and BAM-PPV coatings on aluminum in contact with 0.5 M NaCl (aq).

Al/CCC vs Al/BAM-PPV

The Bode plots for Al-panels treated with CCC and BAM exhibit significant changes over time, Figure 149. However, the impedances at low frequencies do not significantly change within the first six months of exposure to the salt solution. Specifically, the total resistances do not deviate significant from 10^4-10^5 ohms regardless of the coating, Figure 150. There are different frequency dependent processes occurring with the two surfaces. For example, at high frequencies (10^4-10^6 Hz) the total impedance

of the Al/BAM-PPV surface initially has both resistive and capacitive elements. Over time, the capacitive nature of this high-frequency process diminishes. By contrast the high-frequency impedance of the chromate conversion treated aluminum is purely resistive at these frequencies.

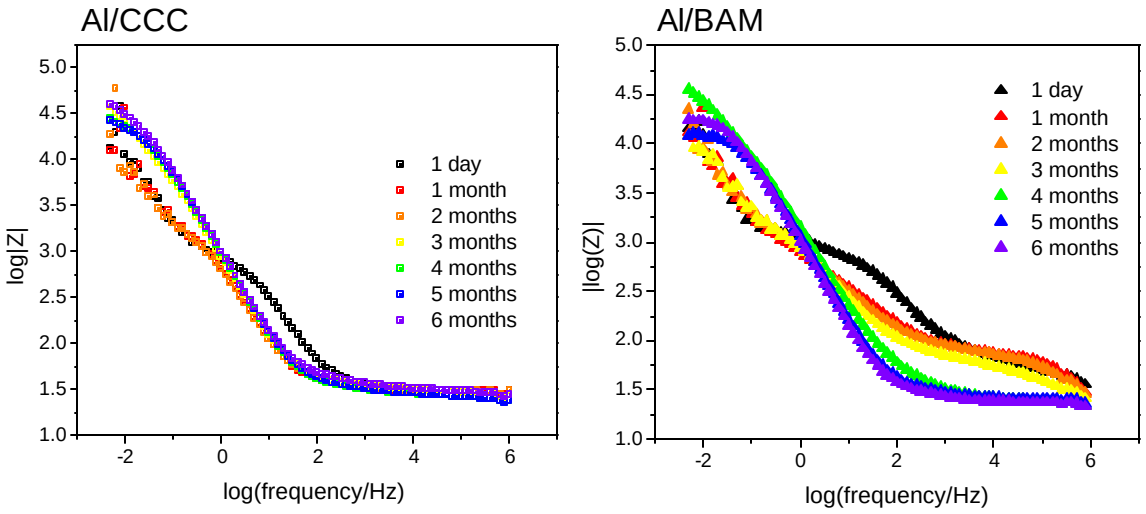

Figure 149: Bode plots of (left) Al/CCC and (right) Al/BAM exposed to 0.5 M NaCl (aq) over six months.

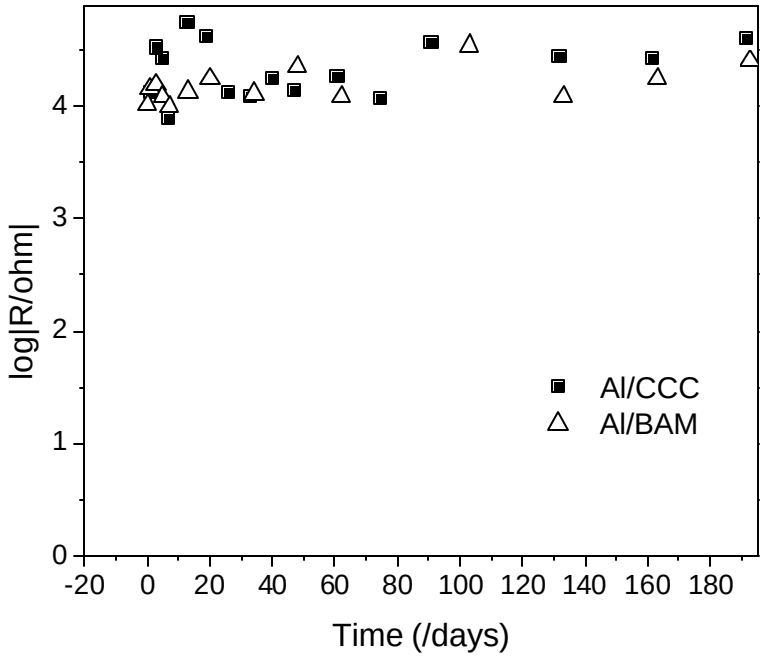

Figure 150: Total resistance obtained at low frequencies for Al/CCC (black squares) and Al/BAM (white triangles) in contact with 0.5 M NaCl (aq).

Al/CCC/Cr-primer vs Al/BAM-PPV/Cr-primer

The differences between the Al/CCC/Cr-primer and Al/BAM-PPV/Cr-primer coated surfaces were significantly more pronounced than the difference between the Al/CCC and Al/BAM-PPV panels. With the chromate primer, initial impedance measurements were dominated by the highly resistive Cr-primer film, Figure 151. Over time and exposure to 0.5 M NaCl (aq), the Cr-primer layer swells with water, delaminates, and bubbles. These processes allow greater access of the underlying aluminum with the BAM-PPV or CCC treatment to the liquid phase. Consequently, the total impedance of the Al-coatings gradually decreases with time. However, the total decrease in the impedance of the cells is much greater for the Al/CCC/Cr-primer treatment than for the Al/BAM-PPV/Cr-primer. After six months of exposure to the salt solution, the resistance of the Al/CCC/Cr-primer panel is 1000 times smaller than that of the Al/BAM-PPV/Cr-primer coating, Figure 152. Unfortunately, it is unclear from the data which mechanism (delamination, pore formation, film swelling, etc.) is the main cause for the decrease in resistance. Nevertheless, it is quite clear from the data that the BAM-PPV film in these cases outperforms the CCC treatment by maintaining a higher resistance.

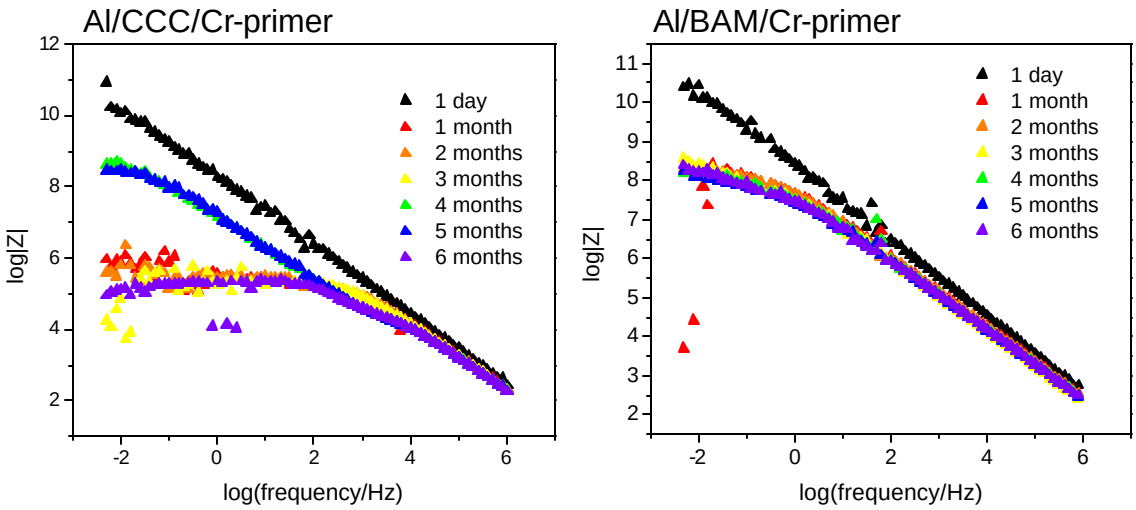

Figure 151: Bode plots of (left) Al/CCC/Cr-primer and (right) Al/BAM/Cr-primer exposed to 0.5 M NaCl (aq) over six months.

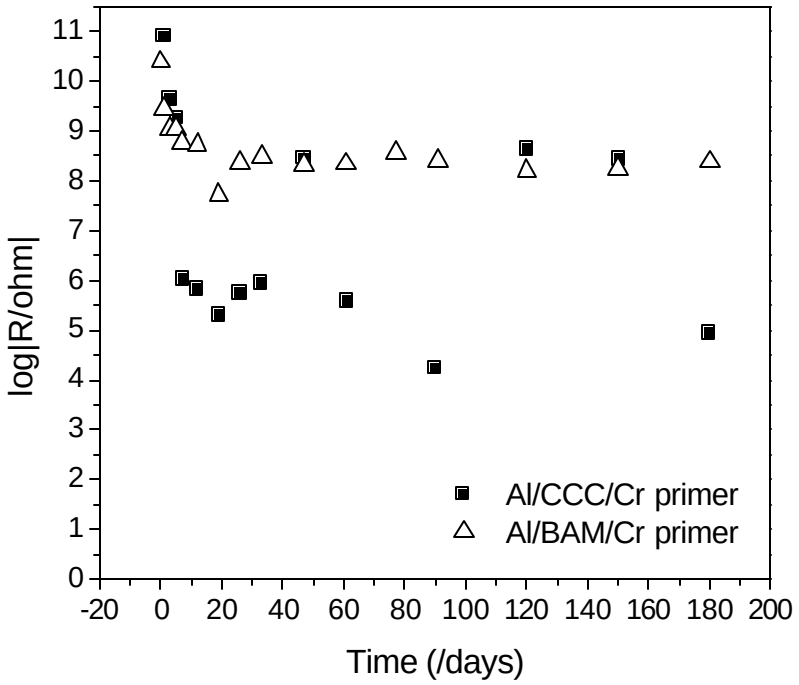

Figure 152: Total resistance obtained at low frequencies for Al/CCC/Cr-primer (black squares) and Al/BAM/Cr-primer (white triangles) in contact with 0.5 M NaCl (aq).

Al/CCC/non-Cr-primer vs Al/BAM-PPV/non-Cr-primer

Differences in the impedance of the Al/CCC/non-Cr-primer and Al/BAM-PPV/non-Cr-primer panels exposed to 0.5 M NaCl (aq) are subtle and inconclusive. These data are complicated by the largely capacitive nature of the response at the low frequencies, Figure 153. Consequently, only lower limits of the total resistance can be estimated. Since the true resistance can be considerably higher, these values are less useful for making conclusions regarding the effectiveness of the two coatings. In both cases the initial impedances were relatively low compared to that of the Cr-primer samples, Figure 153. However, as stated above, it is unclear how meaningful these differences are. In addition, the differences between the Al/CCC/non-Cr-primer and Al/BAM-PPV/non-Cr-primer are insignificant with regard to the lower limit estimate, Figure 154. The presence of the low-frequency capacitive element is likely a property of the non-Cr-primer coating. It is unclear what component of the non-Cr-primer gives rise to this capacitive property since both the non-Cr-primer and the Cr-primer are composed of the same epoxy polymer. One source of this capacitive behavior may be the phosphonate additives to the non-Cr-primer. If these additives are sufficiently mobile, their motion may contribute to the capacitance at these frequencies.

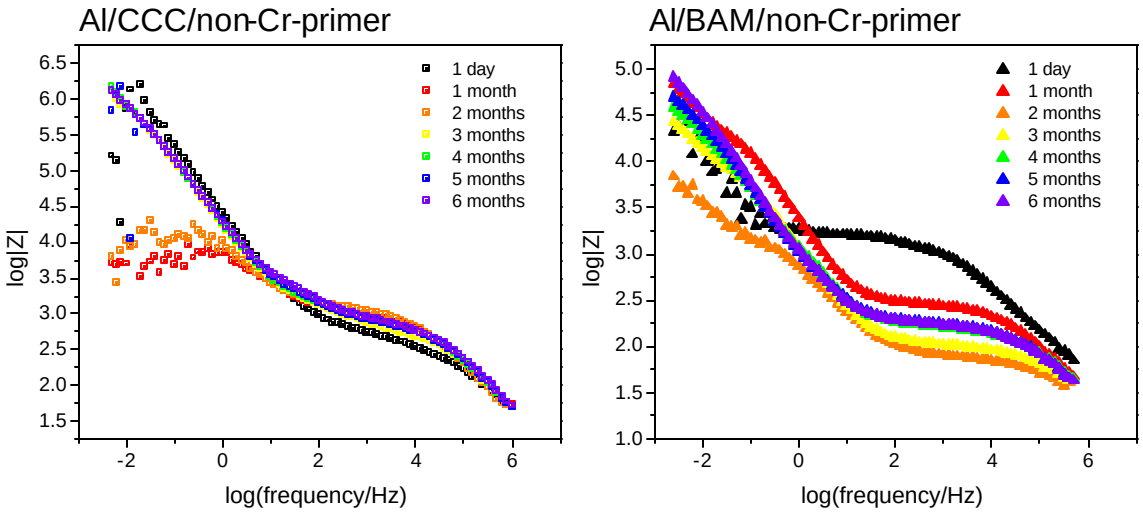

Figure 153: Bode plots of (left) Al/CCC/non-Cr-primer and (right) Al/BAM/non-Cr-primer exposed to 0.5 M NaCl (aq) over six months.

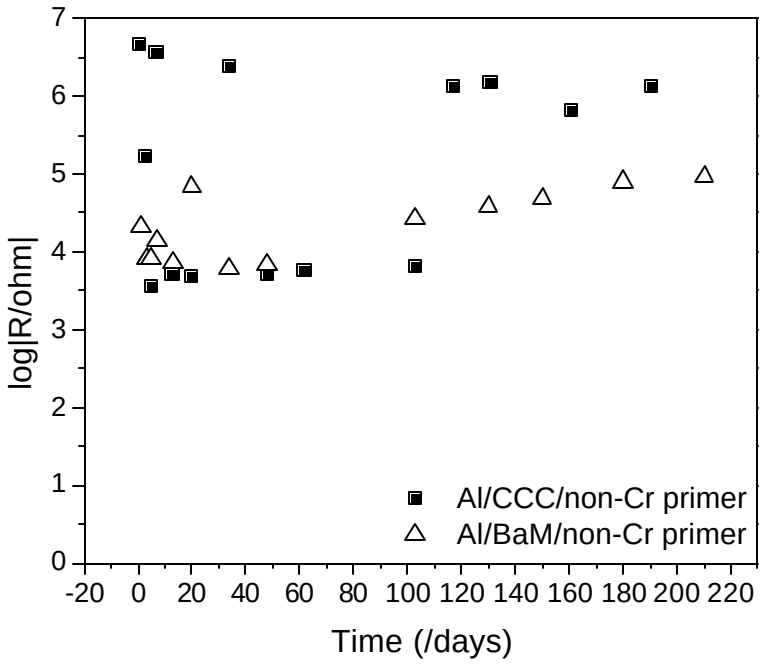

Figure 154: Total resistance obtained at low frequencies for Al/CCC/non-Cr-primer (black squares) and Al/BAM/non-Cr-primer (white triangles) in contact with 0.5 M NaCl (aq).

EIS Study of BAM-PPV Powder Coated Panels:

The panels were examined for corrosion prevention using EIS in 0.5N NaCl solution. The results displayed in Figure 155 show that both compositions show high protective activity as evidenced by the fact that the spectra were capacitive in the entire frequency region and did not change with time. Very similar C_c values were obtained which did not change significantly over time. Since no significant changes in impedance spectra were observed after 3 weeks, one sample of each type of coating was scribed with one small line. The spectra for these scribed samples reflected coating damage. Initially the spectra were similar to those observed for pitting of Al alloys. After one week an additional time constant was observed. After three weeks an additional small scribe was made in each panel coating. The impedance values increased with time for the panel with 1% BAM-PPV. This was also accompanied by an increase in the E_{corr}, which suggests that the overall corrosion damage was decreasing with time.

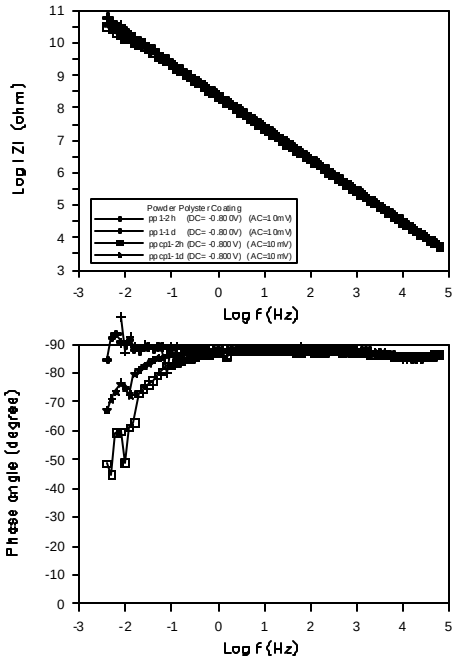

Figure 155: EIS Measurements of Powder Coating Al 2024-T3

Scanning Vibrating Electrode Technique (SVET) and the Electrochemical Noise Method (ENM) Studies of BAM-PPV Coatings:

General Analytical Methods:

The SVET sample cell configurations consisted of a single polymer-coated (BAM-PPV) Al 2024-T3 sample was mounted in a Teflon sample cell and the substrate was masked by a polyester tape (3M) with a 2-mm x 2-mm opening, which determined the exposed area for SVET scanning. An artificial defect was introduced by scribing through the coating to the metal substrate surface. The area of the defect ranged from 0.1 to 0.3 mm^2.

Scans were initiated within 5 minutes of immersion and typically were collected every 20 minutes for the duration of the experiment (approximately 1-day). Each scan consisted of 400 data points obtained on a 20 x 20 grid, with an integration time of 1-second per point. A complete scan required 10 minutes, followed by a 10-minute rest period prior to the next scan. The separation distance between the vibrating probe and the sample surface was about 200 µm. The current density maps are displayed in two ways. In one method, the normal or z-component of the measured current density in the plane of the vibrating electrode is plotted in 3-dimensional format over the scan area, with positive and negative current densities representing anodic and cathodic regions, respectively. In the other method, vectors representing current density magnitude and direction are superimposed onto an optical image of the immersed sample. In all cases, the bottom edge of the optical micrograph corresponds to the x-axis of the 3-dimensional plot. The measurements were taken at the open-circuit potential. The immersion electrolyte is the Dilute Harrison Solution (0.35% ammonium sulfate with 0.05% sodium chloride, (DHS)). Four specimens were cut respectively from four different panels and scanned to assess reproducibility of the observed phenomena.

The noise measurements were conducted using Gamry® PC4 Electrochemical Signal Analyzer (Gamry Instruments,Inc., Willow Grove, PA): ESA 400 Electrochemical Noise System. For each form of polymer-coated sample, four pairs of the same samples were measured. Of the four pairs of samples, two pairs were crossed-scratched and the other two were non-scratched. As shown in 156 two identical specimens (either both scratched or both non-scratched) were treated as two working electrodes and a saturated calomel electrode was used as a reference. The two identical panels were connected using an agar salt bridge.

The two working electrodes were immersed in the DHS. Both current and voltage noises can be measured simultaneously through the system using the ZRA mode. In this mode, the current fluctuation between two identical corrosion specimens was measured along with the potential difference between the specimens and a reference electrode. The sample area under the immersion is about 7.5 cm^2. The panels were allowed to equilibrate for 30 minutes' immersion before initial measurement. At periodic intervals, the current and potential noise was recorded for a period of 5 minutes at a sampling frequency of 1 Hz. For each of these 5-min. periods the standard deviation of the current (s_I) and of the potential (s_V) were computed from the data and the noise resistance R_n was calculated using $R_n = s_V/s_I$.

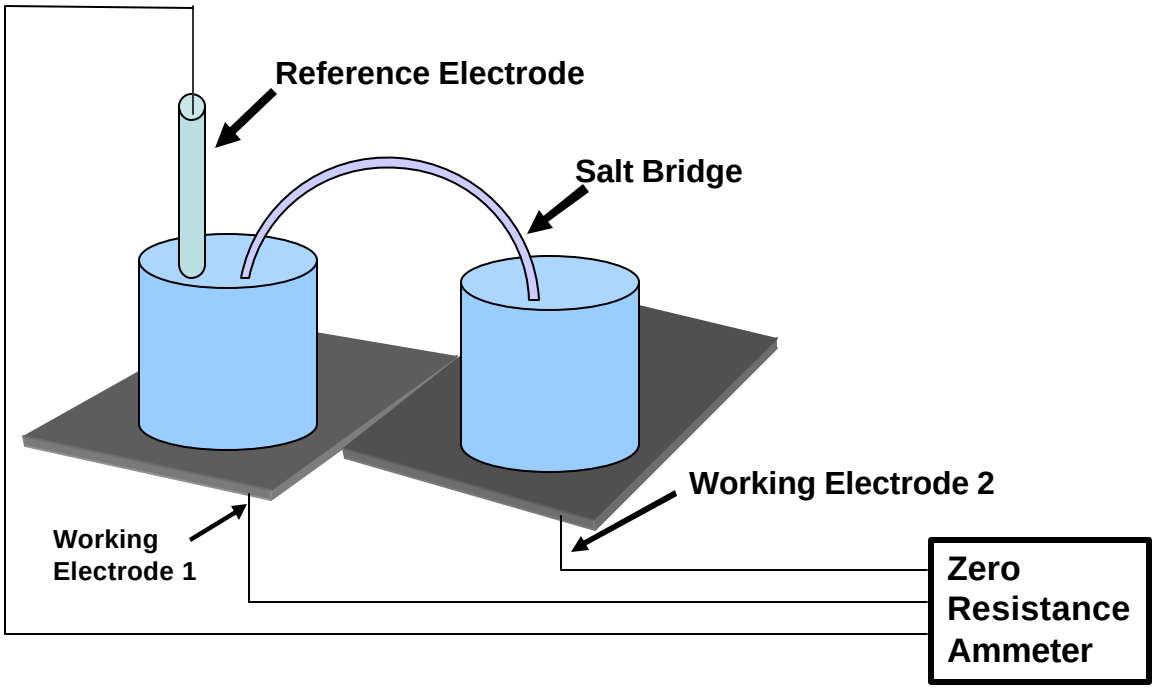

Figure 156. The Experimental Setup of Electrochemical Noise Method

Methods:

SVET Studies on BAM-PPV coated Al 2024-T3:

The chemically synthesized BAM-PPV was a non-doped conjugated polymer and as a result exhibited low conductivity. Typical SVET results are shown in Figure 157 and 158. An anodic and a cathodic couple with current density of about 10 $\mu A/cm^2$ was immediately observed within the defect area after 5 minutes of immersion (Figure 157). This observation was consistent with these films having low initial electrical conductivity incapable of supporting oxygen reduction at the initial period of immersion. The low conductivity of the BAM-PPV coating would impede electron transfer through the coating to the polymer/electrolyte interface. Thus, all current flow was forced to occur only within the defect area. The magnitude of the oxidation current increased with time, reaching 80 $\mu A/cm^2$ after 6 hours and 10 minutes of immersion (Figure 158). The corresponding optical micrograph with overlaid current density vectors indicated that the oxidation current was at the visually corroded area (darker area in the micrograph) of the defect, while the reduction current appeared to occur both within the defect (shiny region of the defect) and also to some extent at the polymer film surface, which may due to the polymer undergoing spontaneous oxidation/doping and rendering itself sufficiently conductive to mediate electron transfer from the metal/polymer interface to polymer/solution interface. The oxidation current then slowly decreased and reached about 10 $\mu A/cm^2$ after ca. 24 hours of immersion, at which point the experiment was terminated (Figure 159). The corresponding electronic or electrochemical interaction between the polymer and the metal may provide evidence for passivation of the metal. Some white corrosion products were observed at the defect and the coating around the defect area was found to have delaminated.

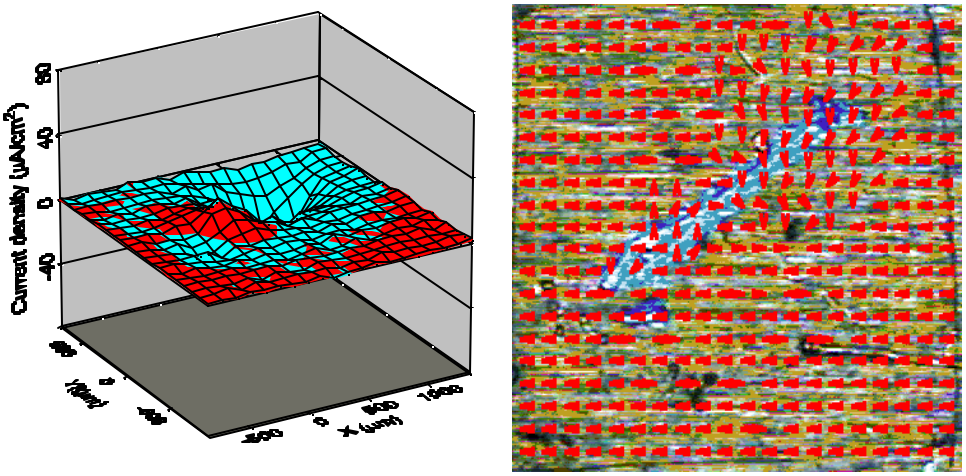

Figure 157. Current density map (left) and optical micrograph with current density vectors (right) for BAM-PPV coating on Al 2024-T3 after 5-minutes of immersion in DHS.

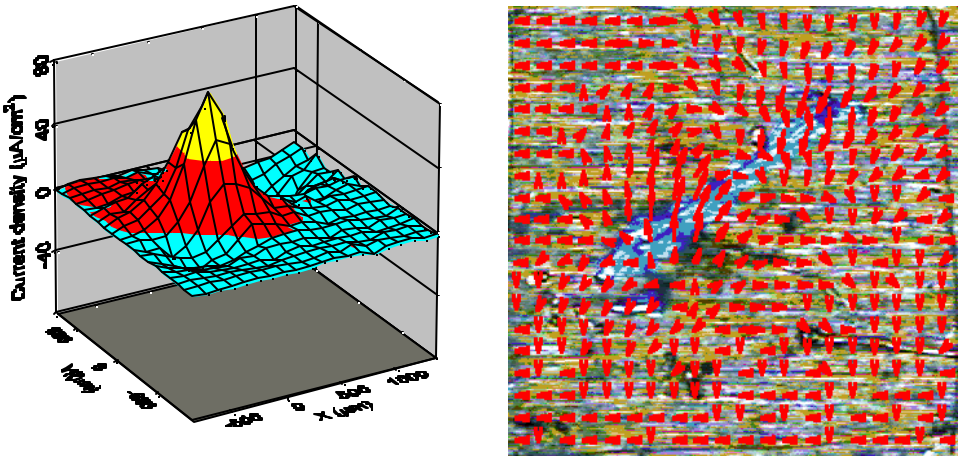

Figure 158. Current density map (left) and optical micrograph with current density vectors (right) for BAM-PPV coating on Al 2024-T3 after 6-hours and 10-minutes of immersion in DHS**.**

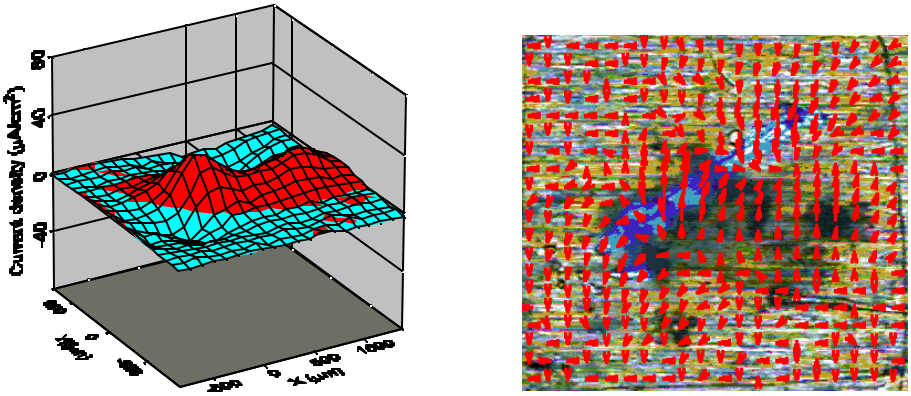

Figure 159: Current density map (left) and optical micrograph with current density vectors (right) for BAM-PPV coating on Al 2024-T3 after 24 hours of immersion in DHS.

BAM-PPV/polyester (TGIC) composite-coated Al 2024:

The BAM-PPV was blended with commercially available polyester TGIC resin and the composite coating was coated on Al 2024 substrate via e-coat. The current density mapping is shown in Figure 160. A significant oxidation current of 10 $\mu A/cm^2$ was found at the artificial surface defect area after 1 hour of immersion. The current continuously increased and reached the maximum value (about 20 $\mu A/cm^2$) after 48 hours, at which point a coupled cathodic current was also clearly observed at the defect area. This redox current couple then decreased slowly to about 5 $\mu A/cm^2$ after 72 hours of immersion. Some black corrosion products were found at the defect. For comparison reason, a TGIC polyester coated Al 2024 was used as a control, the result of which is shown in Figure 161. A typical oxidation/reduction current couple (10 $\mu A/cm^2$) was also found at the metal defect area after 2 hours immersion. The current decreased to the noise level after 75 hour. Some black corrosion product was also observed at the defect area.

The observation that both the oxidation and reduction currents occurred at the metal surface within the defect area is typical behavior for an electrically insulating coating. Since the weight composition of the BAM-PPV in the coating system is only 1%, the electrical conductivity of the composite coating is very low, less than that of the pure conjugated polymer, and the absence of current flow at the coating surface is, thus, not surprising.

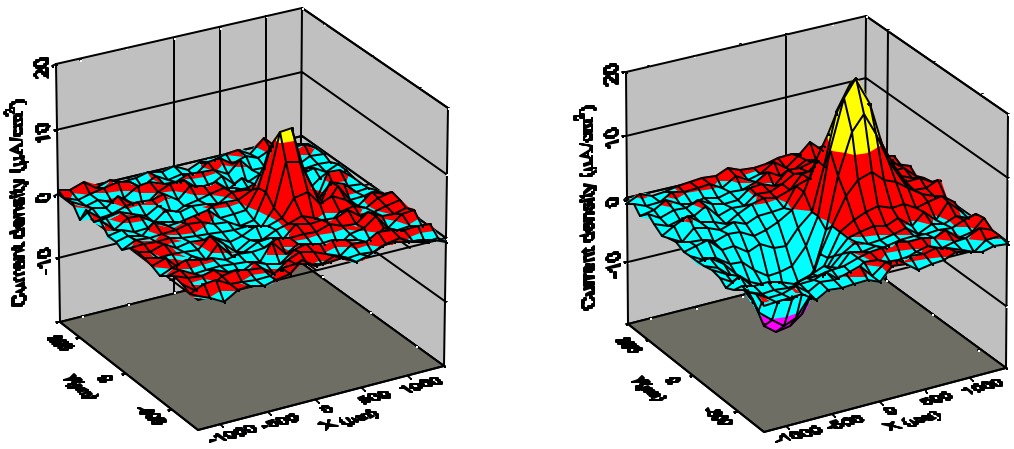

Figure 160: Current density map of BAM-PPV/TGIC coating on Al 2024 after 1-hour and 48-hours of immersion in DHS

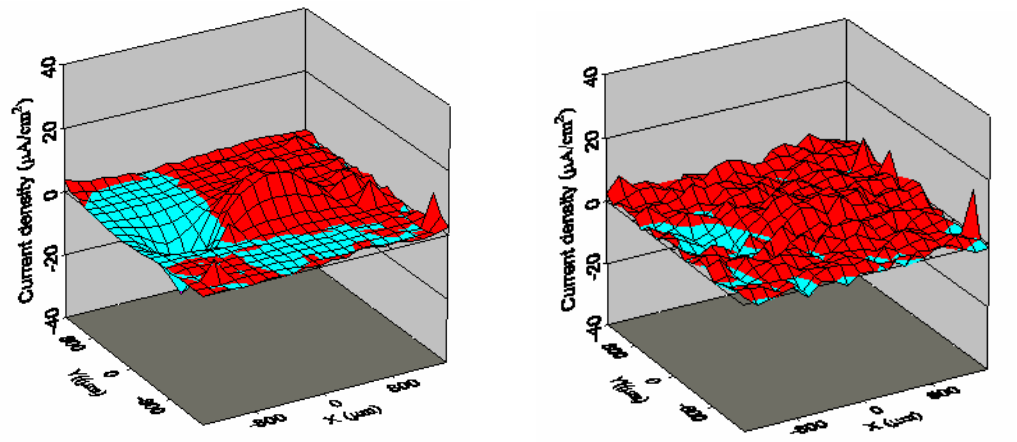

Figure 161: Current density map of TGIC coated Al 2024 after 2-hour and 75-hours of immersion in DHS

BAMPPV with a non-chrome primer and a topcoat on Al 2024:

The current density mapping of the BAMPPV polymer combined with a non-chrome primer (epoxy based, non-chrome primer, Mil-P-53022) and a topcoat (polyurethane, Mil-PRF-85285) on Al 2024-T3. A typical result is shown in Figure 162. After 1.5 hours of immersion, an oxidation/reduction current couple was clearly observed at surface of the defect area. The current increased as a function of time and reached the maximum (30 $\mu A/cm^2$) after 18.5 hour and then began to decrease. After 65 hours, the current reached the noise level (± 3 $\mu A/cm^2$), at which point the experiment was stopped. Some black corrosion product was also found at the defect area. A typical current density mapping for the chromate containing coating (a chromate conversion coating with a chromate primer (solvent-borne epoxy primer w/strontium chromates, Mil-PRF-23377G, Type I, Class C) and a polyurethane topcoat (Mil-PRF-85285C)) on Al 2024-T3 is shown in Figure 163. Basically, no significant current was found during 48 hours of immersion. The surface defect looked shiny and no corrosion product was found visually.

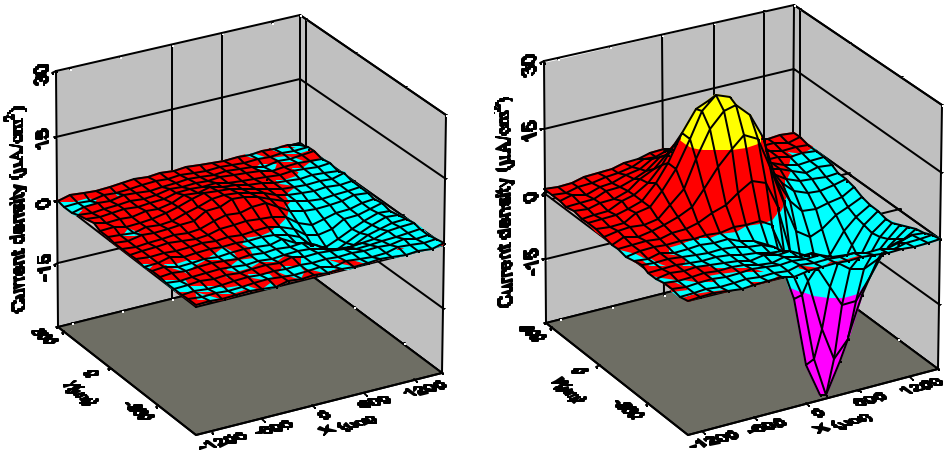

Figure 162: Current density map for BAM-PPV/Primer/Topcoat on Al 2024-T3 after 1.5 hours and 18.5 hours of immersion in DHS.

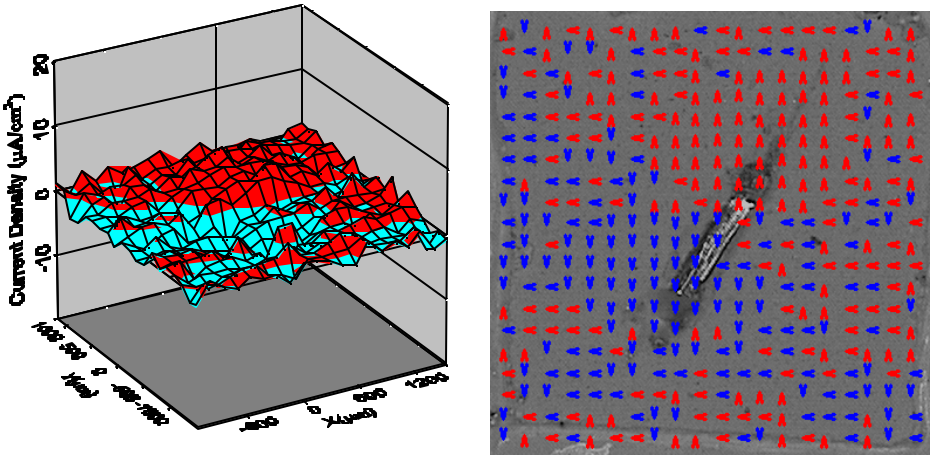

Figure163: Current density map (left) and optical micrograph with current density vectors (right) for a chromate containing coating on Al 2024-T3 after 48 hours of immersion in DHS

ENM Studies on BAM-PPV Coated Al 2024-T3

ENM was used to evaluate the corrosion protection of the BAMPPV-coated Al 2024-T3 in a long-term immersion study. The immersion time was limited to 42 days. The noise resistance of BAM-PPV-coated Al 2024-T3 as a function of time is shown in Figure 164. The thin BAM-PPV coating (film thickness 0.4 µm) is not expected to provide particularly good barrier properties, and the magnitudes of the measured noise resistances were quite low (10^4 to 10^5 ohm), consistent with this view. For the cross-scratched samples (Q&R and U&V), the noise resistance showed an initial value of about 5×10^4 Ω on the first three days of immersion. The resistance dropped to 1×10^4 Ω by the tenth day of immersion and maintained this steady resistance through day 42. Some white and flaky corrosion products were found on day 7. For the non-scratched sample

(P&M and O&N), the average initial noise resistance (1 x 10^5 Ω) was higher than that of cross-scratched samples as expected. The resistance increased and reached the maximum on day 3 (O&N) or day 7 (P&M), then dropped to about 5 x 10^4 Ω on day 10. The fluctuating noise resistance as a function of immersion time may due to the formation/breakdown activities of a passive oxide film at the metal/conjugated polymer interface. Some corrosion products were found after 7 days of immersion. By day 30, the noise resistance of all samples had decreased to 1-2 x 10^4 O indicating complete coating failure.

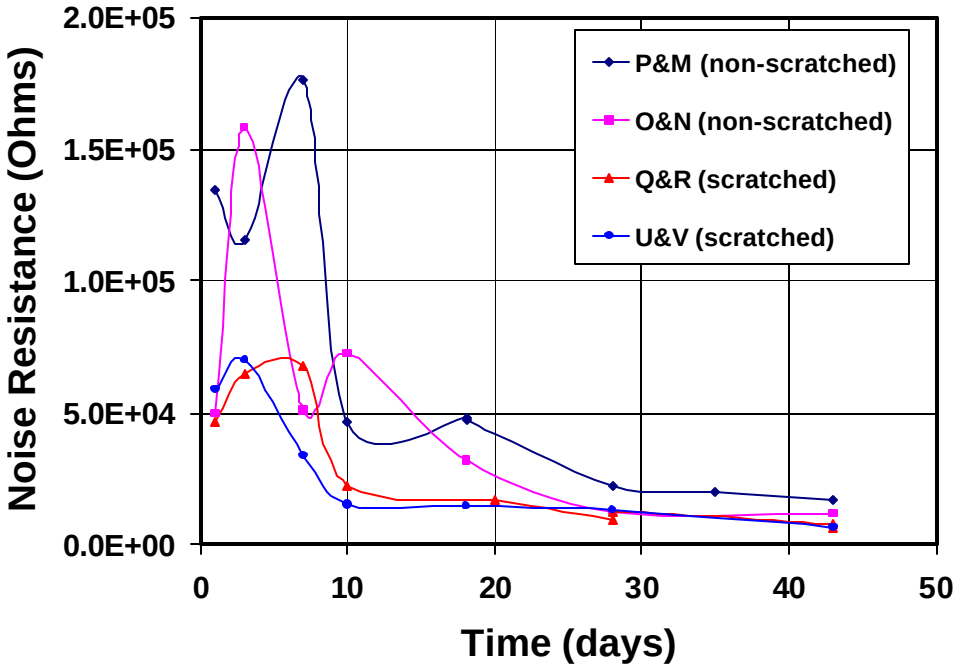

Figure 164: Noise resistance of BAMPPV-coated Al 2024 as a function of immersion time

BAM-PPV/polyester (TGIC) composite-coated Al 2024:

The noise resistance of the non-scratched BAM-PPV/TGIC composite (10^7 Ω) was much higher than the respective BAM-PPV primer coated sample, reflecting a better barrier property of the composite coating against aggressive ions in the electrolyte (Figure 165). The fluctuating noise resistance for the BAM-PPV/TGIC composite was found during the initial period of 60 days, possibly indicating the formation/breakdown activities of a passive oxide film. The non-scratched samples (both with and without BAM-PPV) exhibited noise resistance at the end of the immersion period that was similar to that at the start, indicating little or no degradation of these coatings during the immersion period.

It is interesting to note from Figure 165 that the noise resistance of the composite material (both scratched and non-scratched) is about one order of magnitude lower than that of the TGIC coated metal (without BAM-PPV). It is conjectured that the BAM-PPV in the composite may have undergone spontaneous oxidation/doping during the immersion period, leading to increased conductivity. We have reported that conjugated polymer films placed between a metal and a topcoat results in lower impedance in the low frequency region than in control samples where the conjugated polymer (CP) film was omitted.[30] Similarly, incorporating polypyrrole particles into an acrylic paint resulted

in significantly lower impedance than for a control sample without polypyrrole.[31] These studies indicate that the lowering of the coating impedance by conjugated polymers is due to their ability to conduct current by both ion and electron movement through the polymer, thereby facilitating charge transfer between metals (electronic conductors) and electrolytes and/or barrier coatings (ionic conductors). Ions are readily exchanged at CP/electrolyte or CP/barrier coating interfaces, whereas electrons are readily exchanged at CP/metal interfaces. Thus, overall charge transfer between electrolyte and metal is facilitated and, as a result, the impedance is lowered.

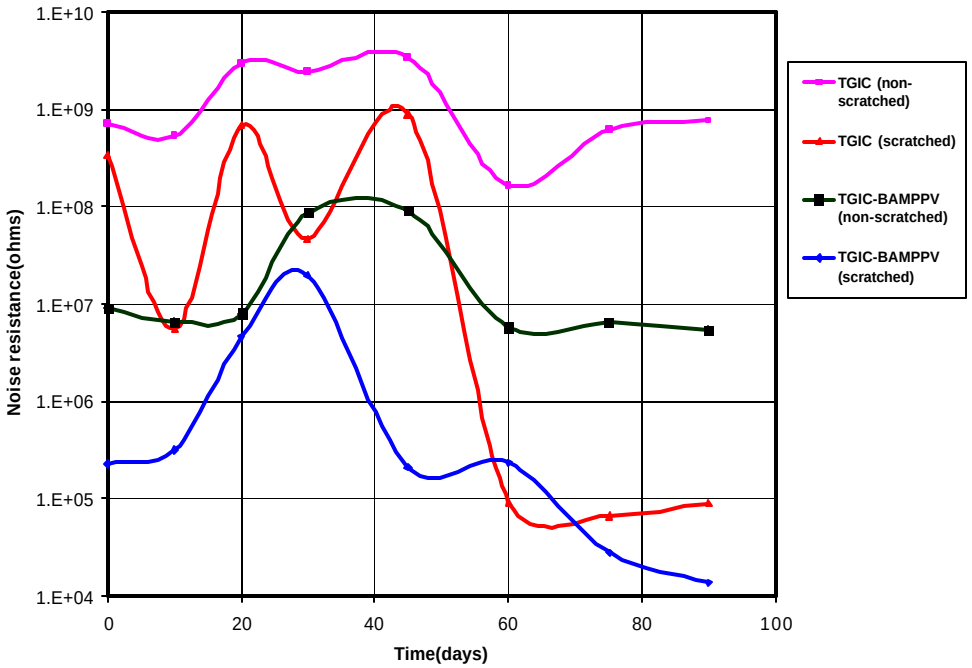

Figure 165: Noise resistance of BAM-PPV/TGIC polyester coating on Al 2024-T3

BAM-PPV with a non-chrome primer and a topcoat on Al 2024-T3:

For the non-scribed sample, a very good barrier property was found and the corresponding noise resistance measurement was difficult to make with the Gamry PC-4 potentiostat (the operation amplifier used in the PC-4 ZRA has input bias currents that become significant for such high impedance coatings). Meaningful data could be obtained on scratched samples and a typical result for a scratched sample is shown in Figure 166. The initial noise resistance on day 1 was about 10^6 Ω. The noise resistance decreased rather continuously as a function of time, reaching about 10^4 Ω at day 78. Some white corrosion product was found around the defect area. These results indicate that the coating system was unable to control corrosion that occurred at the defect area during the immersion period. Compared to a chromated coating system (Figure 166), the noise resistance of the BAM-PPV with a non-chromate primer and a topcoat coated sample was about one order of magnitude lower, indicating better long-term corrosion protection by the chromate-containing coating system.

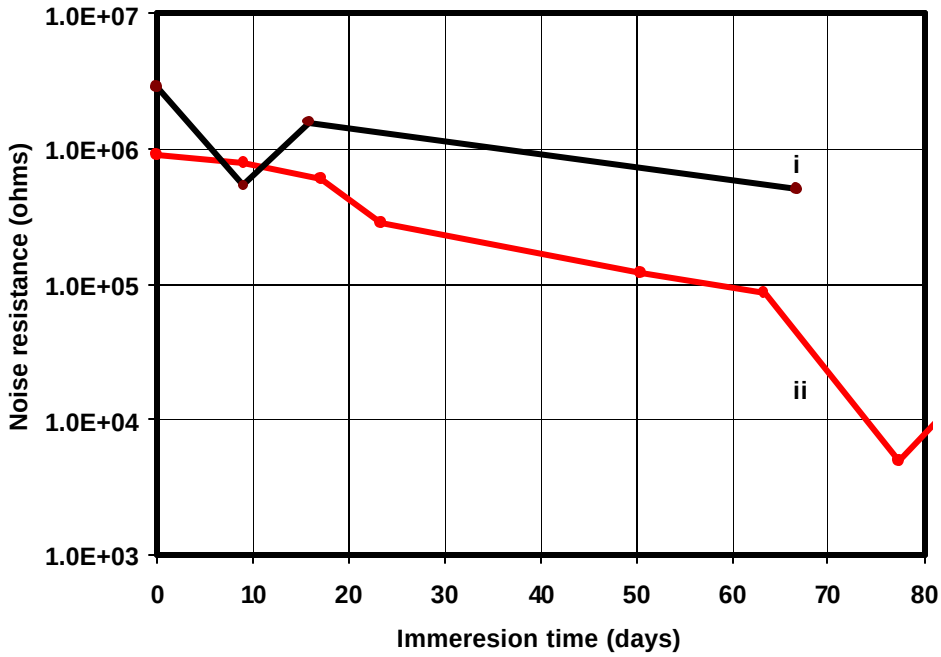

Figure 166: Noise resistance of a chromate containing coating on Al 2024 (i) and a BAMPPV with a non-chromate primer and a conventional polymer topcoat on Al 2024 (ii)

SVET Studies on 1008 Steel:

A typical SVET result of BAM-PPV with a non-chromate primer and a conventional polymer topcoat on 1008 steel is shown in Figure 167. An anodic/cathodic couple with current density of about 8 $\mu A/cm^2$ was immediately found within the defect area after 5 minutes of immersion (Figure 167). The magnitude of the oxidation current increased with time, reaching 20 $\mu A/cm^2$ after 1 hour of immersion. The oxidation current then slowly decreased and reached about 3 $\mu A/cm^2$ after ca. 23 hours of immersion, at which point the experiment was terminated. Some black corrosion products were observed at the defect area.

ENM Studies on 1008 Steel:

A typical ENM result of a scratched BAM-PPV/primer/topcoat sample on 1008 steel is shown in Figure 168. The initial noise resistance at day 1 was about 5×10^4 Ω. The noise resistance decreased throughout the immersion period, reaching a low value of 10^3 Ω, suggesting failure of the coating. Brown-yellow corrosion products were observed on day 1 in the defect area. The combined ENM and SVET results on 1008 steel indicate little corrosion protection by the BAM-PPV coating system.

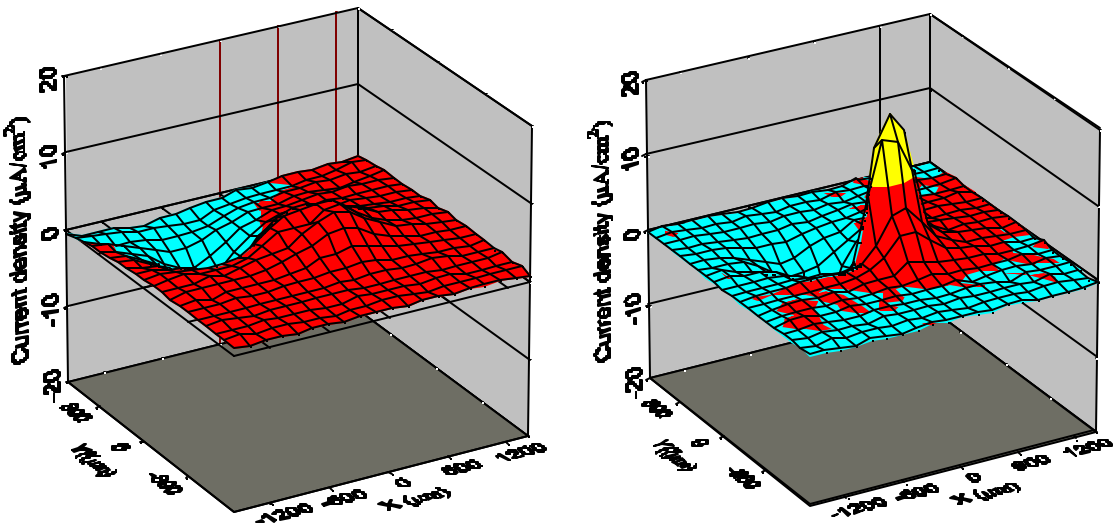

Figure 167: Current density map for BAMPPV/primer/topcoat on steel after 5 minutes (left) and 1 hour (right) of immersion in DHS.

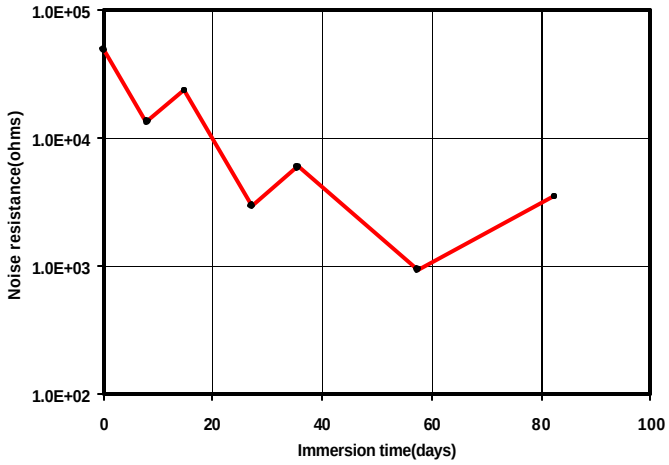

Figure 168: Noise resistance of scratched BAMPPV/primer/topcoat on steel as a function of immersion time in DHS.

X-ray Photoelectron Spectroscopy (XPS) Analysis of BAM-PPV Film Used as a Pretreatment Coating

General Analytical Method:

XPS measurements were taken of bare aluminum, CCC, epoxy (commercial source, Deft), and BAM-PPV coated Al 2024-T3 coupons exposed to air (scribed either 5 minutes or 24 hours prior to analysis) and neutral salt fog spray for 24 hours. After being scribed, the panels were exposed to air or salt fog for the specified duration, and the

scribed areas were examined using XPS. Detailed spectra for the Al 3p peak were collected; binding energies were referenced to the C 1s peak at 286eV. Data were collected with an M-probe spectrometer (VG Instruments) pumped by a CTI Cryogenics-8 cryo pump. Surfaces were exposed to monochromatic Al Kα X-rays at a 35° angle of incidence relative to the surface horizontal, and photoelectrons were collected by a hemispherical analyzer at a takeoff angle of 35° from the sample surface.

Methods:

Spectra for the various aluminum panels are shown in Figure 169. Qualitatively, there is little difference in the XPs spectra for the different coatings. Two peaks are observed in the Al 3p region for the air-exposed panels. One peak is centered at 73eV, a value consistent for reduced aluminum metal. The second peak at 75eV suggests the presence of higher valent aluminum such as that in aluminum oxide. The intensity of the higher binding energy peak is slightly larger after 24h than after only 5min of exposure. The increase in the 75eV-centered peak suggests that the oxidation process occurs over a period of days. Spectra acquired after exposure to air for 1 week also exhibit two peaks, with an increase in the intensity of the higher binding energy peak relative to the lower binding energy peak. These results indicate that the oxidation rate for the differently modified surfaces is not significantly altered.

After exposure to salt fog mist for 24h, the peak at 73eV is absent. Only the Al 3p peak at higher binding energy is present (Figure 169, light blue traces). These results suggest that the surface is completely oxidized and only Al^{+3} is being detected with the XPS. The layer of oxidized aluminum (an insulator) on the surface contributes to a significant amount of surface charging. Consequently, the signal-to-noise ratio is attenuated for these spectra. Interestingly, the higher binding energy peak for the BAM-PPV coated surfaces is very broad. This broadness is likely due to surface charging; however, it is unclear why the Al peak in the BAM-PPV coated surface is broadened and the others are not. A potential explanation can be that the BAM-PPV produces a more insulating effect due to greater amount of oxidized product present in the scribed area. A peak edge is observed in the 68-70eV region of the spectrum for the epoxy-coated aluminum panel exposed to neutral salt fog. This peak is likely due to the neighboring Na 2p peak centered at 63eV. The sodium is likely a residue from incomplete rinsing after the salt fog exposure. Both sodium and chlorine are evident in the survey spectrum for this surface.

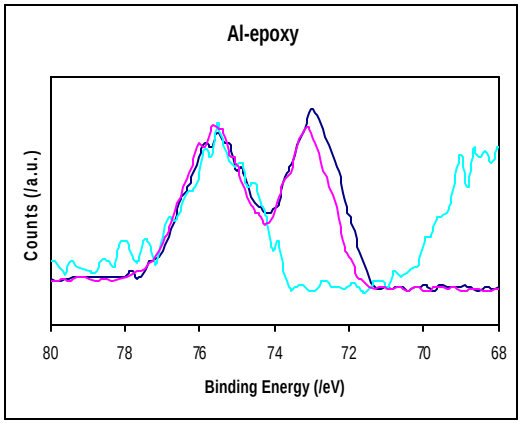

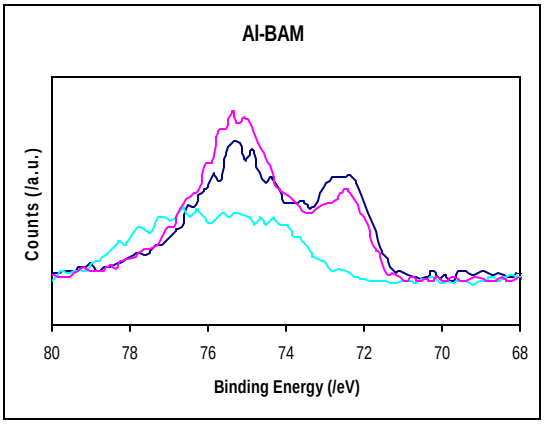

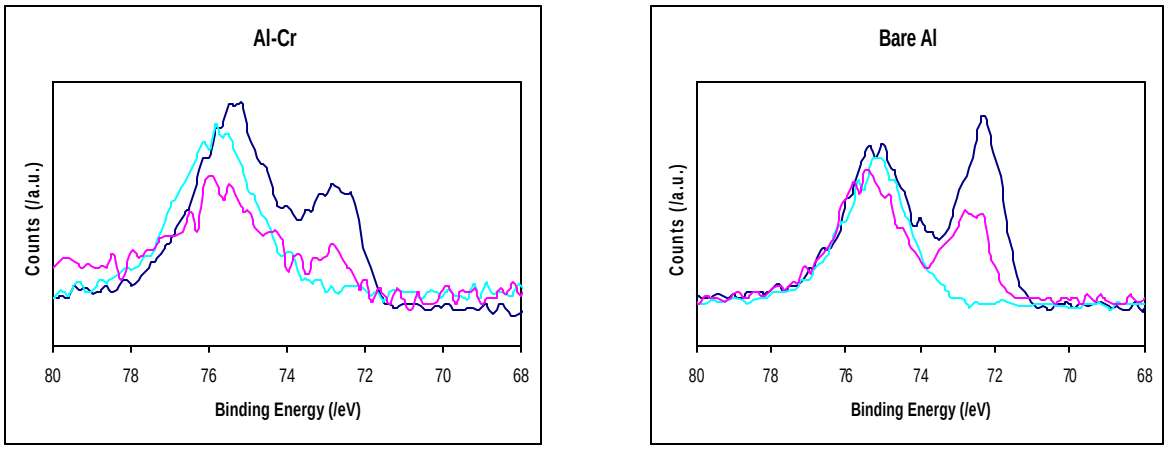

Figure 169: XPS spectra of the Al 3p region for epoxy (top left), BAM-PPV (top right), CCC (bottom left), and bare (bottom right) aluminum panels. Panels are exposed to air for 5min (dark blue), air for 24h (pink), and salt fog for 24h (light blue).

Positron Annihilation Lifetime Spectroscopy (PALS)/Doppler Broadening of Annihilation Radiation (DBAR) Analysis of BAM-PPV Films as a Pretreatment Coating:

Method:

BAM-PPV films were analyzed using DBAR and PALS to predict the performance of thin films of BAM-PPV before and after exposure to salt fog. These tests would allow a simple method to predict the lifetimes of a pretreatment coating system. The samples were prepared as follows: sample Al-507A was prepared by spraying a solution of BAM-PPV dissolved in THF onto the aluminum substrate (Al 2024-T3), and sample Al-507B was prepared by spaying a solution of BAM-PPV dissolved in xylenes. The approximate thicknesses of Al-507A and Al-507B were 1.52 µm and 1.04 µm, respectively. The two panels were coated only with the conductive polymer (BAM-PPV); no topcoat has been added. The samples were heated under vacuum (17 in Hg, 100^{o}C) to remove the residual solvents. Two additional virgin samples similar to Al-507A and Al-507B, prepared as above, were also exposed in neutral salt fog ASTM B117 for 240 hours. After exposure, the samples were rinsed with deionized water and dried with Kim-wipes under ambient conditions. Doppler broadening of annihilation radiation (DBAR) was performed in the Oak Ridge National Laboratory under the direction of Dr. Jun Xu. DBAR was carried out by using slow positron beam with well-defined incident energy varying from 0 to 30keV. The S and W parameters and 3g/2g ratio were automatically calculated from each Doppler Broadening Energy Spectrum (DBES) with a total of 1 million counts. The S parameter is the ratio of the central area from 509.51 to 512.59keV to the total counts after background subtraction. For each sample, 29 DBES spectra were taken in about 3 hours to avoid any interference from radioactive exposure. PALS coupled with slow positron beam was carried out in the National Institute of Advanced

Industrial Science and Technology Japan. *No SERDP funds were used for the PALS experiments.* The lifetime resolution was 250ps at a counting rate of 1000-2000 cps, depending on the incident energy of positron beam. The detail experimental setup is given elsewhere. The lifetime spectra were analyzed using CONTIN and PATFIT programs for determination of least squares fit of PALS data.

In Figure 170, the S parameter vs. positron incident energies for coating Al-507A and Al-507B are shown for as received samples. The corresponding depth of positrons injecting into polymer is indicated in the upper abscissa. The density of pure polymer, ? = 1.13 g/cc, was used for the calculation based on the following equation:

$$Z_0(E) = (40/\rho)E^{1.6}$$

where Z_0 is expressed in nm, E in keV, and ρ is the density in g/cm^3. There are two noticeable differences between these two samples. First, the S parameter of Al-507B is much higher than that of Al-507A. This may be because the free volume in Al-507B is larger than that in Al-507A. Second, from the surface to the bulk, the S parameter of Al-507B increases very rapidly while the S parameter of Al-507A gradually reaches the final plateau. This increase is not due to either positron or positronium diffusion, because 3γ/2γ data do not show such a long diffusion, as shown in Figure 171. One possible explanation for this is that the free volume in the near surface is less than that located within the coatings. Another possible explanation is that advantageous chemicals exist after the material is coated on the aluminum plate. The chemicals may be distributed in the coatings with a gradient from the surface to the substrate metal. It is interesting to notice that, on the surface, the S parameter of both samples converges to the same point. This is probably due to positron annihilation with the high momentum surface electrons. On the other hand, at the high energy part (E > 20keV) of Figure 170, the S parameter of both samples reaches the plateau of the same value, indicating all positrons annihilate in the aluminum substrate. If we further examine the behavior of S parameter in both samples, we find that there are two layers in Al-507A: the near-surface layer, which ranges from 0 to 0.4μm, and the bulk layer, which ranges from 0.4 to1.52μm. For Al-507B, the two layers are not apparent. This can be seen more from W-S correlations in Figure 171. In the figure, only one fitted line presents the entire coating layer for Al-507B, while for Al-507A, the experimental points can be fitted into two lines. The interception point in Al-507A

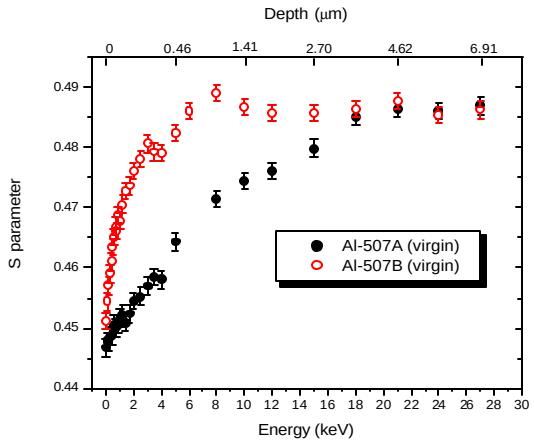

Figure 170: S parameter vs. positron incident energy for Al-507A and Al-507B

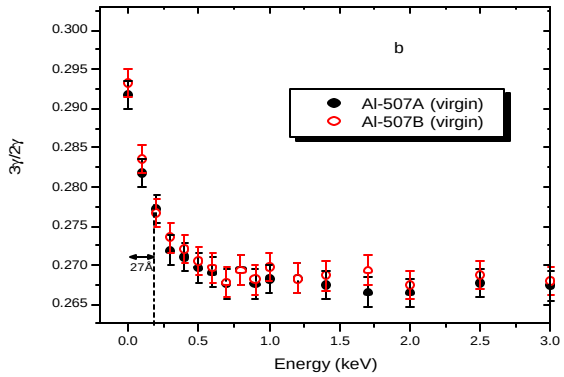

Figure 171: The ratio of 3γ to 2γ

corresponds to around 0.4μm in depth. In addition, it should be noted that the correlation for both samples converges to the same values at two ends, one corresponding to the surface and the other corresponding to Al substrate. This *two-layer* feature for Al-507A is confirmed after the sample is exposed to neutral salt fog.

PALS coupled with slow positron beam was measured for the two samples. Positron beam with 3keV kinetic energy was selected to obtain the free volume information in the film of both samples. The free volume hole size was calculated using the following equation:

$$\tau_3 = 0.5\,\text{ns}\left[1-\frac{R}{R_0}+\frac{1}{2\pi}\sin\left(\frac{2\pi R}{R_0}\right)\right]^{-1}$$

where $R = R_0 - \Delta R$ in Å. 0.5ns is the spin-averaged Ps lifetime. ΔR is a semi-empirical constant, and it is determined to be 1.656Å for well-defined cavity sizes, such as those found in zeolites and organic molecules.

Using the CONTIN program, we could obtain the distribution of *o*-Ps lifetime in the samples, as shown in Figure 171. From this figure, it can be observed that the probability density function (PDF) of *o*-Ps lifetime distribution in Al-507B is higher than that in Al-507A. Several meaningful parameters can be resolved from CONTIN results: (a), the area under the PDF curve, meaning the number of free volume quantity; for Al-507A, the area is 0.13 and for Al-507B the area is 0.21. So the free volume concentration in Al-507B is 1.58 times of that in Al-507A. (b), the peak position of the curve, meaning the maximum possibility of free volume hole size. Both peaks appear at the exactly same position, 2.35ns. (c), the width of the curve, meaning the range of hole size distributed in two samples. The width for Al-507A is 1.39ns and for Al-507B is 1.52ns. So the hole size distribution in Al-507B is broader than that in Al-507A. These parameters are consistent with S measurements, in which the S parameter is much higher in Al-507B than in Al-507A.

Using the PATFIT program, PALS spectra of two samples were resolved into 3 discrete lifetimes, *p*-Ps lifetime, free e^+ lifetime and *o*-Ps lifetime. According to above equation, the free volume hole size was calculated from each *o*-Ps lifetime. The lifetime of *o*-Ps in Al-507A is 2.38 ± 0.02ns, corresponding hole size of 3.17 ± 0.02Å, and the lifetime of *o*-Ps in Al-507B is 2.43 ± 0.02ns, corresponding hole size of 3.21 ± 0.02Å. Therefore, the average free volume size for both samples is very similar, within experimental uncertainty, while free volume concentration in Al-507B is larger than that for Al-507A.

When interpreting $S_B > S_A$, we proposed two possible reasons, first, overall free volume in sample Al-507B is larger than that in sample Al-507A. Second, solvent was not completely removed, which resulting to a solvent diffusion pattern in Al-507A. With the lifetime data, it is clear that the higher free volume in Al-507B should be responsible for the higher S parameter. Chemical composition might still play a role, but it is not clear at this point. Another caveat is that Cl ion may affect the S parameter profile. Cl concentration in those samples is found to be around 15ppm in number concentration of atoms. Earlier work by Dlubek *et al.* indicates that for an observed S effect of Cl in chlorine-containing polymers, a minimum concentration of 10% Cl is required.[32] Therefore, Cl is probably not responsible for the difference in S parameters between the two samples. As a result, it is reasonably concluded that differences in S parameters between the two samples depend primarily upon differences in free volume.

The two samples (Al-507A and Al-507B) exhibit very different responses to the salt spray treatment, as seen in Figures 172 and 173. Several interesting observations can be found from these two plots: first, Al-507A was severely degraded while Al-507B showed very little change when both samples were subjected to the salt spray. Second, the S parameter exhibits a large change in the near-surface layer, while it exhibits only a very small change in the bulk layer in Al-507A. However, after salt spray degradation, the two-layer feature in this sample becomes more pronounced, as we mentioned earlier in this discussion. The different behaviors in response to salt treatment might be attributed to differences in free volume; salt spray degradation may increase free volume. Prior to salt spray exposure, the free volume in Al-507A is less than that of Al-507B.

Exposure to salt spray appears to increase free volume in Al-507A. Note that it seems at the outermost layer of surface, the S parameter does not change for both samples before and after salt treatment. This suggests that the chemical compositions of Al-507A and Al-507B are similar and are not changed by the salt treatment.

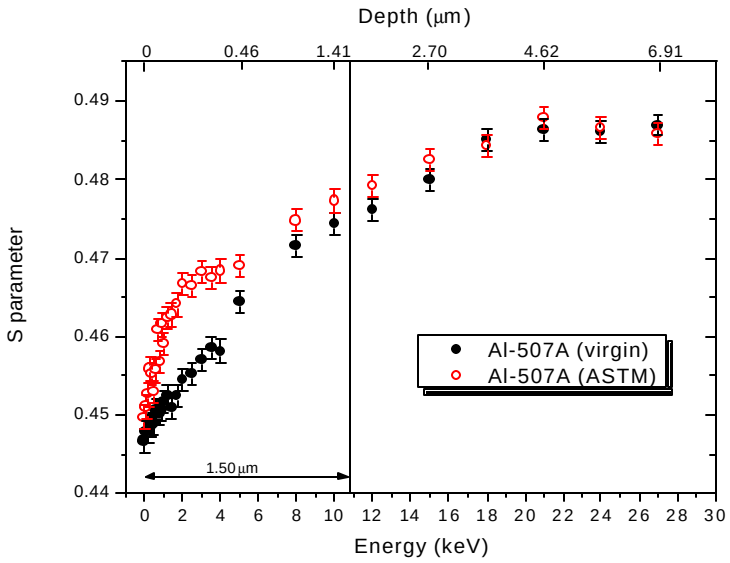

Figure 172: Comparison of the S parameter of virgin and salt treated Al507A

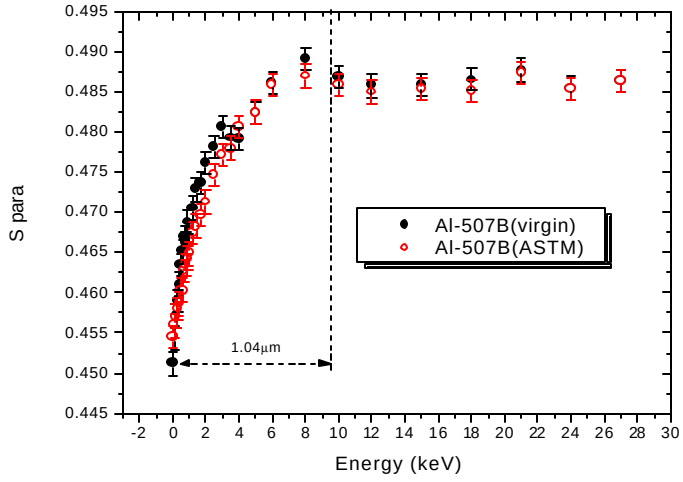

Figure 173: Comparison of the S parameter of virgin and salt treated Al507B

Thus from these experiments it is apparent that there is a significant difference in the two samples with regard to their free volume holes. The average diameters of the free volume holes for both samples were evaluated and they were found to be very similar,

around 0.32nm. However, the free volume in Al-507B is almost 1.6 times of that in Al-507A. This is consistent with S parameter measurements; the S parameter of sample Al-507B is much higher than the S parameter of Al-507A. From the S parameter as a function of depth from the surface, it is found that there are two layers in sample Al-507A, surface layer and bulk layer, while there is only one layer in sample Al-507B. After both samples were treated with neutral salt spray for 240h they exhibit very different responses. The S parameter in Al-507A increases but the S parameter in Al-507B shows only a small change. The degradation caused by salt fog spray occurs mostly in the near-surface layer of Al-507A. From the change in S parameters in both samples upon the neutral salt fog treatment, it is found that sample Al-507B has a stronger resistance to the neutral salt fog exposure. This result shows consistency with previous investigations regarding the solubility of BAM-PPV in various solvents. Depending on the processing of the BAM-PPV solutions, differences in film formation and uniformity can occur. An investigation by B. J. Schwartz *et al.* showed that by proper choice of solvent and processing conditions, a BAM-PPV light emitting diode device performance could be enhanced.[33] This same type of result is found from PALS and DBAR in which the proper selection of solvent and processing of BAM-PPV solutions results in enhanced corrosion protection.

Section VIII

SERDP FY 00-02

Results and Accomplishments:

The initial scale-up of BAM-PPV resulted in 1kg of the polymer available for use in January 2002. Cool combustion spray technology has been used to deposit pure BAM-PPV on aluminum and steel coupons; adhesion testing has been performed, and good adhesion was demonstrated. Initial neutral salt fog tests were conducted at China Lake and the MCT coating on Al 2024-T3 vs. the CCC showed similar performance up to 1146 hours. At 3000 hours, extensive corrosion was evident in both the BAM-PPV and CCC Al panels. Alternative routes were investigated to reduce the amount of steps, waste, and cost required for the production of BAM-PPV with several methods adopted during this time period ands several processes that resulted in failure. Oligomers of aniline were prepared by the RPI group and showed redox behavior. The oligomers were thoroughly characterized during this period of study.

The scale-up synthesis of BAM-PPV was completed by the end of FY02 providing 3.2kg of unpurified polymer. Modifications to the synthesis have resulted in reduction in the total number of steps required for the reaction and replacement of several reagents with more environmentally friendly and/or less expensive alternatives. BAM-PPV underwent a vigorous purification study to remove salt that are formed during the polymerization process. This method could be scaled for future industrial use. The purification process gave over 2.0 kg of pure polymer as confirmed by elemental analysis. BAM-PPV was characterized via FTIR, NMR and thermal analysis.

Polymethacrylamides containing pendant oligo-aniline groups have been prepared and were fully characterized.

Neutral salt fog tests have shown that pure BAM-PPV solvent sprayed onto Al 2024-T3 can pass 336 hours for a potential replacement of CCC. BAM-PPV coatings have not lasted as long as CCC or TCP in neutral salt fog. During this period initial experiments have shown that BAM-PPV can be swollen in $SCCO_2$ as a potential environmentally benign coating method.

SERDP FY 03-04

BAM-PPV was further characterized using thermal analysis for solubility into $SCCO_2$ solvent at VCU. The VCU studies confirmed the thermal properties of BAM-PPV (T_g, T_m, and T_d) within experimental error to the work at NAWCWD. BAM-PPV is a robust material that can undergo normal processing conditions to give high quality films. However, the $SCCO_2$ processing of BAM-PPV did reveal that even with a co-solvent, high quality films were not obtained.

BAM-PPV as a pretreatment system showed good performance in neutral salt fog exposure tests when the coating thickness was greater than 1.5 microns. BAM-PPV can be processed by a variety of methods including zero VOC powder formulations, solvent based and environmentally friendly solvents.

BAM-PPV films processed from solvent and environmentally friendly solvents gave superior performance when compared to AC131 and Alodine 5700 but could not perform as well as CCC or TCP. Polyaniline films did not pass the 336 hour neutral salt fog exposure test. BAM-PPV incorporated into a military coating containing non-chrome primers with topcoat did not pass the 2000 hour neutral salt fog test. However, when compared to TCP and CCC pretreatment and non-chrome primers with topcoat they all showed very similar performance. BAM-PPV powder formulations did not meet the 2000 hour neutral salt fog test, both the control and BAM-PPV powder formulation failed at 1500 hours. BAM-PPV was incorporated into a CARC military coating but failed during exposure in neutral salt fog testing.

BAM-PPV coatings were examined for the mechanism of corrosion protection in corrosive environments by using a variety of advanced analytical techniques. ENM and SVET showed that BAM-PPV films may passivate the metal surface in DHS. XPS data also indicates that BAM-PPV performs differently than standard coatings (e.g. CCC, bare and epoxy) in neutral salt fog tests. EIS studies on the stability of BAM-PPV films in various pH solutions showed that BAM-PPV is robust without evidence of delamination or blistering. Further EIS studies of BAM-PPV films showed that it can perform in some cases as well as a chromated system.

Section IX

Conclusions:

A fully successful SERDP program (WP 1148) was accomplished over the past four years of study (FY00-04). EAP polymers have shown that they can meet the minimum requirement for a viable alternative to CCC. These EAP polymers can be incorporated into military coatings and in most cases can perform as well as the CCC and TCP based military coating with non-chrome primers and topcoats. In general the alternatives to fully chromated systems do not meet the minimum requirement for neutral salt fog. However, the BAM-PPV pretreatment film is a potentially viable alternative to the currently approved pretreatment (TCP) coating system. BAM-PPV does not contain any heavy metals in the system (e.g. chromium: hexavalent or trivalent). This represents a significant improvement over heavy metal based coatings (e.g. TCP) that contain chromium. Trivalent chromium is not considered a carcinogen but with potential restrictions on the future use of chromium (in any form), a fully chromium free coating will be more attractive to military installations as they seek to comply with future regulations.

Currently, this SERDP program has been transitioned to a demonstration/validation program. It is now in the first year of an ESTCP program (FY05-08) to determine the viability of BAM-PPV pretreatment as a field-tested alternative to CCC and TCP.

Section X: Appendices

Appendix A-References:

1. *Non-Chromate Aluminum Pretreatments Phase I Report*, Project # PP0025, Environmental Security Technology Certification Program (ESTCP), August 2003.
2. Korinek, K. A., *Chromate Conversion Coatings*, in ASM Hanbook, Volume 13 Corrosion, Eds. Lawrence J. Korb and David L. Olson, p. 389, ASM International Handbook, 1987.
3. Blasiak, J., and Kowalik, J., *Mutation Research*, **469**, 135 (2000).
4. National Emission Standards for Chromium Emissions from Hard and Decorative Chromium Electroplating and Chromium Anodizing Tanks, Environmental Protection Agency, Federal Register, RIN 2060-AC14, January 25, 1995.
5. AES/EPA Conference, *Hexavalent Chrome PEL AESF Presentation*, January 2004.
6. Jacobs, P. B., and Yu, P.C., *Journal of Coatings Technology*, **65(822**), 45 (1993).
7. Kolcum, E. H., *Aviation Week and Space Technology*, June 24, 1991 p. 67.
8. Thompson, K. G., Byran, C. J., Benicewicz, B. C., and Wrobleski, D. A., *Los Alamos National Laboratory Report* , LA-UR-92-360 (1991).
9. Wrobleski, D.A., Benicewicz, B. C., Thomposon, K. G., and Byran, B. J., *ACS Polym. Prepr.*, **35(1)**, 265 (1994).
10. Mengoli, G., Munari, M. T., Bianco, P., and Musiana, M. M., *J. Appl. Polym. Sci.*, **26**, 4247 (1981).
11. DeBerry D. W., *J. Electrochem. Soc*., **132**, 1022 (1985).
12. Jain, F. C., Rosato, J. J., Laonia, and Agarwala,V. S., *Corrosion,* **42,** 700 (1986).
13. Wessling, B., *Synth. Met*. **93**, 143 (1998).
14. Kinlen, P. J., Ding, Y., and Silverman, D. C., *Corrosion*, **58(6)**, 490 (2002).
15. Kendig, M., and Hon, M., *Corrosion*, **60**, 1024 (2004).
16. Zarras, P., Anderson, N., Webber, C., Guenthner, A, Prokopuk, N., and Stenger-Smith, J. D., *Polymers in Aggressive and Corrosive Environments PACE 2004*, September 8-9, 2004, Cologne, Germany, Conference Proceedings, p. 175.
17. Stenger-Smith, J. D., Zarras, P., Mwerwin, L. H., Shaheen, S. E., Kippelen, B., and Peyghambarian, N. M., *Macromolecules*, **31(21)**, 7566 (1998).
18. Stenger-Smith, J. D., Zarras, P., Ostrom, G., and Miles, M. H., Review of *Poly(bis-dialkylamino-p-phenylene vinylene)s as Corrosion Inhibiting Materials*, ACS Symposium Series 735, Eds. B. R. Hsieh and Y. Wei, ACS Washington DC, Chapter 18, p. 180, 1999.
19. M. Lora; J. S. Lim; M. A. McHugh, *J. Phys. Chem. B*, **103**, 2818, (1999).
20. Mulder, M., *Basic Principles of Membrane Technology*, 2nd Ed., Kluwer Academic Publishers, Boston, 1997.
21. Winkler B., Dai, L.M., and Mau A.W.-H., *Chemistry of Materials*,**11(3),** 704 (1999).
22. Bicerano, J., *Prediction of Polymer Properties*, 3rd Ed., Chapters, 3, 4, 5 and 6, Marcel Dekker Inc., New York, 2002.
23. Seitz, J.T., *J. Appl. Polym. Sci.* **49**, 1331 (1993).

24. ASTM B117, *Annual Book of ASTM Standards*, ASTM, West Conshohochen, PA 2001, **vol. 03.02**, p. 1.
25. Kanegsberg, B., and Kanegsberg, E., *Handbook for Critical Cleaning*, CRC Press, Washington DC, 2001, p.175, Chapter 1.12.
26. Shao, H. B., Wang, J. M., Zhang, Z., and Cao, C. N., *J. Electroanalyst. Chem*., **549**, 145 (2003).
27. Metikoš-Hukovic, M., Babic, R., Grubac, Z., *J. Appl. Electrochem*. **32**, 35, (2002).
28. Mansfeld, F., *J. Appl. Electrochem*. **25**, 187, (1995).
29. He, J., Gelling, V. J., Tallman, D. E., and Bierwagen, G. P., *J. Electrochem. Soc.* **147**, 3661 (2000).
30. Tallman, D. E., Pae Y., and Bierwagen, G. P., *Corrosion* **56,** 401, (2000).
31. Truong V. T., *et al.*, *Synthetic Metals*, **110,** 7, (2000).
32. Dlubek *et al.* , *Macromolecules*, **33**, 187, (2000).
33. Schwartz, J., *et al.*, *J. Chem. Phys*., **116(8),** 8198 (2002).

Appendix B-List of Publication FY00-04

1. P. Zarras, N. Anderson, R. L. Quintana, A. Guenthner, N. Prokopuk, C. Webber, L. Baldwin, J. D. Stenger-Smith, and J. M. Pentony, "Electroactive Polymer Coatings as Replacements for Chromate Conversion Coatings, in Smart Coatings, ACS Symposium Book Series, Eds. T. Provder, Washington DC, in press, 2006.
2. E. Kus, M. Grunlan, C. Webber, N. Anderson, P. Zarras and F. Mansfeld, "Evaluation of the Protective Properties of Novel Chromate-Free Polymer Coatings Using Electrochemical Impedance Spectroscopy (EIS)," in New Developments in Coatings Technology, Eds. P. Zarras, T. Wood,, B. Richey and B. C. Benicewicz, ACS Symposium Book Series, Washington DC in press, 2006.
3. P. Zarras, N. Prokopuk, N. Anderson, A. Guenthner, C. Webber and J. D. Stenger-Smith, "Poly(2,5-bis(N-methyl-N-hexylamino)Phenylene vinylene): A new Smart Conjugated Polymer Coating: Synthesis, Properties, Corrosion Prevention Using X-Ray Photoelectron Spectroscopy Study," *ACS Polymer Prepr*., **46(1)**, 535 (2005).
4. N.Anderson, "Conductive Polymers as Green Alternatives to Hexavalent Chromium," *The Navy's Environmental Magazine: Currents*, pp. 60-62, Spring 2005.
5. P. Zarras, N. Anderson, C. Webber, D. J. Irvin, J. A. Irvin, N. Prokopuk, J. D. Stenger-Smith, A. Guenthner, A. Bishop, M. Fleszar, B. Benicewicz, J. Xu and D. E. Tallman, "Novel Conductive Polymers as Environmentally Compliant Coatings for Corrosion Protection, SERDP/ESTCP Annual Symposium and Technical Workshop, Washington, DC, November 30-December 2, 2004, p. 191.
6. R. Chen and B.C. Benicewicz, "Oligoanilines and Poly(acrylamides) Containing Oligoanilines," *ACS Polymer Preprints*, 45(1), 256 (2004).
7. P. Zarras, N. Anderson, C. Webber, A. Guenthner, N. Prokopuk and J. D. Stenger-Smith, "Novel Conjugated Polymers Based on Derivatives of Poly(phenylene vinylene)s as Corrosion Protective Coatings in Marine Environments," Polymer in Aggressive and Corrosive Environments, PACE 2004, Conference Proceedings, September 8-9, 2004, Cologne, Germany, p. 175.
8. J. D. Stenger-Smith, N. Anderson, C. Webber and P. Zarras, "Poly(2,5-bis(N-methyl-N-hexylamino)Phenylene vinylene)As a Replacement for Chromate Conversion Coatings," *ACS Polym. Prepr*., **45(2),** 150 (2004).
9. R. Chen, V. Raghunadh and B. C. Benicewicz, "New Electroactive Polymers for Anti-Corrosion Coatings," *ACS Polym. Prepr*., **45(2),** 151 (2004).
10. E. Kus, N. Anderson, P. Zarras and F. Mansfeld, "Evaluation of the Protective Properties of Chromate-Free BAM-PPV Polymer Based Coatings using Electrochemical Impedance Spectroscopy (EIS)," *ACS Polym. Prepr*., **45(2),** 207 (2004).
11. J. Xu, R. Zhang, P. Zarras, C. Webber and N. Anderson, "Positron Metrology for Corrosion Analysis of Coatings," *ACS Polym. Prepr*., **45(2)**, 198 (2004).
12. D. E. Tallman, J. He, and G. P. Bierwagen," Polypyrrole Coatings for Corrosion Control of Aluminum Alloys: Scanning Vibrating Electrode Studies of Polymer-Metal Interface," *ACS Polym. Prepr*., **45(2)**, 197 (2004).

13. R. Chen and B.C. Benicewicz, "Preparation and Properties of Poly(methacrylamide)s Containing Oligoaniline Side Chains," *Macromolecules*, **36**, 6333 (2003).
14. P. Zarras, N. Anderson, C. Webber, D. J. Irvin, J. A. Irvin, A. Guenthner and J. D. Stenger-Smith, "Current Issues Facing Conductive Polymers as Corrosion Inhibitors," *Radiation Physics and Chemistry*, **68,** 387 (2003).
15. P. Zarras and J. D. Stenger-Smith, "An Introduction to Corrosion Protection Using Electroactive Polymers," in *Electroactive Polymers for Corrosion Control/Prevention*, P. Zarras, J. D. Stenger-Smith, and Y. Wei., Eds., *ACS Symposium Series 843*, American Chemical Society, Washington DC, Chapter 1, pp.2-17, 2003.
16. N. Anderson, D. J. Irvin, J. A. Irvin, J. D. Stenger-Smith, A. Guenthner, C. Webber and P. Zarras, "Improved Synthesis and Corrosion Properties of Poly(bis-(dialkylamino)phenylene vinylene)s (BAMPPV)," in *Electroactive Polymers for Corrosion Control/Prevention*, P. Zarras, J. D. Stenger-Smith and Y. Wei., Eds., *ACS Symposium Series 843*, American Chemical Society, Washington DC, Chapter 8, pp. 140-155, 2003.
17. P. Zarras and J. Irvin, *Electrically Active Polymers*, in Encyclopedia of Polymer Science and Technology, John Wiley & Sons, Inc., online posting date: April 15, 2003; http://www.mrw.interscience.wiley.com/epst/articles/pst107.
18. P. Zarras, N. Anderson, C. Webber, D. J. Irvin, J. A. Irvin, A. Guenthner and J. D. Stenger-Smith, "Progress in Using Conductive Polymers as Corrosion-inhibiting Coatings," *Radiation Physics and Chemistry*, **68**, 387-394 (2003).
19. K. G. Thompson and B. C. Benicewicz, "Corrosion-Protective Coatings from Electroactive Polymers," in *Electroactive Polymers for Corrosion Control/Prevention*, P. Zarras, J. D. Stenger-Smith and Y. Wei, Eds., *ACS Symposium Series 843*, American Chemical Society, Washington, D.C. 2003, p. 18.
20. R. Chen and B. C. Benicewicz, "Synthesis and Characterization of Polymers with Oligoaniline Side Chains," in *Electroactive Polymers for Corrosion Control/Prevention*, P. Zarras, J. D. Stenger-Smith and Y. Wei, Eds., *ACS Symposium Series 843*, American Chemical Society, Washington, D.C. 2003, p. 126.
21. N. Anderson, D. J. Irvin, C. Webber, J. D. Stenger-Smith, and P. Zarras, "Scale-up and Corrosion Inhibition of Poly(bis(dialkylamino)phenylene vinylenes)," *ACS PMSE Preprints*, **86**, 7 (2002).
22. D. J. Irvin, N. Anderson, C. Webber, S. Fallis, and P. Zarras, "New Synthetic Routes to Poly(bis(dialkylamino)phenylene vinylenes)", *ACS PMSE Preprints*, **86**, 61 (2002).
23. N. Anderson, D. J. Irvin, J. D. Stenger-Smith, A. Guenthner, C. Webber and P. Zarras, "Electroactive Polymers as Alternative Corrosion Protective Coatings," Proceedings Tri-Service Corrosion Conference, San Antonio, TX. January 15-19, 2002.
24. R. Chen and B. C. Benicewicz, "Synthesis and Characterization of Electroactive Polymers with Oligoaniline Side Chains," *ACS PMSE Preprints*, **86**, 42 (2002).

25. N. Anderson, J. D. Stenger-Smith, D.J. Irvin, A. J. Guenthner, and P. Zarras, P. In *A Review of Electroactive polymers as Environmentally Benign Corrosion Control Coatings*, Proceedings of the Navy Corrosion Information and Technology Exchange, Louisville, KY, July 16-20, 2001
25. P. Zarras, J. D. Stenger-Smith, "A Tutorial on the Use of Electroactive Polymers as Corrosion Inhibiting Materials," *ACS Polymer Preprints*, **2000**, *41(2)***,** 1730.
26. J. D. Stenger-Smith, P. Zarras, P. C. Webber, and N. Anderson, "Poly(bisdialkylaminophenylene vinylene)s as Potential Replacements for Chromium," *Poly Millennial 2000 Abstracts*, p. 378, Waikoloa Hawaii, December 9-13, 2000.

Appendix C-List of Presentation FY00-04

1. P. Zarras, N. Anderson, C. Webber, D. J. Irvin, J. A. Irvin, N. Prokopuk, J. D. Stenger-Smith, A. Guenthner, A. Bishop, M. Fleszar, B. Benicewicz, J. Xu and D. E. Tallman, "Novel Conductive Polymers as Environmentally Compliant Coatings for Corrosion Protection, SERDP/ESTCP Annual Symposium and Technical Workshop, Washington, DC, November 30-December 2, 2004, (Marriot Wardman Park Hotel, Washington DC) p. 191.
2. P. Zarras, N. Anderson, C. Webber, A. Guenthner, N. Prokopuk and J. D. Stenger-Smith, "Novel Conjugated Polymers Based on Derivatives of Poly(phenylene vinylene)s as Corrosion Protective Coatings in Marine Environments," Polymer in Aggressive and Corrosive Environments, PACE 2004, Conference Proceedings, September 8-9, 2004, Cologne, Germany, p. 175.
3. J. D. Stenger-Smith, N. Anderson, C. Webber and P. Zarras, "Poly(2,5-bis(N-methyl-N-hexylamino) phenylene vinylene) as a Replacement for Chromate Conversion Coatings," *ACS Polym. Prepr.*, (ACS Fall National Meeting, Philadelphia, PA) **45(2),** 150 (2004).
4. R. Chen, V. Raghunadh and B. C. Benicewicz, "New Electroactive Polymers for Anti-Corrosion Coatings," *ACS Polym. Prepr.*, (ACS Fall National Meeting, Philadelphia, PA) **45(2),** 151 (2004).
5. E. Kus, N. Anderson, P. Zarras and F. Mansfeld, "Evaluation of the Protective Properties of Chromate-Free BAM-PPV Polymer Based Coatings using Electrochemical Impedance Spectroscopy (EIS)," *ACS Polym. Prepr.*, (ACS Fall National Meeting, Philadelphia, PA) **45(2),** 207 (2004).
6. J. Xu, R. Zhang, P. Zarras, C. Webber and N. Anderson, "Positron Metrology for Corrosion Analysis of Coatings," *ACS Polym. Prepr.*, (ACS Fall National Meeting, Philadelphia, PA) **45(2)**, 198 (2004).
7. N. Anderson, "Updates on Using BAM-PPV as a Replacement For Chrome Conversion Coatings," Navy Corrosion Conference, 'Rust 2004', July 2004, Louisville, KY.
8. Conductive Polymers As Alternative Corrosion Control Coatings," Presented by N. Anderson at the Aerospace Coatings and Coating Removal Conference, May 20-22, 2003, Colorado Springs, CO.
9. A New Conductive Polymer As A Replacement For Chrome Conversion Coatings, " Presented by N. Anderson at the Navy Corrosion Conference, 'Rust 2003', July 14-17, 2003, Louisville, KY.
10. Conductive Polymer BAMPPV in Corrosion Inhibiting Coatings, Presented by N. Anderson at the Tri-Service Corrosion Conference, November 17-21, Las Vegas, NV.
11. Electroactive Polymers for Charge Storage and Corrosion Protection, Presented by J. Stenger-Smith at the University of Florida, Gainesville, January 7, 2003.
12. Electroactive Polymers for Charge Storage and Corrosion Protection, Presented by J. Stenger-Smith at the American Chemical Society Polymer Research Section Meeting, Rayleigh-Durham NC, May 6, 2003.

13. P. Zarras, Positron and Positronium Chemistry (PPC-7) Conference, Knoxville, TN., July 7-12, 2002.
14. P. Zarras. Poster presentation, Gordon Research Conference-Aqueous Corrosion, New London, NH., July 14-19, 2002.
15. National Defense Industrial Symposium (NDIA) - Industrial Ecology in Support of the Transformation-Environmental Energy and Corrosion Topics-Morristown, NJ, October 30-31, 2002.
16. SERDP/ESTCP Partners in Environmental Technology Technical Symposium and Workshop, Poster Presentation, Washington DC, December 3-5, 2002.
17. N. Anderson, Air Force Corrosion Conference, Macon, GA, March 9-14, 2002.
18. N. Anderson, J. D. Stenger-Smith, D.J. Irvin, A. J. Guenthner, and P. Zarras, Proceedings of the Navy Corrosion Information and Technology Exchange, Louisville, KY, July 16-20, 2001
19. P. Zarras, J. D. Stenger-Smith, "A Tutorial on the Use of Electroactive Polymers as Corrosion Inhibiting Materials," *ACS Polymer Preprints*, **2000**, *41(2)***,** 1730.
20. J. D. Stenger-Smith, P. Zarras, P. C. Webber, and N. Anderson, *Poly Millennial 2000 Abstracts*, p. 378, Waikoloa Hawaii, December 9-13, 2000.

Appendix D- Toxicity Test of BAM-PPV Powder

The following is the toxicity test data generated by CalScience Environmental Laboratories, Inc., San Diego, California. The "CalWet" test was performed according to EPA method 8260B. This test was in response to a request by the SERDP IPR FY02 to demonstrate that BAM-PPV does not pose environmental hazards.

SEE SEPARATE FILE LISTED BAM TOX TEST.PDF

Calscience
Environmental
Laboratories, Inc.

June 18, 2003

Lyn Vasquez
Navy Public Works Center
2730 McKean Street, Suite 1
San Diego, CA 92136-5294

Subject: **Calscience Work Order No.:** **03-06-0385**
Client Reference: **CEL-0284 / LAB#31338 / Proj#144-01**

Dear Client:

Enclosed is an analytical report for the above-referenced project. The samples included in this report were received 6/6/2003 and analyzed in accordance with the attached chain-of-custody.

Unless otherwise noted, all analytical testing was accomplished in accordance with the guidelines established in our Quality Assurance Program Manual, applicable standard operating procedures, and other related documentation. The original report of any subcontracted analysis is provided herein, and follows the standard Calscience data package. The results in this analytical report are limited to the samples tested and any reproduction thereof must be made in its entirety.

If you have any questions regarding this report, please do not hesitate to contact the undersigned.

Sincerely,

Calscience Environmental
Laboratories, Inc.
Jody McInerney
Project Manager

Michael J. Crisostomo
Quality Assurance Manager

Calscience Environmental Laboratories, Inc.

ANALYTICAL REPORT

Navy Public Works Center	Date Sampled:	06/03/03
2730 McKean Street, Suite 1	Date Received:	06/06/03
San Diego, CA 92136-5294	Date Analyzed:	06/11/03
	Work Order No.:	03-06-0385
	Preparation:	STLC
Attn: Lyn Vasquez	Method:	EPA 8260B
RE: CEL-0284 / LAB#31338 / Proj#144-01	Page 1 of 1	

All concentrations are reported in µg/L (ppb).

Sample Number	Hexachloro-1,3-Butadiene Concentration	Reporting Limit
31338-01 BAM-PPV	ND	2000
Method Blank	ND	2000

ND denotes not detected at indicated reportable limit.

Each sample was received by CEL chilled, intact, and with chain-of-custody attached.

Calscience Environmental Laboratories, Inc.

ANALYTICAL REPORT

Navy Public Works Center
2730 McKean Street, Suite 1
San Diego, CA 92136-5294

Date Received: 06/06/03
Work Order No: 03-06-0385
Preparation: STLC
Method: EPA 8260B

Project: CEL-0284 / LAB#31338 / Proj#144-01

Client Sample Number	Lab Sample Number	Date Collected	Matrix	Date Prepared	Date Analyzed	QC Batch ID
31338-01 BAM-PPV	**03-06-0385-1**	**06/03/03**	**Solid**	**06/06/03**	**06/11/03**	**030610L05**

Parameter	Result	RL	DF	Qual	Units	Parameter	Result	RL	DF	Qual	Units
Acetone	ND	1000	100		ug/L	1,3-Dichloropropane	ND	100	100		ug/L
Benzene	ND	50	100		ug/L	2,2-Dichloropropane	ND	100	100		ug/L
Bromobenzene	ND	100	100		ug/L	1,1-Dichloropropene	ND	100	100		ug/L
Bromochloromethane	ND	100	100		ug/L	c-1,3-Dichloropropene	ND	50	100		ug/L
Bromodichloromethane	ND	100	100		ug/L	t-1,3-Dichloropropene	ND	50	100		ug/L
Bromoform	ND	100	100		ug/L	Ethylbenzene	ND	100	100		ug/L
Bromomethane	ND	100	100		ug/L	2-Hexanone	ND	1000	100		ug/L
2-Butanone	ND	1000	100		ug/L	Isopropylbenzene	ND	100	100		ug/L
n-Butylbenzene	ND	100	100		ug/L	p-Isopropyltoluene	ND	100	100		ug/L
sec-Butylbenzene	ND	100	100		ug/L	Methylene Chloride	ND	1000	100		ug/L
tert-Butylbenzene	ND	100	100		ug/L	4-Methyl-2-Pentanone	ND	1000	100		ug/L
Carbon Disulfide	ND	1000	100		ug/L	Naphthalene	ND	1000	100		ug/L
Carbon Tetrachloride	ND	50	100		ug/L	n-Propylbenzene	ND	100	100		ug/L
Chlorobenzene	ND	100	100		ug/L	Styrene	ND	100	100		ug/L
Chloroethane	ND	100	100		ug/L	1,1,1,2-Tetrachloroethane	ND	100	100		ug/L
Chloroform	ND	100	100		ug/L	1,1,2,2-Tetrachloroethane	10000	100	100		ug/L
Chloromethane	ND	100	100		ug/L	Tetrachloroethene	ND	100	100		ug/L
2-Chlorotoluene	ND	100	100		ug/L	Toluene	1200	100	100		ug/L
4-Chlorotoluene	ND	100	100		ug/L	1,2,3-Trichlorobenzene	ND	100	100		ug/L
Dibromochloromethane	ND	100	100		ug/L	1,2,4-Trichlorobenzene	ND	100	100		ug/L
1,2-Dibromo-3-Chloropropane	ND	500	100		ug/L	1,1,1-Trichloroethane	ND	100	100		ug/L
1,2-Dibromoethane	ND	100	100		ug/L	1,1,2-Trichloroethane	ND	100	100		ug/L
Dibromomethane	ND	100	100		ug/L	Trichloroethene	540	100	100		ug/L
1,2-Dichlorobenzene	ND	100	100		ug/L	Trichlorofluoromethane	ND	1000	100		ug/L
1,3-Dichlorobenzene	ND	100	100		ug/L	1,2,3-Trichloropropane	ND	100	100		ug/L
1,4-Dichlorobenzene	ND	100	100		ug/L	1,2,4-Trimethylbenzene	ND	100	100		ug/L
Dichlorodifluoromethane	ND	100	100		ug/L	1,3,5-Trimethylbenzene	ND	100	100		ug/L
1,1-Dichloroethane	ND	100	100		ug/L	Vinyl Acetate	ND	1000	100		ug/L
1,2-Dichloroethane	ND	50	100		ug/L	Vinyl Chloride	ND	50	100		ug/L
1,1-Dichloroethene	ND	100	100		ug/L	p/m-Xylene	180	100	100		ug/L
c-1,2-Dichloroethene	ND	100	100		ug/L	o-Xylene	180	100	100		ug/L
t-1,2-Dichloroethene	ND	100	100		ug/L	Methyl-t-Butyl Ether (MTBE)	ND	100	100		ug/L
1,2-Dichloropropane	ND	100	100		ug/L						

Surrogates:	REC (%)	Control Limits	Qual	Surrogates:	REC (%)	Control	Qual
Dibromofluoromethane	108	86-118		Toluene-d8	101	88-110	
1,4-Bromofluorobenzene	100	86-115					

RL - Reporting Limit , DF - Dilution Factor , Qual - Qualifiers

Calscience Environmental Laboratories, Inc.

ANALYTICAL REPORT

Navy Public Works Center
2730 McKean Street, Suite 1
San Diego, CA 92136-5294

Date Received: 06/06/03
Work Order No: 03-06-0385
Preparation: STLC
Method: EPA 8260B

Project: CEL-0284 / LAB#31338 / Proj#144-01

Client Sample Number	Lab Sample Number	Date Collected	Matrix	Date Prepared	Date Analyzed	QC Batch ID
Method Blank	**095-01-026-2,201**	**N/A**	**Aqueous**	**06/06/03**	**06/11/03**	**030610L05**

Parameter	Result	RL	DF	Qual	Units	Parameter	Result	RL	DF	Qual	Units
Acetone	ND	1000	100		ug/L	1,3-Dichloropropane	ND	100	100		ug/L
Benzene	ND	50	100		ug/L	2,2-Dichloropropane	ND	100	100		ug/L
Bromobenzene	ND	100	100		ug/L	1,1-Dichloropropene	ND	100	100		ug/L
Bromochloromethane	ND	100	100		ug/L	c-1,3-Dichloropropene	ND	50	100		ug/L
Bromodichloromethane	ND	100	100		ug/L	t-1,3-Dichloropropene	ND	50	100		ug/L
Bromoform	ND	100	100		ug/L	Ethylbenzene	ND	100	100		ug/L
Bromomethane	ND	100	100		ug/L	2-Hexanone	ND	1000	100		ug/L
2-Butanone	ND	1000	100		ug/L	Isopropylbenzene	ND	100	100		ug/L
n-Butylbenzene	ND	100	100		ug/L	p-Isopropyltoluene	ND	100	100		ug/L
sec-Butylbenzene	ND	100	100		ug/L	Methylene Chloride	ND	1000	100		ug/L
tert-Butylbenzene	ND	100	100		ug/L	4-Methyl-2-Pentanone	ND	1000	100		ug/L
Carbon Disulfide	ND	1000	100		ug/L	Naphthalene	ND	1000	100		ug/L
Carbon Tetrachloride	ND	50	100		ug/L	n-Propylbenzene	ND	100	100		ug/L
Chlorobenzene	ND	100	100		ug/L	Styrene	ND	100	100		ug/L
Chloroethane	ND	100	100		ug/L	1,1,1,2-Tetrachloroethane	ND	100	100		ug/L
Chloroform	ND	100	100		ug/L	1,1,2,2-Tetrachloroethane	ND	100	100		ug/L
Chloromethane	ND	100	100		ug/L	Tetrachloroethene	ND	100	100		ug/L
2-Chlorotoluene	ND	100	100		ug/L	Toluene	ND	100	100		ug/L
4-Chlorotoluene	ND	100	100		ug/L	1,2,3-Trichlorobenzene	ND	100	100		ug/L
Dibromochloromethane	ND	100	100		ug/L	1,2,4-Trichlorobenzene	ND	100	100		ug/L
1,2-Dibromo-3-Chloropropane	ND	500	100		ug/L	1,1,1-Trichloroethane	ND	100	100		ug/L
1,2-Dibromoethane	ND	100	100		ug/L	1,1,2-Trichloroethane	ND	100	100		ug/L
Dibromomethane	ND	100	100		ug/L	Trichloroethene	ND	100	100		ug/L
1,2-Dichlorobenzene	ND	100	100		ug/L	Trichlorofluoromethane	ND	1000	100		ug/L
1,3-Dichlorobenzene	ND	100	100		ug/L	1,2,3-Trichloropropane	ND	100	100		ug/L
1,4-Dichlorobenzene	ND	100	100		ug/L	1,2,4-Trimethylbenzene	ND	100	100		ug/L
Dichlorodifluoromethane	ND	100	100		ug/L	1,3,5-Trimethylbenzene	ND	100	100		ug/L
1,1-Dichloroethane	ND	100	100		ug/L	Vinyl Acetate	ND	1000	100		ug/L
1,2-Dichloroethane	ND	50	100		ug/L	Vinyl Chloride	ND	50	100		ug/L
1,1-Dichloroethene	ND	100	100		ug/L	p/m-Xylene	ND	100	100		ug/L
c-1,2-Dichloroethene	ND	100	100		ug/L	o-Xylene	ND	100	100		ug/L
t-1,2-Dichloroethene	ND	100	100		ug/L	Methyl-t-Butyl Ether (MTBE)	ND	100	100		ug/L
1,2-Dichloropropane	ND	100	100		ug/L						

Surrogates:	REC (%)	Control Limits	Qual	Surrogates:	REC (%)	Control	Qual
Dibromofluoromethane	107	86-118		Toluene-d8	101	88-110	
1,4-Bromofluorobenzene	101	86-115					

RL - Reporting Limit , DF - Dilution Factor , Qual - Qualifiers

Calscience Environmental Laboratories, Inc.

EPA 8260B(STLC) Tentatively Identified Compound List

Work Order	CEL Sample ID	Client ID	Q	Compound	CAS Number	RT	On Column Conc. µg/L	Estimated Conc. µg/L
03-06-0385	1	31338-01 BAM-PPV	83	Hexanal	66-25-1	11.00	8.9	890

Q: Qualifier
RT: Retention Time

Calscience Environmental Laboratories, Inc.

ANALYTICAL REPORT

Navy Public Works Center	Date Sampled:	06/03/03
2730 McKean Street, Suite 1	Date Received:	06/06/03
San Diego, CA 92136-5294	Date Analyzed:	06/11/03
	Work Order No.:	03-06-0385
	Preparation:	EPA 1311
Attn: Lyn Vasquez	Method:	EPA 8260B
RE: CEL-0284 / LAB#31338 / Proj#144-01	Page 1 of 1	

All concentrations are reported in µg/L (ppb).

Sample Number	Hexachloro-1,3-Butadiene Concentration	Reporting Limit
31338-01 BAM-PPV	ND	2000
Method Blank	ND	2000

ND denotes not detected at indicated reportable limit.

Each sample was received by CEL chilled, intact, and with chain-of-custody attached.

Calscience Environmental Laboratories, Inc.

ANALYTICAL REPORT

Navy Public Works Center
2730 McKean Street, Suite 1
San Diego, CA 92136-5294

Date Received: 06/06/03
Work Order No: 03-06-0385
Preparation: EPA 1311
Method: EPA 8260B

Project: CEL-0284 / LAB#31338 / Proj#144-01

Client Sample Number	Lab Sample Number	Date Collected	Matrix	Date Prepared	Date Analyzed	QC Batch ID
31338-01 BAM-PPV	**03-06-0385-1**	**06/03/03**	**Solid**	**06/06/03**	**06/11/03**	**030610L04**

Parameter	Result	RL	DF	Qual	Units	Parameter	Result	RL	DF	Qual	Units
Acetone	ND	1000	1		ug/L	1,3-Dichloropropane	ND	100	1		ug/L
Benzene	ND	50	1		ug/L	2,2-Dichloropropane	ND	100	1		ug/L
Bromobenzene	ND	100	1		ug/L	1,1-Dichloropropene	ND	100	1		ug/L
Bromochloromethane	ND	100	1		ug/L	c-1,3-Dichloropropene	ND	50	1		ug/L
Bromodichloromethane	ND	100	1		ug/L	t-1,3-Dichloropropene	ND	50	1		ug/L
Bromoform	ND	100	1		ug/L	Ethylbenzene	ND	100	1		ug/L
Bromomethane	ND	1000	1		ug/L	2-Hexanone	ND	1000	1		ug/L
2-Butanone	ND	1000	1		ug/L	Isopropylbenzene	ND	100	1		ug/L
n-Butylbenzene	ND	100	1		ug/L	p-Isopropyltoluene	ND	100	1		ug/L
sec-Butylbenzene	ND	100	1		ug/L	Methylene Chloride	ND	1000	1		ug/L
tert-Butylbenzene	ND	100	1		ug/L	4-Methyl-2-Pentanone	ND	1000	1		ug/L
Carbon Disulfide	ND	1000	1		ug/L	Naphthalene	ND	1000	1		ug/L
Carbon Tetrachloride	ND	50	1		ug/L	n-Propylbenzene	ND	100	1		ug/L
Chlorobenzene	ND	100	1		ug/L	Styrene	ND	100	1		ug/L
Chloroethane	ND	100	1		ug/L	1,1,1,2-Tetrachloroethane	ND	100	1		ug/L
Chloroform	ND	100	1		ug/L	1,1,2,2-Tetrachloroethane	8400	100	1		ug/L
Chloromethane	ND	100	1		ug/L	Tetrachloroethene	ND	100	1		ug/L
2-Chlorotoluene	ND	100	1		ug/L	Toluene	860	100	1		ug/L
4-Chlorotoluene	ND	100	1		ug/L	1,2,3-Trichlorobenzene	ND	100	1		ug/L
Dibromochloromethane	ND	100	1		ug/L	1,2,4-Trichlorobenzene	ND	100	1		ug/L
1,2-Dibromo-3-Chloropropane	ND	500	1		ug/L	1,1,1-Trichloroethane	ND	100	1		ug/L
1,2-Dibromoethane	ND	100	1		ug/L	1,1,2-Trichloroethane	ND	100	1		ug/L
Dibromomethane	ND	100	1		ug/L	Trichloroethene	440	100	1		ug/L
1,2-Dichlorobenzene	ND	100	1		ug/L	Trichlorofluoromethane	ND	1000	1		ug/L
1,3-Dichlorobenzene	ND	100	1		ug/L	1,2,3-Trichloropropane	ND	500	1		ug/L
1,4-Dichlorobenzene	ND	100	1		ug/L	1,2,4-Trimethylbenzene	ND	100	1		ug/L
Dichlorodifluoromethane	ND	100	1		ug/L	1,3,5-Trimethylbenzene	ND	100	1		ug/L
1,1-Dichloroethane	ND	100	1		ug/L	Vinyl Acetate	ND	1000	1		ug/L
1,2-Dichloroethane	ND	50	1		ug/L	Vinyl Chloride	ND	50	1		ug/L
1,1-Dichloroethene	ND	100	1		ug/L	p/m-Xylene	120	100	1		ug/L
c-1,2-Dichloroethene	ND	100	1		ug/L	o-Xylene	120	100	1		ug/L
t-1,2-Dichloroethene	ND	100	1		ug/L	Methyl-t-Butyl Ether (MTBE)	ND	100	1		ug/L
1,2-Dichloropropane	ND	100	1		ug/L						

Surrogates:	REC (%)	Control Limits	Qual	Surrogates:	REC (%)	Control	Qual
Dibromofluoromethane	108	86-118		Toluene-d8	101	88-110	
1,4-Bromofluorobenzene	101	86-115					

RL - Reporting Limit . DF - Dilution Factor . Qual - Qualifiers

Calscience Environmental Laboratories, Inc.

ANALYTICAL REPORT

Navy Public Works Center
2730 McKean Street, Suite 1
San Diego, CA 92136-5294

Date Received: 06/06/03
Work Order No: 03-06-0385
Preparation: EPA 1311
Method: EPA 8260B

Project: CEL-0284 / LAB#31338 / Proj#144-01

Client Sample Number	Lab Sample Number	Date Collected	Matrix	Date Prepared	Date Analyzed	QC Batch ID
Method Blank	**099-10-006-7,716**	**N/A**	**Aqueous**	**06/06/03**	**06/11/03**	**030610L04**

Parameter	Result	RL	DF	Qual	Units	Parameter	Result	RL	DF	Qual	Units
Acetone	ND	1000	1		ug/L	1,3-Dichloropropane	ND	100	1		ug/L
Benzene	ND	50	1		ug/L	2,2-Dichloropropane	ND	100	1		ug/L
Bromobenzene	ND	100	1		ug/L	1,1-Dichloropropene	ND	100	1		ug/L
Bromochloromethane	ND	100	1		ug/L	c-1,3-Dichloropropene	ND	50	1		ug/L
Bromodichloromethane	ND	100	1		ug/L	t-1,3-Dichloropropene	ND	50	1		ug/L
Bromoform	ND	100	1		ug/L	Ethylbenzene	ND	100	1		ug/L
Bromomethane	ND	1000	1		ug/L	2-Hexanone	ND	1000	1		ug/L
2-Butanone	ND	1000	1		ug/L	Isopropylbenzene	ND	100	1		ug/L
n-Butylbenzene	ND	100	1		ug/L	p-Isopropyltoluene	ND	100	1		ug/L
sec-Butylbenzene	ND	100	1		ug/L	Methylene Chloride	ND	1000	1		ug/L
tert-Butylbenzene	ND	100	1		ug/L	4-Methyl-2-Pentanone	ND	1000	1		ug/L
Carbon Disulfide	ND	1000	1		ug/L	Naphthalene	ND	1000	1		ug/L
Carbon Tetrachloride	ND	50	1		ug/L	n-Propylbenzene	ND	100	1		ug/L
Chlorobenzene	ND	100	1		ug/L	Styrene	ND	100	1		ug/L
Chloroethane	ND	100	1		ug/L	1,1,1,2-Tetrachloroethane	ND	100	1		ug/L
Chloroform	ND	100	1		ug/L	1,1,2,2-Tetrachloroethane	ND	100	1		ug/L
Chloromethane	ND	100	1		ug/L	Tetrachloroethene	ND	100	1		ug/L
2-Chlorotoluene	ND	100	1		ug/L	Toluene	ND	100	1		ug/L
4-Chlorotoluene	ND	100	1		ug/L	1,2,3-Trichlorobenzene	ND	100	1		ug/L
Dibromochloromethane	ND	100	1		ug/L	1,2,4-Trichlorobenzene	ND	100	1		ug/L
1,2-Dibromo-3-Chloropropane	ND	500	1		ug/L	1,1,1-Trichloroethane	ND	100	1		ug/L
1,2-Dibromoethane	ND	100	1		ug/L	1,1,2-Trichloroethane	ND	100	1		ug/L
Dibromomethane	ND	100	1		ug/L	Trichloroethene	ND	100	1		ug/L
1,2-Dichlorobenzene	ND	100	1		ug/L	Trichlorofluoromethane	ND	1000	1		ug/L
1,3-Dichlorobenzene	ND	100	1		ug/L	1,2,3-Trichloropropane	ND	500	1		ug/L
1,4-Dichlorobenzene	ND	100	1		ug/L	1,2,4-Trimethylbenzene	ND	100	1		ug/L
Dichlorodifluoromethane	ND	100	1		ug/L	1,3,5-Trimethylbenzene	ND	100	1		ug/L
1,1-Dichloroethane	ND	100	1		ug/L	Vinyl Acetate	ND	1000	1		ug/L
1,2-Dichloroethane	ND	50	1		ug/L	Vinyl Chloride	ND	50	1		ug/L
1,1-Dichloroethene	ND	100	1		ug/L	p/m-Xylene	ND	100	1		ug/L
c-1,2-Dichloroethene	ND	100	1		ug/L	o-Xylene	ND	100	1		ug/L
t-1,2-Dichloroethene	ND	100	1		ug/L	Methyl-t-Butyl Ether (MTBE)	ND	100	1		ug/L
1,2-Dichloropropane	ND	100	1		ug/L						

Surrogates:	REC (%)	Control Limits	Qual	Surrogates:	REC (%)	Control	Qual
Dibromofluoromethane	106	86-118		Toluene-d8	100	88-110	
1,4-Bromofluorobenzene	100	86-115					

RL - Reporting Limit . DF - Dilution Factor . Qual - Qualifiers

Calscience Environmental Laboratories, Inc.

EPA 1311/8260BTentatively Identified Compound List

Work Order	CEL Sample ID	Client ID	Q	Compound	CAS Number	RT	On Column Conc. µg/L	Estimated Conc. µg/L
03-06-0385	1	31338-01 BAM-PPV	2	2,2-Difluoropropane	42045-1	4.86	5.5	550

Q: Qualifier
RT: Retention Time

Calscience Environmental Laboratories, Inc.

ANALYTICAL REPORT

Navy Public Works Center		Date Received:	06/06/03
2730 McKean Street, Suite 1		Work Order No:	03-06-0385
San Diego, CA 92136-5294		Preparation:	STLC
		Method:	EPA 8270C

Project: CEL-0284 / LAB#31338 / Proj#144-01

Client Sample Number	Lab Sample Number	Date Collected	Matrix	Date Prepared	Date Analyzed	QC Batch ID
31338-01 BAM-PPV	**03-06-0385-1**	**06/03/03**	**Solid**	**06/09/03**	**06/11/03**	**030609L05**

Parameter	Result	RL	DF	Qual	Units	Parameter	Result	RL	DF	Qual	Units
N-Nitrosodimethylamine	ND	100	10		ug/L	2,4-Dinitrophenol	ND	500	10		ug/L
Aniline	ND	100	10		ug/L	4-Nitrophenol	ND	100	10		ug/L
Phenol	ND	100	10		ug/L	Dibenzofuran	ND	100	10		ug/L
Bis(2-Chloroethyl) Ether	ND	250	10		ug/L	2,4-Dinitrotoluene	ND	100	10		ug/L
2-Chlorophenol	ND	100	10		ug/L	2,6-Dinitrotoluene	ND	100	10		ug/L
1,3-Dichlorobenzene	ND	100	10		ug/L	Diethyl Phthalate	ND	100	10		ug/L
1,4-Dichlorobenzene	ND	100	10		ug/L	4-Chlorophenyl-Phenyl Ether	ND	100	10		ug/L
Benzyl Alcohol	ND	100	10		ug/L	Fluorene	ND	100	10		ug/L
1,2-Dichlorobenzene	ND	100	10		ug/L	4-Nitroaniline	ND	100	10		ug/L
2-Methylphenol	ND	100	10		ug/L	Azobenzene	ND	100	10		ug/L
Bis(2-Chloroisopropyl) Ether	ND	100	10		ug/L	4,6-Dinitro-2-Methylphenol	ND	500	10		ug/L
3/4-Methylphenol	ND	100	10		ug/L	N-Nitrosodiphenylamine	ND	100	10		ug/L
N-Nitroso-di-n-propylamine	ND	100	10		ug/L	4-Bromophenyl-Phenyl Ether	ND	100	10		ug/L
Hexachloroethane	ND	100	10		ug/L	Hexachlorobenzene	ND	100	10		ug/L
Nitrobenzene	ND	250	10		ug/L	Pentachlorophenol	ND	100	10		ug/L
Isophorone	ND	100	10		ug/L	Phenanthrene	ND	100	10		ug/L
2-Nitrophenol	ND	100	10		ug/L	Anthracene	ND	100	10		ug/L
2,4-Dimethylphenol	ND	100	10		ug/L	Di-n-Butyl Phthalate	ND	100	10		ug/L
Benzoic Acid	ND	500	10		ug/L	Fluoranthene	ND	100	10		ug/L
Bis(2-Chloroethoxy) Methane	ND	100	10		ug/L	Benzidine	ND	500	10		ug/L
2,4-Dichlorophenol	ND	100	10		ug/L	Pyrene	ND	100	10		ug/L
1,2,4-Trichlorobenzene	ND	100	10		ug/L	Pyridine	ND	100	10		ug/L
Naphthalene	ND	100	10		ug/L	Butyl Benzyl Phthalate	ND	100	10		ug/L
4-Chloroaniline	ND	100	10		ug/L	3,3'-Dichlorobenzidine	ND	250	10		ug/L
Hexachloro-1,3-Butadiene	ND	100	10		ug/L	Benzo (a) Anthracene	ND	100	10		ug/L
4-Chloro-3-Methylphenol	ND	100	10		ug/L	Bis(2-Ethylhexyl) Phthalate	ND	100	10		ug/L
2-Methylnaphthalene	ND	100	10		ug/L	Chrysene	ND	100	10		ug/L
Hexachlorocyclopentadiene	ND	250	10		ug/L	Di-n-Octyl Phthalate	ND	100	10		ug/L
2,4,6-Trichlorophenol	ND	100	10		ug/L	Benzo (k) Fluoranthene	ND	100	10		ug/L
2,4,5-Trichlorophenol	ND	100	10		ug/L	Benzo (b) Fluoranthene	ND	100	10		ug/L
2-Chloronaphthalene	ND	100	10		ug/L	Benzo (a) Pyrene	ND	100	10		ug/L
2-Nitroaniline	ND	100	10		ug/L	Benzo (g,h,i) Perylene	ND	100	10		ug/L
Dimethyl Phthalate	ND	100	10		ug/L	Indeno (1,2,3-c,d) Pyrene	ND	100	10		ug/L
Acenaphthylene	ND	100	10		ug/L	Dibenz (a,h) Anthracene	ND	100	10		ug/L
3-Nitroaniline	ND	100	10		ug/L	1-Methylnaphthalene	ND	100	10		ug/L
Acenaphthene	ND	100	10		ug/L						

Surrogates:	REC (%)	Control Limits	Qual	Surrogates:	REC (%)	Control	Qual
2-Fluorophenol	73	15-138		Phenol-d6	74	17-141	
Nitrobenzene-d5	76	56-123		2-Fluorobiphenyl	71	45-120	
2,4,6-Tribromophenol	76	32-143		p-Terphenyl-d14	73	46-133	

RL - Reporting Limit , DF - Dilution Factor , Qual - Qualifiers

Calscience Environmental Laboratories, Inc.

ANALYTICAL REPORT

Navy Public Works Center
2730 McKean Street, Suite 1
San Diego, CA 92136-5294

Date Received: 06/06/03
Work Order No: 03-06-0385
Preparation: STLC
Method: EPA 8270C

Project: CEL-0284 / LAB#31338 / Proj#144-01

Client Sample Number	Lab Sample Number	Date Collected	Matrix	Date Prepared	Date Analyzed	QC Batch ID
Method Blank	**095-01-003-1,281**	**N/A**	**Aqueous**	**06/09/03**	**06/11/03**	**030609L05**

Parameter	Result	RL	DF	Qual	Units	Parameter	Result	RL	DF	Qual	Units
N-Nitrosodimethylamine	ND	100	10		ug/L	2,4-Dinitrophenol	ND	500	10		ug/L
Aniline	ND	100	10		ug/L	4-Nitrophenol	ND	100	10		ug/L
Phenol	ND	100	10		ug/L	Dibenzofuran	ND	100	10		ug/L
Bis(2-Chloroethyl) Ether	ND	250	10		ug/L	2,4-Dinitrotoluene	ND	100	10		ug/L
2-Chlorophenol	ND	100	10		ug/L	2,6-Dinitrotoluene	ND	100	10		ug/L
1,3-Dichlorobenzene	ND	100	10		ug/L	Diethyl Phthalate	ND	100	10		ug/L
1,4-Dichlorobenzene	ND	100	10		ug/L	4-Chlorophenyl-Phenyl Ether	ND	100	10		ug/L
Benzyl Alcohol	ND	100	10		ug/L	Fluorene	ND	100	10		ug/L
1,2-Dichlorobenzene	ND	100	10		ug/L	4-Nitroaniline	ND	100	10		ug/L
2-Methylphenol	ND	100	10		ug/L	Azobenzene	ND	100	10		ug/L
Bis(2-Chloroisopropyl) Ether	ND	100	10		ug/L	4,6-Dinitro-2-Methylphenol	ND	500	10		ug/L
3/4-Methylphenol	ND	100	10		ug/L	N-Nitrosodiphenylamine	ND	100	10		ug/L
N-Nitroso-di-n-propylamine	ND	100	10		ug/L	4-Bromophenyl-Phenyl Ether	ND	100	10		ug/L
Hexachloroethane	ND	100	10		ug/L	Hexachlorobenzene	ND	100	10		ug/L
Nitrobenzene	ND	250	10		ug/L	Pentachlorophenol	ND	100	10		ug/L
Isophorone	ND	100	10		ug/L	Phenanthrene	ND	100	10		ug/L
2-Nitrophenol	ND	100	10		ug/L	Anthracene	ND	100	10		ug/L
2,4-Dimethylphenol	ND	100	10		ug/L	Di-n-Butyl Phthalate	ND	100	10		ug/L
Benzoic Acid	ND	500	10		ug/L	Fluoranthene	ND	100	10		ug/L
Bis(2-Chloroethoxy) Methane	ND	100	10		ug/L	Benzidine	ND	500	10		ug/L
2,4-Dichlorophenol	ND	100	10		ug/L	Pyrene	ND	100	10		ug/L
1,2,4-Trichlorobenzene	ND	100	10		ug/L	Pyridine	ND	100	10		ug/L
Naphthalene	ND	100	10		ug/L	Butyl Benzyl Phthalate	ND	100	10		ug/L
4-Chloroaniline	ND	100	10		ug/L	3,3'-Dichlorobenzidine	ND	250	10		ug/L
Hexachloro-1,3-Butadiene	ND	100	10		ug/L	Benzo (a) Anthracene	ND	100	10		ug/L
4-Chloro-3-Methylphenol	ND	100	10		ug/L	Bis(2-Ethylhexyl) Phthalate	ND	100	10		ug/L
2-Methylnaphthalene	ND	100	10		ug/L	Chrysene	ND	100	10		ug/L
Hexachlorocyclopentadiene	ND	250	10		ug/L	Di-n-Octyl Phthalate	ND	100	10		ug/L
2,4,6-Trichlorophenol	ND	100	10		ug/L	Benzo (k) Fluoranthene	ND	100	10		ug/L
2,4,5-Trichlorophenol	ND	100	10		ug/L	Benzo (b) Fluoranthene	ND	100	10		ug/L
2-Chloronaphthalene	ND	100	10		ug/L	Benzo (a) Pyrene	ND	100	10		ug/L
2-Nitroaniline	ND	100	10		ug/L	Benzo (g,h,i) Perylene	ND	100	10		ug/L
Dimethyl Phthalate	ND	100	10		ug/L	Indeno (1,2,3-c,d) Pyrene	ND	100	10		ug/L
Acenaphthylene	ND	100	10		ug/L	Dibenz (a,h) Anthracene	ND	100	10		ug/L
3-Nitroaniline	ND	100	10		ug/L	1-Methylnaphthalene	ND	100	10		ug/L
Acenaphthene	ND	100	10		ug/L						

Surrogates:	REC (%)	Control Limits	Qual	Surrogates:	REC (%)	Control	Qual
2-Fluorophenol	91	15-138		Phenol-d6	91	17-141	
Nitrobenzene-d5	91	56-123		2-Fluorobiphenyl	83	45-120	
2,4,6-Tribromophenol	90	32-143		p-Terphenyl-d14	88	46-133	

RL - Reporting Limit , DF - Dilution Factor , Qual - Qualifiers

Calscience Environmental Laboratories, Inc.

EPA 8270C(STLC) Tentatively Identified Compound List

Work Order	CEL Sample ID	Client ID	Q	Compound	CAS Number	RT	On Column Conc. µg/L	Estimated Conc. µg/L
03-06-0385	1	31338-01 BAM-PPV	72	1-Pentanol	71-41-0	4.05	9.0	180
03-06-0385	1	31338-01 BAM-PPV	94	Toluene	108-88-3	4.10	18	350
03-06-0385	1	31338-01 BAM-PPV	72	Hexanal	66-25-1	4.39	11	214
03-06-0385	1	31338-01 BAM-PPV	83	1-Hexanol	111-27-3	5.04	66	1314
03-06-0385	1	31338-01 BAM-PPV	90	1,4-Dichlorobutane	110-56-5	5.44	12	248
03-06-0385	1	31338-01 BAM-PPV	98	1,1,2,2-Tetrachloroethane	79-34-5	5.49	120	2404
03-06-0385	1	31338-01 BAM-PPV	83	2-Methylhexanoic acid	4536-23-6	6.51	7.5	150
03-06-0385	1	31338-01 BAM-PPV	43	Dimethyl(2-octyl) amine	1000216-65-3	8.17	16	320
03-06-0385	1	31338-01 BAM-PPV	38	2,6-Bis[(trimethylsilyl)oxy]-, trime...benzoic acid*	3782-85-2	10.47	8.2	164
03-06-0385	1	31338-01 BAM-PPV	42	1,1,1,5,7,7,7-Heptamethyl-3,3-bis(trimethylsiloxy)...*	38147-00-1	11.29	7.5	150
03-06-0385	1	31338-01 BAM-PPV	90	11-[(trimethylsilyl)oxy]-, bi...pregnane-3,20-dione*	57305-27-8	12.02	8.6	172
03-06-0385	1	31338-01 BAM-PPV	43	1,1,1, 5, 5, 5-Hexamethyl-3,3-bis[(trime...trisiloxane*	3555-47-3	12.69	12	236
03-06-0385	1	31338-01 BAM-PPV	58	Octadecamethylcyclononasiloxane*	556-71-8	14.11	21	422
03-06-0385	1	31338-01 BAM-PPV	60	2, 3-Bis[(trimethls...9,12,15-octadecatrienoic acid*	55521-22-7	14.94	27	536
03-06-0385	1	31338-01 BAM-PPV	50	Octadecamethylcyclononasiloxane*	556-71-8	15.89	27	548
03-06-0385	1	31338-01 BAM-PPV	64	Octadecamethylcyclononasiloxane*	556-71-8	16.93	38	752
03-06-0385	1	31338-01 BAM-PPV	64	Octadecamethylcyclononasiloxane*	556-71-8	18.04	30	590
03-06-0385	1	31338-01 BAM-PPV	59	Octadecamethylcyclononasiloxane*	556-71-8	19.25	23	454
03-06-0385	1	31338-01 BAM-PPV	35	3,6-Dioxa-2,4,5,7-tetrasilaoctane, 2, 2, 4, 4, 5, 5, 7, 7,...*	4342-25-0	20.74	12	248
03-06-0385	1	31338-01 BAM-PPV	33	3-Isopropoxy-1,1,1, 7, 7, 7-hexamethyl-3, 5, 5-tris(tri...*	71579-69-6	22.56	7.0	140

Q: Qualifier
RT: Retention Time
Note: * Compound attributed to column bleed.

Calscience Environmental Laboratories, Inc.

ANALYTICAL REPORT

Navy Public Works Center		Date Received:	06/06/03
2730 McKean Street, Suite 1		Work Order No:	03-06-0385
San Diego, CA 92136-5294		Preparation:	EPA 1311
		Method:	EPA 8270C

Project: CEL-0284 / LAB#31338 / Proj#144-01

Client Sample Number	Lab Sample Number	Date Collected	Matrix	Date Prepared	Date Analyzed	QC Batch ID
31338-01 BAM-PPV	**03-06-0385-1**	**06/03/03**	**Solid**	**06/09/03**	**06/12/03**	**030609L06**

Parameter	Result	RL	DF	Qual	Units	Parameter	Result	RL	DF	Qual	Units
N-Nitrosodimethylamine	ND	250	1		ug/L	3-Nitroaniline	ND	250	1		ug/L
Aniline	ND	250	1		ug/L	Acenaphthene	ND	250	1		ug/L
Pyridine	ND	250	1		ug/L	2,4-Dinitrophenol	ND	500	1		ug/L
Phenol	ND	250	1		ug/L	4-Nitrophenol	ND	500	1		ug/L
Bis(2-Chloroethyl) Ether	ND	250	1		ug/L	Dibenzofuran	ND	250	1		ug/L
2-Chlorophenol	ND	250	1		ug/L	2,4-Dinitrotoluene	ND	130	1		ug/L
1,3-Dichlorobenzene	ND	250	1		ug/L	2,6-Dinitrotoluene	ND	250	1		ug/L
1,4-Dichlorobenzene	ND	250	1		ug/L	Diethyl Phthalate	ND	250	1		ug/L
Benzyl Alcohol	ND	250	1		ug/L	4-Chlorophenyl-Phenyl Ether	ND	250	1		ug/L
1,2-Dichlorobenzene	ND	250	1		ug/L	Fluorene	ND	250	1		ug/L
2-Methylphenol	ND	250	1		ug/L	4-Nitroaniline	ND	250	1		ug/L
Bis(2-Chloroisopropyl) Ether	ND	250	1		ug/L	Azobenzene	ND	250	1		ug/L
3/4-Methylphenol	ND	250	1		ug/L	4,6-Dinitro-2-Methylphenol	ND	500	1		ug/L
N-Nitroso-di-n-propylamine	ND	250	1		ug/L	N-Nitrosodiphenylamine	ND	250	1		ug/L
Hexachloroethane	ND	250	1		ug/L	4-Bromophenyl-Phenyl Ether	ND	250	1		ug/L
Nitrobenzene	ND	250	1		ug/L	Hexachlorobenzene	ND	130	1		ug/L
Isophorone	ND	250	1		ug/L	Pentachlorophenol	ND	500	1		ug/L
2-Nitrophenol	ND	250	1		ug/L	Phenanthrene	ND	250	1		ug/L
2,4-Dimethylphenol	ND	250	1		ug/L	Anthracene	ND	250	1		ug/L
Benzoic Acid	ND	500	1		ug/L	Di-n-Butyl Phthalate	ND	250	1		ug/L
Bis(2-Chloroethoxy) Methane	ND	250	1		ug/L	Fluoranthene	ND	250	1		ug/L
2,4-Dichlorophenol	ND	250	1		ug/L	Benzidine	ND	500	1		ug/L
1,2,4-Trichlorobenzene	ND	250	1		ug/L	Pyrene	ND	250	1		ug/L
Naphthalene	ND	250	1		ug/L	Butyl Benzyl Phthalate	ND	250	1		ug/L
4-Chloroaniline	ND	500	1		ug/L	3,3'-Dichlorobenzidine	ND	250	1		ug/L
Hexachloro-1,3-Butadiene	ND	250	1		ug/L	Benzo (a) Anthracene	ND	250	1		ug/L
4-Chloro-3-Methylphenol	ND	250	1		ug/L	Bis(2-Ethylhexyl) Phthalate	ND	250	1		ug/L
2-Methylnaphthalene	ND	250	1		ug/L	Chrysene	ND	250	1		ug/L
Hexachlorocyclopentadiene	ND	2500	1		ug/L	Di-n-Octyl Phthalate	ND	250	1		ug/L
2,4,6-Trichlorophenol	ND	250	1		ug/L	Benzo (k) Fluoranthene	ND	250	1		ug/L
2,4,5-Trichlorophenol	ND	250	1		ug/L	Benzo (b) Fluoranthene	ND	250	1		ug/L
2-Chloronaphthalene	ND	250	1		ug/L	Benzo (a) Pyrene	ND	250	1		ug/L
2-Nitroaniline	ND	250	1		ug/L	Dibenz (a,h) Anthracene	ND	250	1		ug/L
Dimethyl Phthalate	ND	250	1		ug/L	Indeno (1,2,3-c,d) Pyrene	ND	250	1		ug/L
Acenaphthylene	ND	250	1		ug/L	Benzo (g,h,i) Perylene	ND	250	1		ug/L

Surrogates:	REC (%)	Control Limits	Qual	Surrogates:	REC (%)	Control	Qual
2-Fluorophenol	69	21-100		Phenol-d6	76	10-94	
Nitrobenzene-d5	79	35-114		2-Fluorobiphenyl	78	43-116	
2,4,6-Tribromophenol	91	10-123		p-Terphenyl-d14	80	33-141	

RL - Reporting Limit , DF - Dilution Factor , Qual - Qualifiers

Calscience Environmental Laboratories, Inc.

ANALYTICAL REPORT

Navy Public Works Center
2730 McKean Street, Suite 1
San Diego, CA 92136-5294

Date Received: 06/06/03
Work Order No: 03-06-0385
Preparation: EPA 1311
Method: EPA 8270C

Project: CEL-0284 / LAB#31338 / Proj#144-01

Client Sample Number	Lab Sample Number	Date Collected	Matrix	Date Prepared	Date Analyzed	QC Batch ID
Method Blank	**096-02-007-650**	**N/A**	**Aqueous**	**06/09/03**	**06/12/03**	**030609L06**

Parameter	Result	RL	DF	Qual	Units	Parameter	Result	RL	DF	Qual	Units
N-Nitrosodimethylamine	ND	250	1		ug/L	3-Nitroaniline	ND	250	1		ug/L
Aniline	ND	250	1		ug/L	Acenaphthene	ND	250	1		ug/L
Pyridine	ND	250	1		ug/L	2,4-Dinitrophenol	ND	500	1		ug/L
Phenol	ND	250	1		ug/L	4-Nitrophenol	ND	500	1		ug/L
Bis(2-Chloroethyl) Ether	ND	250	1		ug/L	Dibenzofuran	ND	250	1		ug/L
2-Chlorophenol	ND	250	1		ug/L	2,4-Dinitrotoluene	ND	130	1		ug/L
1,3-Dichlorobenzene	ND	250	1		ug/L	2,6-Dinitrotoluene	ND	250	1		ug/L
1,4-Dichlorobenzene	ND	250	1		ug/L	Diethyl Phthalate	ND	250	1		ug/L
Benzyl Alcohol	ND	250	1		ug/L	4-Chlorophenyl-Phenyl Ether	ND	250	1		ug/L
1,2-Dichlorobenzene	ND	250	1		ug/L	Fluorene	ND	250	1		ug/L
2-Methylphenol	ND	250	1		ug/L	4-Nitroaniline	ND	250	1		ug/L
Bis(2-Chloroisopropyl) Ether	ND	250	1		ug/L	Azobenzene	ND	250	1		ug/L
3/4-Methylphenol	ND	250	1		ug/L	4,6-Dinitro-2-Methylphenol	ND	500	1		ug/L
N-Nitroso-di-n-propylamine	ND	250	1		ug/L	N-Nitrosodiphenylamine	ND	250	1		ug/L
Hexachloroethane	ND	250	1		ug/L	4-Bromophenyl-Phenyl Ether	ND	250	1		ug/L
Nitrobenzene	ND	250	1		ug/L	Hexachlorobenzene	ND	130	1		ug/L
Isophorone	ND	250	1		ug/L	Pentachlorophenol	ND	500	1		ug/L
2-Nitrophenol	ND	250	1		ug/L	Phenanthrene	ND	250	1		ug/L
2,4-Dimethylphenol	ND	250	1		ug/L	Anthracene	ND	250	1		ug/L
Benzoic Acid	ND	500	1		ug/L	Di-n-Butyl Phthalate	ND	250	1		ug/L
Bis(2-Chloroethoxy) Methane	ND	250	1		ug/L	Fluoranthene	ND	250	1		ug/L
2,4-Dichlorophenol	ND	250	1		ug/L	Benzidine	ND	500	1		ug/L
1,2,4-Trichlorobenzene	ND	250	1		ug/L	Pyrene	ND	250	1		ug/L
Naphthalene	ND	250	1		ug/L	Butyl Benzyl Phthalate	ND	250	1		ug/L
4-Chloroaniline	ND	500	1		ug/L	3,3'-Dichlorobenzidine	ND	250	1		ug/L
Hexachloro-1,3-Butadiene	ND	250	1		ug/L	Benzo (a) Anthracene	ND	250	1		ug/L
4-Chloro-3-Methylphenol	ND	250	1		ug/L	Bis(2-Ethylhexyl) Phthalate	ND	250	1		ug/L
2-Methylnaphthalene	ND	250	1		ug/L	Chrysene	ND	250	1		ug/L
Hexachlorocyclopentadiene	ND	2500	1		ug/L	Di-n-Octyl Phthalate	ND	250	1		ug/L
2,4,6-Trichlorophenol	ND	250	1		ug/L	Benzo (k) Fluoranthene	ND	250	1		ug/L
2,4,5-Trichlorophenol	ND	250	1		ug/L	Benzo (b) Fluoranthene	ND	250	1		ug/L
2-Chloronaphthalene	ND	250	1		ug/L	Benzo (a) Pyrene	ND	250	1		ug/L
2-Nitroaniline	ND	250	1		ug/L	Dibenz (a,h) Anthracene	ND	250	1		ug/L
Dimethyl Phthalate	ND	250	1		ug/L	Indeno (1,2,3-c,d) Pyrene	ND	250	1		ug/L
Acenaphthylene	ND	250	1		ug/L	Benzo (g,h,i) Perylene	ND	250	1		ug/L

Surrogates:	REC (%)	Control Limits	Qual	Surrogates:	REC (%)	Control	Qual
2-Fluorophenol	79	21-100		Phenol-d6	80	10-94	
Nitrobenzene-d5	87	35-114		2-Fluorobiphenyl	85	43-116	
2,4,6-Tribromophenol	96	10-123		p-Terphenyl-d14	86	33-141	

RL - Reporting Limit , DF - Dilution Factor , Qual - Qualifiers

Calscience Environmental Laboratories, Inc.

EPA 1311/8270C Tentatively Identified Compound List

Work Order	CEL Sample ID	Client ID	Q	Compound	CAS Number	RT	On Column Conc. µg/L	Estimated Conc. µg/L
03-06-0385	1	31338-01 BAM-PPV	97	Trichloroethylene	79-01-6	3.41	6.4	128
03-06-0385	1	31338-01 BAM-PPV	91	Toluene	108-88-3	4.10	31	616
03-06-0385	1	31338-01 BAM-PPV	83	Hexanal	66-25-1	4.40	59	1180
03-06-0385	1	31338-01 BAM-PPV	95	2-n-Butylacrolein	1070-66-2	5.01	16	328
03-06-0385	1	31338-01 BAM-PPV	97	p-Xylene	106-42-3	5.34	7.5	150
03-06-0385	1	31338-01 BAM-PPV	86	1,4-Dichlorobutane	110-56-5	5.45	22	434
03-06-0385	1	31338-01 BAM-PPV	95	1,1,2,2-Tetrachloroethane	79-34-5	5.50	127	2542
03-06-0385	1	31338-01 BAM-PPV	59	1-Butanol, 4-chloro, acetate	6962-92-1	6.73	6.3	126
03-06-0385	1	31338-01 BAM-PPV	43	N,N-Dipropylacetamide	1116-24-1	8.18	19	386
03-06-0385	1	31338-01 BAM-PPV	22	2,4-bis[(trimethylsilyl)oxy]-, trim...benzoic acid*	10586-16-0	10.49	9.5	190
03-06-0385	1	31338-01 BAM-PPV	37	3-Isopropoxy-1,1,1, 7, 7, 7-hexamethyl...*	71579-69-6	11.3	9.2	184
03-06-0385	1	31338-01 BAM-PPV	42	1,1,1, 5, 5, 5-Hexamethyl-3,3-bis[(trime...trisiloxane*	3555-47-3	12.03	10	200
03-06-0385	1	31338-01 BAM-PPV	42	1-Monolinoleoylglycerol trimethylsilyl ether*	54284-45-6	12.70	13	254
03-06-0385	1	31338-01 BAM-PPV	56	1,1,1,5,7,7,7-Heptamethyl-3, 3-bis(trimethylsiloxy) ...*	38147-00-1	14.13	20	390
03-06-0385	1	31338-01 BAM-PPV	50	Octadecamethylcyclononasiloxane*	556-71-8	14.97	23	452
03-06-0385	1	31338-01 BAM-PPV	53	Octadecamethylcyclononasiloxane*	556-71-8	15.91	23	468
03-06-0385	1	31338-01 BAM-PPV	36	1-Monolinoleoylglycerol trimethylsilyl ether*	54284-45-6	16.95	38	756
03-06-0385	1	31338-01 BAM-PPV	87	Octadecamethylcyclononasiloxane*	556-71-8	18.07	29	582
03-06-0385	1	31338-01 BAM-PPV	90	Octadecamethylcyclononasiloxane*	556-71-8	19.29	21	418
03-06-0385	1	31338-01 BAM-PPV		3,6-Dioxa-2,4,5,7-tetrasilaoctane, 2, 2, 4, 4, 5, 5, 7, 7...*	4342-25-0	20.78	11	222

Q: Qualifier
RT: Retention Time
Note: * Compound attributed to column bleed.

Calscience Environmental Laboratories, Inc.

Quality Control - Spike/Spike Duplicate

Navy Public Works Center
2730 McKean Street, Suite 1
San Diego, CA 92136-5294

Date Received: 06/06/03
Work Order No: 03-06-0385
Preparation: STLC
Method: EPA 8260B

Project: CEL-0284 / LAB#31338 / Proj#144-01

Quality Control Sample ID	Matrix	Instrument	Date Prepared	Date Analyzed	MS/MSD Batch Number
31338-01 BAM-PPV	Solid	GC/MS O	06/06/03	06/11/03	030610S03

Parameter	MS %REC	MSD %REC	%REC CL	RPD	RPD CL	Qualifiers
Benzene	96	95	72-127	1	0-25	
Carbon Tetrachloride	97	97	70-130	0	0-25	
Chlorobenzene	98	98	72-131	0	0-25	
1,2-Dichlorobenzene	98	98	70-130	1	0-25	
1,1-Dichloroethene	106	104	69-127	2	0-25	
Toluene	97	97	75-124	0	0-25	
Trichloroethene	86	85	60-137	1	0-25	
Vinyl Chloride	103	101	70-130	2	0-25	
Methyl-t-Butyl Ether (MTBE)	94	93	80-120	1	0-25	

Calscience Environmental Laboratories, Inc.

Quality Control - Spike/Spike Duplicate

Navy Public Works Center
2730 McKean Street, Suite 1
San Diego, CA 92136-5294

Date Received: 06/06/03
Work Order No: 03-06-0385
Preparation: EPA 1311
Method: EPA 8260B

Project: CEL-0284 / LAB#31338 / Proj#144-01

Quality Control Sample ID	Matrix	Instrument	Date Prepared	Date Analyzed	MS/MSD Batch Number
31338-01 BAM-PPV	Solid	GC/MS O	06/06/03	06/11/03	030610S02

Parameter	MS %REC	MSD %REC	%REC CL	RPD	RPD CL	Qualifiers
Benzene	95	97	81-123	2	0-15	
Carbon Tetrachloride	98	98	61-133	0	0-17	
Chlorobenzene	98	98	82-124	0	0-15	
1,2-Dichlorobenzene	99	98	82-124	1	0-16	
1,1-Dichloroethene	105	103	70-136	2	0-20	
Toluene	99	99	87-123	1	0-15	
Trichloroethene	84	85	66-108	1	0-16	
Vinyl Chloride	102	100	61-133	2	0-20	
Methyl-t-Butyl Ether (MTBE)	92	93	67-127	1	0-20	

Calscience Environmental Laboratories, Inc.

Quality Control - Spike/Spike Duplicate

Navy Public Works Center		Date Received:	06/06/03
2730 McKean Street, Suite 1		Work Order No:	03-06-0385
San Diego, CA 92136-5294		Preparation:	EPA 1311
		Method:	EPA 8270C

Project: CEL-0284 / LAB#31338 / Proj#144-01

Quality Control Sample ID	Matrix	Instrument	Date Prepared	Date Analyzed	MS/MSD Batch Number
31338-01 BAM-PPV	**Solid**	**GC/MS P**	**06/09/03**	**06/12/03**	**030609S06**

Parameter	MS %REC	MSD %REC	%REC CL	RPD	RPD CL	Qualifiers
Phenol	88	83	20-120	5	0-42	
2-Chlorophenol	81	80	23-134	2	0-40	
1,4-Dichlorobenzene	79	76	20-124	4	0-28	
N-Nitroso-di-n-propylamine	82	78	0-230	4	0-38	
1,2,4-Trichlorobenzene	81	77	44-142	5	0-28	
Acenaphthene	86	84	47-145	2	0-31	
2,4-Dinitrotoluene	90	89	39-139	1	0-38	

Calscience Environmental Laboratories, Inc.

Quality Control - Laboratory Control Sample

Navy Public Works Center
2730 McKean Street, Suite 1
San Diego, CA 92136-5294

Project: CEL-0284 / LAB#31338 / Proj#144-01

Date Received: 06/06/03
Work Order No: 03-06-0385
Preparation: STLC
Method: EPA 8260B

Quality Control Sample ID	Matrix	Instrument	Date Analyzed	Lab File ID	LCS Batch Number
095-01-026-2,201	Aqueous	GC/MS O	06/11/03	10JUN029	030610L05

Parameter	Conc Added	Conc Recovered	%Rec	%Rec CL	Qualifiers
Benzene	50	48	96	72-127	
Carbon Tetrachloride	50	51	101	70-130	
Chlorobenzene	50	50	100	72-131	
1,2-Dichlorobenzene	50	50	99	70-130	
1,1-Dichloroethene	50	54	109	69-127	
Toluene	50	49	98	75-124	
Trichloroethene	50	44	87	60-137	
Vinyl Chloride	50	54	107	79-118	
Methyl-t-Butyl Ether (MTBE)	50	45	91	80-120	

Calscience Environmental Laboratories, Inc.

Quality Control - Laboratory Control Sample

Navy Public Works Center
2730 McKean Street, Suite 1
San Diego, CA 92136-5294

Date Received: 06/06/03
Work Order No: 03-06-0385
Preparation: EPA 1311
Method: EPA 8260B

Project: CEL-0284 / LAB#31338 / Proj#144-01

Quality Control Sample ID	Matrix	Instrument	Date Analyzed	Lab File ID	LCS Batch Number
099-10-006-7,716	Aqueous	GC/MS O	06/11/03	10JUN029	030610L04

Parameter	Conc Added	Conc Recovered	%Rec	%Rec CL	Qualifiers
Benzene	50	48	96	84-120	
Carbon Tetrachloride	50	51	101	66-132	
Chlorobenzene	50	50	100	89-119	
1,2-Dichlorobenzene	50	50	99	89-119	
1,1-Dichloroethene	50	54	109	80-128	
Toluene	50	49	98	84-126	
Trichloroethene	50	44	87	69-105	
Vinyl Chloride	50	54	107	70-124	
Methyl-t-Butyl Ether (MTBE)	50	45	91	68-134	
Tert-Butyl Alcohol (TBA)	250	260	102	48-144	
Diisopropyl Ether (DIPE)	50	45	90	79-121	
Ethyl-t-Butyl Ether (ETBE)	50	44	88	74-134	
Tert-Amyl-Methyl Ether (TAME)	50	41	83	73-127	
Ethanol	500	540	109	49-133	

Calscience Environmental Laboratories, Inc.

Quality Control - LCS/LCS Duplicate

Navy Public Works Center
2730 McKean Street, Suite 1
San Diego, CA 92136-5294

Date Received: 06/06/03
Work Order No: 03-06-0385
Preparation: STLC
Method: EPA 8270C

Project: CEL-0284 / LAB#31338 / Proj#144-01

Quality Control Sample ID	Matrix	Instrument	Date Prepared	Date Analyzed	LCS/LCSD Batch Number
095-01-003-1,281	Aqueous	GC/MS J	06/09/03	06/11/03	030609L05

Parameter	LCS %REC	LCSD %REC	%REC CL	RPD	RPD CL	Qualifiers
Phenol	85	82	12-151	4	0-23	
2-Chlorophenol	83	81	45-135	2	0-18	
1,4-Dichlorobenzene	82	74	36-118	11	0-26	
N-Nitroso-di-n-propylamine	85	75	52-128	12	0-13	
1,2,4-Trichlorobenzene	83	78	42-120	5	0-21	
4-Chloro-3-Methylphenol	86	79	20-150	9	0-40	
Acenaphthene	84	84	51-137	1	0-11	
4-Nitrophenol	74	70	20-150	7	0-40	
2,4-Dinitrotoluene	78	81	25-143	3	0-36	
Pentachlorophenol	84	73	20-150	14	0-40	
Pyrene	75	67	45-135	11	0-20	

Calscience Environmental Laboratories, Inc.

Quality Control - Laboratory Control Sample

Navy Public Works Center
2730 McKean Street, Suite 1
San Diego, CA 92136-5294

Project: CEL-0284 / LAB#31338 / Proj#144-01

Date Received: 06/06/03
Work Order No: 03-06-0385
Preparation: EPA 1311
Method: EPA 8270C

Quality Control Sample ID	Matrix	Instrument	Date Analyzed	Lab File ID	LCS Batch Number
096-02-007-650	Aqueous	GC/MS P	06/12/03	12JUN008	030609L06

Parameter	Conc Added	Conc Recovered	%Rec	%Rec CL	Qualifiers
Phenol	2000	1700	84	20-120	
2-Chlorophenol	2000	1600	79	23-134	
1,4-Dichlorobenzene	2000	1600	78	20-124	
N-Nitroso-di-n-propylamine	2000	1700	83	0-230	
1,2,4-Trichlorobenzene	2000	1500	77	44-142	
Acenaphthene	2000	1600	82	47-145	
2,4-Dinitrotoluene	2000	1800	91	39-139	

Calscience Environmental Laboratories, Inc.

GLOSSARY OF TERMS AND QUALIFIERS

Work Order Number: 03-06-0385

Qualifier	Definition
ND	Not detected at indicated reporting limit.

Calscience
Environmental
Laboratories, Inc.

Navy Public Works Center
2730 McKean Street, Suite 1
San Diego, CA 92136-5294

Date Received: 06/16/03
Work Order No.: 03-06-0385

Project: CEL-0284 / LAB#31338 / Proj#144-01

Department	Analyst
VOC	VT
SVOC	LL

Calscience Environmental Laboratories, Inc.

WORK ORDER #: 03 - 06 - 0385

Cooler 1 of 1

SAMPLE RECEIPT FORM

CLIENT: Ware DATE: 6/6/13

TEMPERATURE – SAMPLES RECEIVED BY:

CALSCIENCE COURIER:

- _____ Chilled, cooler with temperature blank provided.
- _____ Chilled, cooler without temperature blank.
- ✓ Chilled and placed in cooler with wet ice.
- _____ Ambient and placed in cooler with wet ice.
- _____ Ambient temperature.
- 5 °C Temperature blank.

LABORATORY (Other than Calscience Courier):

- _____ °C Temperature blank.
- _____ °C IR thermometer.
- _____ Ambient temperature.

Initial: [signature]

CUSTODY SEAL INTACT:

Sample(s): _____ Cooler: _____ No (Not Intact) : _____ Not Applicable (N/A): ✓

Initial: [signature]

SAMPLE CONDITION:

	Yes	No	N/A
Chain-Of-Custody document(s) received with samples	✓		
Sample container label(s) consistent with custody papers	✓		
Sample container(s) intact and good condition	✓		
Correct containers for analyses requested	✓		
Proper preservation noted on sample label(s)			✓
VOA vial(s) free of headspace.			✓
Tedlar bag(s) free of condensation			✓

Initial: [signature]

COMMENTS:

03-06-0385

Due Date: **6/18/03**

Work Request Number: **cel-0284**

Project#: 144-01

Collect By: WEBBER

Navy Region Environmental Chemistry Laboratory
Building M-9
San Diego, CA 92135

Contact: Lyn Vasquez
Alt. Contact: Carolyn Brodish
Phone: (619)545-8431
Fax: (619)545-0793

Ship Samples To:

Calscience Environmental Lab

7440 Lincoln Way
Garden Grove CA 92841-14

Contact: Jody McInerney
Phone: (800)888-5221
Fax: (714)894-7501

Container Type/ Bottle ID/ Preservative: E/SV/NA

Analysis ID

See SWR for analytical requirements. Numberd boxes indicate special instructions.

Lab#:	SampleID:	Collect Date:	Collect Time:	SampleType:	NO. OF Containers:	8260-STLC	8260-TCLP	8270-STLC	8270-TCLP	STLC TO ONLY	STLC PREP	TCLP PREP NONZHE	TCLP PREP ZHE
31338-01	BAM-PPV	06/03/03	0:00	Solid		X	X	X	X	X	X	X	X

Relinquished By: A. BURGI Date/Time: 6/6/3 1305

Received By:

Relinquished By: Date/Time:

Received By:

CONTAINER TYPE:
A= 125ml clear glass AA= 125ml amber glass B= BACTI bottle BRASS= brass sleeve C= 250ml clear glass D= 500ml clear glass DD= 500ml amber glass E= 1liter clear glass EE= 1 liter amber glass F= 1 liter plastic(collapsible),G= 1 gal plastic(collapsible) GG= 1 gal amber glass H= 250ml plastic I= 500ml plastic J= 1 liter plastic JJ= 1 liter amber plastic S= 20ml vial V= 40ml VOA vial V V= 40ml amber VOA vial Z= ziplock bag

PRESERVATIVE:
1 = Nitric Acid(HNO3) 2 = Hydrochloric Acid(HCl) 3 =Sulfuric Acid(H2SO4) 4 = Sodium Hydroxide(NaOH) 5 = Zinc Acetate(ZnC2H3O2) 6 = Sodium Thiosulfate(Na2S2O3) 7 = Ascorbic Acid(C6H8O6) 8 = Sodium Bisulfate(NaHSO4) ,9= Monochloroacetic acid(C2H3O2Cl) NA = Not applicable

Special Instructions: x= ~~Standard analysis, No special instructions~~

* = See attachment for BAM-PPV Physical Data This polymer varies in color from batch to batch, ...

** = Pls return any unused portion and any extracts. Ordinary storage is room temperature.

*** = Spike with Fenuron.

(03-C06-0355)

NAVAL AVIATION SYSTEMS TEAM

Originally prepared: January 18, 2001
Revised: February 26, 2002

BAM-PPV Physical Property Data

Appearance and Density

Color	Dark Orange
Fluorescence	Fluorescent orange under blue light
Product Form	Fibrous Solid Flakes
Pure Density:	1.13 g / cc*
Bulk Density:	0.1 g / cc (uncompacted)
Density after Compression Molding …	1.15 g / cc

Phase Behavior

Crystallinity:	Semi-crystalline (crystallinity varies with processing conditions)
Melting Point (virgin material)	150-160 C (302-320 F)
Melting Point (recrystallized material)	170-177 C (338-347 F)
Boiling Point	None (Decomposes below boiling point)
Vapor Pressure	Negligible

Solubility

Solubility Parameter	8.8 cal/cc $^{1/2}$ *
Solvents	Xylene, Trimethylbenzene, 1,1,2,2-tetrachloroethane, Methylene Chloride (up to a few per cent)
Solution appearance	Fluorescent orange liquid, generally will not pass through filters with pore size 1 micron or less

Thermal Properties

Maximum Use Temperature	200 C (392 F) unstabilized

Safet Handling and Use

Precautions: Solution can stain containers, especially glassware. Wear gloves and eye protection when handling. Use adequate ventilation if processing in solvents. Do not breathe dust or fine powder.

Stability: Stable at room temperature. Degradation accelerated by exposure to blue and ultraviolet light, as well as oxygen exposure. Avoid long-term exposure to light and UV radiation.

* estimate

Subcontract Work Request (SWR)

Ship Samples to:
Calscience Environmental Lab
7440 Lincoln Way
Garden Grove CA 92841-1
Attnt: Jody McInerney
Phone: (800)888-5221 Fax: (714)894-7501

Report Results to:
US Navy Environmental Chemistry Lab. San Diego
Navy Public Works Center
2730 McKean Street
San Diego, CA 92136-5294
Attn: Lyn Vasquez Phone:(619)545-8431 Fax:(619)545-0793

Invoice to:
ROICC
CORONADO
PO BOX 357007
BLDG 242 NAS

All work under this work request must comply with the terms and conditions stated in the Navy Sucontract description/specifications/work statement.

PWC SDG#: 31338

SWR#: CEL-0284

Include SWR number on all reports.

Contract No: N68711-02-A-5013

CALL# 0284

Include CALL# and Contract No. on invoice

Due Date: 6/18/03 TestGroupID: 8260-STLC TestGroupName: STLC: VOLATILE ORGANICS
Hold Date: 6/17/03
1 Samples Totaling: $105.00
Total Cost for 8 Day TAT: $0.00
Total Cost for Testgroup: $105.00

Report MISC. ORGANICS To: mg/L (ppm) Prep/Analyze By: 1311A ZHE / 8260B/TCLP

Due Date: 6/18/03 TestGroupID: 8260-TCLP TestGroupName: TCLP: VOLATILE ORGANICS
Hold Date: 6/17/03
1 Samples Totaling: $130.00
Total Cost for 8 Day TAT: $0.00
Total Cost for Testgroup: $130.00

Report MISC. ORGANICS To: mg/L (ppm) Prep/Analyze By: 1311A ZHE / 8260B/TCLP

Due Date: 6/18/03 TestGroupID: 8270-STLC TestGroupName: STLC: SEMIVOLATILE ORGANICS
Hold Date: 6/10/03
1 Samples Totaling: $215.00
Total Cost for 8 Day TAT: $0.00
Total Cost for Testgroup: $215.00

Report MISC. ORGANICS To: mg/L (ppm) Prep/Analyze By: 1311/3510C / 8270C/TCLP

Printed: 6/6/03 9:48:54 AM

Subcontract Work Request (SWR)

Ship Samples to:
Calscience Environmental Lab
7440 Lincoln Way
Garden Grove CA 92841-1
Attnt: Jody McInerney
Phone: (800)888-5221 Fax: (714)894-7501

All work under this work request must comply with the terms and conditions stated in the Navy Sucontract description/specifications/work statement.

Report Results to:
US Navy Environmental Chemistry Lab, San Diego
Navy Public Works Center
2730 McKean Street
San Diego, CA 92136-5294
Attn: Lyn Vasquez Phone:(619)545-8431 Fax:(619)545-0793

PWC SDG#: 31338

SWR#: CEL-0284

Include SWR number on all reports.

Invoice to:
ROICC
CORONADO
PO BOX 357007
BLDG 242 NAS

Contract No: N68711-02-A-5013

CALL# 0284

Include CALL# and Contract No. on invoice

Due Date: 6/18/03 TestGroupID: 8270-TCLP TestGroupName: TCLP: SEMIVOLATILE ORGANICS
Hold Date: 6/10/03
1 Samples Totaling: $215.00
Total Cost for 8 Day TAT: $0.00
Total Cost for Testgroup: $215.00

Report MISC. ORGANICS To: mg/L (ppm) Prep/Analyze By: 1311/3510C / 8270C/TCLP

Due Date: 6/18/03 TestGroupID: STLC IQ ONLY TestGroupName: WASTE EXTRACTION TEST
Hold Date: 6/17/03
1 Samples Totaling: $35.00
Total Cost for 8 Day TAT: $0.00
Total Cost for Testgroup: $35.00

Report STLC CA WET To: Prep/Analyze By: WET / WET

Due Date: 6/18/03 TestGroupID: STLC PREP TestGroupName: WASTE EXTRACTION TEST
Hold Date: 6/17/03
1 Samples Totaling: $45.00
Total Cost for 8 Day TAT: $0.00
Total Cost for Testgroup: $45.00

Report STLC CA WET To: Prep/Analyze By: WET / WET

Printed: 6/6/03 9:48:55 AM

Subcontract Work Request (SWR)

Ship Samples to:
Calscience Environmental Lab
7440 Lincoln Way
Garden Grove CA 92841-1
Attnt: Jody McInerney
Phone: (800)888-5221 Fax: (714)894-7501

Report Results to:
US Navy Environmental Chemistry Lab, San Diego
Navy Public Works Center
2730 McKean Street
San Diego, CA 92136-5294
Attn: Lyn Vasquez Phone:(619)545-8431 Fax:(619)545-0793

Invoice to:
ROICC
CORONADO
PO BOX 357007
BLDG 242 NAS

All work under this work request must comply with the terms and conditions stated in the Navy Sucontract description/specifications/work statement.

PWC SDG#: 31338

SWR#: CEL-0284

Include SWR number on all reports.

Contract No: N68711-02-A-5013

CALL# **0284**

Include CALL# and Contract No. on invoice

Due Date:	6/18/03	TestGroupID:	TCLP PREP NONZHE	TestGroupName:	PREP BY 1311(TCLP) NON ZHE		
		Hold Date:	6/17/03		1 Samples Totaling:		$35.00
					Total Cost for 8 Day TAT:		$0.00
					Total Cost for Testgroup:		$35.00

Report To: Prep/Analyze By: EPA1311/TCLP / EPA1311/TCLP

Due Date:	6/18/03	TestGroupID:	TCLP PREP ZHE	TestGroupName:	PREP BY 1311(TCLP) ZHE		
		Hold Date:	6/17/03		1 Samples Totaling:		$70.00
					Total Cost for 8 Day TAT:		$0.00
					Total Cost for Testgroup:		$70.00

Report To: Prep/Analyze By: EPA1311/TCLP / EPA1311/TCLP

Grand Total Cost for SWRN CEL-0284: $850.00